Fraktionierung stabiler Isotope durch anaerobe Bodenmikroorganismen

Dissertation

zur Erlangung
des Doktorgrades der Naturwissenschaften
(Dr. rer. nat.)

dem Fachbereich der Biologie
der Philipps-Universität Marburg/Lahn
vorgelegt von

Holger Penning
aus Erlangen

Marburg/Lahn 2005

Die Untersuchungen zur folgenden Arbeit wurden von Januar 2003 bis Oktober 2005 am Max-Planck-Institut für terrestrische Mikrobiologie in Marburg unter Anleitung von Prof. Dr. Ralf Conrad durchgeführt.

Vom Fachbereich Biologie der Philipps-Universität Marburg als Dissertation angenommen am: 21. November 2005

Erstgutachter: Prof. Dr. Ralf Conrad
Zweitgutachter: Prof. Dr. Rudolf K. Thauer

Tag der Disputation: 9. Dezember 2005

Die in dieser Dissertation beschriebenen Ergebnisse sind in folgenden Originalpublikationen veröffentlicht bzw. zur Veröffentlichung eingereicht:

1. **Penning H., C.M. Plugge, P.E. Galand und R. Conrad** (2005) Variation of carbon isotope fractionation in hydrogenotrophic methanogenic microbial cultures and environmental samples at different energy status (akzeptiert bei Global Change Biology).

2. **Penning, H. und R. Conrad** (2005) Carbon isotope effects associated with mixed-acid fermentation of saccharides by *Clostridium papyrosolvens* (eingereicht bei Geochimica et Cosmochimica Acta am 7. Juli 2005).

3. **Penning, H. und R. Conrad** (2005) Effect of inhibition of acetoclastic methanogenesis on growth of archaeal populations in an anoxic model environment (akzeptiert bei Applied and Environmental Microbiology).

4. **Penning, H., S.C. Tyler und R. Conrad** (2005) Geochemical characterization of the anoxic model system rice roots using thermodynamics, carbon stable isotopes, and specific inhibition of acetoclastic methanogenesis (eingereicht bei Geobiology am 13. Oktober 2005)

Inhalt

Abkürzungen

bp	Basenpaare
CH_3F	Methylfluorid
D	Verdünnungsrate (Chemostat)
f_{ac}	relativer Anteil des aus Acetyl-CoA gebildeten Acetat
FAM	Carboxyfluorescein
f_{lac}	relativer Anteil des aus Pyruvat gebildeten Lactats
f_{mc}	Anteil der hydrogenotrophen Methanogenese an der Methanbildung
IRMS	Isotopen-Verhältnis-Massenspektrometer
p_{H2}	Wasserstoffpartialdruck
qPCR	quantitative *real time* Polymerase Kettenreaktion
RC	Rice Cluster
TIC	gesamter anorganischer Kohlenstoff (*total inorganic carbon*)
T-RF	terminales Restriktionsfragment
T-RFLP	terminaler Restriktionsfragment-Längen-Polymorphismus
ΔG	Änderung der Gibbs freien Energie unter experimentellen Bedingungen
Ω_x	Unterschied der Isotopenfraktionierung zweier Reaktionen in ‰, die x als gemeinsames Substrat haben
$\delta^{13}C$	stabiles Kohlenstoff-Isotopenverhältnis relativ zum internationalen Standard
δ_{ac}	$\delta^{13}C$ von Acetat
ε und α	Isotopen-Fraktionierungsfaktoren (definiert unter Material und Methoden)

Zusammenfassung

Methan ist ein Endprodukt des anaeroben Abbaus organischen Materials und ein klimarelevantes Treibhausgas. Über die Kohlenstoffisotopensignatur atmosphärischen Methans kann der Anteil der unterschiedlichen Methanquellen bestimmt werden. Die bedeutendste Quelle sind terrestrische Systeme wie Sümpfe und Reisfelder, in denen Methan fast ausschließlich aus CO_2 und Acetat gebildet wird. Die Methanbildungswege unterscheiden sich in ihrer Isotopenfraktionierung, so dass für ein anoxisches System der Anteil des hydrogenotroph und acetoklastisch gebildeten Methans über dessen Isotopenverteilung bestimmt werden kann. In dieser Arbeit wurden Isotopenfraktionierungsfaktoren (α), die für die Modellierung der relativen Anteile der Methanbildungswege benötigt werden, bestimmt.

Die Isotopensignatur von Acetat (δ_{ac}) und der Fraktionierungsfaktor der hydrogenotrophen Methanogenese ($\alpha_{CO2/CH4}$) sind Parameter, die für eine solche Modellierung benötigt werden. Sie können experimentell über Hemmung der acetoklastischen Methanogenese mit dem Hemmstoff Methylfluorid (CH_3F) erhalten werden. Hier wurde überprüft, ob CH_3F auch unspezifisch andere Prozesse und archaeelle Gruppen hemmt. Im Reiswurzel-Modellsystem wurde mittels geochemischer und molekularbiologischer Methoden gezeigt, dass nur der Zielprozess, die acetoklastische Methanogenese, und die entsprechenden Zielorganismen, die Familie der *Methanosarcinaceae*, direkt gehemmt wurden. Damit eignen sich Inkubationen mit CH_3F zur Bestimmung von δ_{ac} und $\alpha_{CO2/CH4}$.

Acetat wird zum überwiegenden Teil bei der Fermentation produziert. Daher kann δ_{ac} über Isotopenfraktionierungsfaktoren der Fermentation errechnet werden. Für *Clostridium papyrosolvens* wurde in dieser Arbeit das Fraktionierungsverhalten für die Bildung von Acetat, Ethanol, Lactat, Formiat und CO_2 aufgeklärt. Im linearen Teil des Stoffwechselweges vom Saccharid zum Intermediat Pyruvat wurde in löslichen Sacchariden ^{12}C bevorzugt, während dagegen beim Polysaccharid Cellulose keine Fraktionierung auftrat. Die Verzweigungspunkte Pyruvat und Acetyl-CoA wiesen charakteristische Fraktionierungsmuster auf und ermöglichten die Isotopensignatur der Produkte vorauszusagen. Da in Umweltsystemen Polysaccharide das hauptsächliche Substrat der Fermentation sind, und somit keine Fraktionierung bis zum Pyruvat auftritt,

können die stabilen Isotopensignaturen der Produkte allein über die Isotopensignatur des organisches Materials und den Kohlenstofffluss der Fermentation vorausgesagt werden.

Die Isotopenfraktionierung während der hydrogenotrophen Methanogenese ist ebenfalls ein notwendiger Parameter, der allerdings stark variiert. Die dahinterliegenden Steuerungsfaktoren waren bisher nicht bekannt und wurden daher in dieser Arbeit in Rein- und Kokulturen hydrogenotropher *Archaea* der Familien *Methanomicrobiaceae* und *Methanobacteriaceae* untersucht. Die Isotopenfraktionierung korrelierte mit der Änderung der Gibbs freien Energie (ΔG) der Methanbildung aus H_2 und CO_2. In Böden und Sedimenten, in denen ΔG auf Grund von H_2-Gradienten nicht korrekt über Gasmessungen ermittelt werden kann, ermöglichte die gefundene $\alpha_{CO2/CH4}$-ΔG-Korrelation eine unbeeinflusste Bestimmung von ΔG der hydrogenotrophen Methanogenese. Es zeigte sich, dass den hydrogenotrophen Methanogenen in H_2-Gradienten-beeinflussten Umweltsystemen deutlich mehr freie Energie zur Verfügung steht als bisher angenommen.

Im Reiswurzel-Modellsystem wurden die ermittelten Parameter zur Quantifizierung der relativen Anteile der Methanbildungswege verwendet. Die berechneten Werte stimmten mit anderen geochemischen Daten überein und bestätigten, dass eine solche Bestimmung allein über die Kohlenstoffisotopensignaturen möglich ist. Insgesamt vertiefte diese Arbeit das Verständnis des $^{13}C/^{12}C$-Isotopenflusses in Einzelprozessen und im gesamten Netzwerk des anaeroben Abbaus organischen Materials und vereinfachte damit die Modellierung des Kohlenstoffflusses in diesem System.

I. Einleitung

I.1. Grundlagen der stabilen Isotopenfraktionierung

Leichte Elemente einschließlich Wasserstoff, Kohlenstoff, Stickstoff und Sauerstoff sind von wesentlicher biologischer Bedeutung und besitzen natürlich vorkommende stabile Isotope. Mit Ausnahme von Sauerstoff, ist bei den genannten Elementen das leichtere Isotop häufiger als das eine Masseneinheit schwerere Isotop. Im Folgenden wird ausschließlich das Element Kohlenstoff betrachtet, dessen Isotope sich stark in ihrer Häufigkeit unterscheiden. Das Isotop ^{13}C hat in der Natur einen Anteil von nur 1,1 %, der Rest entfällt auf ^{12}C. Isotope eines Elements besitzen sehr ähnliche chemische Eigenschaften, sind aber nicht identisch. Die Massenunterschiede sind verantwortlich für leicht veränderte Bindungs- und Vibrationsenergien (de Vries, 2005), welche zwei Isotopeneffekte bedingen. In Gleichgewichtsreaktionen sorgt der Gleichgewichtsisotopeneffekt dafür, dass sich die Isotope eines Elements auf Grund unterschiedlicher Bindungsenergien nicht statistisch auf Produkte und Reaktanden verteilen. Es erfolgt normalerweise eine Anreicherung des schwereren Isotops in Verbindungen höherer molekularer Masse. Beim zweiten Isotopeneffekt, dem kinetischen Isotopeneffekt, reagieren die Isotope eines Elements in einer irreversiblen oder unvollständigen Reaktion nicht mit der gleichen Rate. Da das leichtere Isotop eine höhere Vibrationsenergie besitzt, ist die Wahrscheinlichkeit mit dem Reaktionspartner zusammenzutreffen (Kollisionshäufigkeit) höher, so dass Produkte irreversibler Reaktionen generell an ^{12}C angereichert sind. Bei den meisten biologischen Reaktionen handelt es sich nicht um Gleichgewichtsreaktionen, so dass fast ausschließlich kinetische Isotopeneffekte vorliegen.

Isotopeneffekte sind physikalische Phänomene, die nicht direkt beobachtet werden können. Quantitativ messbar hingegen ist die Folge des Isotopeneffekts, die Isotopenfraktionierung, die einen charakteristischen Wert für eine bestimmte Reaktion besitzt. Sie ist beschrieben durch den Fraktionierungsfaktor α:

$$\alpha_{S/P} = \frac{R_S}{R_P} \tag{I-1}$$

wobei S und P das Substrat und Produkt einer Reaktion sind, und R das Isotopenverhältnis $^{13}C/^{12}C$. In einer Reaktion ohne Fraktionierung ist $\alpha = 1$; wird während der Reaktion gegen

das schwerere Isotop diskriminiert (leichtes Isotop bevorzugt) ist $\alpha > 1$ und umgekehrt. Eine Kohlenstoffisotopenfraktionierung von $\alpha > 1$ wird als normal bezeichnet und ist bei unverzweigten irreversiblen Reaktionen auf Grund oben erwähnter Prinzipien die Regel. Die Isotopenfraktionierung des kinetischen Isotopeneffekts einer irreversiblen Reaktion $S \rightarrow P$ kann in einem geschlossenen System immer beobachtet werden (Abbildung I-1). Während die Reaktion von Beginn bis zur vollständigen Umsetzung des Substrats abläuft steigt die Ausbeute von 0 auf 1 an und die Isotopenzusammensetzung des Substrats und Produkts ändern sich kontinuierlich. Bei quantitativer Umsetzung des Substrats (Ausbeute = 1) entspricht das Isotopenverhältnis des Produkts dem Ausgangsisotopenverhältnis des Substrats. Während des Ablaufs der Reaktion reichert sich durch den bevorzugten Verbrauch von ^{12}C-Substrat das schwerere Isotop (^{13}C) im verbliebenen Substrat an. Die Isotopenfraktionierung zwischen dem Anteil des Produkts, das momentan gebildet wird (rote gestrichelte Linie), und dem verbliebenen Substrat bleibt im Verlauf unverändert und entspricht der Größe des Isotopeneffekts. Daher sind die Kurven des Substrats und des momentan gebildeten Produkts immer durch dieselbe y-Differenz getrennt, wogegen die y-Differenz zwischen dem Substrat und dem akkumulierten Produkt stetig zunimmt (Hayes, 2002).

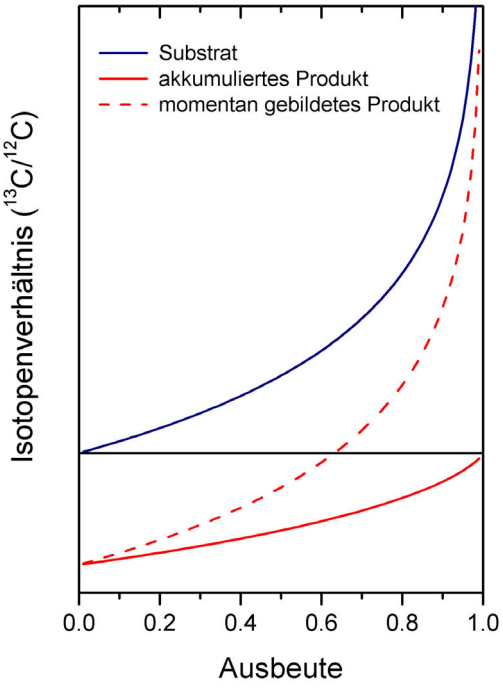

Abbildung I-1. Schematische Darstellung der kinetischen Isotopenfraktionierung im geschlossenen System während des Ablaufs der Reaktion.

Da die Änderungen der Isotopenverhältnisse während einer Reaktion sehr klein sind, wird bei der Betrachtung natürlicher Isotopenverhältnisse die sogenannte Delta-Notierung verwendet:

$$\delta^{13}C = [(R_{Probe} / R_{Standard})-1] \times 10^3 \ [‰] \quad \text{(I-2)}$$

dabei ist R das Isotopenverhältnis $^{13}C/^{12}C$ der Probe oder des verwendeten Standards. Es wurden Standard-Referenzmaterialen definiert, denen der willkürliche Wert 0 ‰ zugeordnet wurde (für Kohlenstoff ein Belemnit der PeeDee-Formation (Kalkstein) in den U.S.A.). Ein Anstieg des δ-Wertes entspricht einem Anstieg des Anteils des schwereren Isotops und umgekehrt.

I.2. Modellierung mittels Kohlenstoffisotopie

In biologischen und geochemischen Kreisläufen entwickelt sich durch eine Vielzahl von aufeinanderfolgenden Reaktionen eine Isotopenstruktur mit unterschiedlichen Isotopenverhältnissen in den vorkommenden Verbindungen. Hierbei werden zwei Arten von Informationen in der Isotopensignatur aufgezeichnet. Einerseits liefert die Fraktionierung Informationen über die Reaktionen und die Bedingungen, bei denen sie ablaufen (Prozessinformation). Andererseits gibt die Isotopenverteilung Aufschluss über den Ursprung einer Verbindung (Quelleninformation). Ein gut untersuchtes Beispiel dafür ist die Kohlenstoffisotopenfraktionierung während der Photosynthese. C_3-Pflanzen haben ein durchschnittliches $\delta^{13}C$ von –27,8 ‰, das damit ungefähr 20 ‰ niedriger ist als das verwendete Substrat (atmosphärisches CO_2 mit $\delta^{13}C_{CO2}$ = -7,4 ‰). Somit spiegelt die Isotopenzusammensetzung dieser Pflanzen sowohl die Quelle (CO_2) als auch die Fraktionierung während der Reaktion wider. In einem Nahrungsnetz ist es damit möglich, die Anteile der jeweiligen Prozesse am Kohlenstoffffluss zu bestimmen, wenn man die charakteristischen Isotopenfraktionierungsfaktoren der beteiligten Reaktionen kennt. Ein entscheidender Vorteil dieser Methode liegt darin, dass ein bereits vorhandenes natürliches Signal, die Kohlenstoffisotopie, zur Quantifizierung des Anteils bestimmter Prozesse am Kohlenstoffffluss verwendet wird. Damit ist eine Störung des untersuchten Systems vor der Probenahme nicht erforderlich, wie es z.B. beim Einsatz radiogener Tracer notwendig ist. Bisher wurde diese Methode jedoch nur in wenigen Bereichen zu Modellierungszwecken eingesetzt, da das Wissen über Isotopenfraktionierungsfaktoren der beteiligten Reaktionen begrenzt ist.

I.3. Anoxischer Abbau organischen Materials

In anoxischen Systemen wird organisches Material bei geringer Verfügbarkeit von alternativen Elektronenakzeptoren (Nitrat, Sulfat oder oxidiertem Eisen und Mangan) zu Methan und Kohlendioxid abgebaut. Typische Umweltsysteme hierfür sind Böden und Süßwassersedimente, die reich an organischem Material sind, wobei Sümpfe, Moore und geflutete Reisfelder am bedeutendsten sind. Im Vergleich zu anderen oxidativen Prozessen hat der anaerobe Abbau organischer Materie zu Methan die geringste Energieausbeute und wird nicht von einem Organismus allein, sondern von mindestens vier funktionellen Gruppen bewältigt (Schink, 1997): Primärfermentierer, Sekundärfermentierer und zwei Arten von Methanogenen (Abbildung I-2). Ausgehend von Polymeren stellen die jeweilig vorgeschalteten Prozesse das Substrat für nachfolgende Reaktionen zur Verfügung.

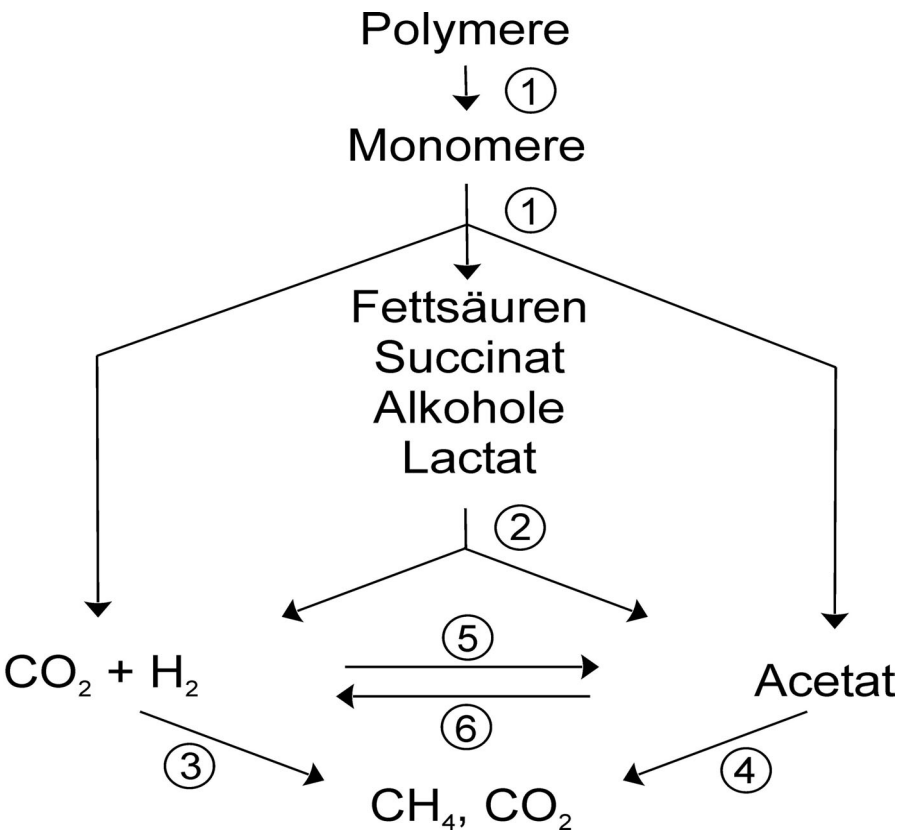

Abbildung I-2. Kohlenstoffffluss während des anaeroben Abbaus komplexer organischer Materie durch Mikroorganismen unterschiedlicher funktioneller Gruppen. (1) Primärfermentierer; (2) Sekundärfermentierer; (3) hydrogenotrophe und (4) acetoklastische methanogene *Archaea*; (5) Homoacetogene *Bacteria*; (6) Syntroph acetatoxidierende *Bacteria*.

Primärfermentierer hydrolysieren Polymere (z.B. Cellulose) zu Oligo- und Monomeren und fermentieren diese zu Acetat, H_2, CO_2, Fettsäuren, Succinat, Alkoholen und Lactat. Die Produkte Acetat, H_2 und CO_2 können direkt von methanogenen *Archaea* zu CH_4 und CO_2 umgesetzt werden, während Sekundärfermentierer aus den übrigen Intermediaten Vorläuferverbindungen für die Methanogenese produzieren. Doch es besteht auch eine Abhängigkeit vorgeschalteter Organismen von der Aktivität jener Organismen, die ihre Produkte verstoffwechseln. So ist z.B. die Vergärung von Fettsäuren durch Sekundärfermentierer thermodynamisch nur bei sehr geringen H_2-Partialdrücken möglich, die durch die Aktivität hydrogenotropher Methanogener eingestellt werden können.

In den meisten terrestrischen Habitaten wird Methan fast ausschließlich entweder aus Acetat (acetoklastisch) oder aus H_2/CO_2 (hydrogenotroph) gebildet:

$$*CH_3COOH \rightarrow CO_2 + *CH_4 \qquad \text{(I-3)}$$

$$CO_2 + 4\ H_2 \rightarrow 2\ H_2O + CH_4 \qquad \text{(I-4)}$$

In Reaktion I-3 wird CH_4 aus der Methylgruppe der Essigsäure produziert (durch * markiert). Methanogene Mikroorganismen gehören ausschließlich der Domäne der *Archaea* an und sind durch ihren obligat methanogenen Stoffwechsel gekennzeichnet. Kultivierte Vertreter von Methanogenen sind die Familien *Methanobacteriaceae* (hydrogenotroph), *Methanomicrobiaceae* (hydrogenotroph), *Methanosaetaceae* (acetoklastisch) und *Methanosarcinaceae* (acetoklastisch und hydrogenotroph). Bei den unkultivierten archaeellen Gruppen konnte bisher nur für *Rice Cluster* I ein hydrogenotroph-methanogener Stoffwechsel nachgewiesen werden (Erkel et al., 2005). Weiterhin kann abhängig von den thermodynamischen Bedingungen Homoacetogenese (Acetat aus H_2/CO_2) oder syntrophe Acetatoxidation (H_2/CO_2 aus Acetat) stattfinden.

Bezogen auf die globale Treibhausgasbilanz sind Feuchtgebiete einschließlich gefluteter Reisfelder die bedeutendste natürliche Quelle des klimarelevanten Gases Methan (Cicerone und Oremland, 1988). Dessen Kohlenstoffisotopenzusammensetzung wird zur Beurteilung der Bedeutung individueller atmosphärischer Methanquellen und -senken verwendet und ermöglicht die Interpretation der atmosphärischen Methanbilanz (Lowe et al., 1994; Quay et al., 1991; Tyler et al., 1999). Ausschlaggebend für die Qualität der Modellierung des Methanbudgets der Atmosphäre ist die genaue Kenntnis der Isotopensignatur der Quellen und Senken. Bei terrestrischen anoxischen Systemen hängt die Isotopensignatur des Methans hauptsächlich vom relativen Anteil der Methanogenese

aus Acetat und H_2/CO_2 ab. Diese Anteile können an Hand der unterschiedlichen Isotopenfraktionierung der Bildungswege bestimmt werden.

I.4. Quantifizierung methanogener Reaktionen

Wie unter I.2 angeführt, ist es möglich die relativen Anteile der Prozesse am Kohlenstoffffluss zu bestimmen, wenn man die Fraktionierungsfaktoren für die jeweiligen Prozesse kennt. Für den Fall der Methanproduktion aus zwei Quellen benötigt man die $\delta^{13}C$-Werte der Methanvorläufer und des gebildeten Methans, sowie die Fraktionierungsfaktoren von acetoklastischer und hydrogenotropher Methanogenese. Damit kann dann der Anteil der hydrogenotrophen Methanogenese (f_{mc}) berechnet werden (Conrad, 2005):

$$\delta_{CH4} = f_{mc}\delta_{mc} + (1-f_{mc})\delta_{ma} \quad \text{(I-5)}$$

aufgelöst nach f_{mc}

$$f_{mc} = (\delta_{CH4} - \delta_{mc})/(\delta_{mc} - \delta_{ma}) \quad \text{(I-6)}$$

wobei δ_{CH4}, δ_{mc}, δ_{ma} die δ-Werte von insgesamt gebildetem, CO_2-abgeleitetem und Acetat-abgeleitetem Methan sind. δ_{mc} und δ_{ma} werden über die Fraktionierungsfaktoren und $\delta^{13}C$-Werte der Methanvorläufer errechnet. Allein die Variable δ_{CH4} wird direkt gemessen.

Die Fraktionierungsfaktoren zur Berechnung von δ_{mc} und δ_{ma} wurden für verschiedene acetoklastische und hydrogenotrophe *Archaea* in Reinkultur bereits bestimmt. Während die Fraktionierungsfaktoren der acetoklastischen Methanogenese innerhalb eines engen Bereichs liegen ($1.021 \leq \alpha \leq 1.027$) (Gelwicks et al., 1994; Krzycki et al., 1987; Zyakun et al., 1988), variieren die berichteten Daten für die hydrogenotrophe Methanogenese zwischen 1,045 und 1,071 (Fey et al., 2004), was eine sinnvolle Modellierung verhindert. Zusätzlich kann δ_{ac} unter natürlichen Bedingungen im Fließgleichgewicht nicht direkt gemessen werden, da die Konzentrationen meist unter dem analytischen Detektionslimit liegen. δ_{ac} kann jedoch berechnet werden, wenn man die Isotopenfraktionierung der anaerob Acetat-produzierenden Organismen kennt. Bisher wurde nur die Isotopenfraktionierung des homoacetogenen Organismus *Acetobacterium woodii* untersucht (Gelwicks et al., 1989). Allerdings produzieren Primärfermentierer in den meisten Habitaten den Großteil an Acetat, wohingegen andere Gruppen wie

Sekundärfermentierer und Homoacetogene nur eine stark untergeordnete Rolle spielen (Krylova et al., 1997; Lovley und Klug, 1983).

In dieser Arbeit sollen daher die bisher noch nicht ausreichend bestimmten, aber für die Quantifizierung des Anteils der methanogenen Reaktionswege benötigten Fraktionierungsfaktoren der hydrogenotrophen Methanogenese und der Fermentation zu Acetat bestimmt werden.

Valentine et al. (2004) vermuteten, dass der Fraktionierungsfaktor der hydrogenotrophen Methanogenese (α_{mc}) vom Wasserstoffpartialdruck (p_{H2}) abhängt. In den hier beschriebenen Versuchen wurden daher unterschiedliche Arten hydrogenotropher Methanogener in Kokultur mit fermentierenden Bakterien gezogen. In obligat syntrophen Kokulturen (mit dem Propionatoxidierer *Synthrophobacter fumaroxidans*) war p_{H2} stets sehr niedrig, während hingegen in nicht obligaten Kokulturen (mit *Clostridium papyrosolvens* und *Acetobacterium woodii*) die Isotopenfraktionierung der Methanogenen in einem weiten Bereich von p_{H2} untersucht werden konnte. Methanogene Umweltsysteme, die sich in ihrem p_{H2} unterscheiden, hier Reisfeldboden, Moor (Conrad, 1999) und Pansen (Hobson, 1997), wurden ebenfalls getestet, um die in den Kulturexperimenten gewonnenen Erkenntnisse mit der Situation unter natürlichen Bedingungen zu vergleichen.

Zur Untersuchung der Isotopenfraktionierung während der Primärfermentation zu Acetat wurde das Bakterium *Clostridium papyrosolvens* ausgewählt. Dieser Organismus wurde bereits aus einem ästuarinen Sediment (Madden et al., 1982), einem Süßwassersumpf (Leschine und Canaleparola, 1983; Pohlschroder et al., 1994) und aus Reisfeldboden (Chin et al., 1998) isoliert und verstoffwechselt unterschiedliche Poly-, Oligo- und Monosaccharide in einer gemischten Säuregärung zu Acetat, CO_2, Ethanol, Lactat und H_2. Unterschiedliche Wachstumsbedingungen wurden gewählt, um die Isotopenfraktionierung in Abhängigkeit des metabolischen Kohlenstoffflusses zu bestimmen.

I.5. Kombination von Hemmstoffen und Kohlenstoffisotopie

Neben der Bestimmung der Isotopenfraktionierung in Kulturen können die benötigten Parameter (α_{mc} und δ_{ac}) auch durch Hemmung der acetoklastischen Methanogenese mit Methylfluorid (Frenzel und Bosse, 1996) in Umweltinkubationen bestimmt werden (Conrad, 2005). Unter der Annahme, dass Methan nur aus Acetat oder H_2/CO_2 gebildet wird, kann α_{mc} berechnet werden, da Methan in diesem Versuchsansatz ausschließlich aus H_2/CO_2 gebildet wird (f_{mc} = 1). δ_{ac} kann direkt gemessen werden, da Acetat im System akkumuliert. Das Prinzip wurde bereits für ein profundales Seesediment getestet (Chan et al., 2005). Allerdings geht der Einsatz von Hemmstoffen mit einer Änderung der *in situ* Bedingungen einher und kann somit das untersuchte System auch verändern. Zudem ist die genaue Wirkungsweise von Methylfluorid (CH_3F) nicht völlig aufgeklärt. Obwohl die Hemmwirkung von CH_3F in Reinkulturen acetoklastisch-methanogener *Archaea* erfolgreich getestet wurde (Janssen und Frenzel, 1997), ist die Spezifität für den acetoklastisch-methanogenen Reaktionsweg noch nicht experimentell abgesichert. Es wurde zwar bisher noch keine Hemmung anderer kultivierter Mikroorganismen mit ähnlichen Stoffwechselwegen beobachtet (Janssen und Frenzel, 1997), jedoch ist nicht auszuschließen, dass abundante unkultivierte archaeelle Gruppen, deren Physiologie noch völlig unbekannt ist, unspezifisch gehemmt werden.

Als Modellsystem zur Untersuchung der Einflüsse von CH_3F auf archaeelle Gruppen wurden anoxisch inkubierte Reiswurzeln gewählt. Dieses System ist sowohl hinsichtlich der archaeellen Lebensgemeinschaft und deren Dynamik (Chin et al., 2004; Lehmann-Richter et al., 1999; Scheid et al., 2004) als auch hinsichtlich seiner biogeochemischen Prozesse (Conrad et al., 2002; Conrad und Klose, 1999a; Lehmann-Richter et al., 1999) gut untersucht. Indirekt über das 16S rRNA-Gen soll mittels molekularbiologischer *Fingerprint*- und quantitativer Methoden die Spezifizität von CH_3F und dessen Einfluss auf bisher nur phylogenetisch charakterisierte Gruppen getestet werden.

I.6. Ziele der Arbeit

Terrestrische anoxische Habitate sind bedeutende Quellen klimarelevanter Treibhausgase. Die Isotopensignatur von Methan, die zur Erstellung globaler Methanbudgets verwendet wird, wird in diesen Habitaten durch hydrogenotrophe und acetoklastische Methanogenese und somit durch den Kohlenstoffffluss beim letzten Schritt der Mineralisierung organischer Materie bestimmt. Der Kohlenstoffffluss während der Mineralisierung zu Methan kann innerhalb des Habitats durch stabile Isotopensignaturen und den Einsatz spezifischer Hemmstoffe modelliert werden. Offene Fragen bezüglich der Fraktionierungsfaktoren bestimmter anaerober Prozesse und bezüglich der Einflüsse des Hemmstoffs Methylfluorid auf Mikroorganismen sollen in dieser Arbeit mit Methoden der stabilen Isotopen-Massenspektrometrie und der molekularen mikrobiellen Ökologie behandelt werden:

- Wie hoch ist die Kohlenstoffisotopenfraktionierung während der gemischten Säuregärung von Sacchariden?
- Wodurch ist die hohe Variabilität der Kohlenstoffisotopenfraktionierung während der hydrogenotrophen Methanogenese bedingt und kann mit Hilfe der Steuerungsfaktoren die Fraktionierung vorausgesagt werden?
- Kann der Hemmstoff CH_3F zur Bestimmung der Isotopenfraktionierung der nicht-acetoklastischen Methanogenese verwendet werden?
- Kann mit den bisherigen Kenntnissen die Quantifizierung der Methanogenesereaktionswege über Isotopenfraktionierung erreicht werden?

II. Material und Methoden

II.1. Sterilisationsverfahren

Die verwendeten Medien, Puffer und Lösungen wurden, soweit nicht anders beschrieben, mit demineralisiertem Wasser angesetzt und durch Autoklavieren (30 min bei 121°C und 2 atm) sterilisiert. Nicht autoklavierbare Bestandteile wurden sterilfiltriert (0,2 µm Porengröße, Nr. FP 30/0,2 CA-5, Schleicher und Schuell GmbH, Dassel) und unter sterilen Bedingungen zugesetzt. Für Kulturen und Inkubationen verwendete Glasmaterialien, Stopfen und Verbindungsstücke wurden vor Benutzung autoklaviert (30 min bei 121°C und 2 atm).

II.2. Chemikalien und Gase

Soweit nicht anders vermerkt, wurden alle Chemikalien in p.A.-Qualität von den Firmen Amersham Pharmacia Biotech (Freiburg), Applied Biosystems (Darmstadt), BioRad Laboratories (München), Biozym Diagnostik (Hessisch Oldendorf), Eppendorf AG (Hamburg), Fermentas (St. Leon-Rot), Fluka (Buchs, Schweiz), Invitrogen (Freiburg), Merck (Darmstadt), MWG (Ebersberg), Promega (Mannheim), Qiagen (Hilden), Roche (Mannheim), Roth (Karlsruhe) und Sigma-Aldrich (Taufkirchen) bezogen.

Von der Firma Messer-Griesheim (Frankfurt) wurden folgende technische Gase eingesetzt. Als Eichgase dienten H_2 in Stickstoff, und ein CH_4-, CO_2-, CO-Gemisch in Stickstoff. Zur Begasung von Proben oder Kulturen wurden N_2, ein H_2/CO_2-Gemisch (80/20 %) und ein $H_2/CO_2/N_2$-Gemisch (5/20/75 %) verwendet. Methylfluorid (CH_3F; 99 %) wurde von ABCR (Karlsruhe) bezogen.

II.3. Mikroorganismen

Methanobacterium bryantii (DSM 863), *Methanospirillum hungatei* (DSM 864), *Methanothermobacter marburgensis* (DSM 2133), *Acetobacterium woodii* (DSM 1030) und *Clostridium papyrosolvens* (DSM 2782) wurden von der Deutschen Sammlung für Mikroorganismen und Zellkulturen bezogen. Die Kokulturen von *Synthrophobacter fumaroxidans* (DSM 10017) mit *Methanospirillum hungatei* (DSM 864) bzw. *Methanobacterium formicicum* (DSM 1535) wurden freundlicherweise von Dr. Caroline

Plugge (Agrotechnology and Food Sciences, Wageningen University) zur Verfügung gestellt.

II.4. Kultivierungsbedingungen

Mit Ausnahme von *M. marburgensis* basierten alle für Rein- und Kokulturen verwendeten Medien auf einem Süßwassermedium mit den unten aufgeführten Stammlösungen. Resazurin diente als Indikator für anoxische Bedingungen. Die Medien unterschieden sich allein in der Endkonzentration der Pufferlösungen (Lösung 1, 2 und 7; siehe Tabelle II-1). Lösungen (1) bis (6) wurden für die unterschiedlichen Kulturen gemischt und auf das Endvolumen abzüglich des Inokulums, der Substratlösung und der Lösungen (7) bis (9) mit Wasser aufgefüllt. Der pH-Wert wurde auf den benötigten Wert eingestellt (Tabelle II-1).

Für Batchversuche wurden die Kulturflaschen mit maximal 50 % Medium befüllt und mit Butylgummistopfen und Aluminium- bzw. Edelstahlkappe verschlossen. Die Gasphase wurde gegen N_2 oder ein H_2/CO_2 (80/20 %)-Gemisch ausgetauscht, was durch einen Wechsel von Vakuum und Begasen für 10 min erfolgte. Danach wiesen die Flaschen einen Druck von 1,6 bar auf. Nach Zugabe der Lösung (7) und (8) wurde das Medium autoklaviert. Die Lösung (9), bestehend aus einem Vitamingemisch (Wolin et al., 1963) und $CaCl_2 \times 2\ H_2O$, sowie die verschiedenen Substrate wurden vor dem Beimpfen steril zugegeben.

Medium für Chemostatversuche wurde in 10 l Glasflaschen mit einem Endvolumen von 10 l angesetzt und mit einem Gummistopfen verschlossen, durch den Schläuche für Belüftung, Entlüftung (mit Watte befüllte Injektionsspritze) und Chemostatzulauf geführt waren. Nach Autoklaviervorgang, bei dem die Entlüftung geöffnet war, wurde das noch ca. 70°C heiße Medium unter Rühren mit sterilfiltriertem N_2 durchgast bis es Raumtemperatur erreicht hatte. Bei noch laufender Durchgasung wurden Lösung (9) und Glucoselösung (Endkonzentration 10 mM) zugegeben. Danach wurde Be- und Entlüftung verschlossen und das Reduktionsmittel (Lösung 8) zugegeben.

Stammlösungen:

(1) Pufferlösung I: 200 mM KH_2PO_4

(2) Pufferlösung II: 200 mM $Na_2HPO_4 \times 2\ H_2O$

(3) Salzlösung (12,5 ml l^{-1}):

448,6 mM NH_4Cl (5,6 mM Endkonzentration)

39,4 mM $MgCl_2 \times 6\ H_2O$ (0,5 mM Endkonzentration)

410,3 mM NaCl (5 mM Endkonzentration)

(4a) saure Spurenelementlösung: 500-fache Stammlösung (2 ml l^{-1}; (Chin et al., 1998))

1,53 ml l^{-1} 35%ige HCl

5,0 mM $FeCl_2 \times 4\ H_2O$

0,5 mM $ZnCl_2$

0,5 mM $MnCl_2 \times 4\ H_2O$

0,1 mM H_3BO_3

0,5 mM $CoCl_2 \times 6H_2O$

0,01mM $CuCl_2 \times 2\ H_2O$

0,1 mM $NiCl_2 \times 6\ H_2O$

(4b) basische Spurenelementlösung: 1000-fache Stammlösung (1 ml l^{-1}; (Stams et al., 1993))

10 mM NaOH

0,1 mM $Na_2SeO_3 \times 5\ H_2O$

0,1 mM $Na_2SeWO_4 \times 2\ H_2O$

0,1 mM $Na_2MoO_4 \times 2\ H_2O$

(5) KCl-Lösung: 2 M (1 ml l^{-1}; 2 mM Endkonzentration)

(6) Resazurinlösung: 2,2mM (1 ml l^{-1}; 2,2 µM Endkonzentration)

(7) Pufferlösung III: 952,4mM $NaHCO_3$

(8) Reduktionsmittel: 0,75 M $Na_2S \times 9\ H_2O$ (2 ml l^{-1}; 1,5 mM Endkonzentration)

(9) Vitamin-Calciumchlorid-Lösung (1 ml l^{-1}):

5,5 g $CaCl_2 \times 2\ H_2O$ / 90 ml H_2O (in Serumflasche mit N_2-Gasphase autoklaviert); dazu wurden 10 ml eines konzentrierten Vitamingemischs (je 20 mg l^{-1} Biotin und Folsäure; 100 mg l^{-1} Vitamin B6; je 50 mg l^{-1} Vitamine B1, B2, B12, Nikotinsäure, D-Ca-Pantothensäure, p-Aminobenzoesäure, Liponsäure) steril filtriert hinzugefügt

Tabelle II-1. Unterschiede in Art und Konzentration der verwendeten Pufferlösungen des für unterschiedliche Rein- und Kokulturen verwendeten Süßwassermediums.

	Substrat	Konzentration [mM]			pH	Gas-phase
		KH_2PO_4	Na_2HPO_4	$NaHCO_3$		
Reinkulturen						
C. papyrosolvens	Glucose Cellobiose Cellulose	14	36	0	7,2	N_2
C. papyrosolvens (Chemostat)	Glucose	7	18	0	7,2	N_2
A. woodii	Glucose	14	36	0	6,8	N_2
A. woodii	H_2/CO_2	3	3	38	6,8	H_2/CO_2
M. hungatei	H_2/CO_2	3	3	38	6,8	H_2/CO_2
M. bryantii	H_2/CO_2	3	3	38	6,8	H_2/CO_2
Kokulturen						
C. papyrosolvens/M. bryantii	Glucose Cellobiose Cellulose	14	36	0	7,2	N_2
C. papyrosolvens/M. hungatei	Glucose Cellobiose Cellulose	14	36	0	7,2	N_2
A. woodii/M. bryantii	Glucose	14	36	0	7,2	N_2
A. woodii/M. hungatei	Glucose	14	36	0	7,2	N_2
S. fumaroxidans/M. hungatei	Propionat	3	3	38	6,8	N_2
S. fumaroxidans/M. formicicum	Propionat	3	3	38	6,8	N_2

M. marburgensis. Kulturen von *M. marburgensis* (Wasserfallen et al., 2000) wurden in bicarbonat- und phosphatgepuffertem Medium (Tabelle II-2) gezogen. Das Medium wurde aerob im später zur Kultivierung (siehe II.4.2) verwendeten 2 l Glasfermenter (New Brunwick, Michigan, USA) angesetzt. Die Anaerobisierung erfolgte durch Begasen mit dem jeweils verwendeten $H_2/CO_2/N_2$-Gasgemisch und 0.1 % H_2S bei 65°C an der Fermenteranlage.

Tabelle II-2. Zusammensetzung des Mediums zur Kultivierung von *M. Marburgensis*

	Komponente	Menge	Endkonzentration
Medium	NH_4Cl	3,18 g	65 mM
	KH_2PO_4	10,2 g	50 mM
	Na_2CO_3	3,82 g	30 mM
	0,2 % (w/v) Resazurin	0,4 ml	3,5 µM
	Spurenelementlösung	1,5 ml	
	H_2O	ad 1,5 l	
Spurenelementlösung	Nitriloessigsäure	30,0 g	160 µM
	H_2O	ad 500 ml	
	mit 10 M NaOH auf pH 6.7 einstellen		
	$MgCl_2 \times 6\ H_2O$	40,0 g	200 µM
	$FeCl_2 \times 4\ H_2O$	10,0 g	50 µM
	$NiCl_2 \times 6\ H_2O$	1,2 g	5 µM
	$CoCl_2 \times 6\ H_2O$	0,2 g	1 µM
	$NaMoO_4 \times 2\ H_2O$	0,2 g	1 µM
	H_2O	ad 1000 ml	

II.4.1 Isotopenfraktionierung der Fermentation

Rein- und Kokulturen von *C. papyrosolvens* in Batch. Zur Untersuchung der Isotopenfraktionierung bei vollständiger Substratumsetzung wurde *C. papyrosolvens* mit Glucose (Merck), Cellobiose (Fluka) und Cellulose (Fluka; Konzentrationen als Anhydroglucose ausgedrückt; M = 162 g mol^{-1}) entweder in Reinkultur oder in Kokultur mit hydrogenotrophen Methanogenen, die Acetat nicht katabolisieren können, gezogen (Tabelle II-3). Jede Kombination von Temperatur, Organismen, Substratart und Substratkonzentration erfolgte in Triplikaten. Die Medien wurden mit exponentiell wachsenden Vorkulturen angeimpft. Nach vollständiger Umsetzung der Saccharide (bestätigt mit enzymatischem Glucosetest (Glucose), HPLC-Analyse (Cellobiose) bzw. Massenbilanz und Wachstumsverlauf (Cellulose)) wurden Gas- und Flüssigproben zur Bestimmung der Konzentration und der Kohlenstoffisotopensignatur entnommen.

Zur Bestimmung des Fraktionierungsverhaltens während der Umsetzung wurde *C. papyrosolvens* in Rein- und Kokulturen auf den o.g. Substraten gezogen, aber in regelmäßigen Abständen im Wachstumsverlauf beprobt (Tabelle II-4).

Tabelle II-3. Kultivierungsbedingungen von *C. papyrosolvens* in Experimenten zur Bestimmung der Isotopenfraktionierung nach vollständigem Umsatz des Substrats.

Mikroorganismen	Saccharid	T [°C]	Saccharid Konzentration [mM]	Kultur-volumen [ml]
Reinkulturen				
C. papyrosolvens	Glucose ($\delta^{13}C$ = -10,67)	15	2,22	50
			4,44	50
			8,88	50
		30	2,22	50
			4,44	50
			8,88	50
	Cellobiose ($\delta^{13}C$ = -25,11)	30	0,59	50
			1,17	50
			2,34	50
	Cellulose ($\delta^{13}C$ = -25,23)	30	2,81	500
Kokulturen				
C. papyrosolvens/ M. hungatei	Glucose ($\delta^{13}C$ = -10,67)	30	2,22	50
			4,44	50
			8,88	50
	Cellobiose ($\delta^{13}C$ = -25,11)	30	1,17	50
			2,34	50
			4,67	50
C. papyrosolvens/ M. bryantii	Glucose ($\delta^{13}C$ = -10,67)	30	2,22	50
			4,44	50
			8,88	50
	Cellobiose ($\delta^{13}C$ = -25,11)	30	1,17	50
			2,34	50
			4,67	50

Tabelle II-4. Kultivierungsbedingungen von *C. papyrosolvens* in Experimenten zur Bestimmung der Isotopenfraktionierung während des Substratabbaus.

Mikroorganismen	Saccharid	T [°C]	Saccharid Konzentration [mM]	Kultur-volumen [ml]
Reinkulturen				
C. papyrosolvens	Glucose ($\delta^{13}C$ = -10,67)	15	2,78	500
	Cellobiose ($\delta^{13}C$ = -25,11)	30	1,46	500
	Cellulose ($\delta^{13}C$ = -25,23)	30	2,81	500
Kokulturen				
C. papyrosolvens/ M. bryantii	Cellulose ($\delta^{13}C$ = -25,23)	30	22,47	250

Reinkulturen von *C. papyrosolvens* im Chemostat. *C. papyrosolvens* wurde als kontinuierliche Kultur in 600 ml Glasfermentern mit Temperiermantel (Ochs, Bovenden-Lenglern) unter Glucoselimitierung (10 mM) gezogen (Abbildung II-1). Der mit temperaturgeregeltem Wasserbad (Julabo, Seelbach) temperierte Fermenter (30°C) wurde aus einem 10 l Mediumvorratsgefäß über eine peristaltische Pumpe mit Medium versorgt. Der pH-Wert im Fermenter wurde von einem pH-/mV-Regler (Mostec AG, Liestal, Schweiz), der mit einer autoklavierbaren Elektrode (Mettler-Toledo GmbH, Gießen) verbunden war, kontrolliert und durch Titration mit 1 M NaOH stabil auf pH 7.2 gehalten. Über einen Ablauf wurde die überschüssige Bakteriensuspension in ein 10 l Abfallgefäß abgeleitet. Alle verwendeten Schläuche, Verbindungen, Dichtungen, Elektroden und Glasgefäße wurden vor Benutzung autoklaviert. Der mit Medium unter N_2-Atmosphäre autoklavierte Fermenter wurde, nachdem die Einzelteile unter sterilen Bedingungen verbunden worden waren, unter Rühren (200 U min^{-1}) mit N_2 gespült und auf 30°C temperiert. Anschließend wurde der Fermenter durch sterile Zugabe der Na_2S-Lösung anaerobisiert. Nach Zugabe der Vitamin-$CaCl_2$- und Glucoselösung wurde der Fermenter

mit einer exponentiell wachsenden Vorkultur angeimpft und zunächst im Batch-Modus betrieben. Nach ca. 24 Stunden war das Wachstum der Kultur durch deutliche Trübung erkennbar und es wurde mit der kontinuierlichen Zugabe von Medium begonnen. Für die Versuche wurden zwei Chemostatanlagen verwendet. In einem wurde die Gasphase mit N_2 gespült (Kulturvolumen 290 ml), so dass die gebildeten Gase stetig ausverdünnt wurden. Der N_2-Gasfluss wurde so eingestellt, dass der Wasserstoffpartialdruck 1 kPa nicht überstieg. Im zweiten Chemostat wurde die Gasphase nicht gespült; somit reicherten sich die gasförmigen Fermentationsprodukte in der Gasphase an (Kulturvolumen 270 ml). *C. papyrosolvens* wurde unter beiden Bedingungen bei Verdünnungsraten von 0,02 bis 0,25 h^{-1} kultiviert. Die Probenahme erfolgte, nachdem das Fließgleichgewicht mindestens für die Dauer des Durchsatzes des 10-fachen Kulturvolumens beibehalten worden war. Dabei wurden Proben zur Bestimmung der Konzentration und der Kohlenstoffisotopensignatur in Gasen und gelösten Verbindungen entnommen. Weiterhin wurden OD_{600} und Kohlenstoffisotopenverteilung in der Biomasse bestimmt.

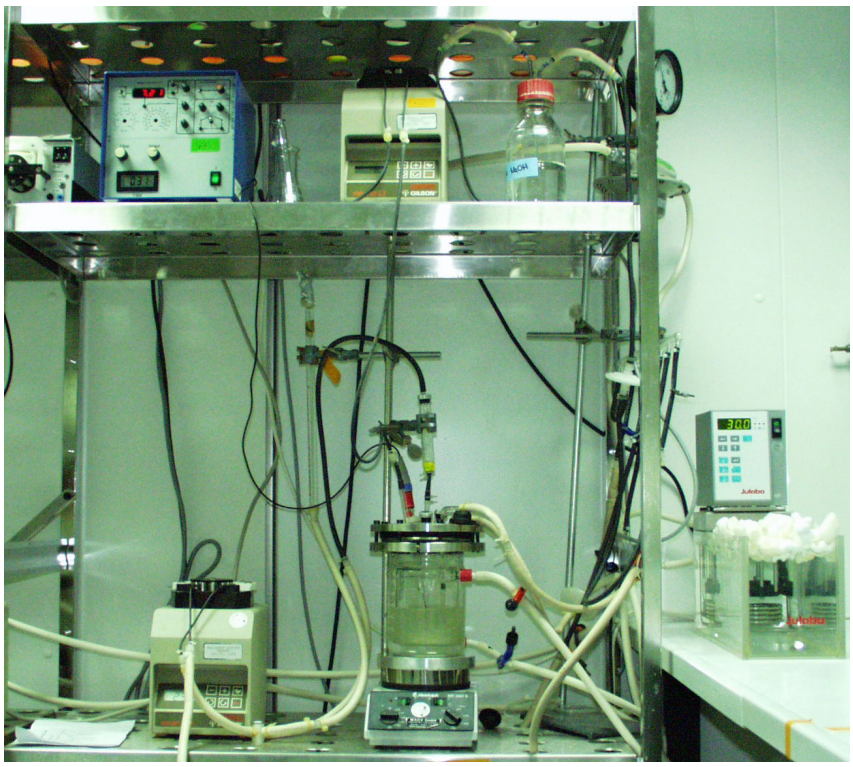

Abbildung II-1. Chemostatanlage. In der Mitte der unteren Bildhälfte ist der Fermenter zu sehen. Links davon die das Medium zuführende peristaltische Pumpe. Im oberen Teil befindet sich der pH-Regler, der die peristaltische Pumpe zur Zufuhr von NaOH steuert.

II.4.2 Isotopenfraktionierung der Methanogenese aus H_2/CO_2

M. marburgensis. *M. marburgensis* wurde in 2 l Glasfermentern bei 65°C unter Rühren (1000 U min^{-1}) gezogen. $H_2/CO_2/N_2$-Gasgemische dienten als Energie- und Kohlenstoffquelle, 0,1 % H_2S-Gas als Reduktionsmittel und Schwefelquelle. 1,5 l Medium wurde mit 1 % Vorkultur angeimpft. Unter H_2-limitierten Bedingungen (5/20/75 % $H_2/CO_2/N_2$-Gemisch) betrug die Gasflussrate 800 ml min^{-1} während des gesamten Versuchs. Unter nicht limitierten Bedingungen (80/20 % H_2/CO_2-Gemisch) wurde die Gasflussrate während des Versuchs auf bis zu 7000 ml min^{-1} erhöht, um den CO_2-Verbrauch bei < 3% zu halten. Dadurch wird sichergestellt, dass die Isotopensignatur des CO_2-Pools stabil bleibt und die Isotopenfraktionierung kann mit Gleichung (1) berechnet werden. In regelmäßigen Abständen wurden Gasproben zur Bestimmung der Konzentration und der Kohlenstoffisotopensignatur entnommen. Flüssigproben wurden zur OD_{600}-Bestimmung entnommen. Vor Versuchsbeginn wurde $\delta^{13}C$ des verwendeten CO_2 bestimmt.

Kokulturen von *C. papyrosolvens* und *A. woodii* in Batch. Fermentierende Bakterien und methanogenen Archaeen wurden in gleicher Zellzahl in das oben beschriebene Süßwassermedium überimpft. Bicarbonat-Konzentrationen zwischen 0,16 und 2,8 mM ergaben sich in Abhängigkeit der zugeimpften Menge an methanogener bicarbonatgepufferter Reinkultur. Folgende Kombinationen von Mikroorgansimen und Substraten wurden jeweils mindestens in Duplikat kultiviert:
C. papyrosolvens/*M. bryantii* (4,44 mM Glucose); *C. papyrosolvens*/*M. bryantii* (2,34 mM Cellobiose); *C. papyrosolvens*/*M. bryantii* (4,94 mM Cellulose); *A. woodii*/*M. bryantii* (4,44 mM Glucose); *C. papyrosolvens*/*M. hungatei* (4,44 mM Glucose); *C. papyrosolvens*/*M. hungatei* (2,34 mM Cellobiose); *C. papyrosolvens*/*M. hungatei* (4,94 mM Cellulose); *A. woodii*/*M. hungatei* (4,44 mM Glucose). Alle Kulturen wurden in 500 ml Glasflaschen (Müller und Krempel, Bülach, Schweiz) mit 250 ml Kulturvolumen gezogen. In regelmäßigen Abständen wurden Gasproben zur Bestimmung der Konzentration und der Kohlenstoffisotopensignatur entnommen.

Methanogene Kokulturen von *S. fumaroxidans.* Kokulturen von *S. fumaroxidans* mit *M. formicium* bzw. *M. hungatei* wurden bei 37°C mit 30 mM Propionat als Kohlenstoff- und Energiequelle gezogen. Beide Kokulturen wurden 10%ig von

Vorkulturen der jeweiligen Kokultur angeimpft und in 1000 ml Glasflaschen (Müller und Krempel, Bülach, Schweiz) mit 500 ml Kulturvolumen in Triplikaten kultiviert. In regelmäßigen Abständen wurden Gasproben zur Bestimmung der Konzentration und der Kohlenstoffisotopensignatur entnommen.

II.5. Inkubationen von Umweltproben

II.5.1 Isotopenfraktionierung der Methanogenese aus H_2/CO_2

II.5.1.1 Moorboden

Im August 2003 wurden die Moorbodenproben von Dr. Pierre Galand im Lakkasuo Moorkomplex in Zentralfinnland (61°48'N, 24°19'E) genommen. Die Proben wurden aus dem anoxischen Bereich eines mesotrophen Niedermoores, eines oligotrophen Niedermoores und eines ombrotrophen Hochmoores entnommen. Nach dem Transport zum Max-Planck-Institut in Marburg wurden die Proben von Dr. Pierre Galand unter anoxischen Bedingungen (N_2-Atmosphäre) bei 10°C inkubiert. Die acetoklastische Methanogenese wurde mit 2 kPa CH_3F gehemmt. Es wurden regelmäßig Gasproben zur Bestimmung der Konzentration und der Kohlenstoffisotopensignatur genommen.

II.5.1.2 Reisfeldboden

Reisfeldboden wurde 1999 aus Reisfeldern des Italian Rice Research Institute in der Nähe von Vercelli in der Po-Ebene, Italien, aus dem Pflughorizont entnommen. Charakteristika und Bewirtschaftung dieses Bodens wurden von Schütz *et al.* (1989a; 1989b) beschrieben. Das Bodenmaterial wurde luftgetrocknet und bei Raumtemperatur in Polyethylenwannen gelagert. Der getrocknete Reisfeldboden wurde grob von Stroh- und Wurzelresten befreit, mit Hilfe eines „Backenbrechers" (Retsch, Dietz-Motoren GmbH & Co. KG, Dettingen und Teck) zerkleinert und auf eine Aggregatgröße ≤ 2 mm gesiebt.

Für die Inkubation wurden 5 g Boden, 20 mg fein zerkleinertes Reisstroh (A11 Basic Analytical Mill, IKA Werke, Staufen) und 5 ml deionisiertes Wasser in ein 26 ml Glassröhrchen gegeben und mit einem Butylstopfen verschlossen. Danach wurden die Inkubationsgefäße mindestens 10 min im Wechsel mit einer Membranpumpe evakuiert und mit N_2 begast und Überdruck von 0,6 bar in den Röhrchen eingestellt. Zur Hemmung der acetoklastischen Methanogenese wurde Methylfluorid mit einer Konzentration von 1 kPa zugegeben. Die Inkubation erfolgte bei 30°C im Dunkeln. Zu jedem Probenahmezeitpunkt

wurden Gaskonzentrationen in drei Röhrchen bestimmt. Danach wurden diese zur Flüssigprobenahme geöffnet.

II.5.2 Archaeelle Lebensgemeinschaft und Geochemie im Reiswurzel-Modellsystem

Für die Reiswurzelinkubationen wurden Reispflanzen (*Oryza sativa*) gezogen. Der gesiebte unter II.5.1.2 beschriebene Boden wurde in einer lichtundurchlässigen Plastikwanne (35 × 27 × 22,5 cm) mit Leitungswasser aufgeschlämmt und geflutet, so dass das Wasser die Bodenoberfläche ca. 5 cm hoch überdeckte. Der geflutete Boden wurde eine Woche im Gewächshaus (Lufttemperatur ca. 25°C; 60 % Luftfeuchtigkeit, je 12 Stunden Licht-/Dunkelphase bei 10-15 kLux Lichtintensität) vorinkubiert. Parallel dazu wurden Reissamen (*O. sativa*, Varietät Roma, Typ Japonica) in eine mit feuchten Papiertüchern ausgelegte Kristallisierschale gelegt, mit durchlöchertem Parafilm abgedeckt und bis zur Keimung an einem lichtgeschützten Ort bei 25°C aufbewahrt. Die Keimlinge wurden im Gewächshaus bis zu einer Höhe von 6 cm herangezogen und anschließend im Abstand von 5 cm in den gefluteten Reisfeldboden eingepflanzt. Der bepflanzte Mikrokosmos wurde regelmäßig mit Leitungswasser gegossen, so dass die Bodenoberfläche stets mit Wasser bedeckt war. Das Auskeimen des Saatgutes wurde als Tag 0 definiert. 90 Tage nach Keimungsbeginn wurden die Reispflanzen aus dem Mikrokosmos entfernt.

Die Reiswurzeln wurden zunächst vorsichtig mit Leitungswasser abgespült, anschließend von der Reispflanze getrennt und in mehreren Waschschritten von anhaftenden Bodenpartikeln gereinigt. Hierfür wurden die Reiswurzeln unter N_2-Begasung in autoklaviertem, deionisiertem Wasser geschwenkt. Dieser Vorgang wurde so lange mit frischem Wasser wiederholt, bis sich keine Bodenpartikel mehr ablösten. Die Reiswurzeln wurden dann in ca. 2 cm lange Stücke geschnitten und zu je 30 g (Feuchtgewicht) in vorbereitete Flaschen (1000 ml; Müller and Krempel, Bülach, Schweiz) gegeben und mit Naturgummistopfen verschlossen. Die Flaschen waren vorher mit jeweils 50 g Marmorgranulat (Merck) und 500 ml anoxischem deionisiertem Wasser befüllt und unter N_2-Atmosphäre autoklaviert worden. Die so angesetzten Inkubationsgefäße wurden mindestens 10 min im Wechsel mit einer Membranpumpe evakuiert und mit N_2 begast. Für die Inkubation wurde ein Überdruck von 0,6 bar in den Glasflaschen eingestellt. Um das Eindringen von Licht zu verhindern, wurden die Gefäße mit Aluminiumfolie umkleidet

und dann bei 25°C in Ruhe inkubiert. In einem Versuchsansatz wurde die acetoklastische Methanogenese mit 1,3 kPa CH_3F gehemmt, ein zweiter Ansatz diente als Kontrolle. Beide Ansätze wurden in drei Parallelen durchgeführt. Während der Inkubation wurden in regelmäßigen Abständen Gas- und Flüssigkeitsproben zur quantitativen, C-Isotopen- und molekularbiologischen Analyse entnommen.

II.6. Chemische Analysen

II.6.1 Quantitative chromatographische Analysen

Vor der Gasanalyse wurden die Kulturen bzw. Inkubationen kurz von Hand geschüttelt, um ein Gleichgewicht zwischen Medium und Gasphase herzustellen. Die Gasproben wurden mit einer 0,25 ml Pressure-Lock-Spritze (VICI, Baton Rouge, LA, USA) unmittelbar vor der Analyse steril durch das Septum entnommen. Das Probenvolumen betrug 0,1 bis 0,25 ml.

II.6.1.1 Analyse von Wasserstoff

Zur Bestimmung niedriger Wasserstoffkonzentrationen (<10 Pa) wurde ein Gaschromatograph GC-8A (Shimadzu, Kyoto, Japan) mit Reduktionsgasdetektor (RGD2, Trace Analytical, Menlo Park, CA, USA) verwendet.

Injektor:	Betriebstemperatur: 100°C
Trägergas:	Synthetische Luft
Säule:	Edelstahlsäule, 1,4 m Länge, 1/2 Zoll Durchmesser
	Trägermaterial: Molsieb 5Å, 80-100 mesh
	Betriebstemperatur: 85°C
Detektor:	HgO-Konversions-Detektor
	Betriebstemperatur: 280°C
Nachweisgrenze:	0,2 ppmv H_2
Auswertung:	Integrator C-R A6 (Shimadzu, Kyoto, Japan)
Eichgas:	H_2 in Stickstoff (50 ppmv)

Wasserstoffkonzentrationen >10 Pa wurden mit einem Gaschromatographen GC-8A (Shimadzu) mit Wärmeleitfähigskeitsdetektor (WLD) bestimmt.

Injektor:	Betriebstemperatur: 120°C
Trägergas:	Stickstoff
Säule:	Edelstahlsäule, 2 m Länge, 1/8 Zoll Durchmesser
	Trägermaterial: Poropack QS 80/100 mesh
	Betriebstemperatur: 110°C
Detektor:	Wärmeleitfähigkeitsdetektor (WLD)
	Betriebstemperatur: 120°C
Nachweisgrenze:	20 ppmv H_2
Auswertung:	Softwareprogramm Peak Simple (SRI Instruments, Torrence, CA, USA)
Eichgas:	H_2 in Stickstoff (1000 ppmv).

II.6.1.2 Analyse von Methan

Die Bestimmung von Methan und Kohlendioxid erfolgte mit einem Gaschromatographen GC-8A (Shimadzu) mit Flammenionisationsdetektor (FID).

Injektor:	Betriebstemperatur: 120°C
Trägergas:	Wasserstoff 5,0
Säule:	Edelstahlsäule, 2 m Länge, 1/8 Zoll Durchmesser
	Trägermaterial: Poropack QS 50/100 mesh
	Betriebstemperatur: 40°C
Methanisator:	Zur Bestimmung von oxidierten Gasen (z.B. CO_2 wird zu CH_4 reduziert); Eigenbau
	Säule: NiCr-Ni-Katalysator (Chrompack, Middelburg, Niederlande), Edelstahlsäule, Länge 20 cm, Innendurchmesser: 1/8 Zoll
	Betriebstemperatur: 350°C
Detektor:	Flammenionisationsdetektor (FID)
	Brenngas: Wasserstoff und FID-Gas
	Quenchgas: Stickstoff 5,0
	Betriebstemperatur: 120°C

Nachweisgrenze:	1 ppmv CH_4
Auswertung:	Integrator C-R A6 (Shimadzu)
Eichgas:	Gemisch aus CH_4, CO_2 und CO in Stickstoff (1000 ppmv)

II.6.1.3 Analyse organischer Säuren und Alkohole

Die Konzentration der organischen Säuren und Alkohole wurde mittels HPLC-(*high performance liquid chromatography*) Analyse bestimmt. Dafür wurden die Proben filtriert (REZIST 13/0,2 PTFE, Schleicher und Schuell, Dassel) und bis zur Analyse bei -20°C gelagert.

Probenaufgeber:	S5200 (Schambeck SFD, Bad Honnef)
HPLC-Anlage:	Pumpe S1000, Säulenofen S4110 (Sykam, Gilching),
Trägermaterial:	Sulfuriertes Divinyl-Benzol-Styren (Aminex HPX-87-H, BioRad)
Fließmittel:	1 mM Schwefelsäure, Flussrate: 0,5 ml min^{-1}
Säule:	Edelstahlsäule, 30 cm Länge, 7,8 mm Durchmesser
Ofentemperatur:	65°C
Detektor:	Refraction Index (RI)-Detektor RI2000 (Schambeck SFD, Bad Honnef) , Betriebstemperatur: 40°C UV-Detektor: S3200 (Schambeck SFD, Bad Honnef), Wellenlänge: 208 nm
Nachweisgrenze:	≈ 5 µM (substanzabhängig)
Auswertung:	Programm Peak Simple (SRI-Instruments)
Eichstandard:	Mischstandard aus Lactat, Formiat, Acetat, Propionat, Butyrat, Ethanol, Valerat und Caproat (je 1 mM)

II.6.2 Stabile Kohlenstoff-Isotopenverhältnismessung

Stabile Isotopenhäufigkeiten werden in dieser Arbeit in der üblichen δ-Notierung dargestellt. Hierbei wird der relative Unterschied des Isotopenverhältnisses ($^{13}C/^{12}C$) der Probe zu einem internationalen Standard in ‰ ausgedrückt. Der Standard für Kohlenstoff-Isotopenverhältnismessungen ist gemäß internationaler Übereinkunft der Vienna Pee Dee Belemnite (V-PDB) mit einem $R_{standard} = 11180.2 \times 10^{-6} \pm 2.8 \times 10^{-6}$ (siehe auch Gleichung 2)

II.6.2.1 CH_4 und CO_2

Die stabile Isotopensignatur von CH_4 und CO_2 wurde mit einem Gaschromatographen mit Verbrennungs-Isotopenverhältnis-Massenspektrometer (GC-C-IRMS, Thermo Electron, Bremen) bestimmt. Das Prinzip dieser Methode wurde von Brand (1996) beschrieben.

GC:	Hewlett Packard 6890 (Waldbronn)
Injektor:	Splitverhältnis 1:10; Betriebstemperatur: 150°C
Trägergas:	Helium 5,0; Flussrate 2,6 ml min^{-1}
Säule:	Pora PLOT Q, 27,5 m Länge; 0,32 mm Durchmesser; Filmdicke 10 µm (Crompack, Frankfurt)
Ofentemperatur:	30°C
GC/C-Interface:	Standard GC Combustion Interface III (Thermo Electron, Bremen) Oxidations-Reaktor bei 940°C Reduktions-Reaktor bei 650°C
Detektor:	IRMS: Finnigan MAT delta plus (Thermo Electron)
Auswertung:	ISODAT™ NT 2.0 (Thermo Electron)
Referenzgas:	CO_2 4,8 (Reinheitsgrad 99.998 %; Messer-Griessheim, Düsseldorf) Das Referenzgas wurde mit dem Arbeitsstandard Methylstearat (Merck) kalibriert. Methylstearat wurde am Max-Planck-Institut für Biogeochemie (Jena) gegen die internationalen Standardmaterialien NBS22 und USGS24 geeicht (Dank an Dr. W.A. Brand)

Die Präzision war bei wiederholter Injektion von 1,3 nmol CH_4 ± 0,2 ‰.

II.6.2.2 Acetat (GC-C-IRMS)

Vor der Bestimmung des $\delta^{13}C$ beider Kohlenstoffatome von Acetat am GC-C-IRMS wurden die wässerigen Proben eingetrocknet (DNA-SpeedVac, DNA 110, Savant Instruments, Farmingdale, NY, USA) und danach in 20 bis 50 µl 0,1 M Ameisensäure in Propanol gelöst.

Das in Propanol gelöste Acetat wurde am unter II.6.2.1 beschriebenen GC-C-IRMS analysiert. Davon abweichende Analysebedingungen sind wie folgt:

Probenaufgeber:	Combi Pal (CTC analysis, Zwingen, Schweiz)
Probenvolumen:	1 µl
Injektor:	Splitlos (30s), Spülfluss 40 ml min^{-1}; Betriebstemperatur: 240°C
Säule:	FFAP; 30 m Länge; 0,32 mm Durchmesser; 0,25 µm Filmdicke (J&W Scientific, Fulsom, CA, USA)
Ofentemperatur:	80°C für 4 min, danach erhöht mit einer Rate von 20°C min^{-1} auf 240°C

II.6.2.3 Methylgruppe von Acetat (*off line*-Pyrolyse und GC-C-IRMS)

Durch eine *off line*-Pyrolyse (Prinzip nach Blair et al., 1985) im Alkalischen wurde die Methylgruppe von Acetat zu Methan umgesetzt und die Isotopenverteilung des entstandenen Methan bestimmt. Flüssigproben aus Umweltinkubationen oder Kulturen wurden gefiltert (REZIST 13/0,2 PTFE, Schleicher und Schuell), mit NaOH auf pH > 10 eingestellt und eingetrocknet (DNA-SpeedVac, DNA 110, Savant Instruments). Die in 45 µl deionisiertem Wasser wieder gelöste Probe wurde mit einem manuellen Injektor (50 µl Probenschleife; S5110, Sykam) auf das unter II.6.1.3 beschriebene HPLC-System aufgebeben. Die Acetat-Fraktion wurde in einem 1,5 ml Reaktionsgefäß, in dem 20 µl 5 N NaOH vorgelegt waren, gesammelt und eingetrocknet. Die Probe wurde wieder in 45 µl Wasser gelöst, mit NaOH (100-fache Menge von Acetat) versetzt und in ein Duran-Glasröhrchen (Außendurchmesser 6 mm) überführt. Hiernach wurde das Reaktionsgemisch unter Vakuum (Membranpumpe) im Wasserbad (60°C) getrocknet. Für die Pyrolyse wurde das Röhrchen verschlossen, evakuiert und für 30 min bei 400°C in einer Heizspule belassen.

Während dieser Zeit wurde die Methylgruppe von Acetat vollständig zu Methan umgesetzt (bestätigt durch Massenbilanzen):

$$Na^*CH_3COO + NaOH \rightarrow {}^*CH_4 + Na_2CO_3 \quad \text{(II-1)}$$

Das gebildete Methan wurde wie unter II.6.2.1 beschrieben gemessen. Da keine internationalen Standards verfügbar sind, wurden zwei in ihrer intramolekularen Isotopie unterschiedlichen Acetatgebinde als Standards verwendet und mit anderen Labors interkalibriert (Dank an Dr. Roland Werner und Dr. Stan C. Tyler).

II.6.2.4 Biomasse (EA-IRMS)

Die Bakteriensuspension wurde bei 4°C für 15 min mit 26000 × g zentrifugiert (RC 5B Plus, Rotor SS34; Sorvall, Langenselbold). Der Überstand wurde abgenommen, die sedimentierten Zellen in 50 mM Phosphatpuffer (pH 7,2) resuspendiert und unter oben genannten Bedingungen zentrifugiert (dieser Schritt wurde zweimal durchgeführt). Der Überstand wurde abgenommen und die Zellen in einem Ofen bei 105°C getrocknet. Die getrocknete Biomasse wurde in Zinnkapseln (IVA, Meerbusch) eingewogen (0.2 bis 1.2 mg).

Die Analyse wurde am Max-Planck-Institut für Biogeochemie in Jena durchgeführt (Dank an Dr. Roland Werner). Das Elementar-Analysator (EA)–IRMS-System war folgendes:

Probenaufgeber:	AS 128 (CE Instruments, Rodano, Italy); Spülfluss 40 ml min^{-1} O_2
Elementaranalysator:	NA 1110 CN (CE Instruments)
Trägergas:	Helium; Flussrate 80 ml min^{-1}
Detektor:	IRMS: Finnigan MAT delta plus XL (Thermo Electron)
ConFlo III:	Eigenbau (Werner et al., 1999)
Referenzmaterialien:	Acetanilid und Coffein. Standardisierung und Berechnung von $\delta^{13}C$-Werten wurde analog wie beschrieben bei Werner und Brand (2001) durchgeführt.

II.6.2.5 Lactat, Formiat, Acetat, Propionat, Ethanol (HPLC-IRMS)

Die Kohlenstoffverbindungen der wässrigen Lösungen wurden über HPLC aufgetrennt und dann mit Natriumperoxodisulfat (0,42 M; Fluka) und Phosphorsäure (1,35 M; Merck) bei 99.9°C vollständig zu CO_2 oxidiert. CO_2 wurde über eine Membran in einen Heliumstrom überführt und zum IRMS weitergeleitet. Das Prinzip dieser Methode wurde von Krummen et al. (2004) beschrieben.

Probenaufgeber:	HTC Pal (CTC Analysis, Zwingen, Schweiz)
HPLC-Anlage:	Pumpe Spectra System P1000 (Thermo Finnigan, Jan Jose, CA, USA) , Säulenofen Mistral (Spark, Emmen, Niederlande),
Trägermaterial:	Sulfuriertes Divinyl-Benzol-Styren (Aminex HPX-87-H, Biorad)
Fließmittel:	1 mM Schwefelsäure, Flussrate: 0,3 ml min^{-1}
Säule:	Edelstahlsäule, 30 cm Länge, 7,8 mm Durchmesser
Oxidationsreagentien:	Natriumperoxodisulfatlösung und Phosphorsäure; Flussrate jeweils 50 µl min^{-1}
Ofentemperatur:	35°C
Interface:	Finnigan LC IsoLink (Thermo Electron, Bremen)
Detektor:	IRMS: Finnigan MAT delta plus advantage (Thermo Electron, Bremen)
Auswertung:	ISODAT™ NT 2.0 (Thermo Electron)
Referenzgas:	CO_2 4,8 (Reinheitsgrad 99.998 %; Messer-Griessheim, Düsseldorf) Das Referenzgas wurde mit dem Arbeitsstandard Methylstearat (Merck, Frankfurt) kalibriert. Methylstearat wurde am Max-Planck-Institut für Biogeochemie (Jena) gegen die internationalen Standardmaterialien NBS22 und USGS24 geeicht (Dank an Dr. W.A. Brand)

II.6.3 Bestimmung des pH-Wertes und der Optischen Dichte (OD_{600})

Für die Bestimmung des pH-Wertes wurde ein digitales pH-Meter (Microprozessor pH Meter 539, Wissenschaftlich-Technische Werkstätten GmbH, Weilheim) mit einer pH-Sonde (InLab 427, pH 2 bis 11, Mettler Toledo, Gießen) verwendet.

Die optische Dichte von mikrobiellen Suspensionen wurde über das Streulicht bei einer Wellenlänge von 600 nm in einem Biophotometer (Eppendorf, Hamburg) bestimmt.

II.6.4 Enzymatische Bestimmung der Glucosekonzentration

Die Glucosekonzentration wurde in Gegenwart von Glucoseoxidase (GOD) und Peroxidase (POD) über gebildetes oxidiertes 2,2'-Azino-di-(3-ethylbenzthiazolinsufonat) (ABTS) bestimmt:

$$\text{Glucose} + O_2 + H_2O \xrightarrow{GOD} \text{Gluconat} + H_2O_2 \qquad \text{(II-2)}$$

$$ABTS_{red} + H_2O_2 \xrightarrow{POD} ABTS_{ox} + 2\ H_2O \qquad \text{(II-3)}$$

Zur Messung wurden 0,9 ml Glucosereagenz (Tabelle II-5) und 0,1 ml Probe bzw. Standard gemischt und 15 min bei 37°C im Ofen inkubiert. Im Anschluss wurde die Absorption am Spektrophotometer (U1100, Hitachi, Tokyo, Japan) bei λ = 436 nm gemessen. Proben wurden zuvor auf 0-40 µM verdünnt. Die unbekannte Konzentration in den Proben wurde über ein Eichreihe (0-40 µM) bestimmt.

Tabelle II-5. Zusammensetzung der verwendeten Glucosereagenz.

Komponente	**Menge**	**Endkonzentration**
$Na_2HPO_4 \times 2\ H_2O$	700 mg	79 mM
$NaH_2PO_4 \times H_2O$	360 mg	52 mM
POD (aus Meerrettich; 200 U mg^{-1}; Sigma-Aldrich)	2 mg	8 U ml^{-1}
GOD (aus *Aspergillus niger*, 200 U mg^{-1}; Fluka)	4 mg	16 U ml^{-1}
ABTS (Sigma-Aldrich)	25 mg	0,91 mM
H_2O	ad 50 ml	

II.6.5 Berechnungen

II.6.5.1 Stoffmenge von Gasen

Die gemessenen Konzentrationen (ppmv) wurden in Stoffmenge (mmol) umgerechnet. Dafür wurde die Zustandsgleichung idealer Gase nach der Stoffmenge *n* aufgelöst:

$$n = \frac{p \times V}{R \times T} \qquad \text{(II-4)}$$

n: Stoffmenge [mol]

p: Partialdruck des gemessenen Gases in [bar] (1 ppmv = 10^{-6} bar)

V: Volumen des Gasraumes im Reaktionsgefäß [l]

R: allgemeine Gaskonstante (0,083144 [l bar K^{-1} mol^{-1}])

II.6.5.2 Stoffmenge von anorganischem Kohlenstoff

CO_2 verteilt sich über die anorganischen Kohlenstoffspezies gasförmiges CO_2 ($CO_{2(g)}$), gelöstes CO_2 ($CO_{2(d)}$; beinhaltet gelöstes CO_2 und Kohlensäure), HCO_3^- und CO_3^-. Zur Bestimmung der Gesamtmenge an anorganischem Kohlenstoff (TIC; Gleichung (II-8)) wurden ausgehend vom $CO_{2(g)}$ die Konzentrationen der einzelnen Spezies und dann ihre Stoffmenge bestimmt (Stumm und Morgan, 1995):

$CO_{2(g)} \leftrightarrows CO_{2(d)}$ $\quad K_0 = 10^{-1,47}$ (II-5)

$CO_{2(d)} + H_2O \leftrightarrows H^+ + HCO_3^-$ $\quad K_1 = 10^{-6,35}$ (II-6)

$HCO_3^- \leftrightarrows H^+ + CO_3^{2-}$ $\quad K_2 = 10^{-10,33}$ (II-7)

$$n(TIC) = n(CO_{2(g)}) + n(CO_{2(d)}) + n(HCO_3^-) + n(CO_3^{2-}) \qquad \text{(II-8)}$$

II.6.5.3 Isotopenfraktionierung

Der Fraktionierungsfaktor $\alpha_{A/B}$ einer Reaktion A → B wurde nach Hayes (1993) definiert (analog zu Gleichung 1, aber unter Verwendung der Deltanotation an Stelle von Isotopenverhältnissen):

$$\alpha_{A/B} = (\delta_A + 1000)/(\delta_B + 1000) \quad \text{(II-9)}$$

dabei ist δ der δ^{13}C-Wert vom Reaktanden A bzw. Produkt B. Isotopenfraktionierung wird häufig auch als ε angegeben ($\varepsilon \equiv 10^3 (1 - \alpha)$).

Unter Annahme eines unendlich großen Substratreservoirs oder eines Fließgleichgewichts kann der Fraktionierungsfaktor wie in Gleichung II-9 bestimmt werden. In geschlossenen Systemen (vgl. Abbildung I-1) kann der Fraktionierungsfaktor ε mit folgenden Näherungsgleichungen nach Mariotti *et al.* (1981), die auf einer Rayleigh Destillation basieren, aus dem Anteil des verbrauchten Reaktanden (*f*) und der Isotopensignatur des Produkts (Gleichung II-10) bzw. Reaktanden (Gleichung II-11) bestimmt werden.

$$\delta_p = \delta_{ri} - \varepsilon(1\text{-}f)[\ln(1\text{-}f)]/f \quad \text{(II-10)}$$

$$\delta_r = \delta_{ri} + \varepsilon[\ln(1\text{-}f)] \quad \text{(II-11)}$$

mit δ_{ri} = δ^{13}C-Wert des Reaktanden zu Beginn ($f = 0$); δ_p und δ_r sind die δ^{13}C-Werte des Produkts bzw. des Reaktanden zu dem Zeitpunkt, an dem *f* bestimmt wurde. Graphisch kann ε durch lineare Regression von δ_p gegen $(1\text{-}f)[\ln(1\text{-}f)]/f$ oder δ_r gegen ln(1-f) als Steigung bestimmt werden.

Die Isotopenfraktionierung an Verzweigungspunkten der Fermentation wurde auf der Massenbilanz basierend über den Unterschied der Isotopensignatur der zwei Produkte ermittelt. Die folgenden Gleichungen, welche für die Kohlenstoffisotopenfraktionierung gültige Vereinfachungen enthalten, können auf Gleichgewichts- und kinetische Isotopeneffekte angewendet werden (Hayes, 2001; Hayes, 2002):

$$\delta_p = \delta_r + (1 - f_p)\,\Omega_d \quad \text{(II–12)}$$

$$\delta_q = \delta_r - f_p\,\Omega_d \quad \text{(II–13)}$$

r: Reaktand

p, q: Produkte der Reaktion am Verzweigungspunkt

f_p: relative Ausbeute des Produkts p

d: Name des Verzweigungspunktes (z.B. Pyruvat)

In einem Diagramm, in dem die Isotopensignaturen von p und q in Abhängigkeit von f_p dargestellt sind, entsprechen gerade Linien dem isotopischen Kohlenstoffffluss zu den Produkten p und q. Die y-Differenz dieser beiden Linien entspricht Ω und ist der Unterschied des Isotopeneffekts beider Reaktionen.

$$\Omega = - \Delta\delta_q / f_p = \Delta\delta_p / (1 - f_p) = \delta_p - \delta_q \quad \text{(II-14)}$$

mit $\Delta\delta_q = (\delta_q - \delta_r)$ und $\Delta\delta_p = (\delta_p - \delta_r)$.

Alternativ kann Ω über die Steigung der Regressionsgeraden der Isotopensignaturen der Produkte bestimmt werden.

Die relative Ausbeute an den Verzweigungspunkten Acetyl-CoA und Pyruvat sind folgendermaßen definiert:

$$f_{ac} = \frac{n(acetate)}{n(acetate) + n(ethanol)} \quad \text{(II-15)}$$

$$f_{lac} = \frac{n(lactate)}{n(lactate) + n(acetate) + n(ethanol)} \quad \text{(II-16)}$$

n: Stoffmenge des akkumulierten Produkts [mol].

II.6.5.4 Kohlenstoffisotopensignatur von anorganischem Kohlenstoff

Die berechneten Stoffmengen der unterschiedlichen anorganischen Kohlenstoffspezies (II.6.5.2) und ihre Isotopensignaturen wurden verwendet, um die Isotopensignatur von TIC zu bestimmen:

$$\delta_{TIC} = X_g\delta_g + X_d\delta_d + X_b\delta_b + X_c\delta_c \quad \text{(II-17)}$$

X: Stoffmengenanteil der jeweiligen Spezies an TIC

δ: $\delta^{13}C$-Wert von *g* = gasförmigem CO_2, *d* = gelöstem CO_2, *b* = HCO_3^-, und *c* = CO_3^{2-}

δ_g wurde gemessen, die übrigen Isotopenverhältnisse wurden mit den Gleichgewichtsisotopen-Fraktionierungsfaktoren für 15 und 30°C (Deines et al., 1974; Mook et al., 1974) bestimmt:

$$\delta_d = \alpha_{d/g}\delta_g + (\alpha_{d/g} - 1)1000 \qquad \text{mit } \alpha_{d/g} = 0{,}999 \text{ für 15 und 30°C} \quad \text{(II-18)}$$

$$\delta_b = \alpha_{b/g}\delta_g + (\alpha_{b/g} - 1)1000 \qquad \text{mit } \alpha_{b/g} = 1{,}009 \text{ für 15°C und } 1{,}007 \text{ für 30°C} \quad \text{(II-19)}$$

$$\delta_c = \alpha_{c/g}\delta_g + (\alpha_{c/g} - 1)1000 \qquad \text{mit } \alpha_{c/g} = 1{,}007 \text{ für 15°C und } 1{,}006 \text{ für 30°C} \quad \text{(II-20)}$$

II.6.5.5 Relativer Anteil methanogener Reaktionswege an der Methanbildung

Der Anteil des aus H_2/CO_2 (f_{mc}) produzierten Methans am Gesamtmethan kann unter der Annahme, dass Methan ausschließlich aus Acetat und H_2/CO_2 gebildet wird, allein aus stabilen Isotopendaten bestimmt werden (Conrad, 2005). Hierfür werden die $\delta^{13}C$-Werte der Methanvorläufer und des gebildeten Gesamtmethans, und weiterhin die Fraktionierungsfaktoren von acetoklastischer und hydrogenotropher Methanogenese benötigt. Es gilt:

$$f_{mc} = (\delta_{CH4} - \delta_{mc})/(\delta_{mc} - \delta_{ma}) \quad \text{(II-21)}$$

wobei δ_{CH4}, δ_{mc}, δ_{ma} die δ-Werte von gesamtgebildetem, CO_2-abgeleitetem und Acetat-abgeleitetem Methan sind. δ_{mc} und δ_{ma} werden folgendermaßen berechnet:

$$\delta_{ma} = (1/\alpha_{ma})(\delta_{ac\text{-}methyl} + 10^3 - \alpha_{ma}\, 10^3) \quad \text{(II-22)}$$

$$\delta_{mc} = (1/\alpha_{mc})(\delta_{CO2} + 10^3 - \alpha_{mc}\, 10^3) \quad \text{(II-23)}$$

wobei α_{ma} und α_{mc} die Fraktionierungsfaktoren der acetoklastischen und hydrogenotrophen Methanogenese sind, $\delta_{ac\text{-}methyl}$ der δ-Wert von Methyl-Acetat.

II.7. Molekularbiologische Analysen

II.7.1 DNA/RNA-Extraktion

Alle folgenden Extraktionsschritte wurden auf Eis oder gekühlt bei 4°C durchgeführt, um die RNA stabil zu halten. Die verwendeten Chemikalien waren RNase-frei, Lösungen wurden in RNAse-freiem Wasser angesetzt. Für die Nukleinsäure-Extraktion, die weitgehend dem von Lueders et al. (2004) beschriebenen Protokoll folgte, wurden 10 ml Flüssigprobe aus Reiswurzelinkubationen zentrifugiert (15 min, 26000 × g, 4°C; RC 5B Plus, Rotor SS34; Sorvall). Der Überstand wurde entfernt, die sedimentierten Zellen in 0,5 ml sterilem Wasser (Sigma) resuspendiert, und vollständig in 2-ml Schraubdeckelreaktionsgefäße überführt. In diese waren bereits etwa 0,7 g hitzesterilisierte (180°C für 4h) und nukleinsäurefreie Zirconium/Silicium Kugeln (0,1 mm; Biospec Products, Bartlesville, OK, USA), 750 µl Na-Phosphat-Puffer (120 mM, pH 5,2) und 250 µl Natriumdodecylsulfat (SDS)-Lösung (10 % SDS; 0,5 M Tris-Puffer pH 7,0; 0,1 M NaCl) vorgelegt. Die Zelllyse wurde in einer Zellmühle (FP120 FastPrep, Savant Instruments) für 45 s bei einer maximalen Beschleunigung von 6,5 m s^{-1} durchgeführt. Zur

Sedimentation der Festbestandteile wurde das Homogenisat für 4 min zentrifugiert (20000 × *g*; 5417R, Eppendorf), der Überstand abgenommen und in ein frisches Reaktionsgefäß überführt.

Proteine, Zellbestandteile und andere Verunreinigungen wurden durch Extraktion mit einem Volumen Phenol/Chloroform/Isoamylalkohol (25:24:1; pH 5) entfernt. Nach Zugabe wurde die Suspension für ca. 20 s geschüttelt und für 4 min zentrifugiert (20000 × *g*). Der Überstand wurde abgenommen und in ein frisches *Phase Lock Gel*^{TM} *Heavy* Reaktionsgefäß (Eppendorf, Hamburg) überführt und ein Volumen Chloroform/Isoamylalkohol (24:1) zugegeben. Nach Schütteln (20 s) und Zentrifugation (4 min, 20000 × *g*) wurde der Überstand zur Nukleinsäurefällung in ein frisches Reaktionsgefäß überführt, 2 Volumina Polyethylenglycol-Lösung (30 % PEG 6000; 1,6 M NaCl) zugegeben und für 60 min zentrifugiert (20000 × *g*). Danach wurde der Überstand abgenommen, der Niederschlag in 0.5 ml Ethanol (70 %) gewaschen und zentrifugiert (15 min; 12000 × *g*). Die Ethanol-Lösung wurde möglichst vollständig entfernt und der Niederschlag in 30 µl RNase-freiem Wasser gelöst und bei -80°C gelagert.

II.7.2 DNA Verdau und RT-PCR von RNA

Von einem Teil der Extrakte wurde die DNA hydrolysiert, um einen reinen RNA-Extrakt zu erhalten. Der Verdau wurde mit RQ1 RNase-freier DNase (Promega) nach Herstellerangaben durchgeführt. Danach wurde die RNA mit einem Volumen Phenol/Chloroform/Isoamylalkohol (25:24:1) extrahiert wie unter II.7.1 beschrieben. Zur gelösten RNA wurde am Ende noch 40 U RNasin Ribonuclease Inhibitor (Promega) gegeben. Der erfolgreiche Verdau wurde über Gelelektrophorese (1,5 % [w/v] TAE-Agarosegel; SeaKem LE, Biozym; in TAE-Puffer) durch Vergleich des RNA-Extrakts mit dem DNA/RNA-Extrakt kontrolliert.

Einzelsträngige cDNA wurde durch RT-PCR von RNA erhalten. Hierbei wurden 8,5 µl RNA-Extrakt, 1 µl 10× Hexanukleotid Mix (1:50 verdünnt; Roche) und 20 U RNasin Ribonuclease Inhibitor (Promega) für 10 min bei 70°C inkubiert (Gesamtvolumen 10 µl). Nach Kühlen auf Eis für eine Minute wurde M-MLV RT 5× Reaktionspuffer (Promega), 100 pmol von jedem Desoxynukleosidtriphosphat (Amersham Pharmacia Biotech) und 200 U M-MLV RT (Promega) zugegeben, mit Wasser auf ein Endvolumen von 25 µl gebracht und für eine Stunde zur cDNA Synthese bei 37°C inkubiert.

II.7.3 PCR-Amplifikation

Mit Hilfe der PCR (Polymerasekettenreaktion) wurden Fragmente des phylogenetischer Markergens 16S rRNA aus DNA-Extrakten vermehrt und die erhaltenen PCR-Produkte für T-RFLP- (Terminaler-Restriktionsfragment-Längen-Polymorphismus) und Sequenzanalysen (II.7.6 und II.7.7) weiterverwendet. Die Real Time-PCR-Methode wurde für die Quantifizierung der Zielmoleküle (= Anzahl der 16S rRNA-Gene) in den DNA-Extrakten eingesetzt. Die verwendeten Primer sind in Tabelle II-6 aufgeführt. Bei jeder Amplifikation wurde als Negativkontrolle eine Reaktion mitgeführt, die anstelle des DNA-Templates das entsprechende Volumen H_2O enthielt. Als Positivkontrolle diente DNA mit dem zu amplifizierenden Zielmolekül.

Tabelle II-6. Beschreibung der verwendeten Primer für quantitative (hier: Real Time) PCR (= qPCR), T-RFLP-Analyse, Sequenzierung (= Seq) des partiellen 16S rRNA-Gens und des Vektorinserts von Klonen (= Klon). Oligonuk. = Oligonukleotid. pGEM-T = pGEM-T Vector System II Cloning Kit (Promega); K = G/T.

Oligonuk.	Sequenz (5´- 3´-Richtung)	Ziel-gruppe	Verwendung	Referenz
A109f	ACKGCTCAGTAACACGT	*Archaea*	T-RFLP, Seq, qPCR	(Grosskopf et al., 1998a)
A915b	GTGCTCCCCCGCCAATTCCT	*Archaea*	T-RFLP, Seq, qPCR	(Stahl und Amann, 1991)
T7f	TAATACGACTCACTATAGGG	Vektor	Klon	pGEM-T
M13b	CAGGAAACAGCTATGAC	Vektor	Klon	pGEM-T

II.7.3.1 Quantifizierung archaeeller 16S rRNA-Gene

Die Quantifizierung des 16S rRNA-Gene der *Archaea* (Primer 109f und 915b; Tabelle II-6) in den DNA-Extrakten, erfolgte mit der Real Time-PCR-Methode (Raeymaekers, 2000; Suzuki et al., 2000) mit dem iCycler IQ Thermocycler (Biorad Laboratories). Die Reaktionen wurden mit einer Antikörper geblockten *Jumpstart* DNA-Polymerase (Sigma-Aldrich) in 96-Well-Mikrotiterplatten (PeqLab, Erlangen) durchgeführt. Eine eventuell mögliche Hemmung der PCR wurde durch eine Verdünnungsreihe der PCR-Extrakte ausgeschlossen. Für die tatsächliche Messung wurden die DNA-Extrakte 1:5 verdünnt und davon je 5 µl in der Mikrotiterplatte vorgelegt. Für die

Eichung wurden jeweils 5 µl einer Verdünnungsreihe eines spezifischen, quantifizierten DNA-Standards (siehe unten) bei jeder Messung (d.h. jeder Mikrotiterplatte) mitgeführt. Alle Proben und Standards wurden in drei Replikaten gemessen. Nach Zugabe der Reaktionslösung wurde die Platte mit einer selbstklebenden optischen Folie (BioRad) verschlossen. Dem Reaktionsgemisch wurde eine Fluoreszeinlösung (= Calibrationdye, 1 mM, BioRad Laboratories) zur Kalibrierung zugegeben, um die Kameraeinstellung zu optimieren. Um die Amplifikations-Kinetik während der PCR verfolgen zu können, enthielt das Reaktionsgemisch den DNA-Farbstoff SybrGreen I, welcher an doppelsträngige DNA bindet. Mit fortschreitender Zyklenzahl und ansteigender Konzentration der doppelsträngigen DNA steigt somit die Fluoreszenzintensität der Lösung. Mit Hilfe einer Digitalkamera wurden die Daten während der DNA-Synthese-Phase dokumentiert. Die PCR-Bedingungen und das verwendete Reaktionsgemisch sind in Tabelle II-7 und Tabelle II-8 zusammengefasst. Das Temperaturprofil der PCR-Reaktionen wurden als Dreischritt-Protokolle durchgeführt. Anstelle des abschließenden DNA-Synthese-Schrittes (DS) erfolgte die Aufnahme der Schmelzkurve. Dabei wurde das entstandene PCR-Produkt während einer Temperaturerhöhung von 75 auf 100°C aufgeschmolzen.

Tabelle II-7. PCR-Bedingungen zur der Quantifizierung (qPCR) und Untersuchung mikrobiellen Diversität der 16S rRNA-Gene: Primer-Anlagerungstemperatur (PAT); Dauer der initialen Denaturierungsphase (D); Dauer der Denaturierung (Dz), der Primeranlagerung (PAz) und der DNA-Synthese während der zyklischen Wiederholung (DSz); Dauer der abschließenden DNA-Synthese (DS). ***** FAM-Markierung für T-RFLP-Analyse; [§] Bestimmung der Fluoreszenzintensität.

Primerkombination	Ziel-gruppe	Anzahl der Zyklen	PAT [°C]	D [min]	Dz [sec]	PAz [sec]	DSz [sec]	DS [min]
A109f / A915b*	*Archaea*	30	55	4	45	60	60	7
A109f / A915b (qPCR)	*Archaea*	40	55	3	40	30	90[§]	-
T7f / M13b	Vektor	25	55	5	60	60	120	7

Tabelle II-8. Zusammensetzung des PCR-Reaktionsgemisches zur Quantifizierung der 16S rRNA-Gene.

Komponente	Hersteller	Konzentration Stammlösung	Zugabe [µl]	Menge
Forward und Reverse Primer	MWG, Ebersberg	33 µM	0,25	8,25 pmol
SYBR Green Jumpstart *Taq* ReadyMix	Sigma-Aldrich, Taufkirchen		12,25	
$MgCl_2$	Invitrogen, Karlsruhe	25 mM	3	37,5 nmol
DNA-Extrakt (1:5)			5	
H_2O			ad 25	

Herstellung eines quantitativen Standards. Für die Eichung wurden archaeelle 16S rRNA-PCR-Produkte von Klon-DNA eingesetzt (Kemnitz et al., 2005), die freundlicherweise von Dr. Dana Kemnitz bereitgestellt wurden. Dafür wurden die Vektorinserts mit dem Primerpaar T7f und M13b (Tabelle II-6) in den flankierenden Sequenzregionen amplifiziert und mit dem QIAquick PCR Purifikation Kit (Qiagen) zweimal nach dem Protokoll des Herstellers aufgereinigt. Die DNA-Konzentrationen der Eichstandards von 1005 bp Länge wurden mit dem PicoGreen dsDNA Quantitation Kit (Molecular Probes, Leiden, Niederlande) nach Herstelleranweisung in einer Microtiterplatte (Nunc, Wiesbaden) in einem Fluorimeter (SAFIRE; TECAN, Crailsheim) vermessen. Die erhaltenen Fluoreszenzwerte eines λ-Phagen-DNA-Mengenstandards wurden dann gegen die Menge [ng] aufgetragen und durch lineare Regression interpoliert. Mittels der erhaltenen Geradengleichung konnte aus den Fluoreszenzwerten des T7-M13-PCR-Produktes die Konzentration der Zielmoleküle (C_w) [ng μl^{-1}] bestimmt werden.

Mit folgender Formel wurde anschließend dieser Wert in die Anzahl der amplifizierbaren Zielmoleküle umgerechnet:

$$C_S = \frac{C_W}{N \times M_N} \times N_A \qquad \text{(II-24)}$$

C_S: Anzahl der amplifizierbaren Zielmoleküle [μl^{-1}]

C_w: Konzentration [ng μl^{-1}]

N_A: Avogadrokonstante ($6{,}022 \times 10^{23} \times 10^{-9}$ $nmol^{-1}$)

N: Länge des Standards in Basenpaaren

M_N: molare Masse eines Basenpaars; 649,5 ng $nmol^{-1}$ (Mittelwert der Nukleotidtriphosphatpaarungen A = T und G ≡ C)

Diese Standardlösung wurde anschließend auf 10^{10} Zielmolekühle × $(5\ \mu l)^{-1}$ mit Elutionspuffer (QIAquick PCR Purifikation Kit) verdünnt und bei -20°C gelagert.

Quantifizierung der Zielmolekülzahlen aus DNA-Extrakten. Aus der Darstellung der Fluoreszenz in Abhängigkeit der Zyklenzahl wurde der Schwellenwertzyklus (= Threshold Cycle [C_T]) bestimmt. Dieser Wert ist definiert als die rationale Zyklenzahl, bei der die Fluoreszenz der Reaktion eine definierte Hintergrundfluoreszenz zu Beginn der exponentiellen Amplifikationsphase übersteigt. Die Auswertung der Rohdaten wurde mit der iCycler IQ Optical System Software V 3.0a (Biorad Laboratories) durchgeführt. Da ein linearer Zusammenhang zwischen dem C_T einer Reaktion und dem Logarithmus der Menge an Zielmolekülen besteht, konnten die Daten mit Hilfe linearer Regression interpoliert werden. Mit der resultierenden Geradengleichung aus den C_T-Werten der Eichstandards (Verdünnungsreihe) wurde die Anzahl der Zielmoleküle in den DNA-Extrakten bestimmt. Die Zielmolekülzahlen wurden in das Programm Excel V7.0 (Microsoft) exportiert und bearbeitet.

II.7.3.2 PCR-Amplifikation zur Untersuchung der archaeellen Diversität

Die PCR-Reaktionen wurden in einem GeneAmp 9700 Thermocycler (Applied Biosystems) mit dem in Tabelle II-9 aufgeführten Reaktionsgemisch durchgeführt. Die Amplifikation von PCR-Produkten für die T-RFLP-Analyse erfolgte mit einem Carboxyfluorescein (= FAM) markierten Primer (5´-Ende). Die Primer-Kombination, Zyklenzahl, Primer-Anlagerungstemperatur und die Dauer der verschiedenen Schritte sind in Tabelle II-7 für jede Reaktion aufgeführt.

Tabelle II-9. Zusammensetzung des PCR-Reaktionsgemisches für die Diversitätsanalyse.

Komponente	Hersteller	Konzentration der Stammlösung	Zugabe [µl]	Menge
Forward und Reverse Primer	MWG	33 µM	0,5	16,5 pmol
Taq-Polymerase	Invitrogen	5 U μl^{-1}	0,25	1,25 U
dNTPs	Amersham Pharmacia Biotech	2 mM	1,25	2,5 nmol
$MgCl_2$	Invitrogen	25 mM	3	75 nmol
Reaktionspuffer	Invitrogen	10-fach	5	1-fach
BSA	Roche	4 µg μl^{-1}	1	4 µg
DNA-Extrakt			1	
H_2O			ad 50	

Nach der PCR wurden Aliquots der erhaltenen Amplifikate durch Gelelektrophorese (1,5 % [w/v] TAE-Agarosegel; SeaKem LE, Biozym; in TAE-Puffer) überprüft. Zur Entfernung von Nukleotiden, Enzymen, Salzen und nicht gebundenen Primern wurden die PCR-Produkte mit dem QIAquick PCR Purifikation Kit (Quiagen GmbH) nach dem Protokoll des Herstellers aufgereinigt.

II.7.4 T-RFLP-Analyse

Mit Hilfe der T-RFLP-Methode wurden genetische Fingerabdrücke für die 16S rRNA der *Archaea* erstellt, die eine direkte Analyse relativer Anteile phylogenetischer Gruppen erlauben (Liu et al., 1997). Diese Methode basiert auf der Analyse von Restriktionsfragmenten, die an einem Ende mit einem fluoreszierenden Farbstoff versehen sind. Dadurch wird nicht das gesamte Fragmentmuster (wie bei einer RFLP-Analyse), sondern nur das terminale Restriktionsfragment detektiert. Mit Hilfe von Klonbibliotheken und anschließender Sequenzanalyse (II.7.6 und II.7.7), können die einzelnen Fragmente bestimmten phylogenetischen Gruppen zugeordnet werden.

Die fluoreszierenden Amplifikate wurden, wie bereits beschrieben (II.7.3.2), durch eine PCR mit einem 5´-FAM-markierten Primer und einem unmarkierten Primer hergestellt. Die Konzentration der aufgereinigten PCR-Produkte wurde durch Bestimmung der Absorption bei einer Wellenlänge von 260 nm in einem Biophotometer (Eppendorf) bestimmt.

Für die Restriktion der 16S rRNA-Gen-Amplifikate wurden etwa 80 ng DNA eingesetzt. Der Restriktionsansatz der archaeellen PCR-Produkte enthielt weiterhin 1 µl Inkubationspuffer und 0,5 µl des Restriktionsenzyms *Taq*I (10 U μl^{-1}, Erkennungssequenz: 5´-TˇCGA-3´; Fermentas). Mit sterilem H_2O wurde auf ein Gesamtvolumen von 10 µl aufgefüllt und für 3 h bei 65°C im Ofen inkubiert. Die verdaute DNA wurde bis zur weiteren Verwendung bei -20°C aufbewahrt.

1,25 µl der verdauten PCR-Produkte wurden mit einem internen Längenstandard (0,4 µl Genescan-1000 Rox; Applied Biosystems) und Formamid Loading Dye (0,85 µl; Amersham Pharmacia Biotech) gemischt, 2 min bei 95°C denaturiert und sofort auf Eis gestellt. Die Auftrennung des Gemisches erfolgte durch Elektrophorese mit einem 6%igen Polyacrylamidgel mit 8,3 M Harnstoff in einem automatischen Sequenziergerät (373A Sequencer, Applied Biosystems) für 6 h bei 2500 V und 40 mA. Die Auswertung wurde mit der Analysesoftware (GeneScan Analysis Version 2.1, Fa. Applied Biosystems) durchgeführt. In den generierten Chromatogrammen entsprachen die Peaks den terminalen Fragmenten unterschiedlicher Länge, die mit dem internen Längenstandard bestimmt wurde. Der relative Anteil der einzelnen Peaks wurde über ihre Peakflächen, die der Intensität der Fluoreszenzsignale entsprechen, im Verhältnis zur Gesamtfläche aller Peaks berechnet.

II.7.5 Erstellung von Klonbibliotheken

Um die phylogenetische Einordnung der 16S rDNA-Sequenzen zu ermöglichen, wurden die aus cDNA- bzw. DNA-Extrakten amplifizierten PCR-Produkte über Klonierung vereinzelt. Die unbehandelten PCR-Produkte wurden mit dem pGEM-T Vector System II Cloning Kit (Promega) nach dem Protokoll des Herstellers kloniert. Die transformierten Zellen wurden auf LB-Ampicillin-X-Gal-Agarplatten (Fast Media^{TM}, LB Agar Amp IPTG/X-Gal, Fermentas) ausplattiert, über Nacht bei 37°C inkubiert und positive Kolonien (Blau-Weiß-Selektion) auf eine Masterplatte überimpft. Die DNA zufällig ausgewählter Klone wurde durch Aufkochen (10 min, 95°C) von Zellpellets in 50 µl sterilem H_2O gewonnen.

II.7.6 Sequenzierung

Die verwendete DNA-Sequenzierungsmethode basiert auf dem Prinzip des „Kettenabbruchs“ (Sanger et al., 1977). Das Reaktionsgemisch enthält neben den üblichen dNTPs vier unterschiedlich 5´-fluoreszenzmarkierte Didesoxynukleotidtriphosphate (ddNTPs = Terminatoren). Letztere führen zum Abbruch der Polymeraseaktivität, wodurch man ein Gemisch unterschiedlich langer 3´-fluoreszenzmarkierter DNA-Fragmente erhält. Vor der eigentlichen Sequenzierreaktion wurde das Insert der Klone direkt mit dem am Vektor bindenden Primerpaar T7f und M13b (II.7.3; Tabelle II-6) amplifiziert und danach aufgereinigt. Die Sequenzierung wurde mit dem *ABI PRISM DNA Sequencing Big Dye^{TM} Terminator Cycle Sequencing Ready Reaction Ki*t (Applied Biosystems) durchgeführt. Dem Reaktionsgemisch wurde in einem Gesamtvolumen von 10 µl 5 pmol des Sequenzier-Primers (T7f oder M13b) und ca. 50 ng Matrizen-DNA zugefügt. Die Reaktion erfolgte mit 25 Zyklen (30 sec 96°C, 25 × [10 sec 96°C, 5 sec 50°C, 4 min 60°C]) mit dem GeneAmp 9700 Thermocycler (Applied Biosystems). Die Produkte der Sequenzierreaktion wurden mit AutoSeq^{TM} G-50-Chromatographiesäulen (Amersham Pharmacia Biotech) aufgereinigt und das Eluat unter Vakuum in der DNA-SpeedVac (DNA 110, Savant Instruments) für 30 min getrocknet. Das Pellet wurde danach in 3 µl Formamid Loading Dye (Amersham Pharmacia Biotech Inc.) resuspendiert, 3 min bei 90°C denaturiert und auf Eis gekühlt. Das Fragmentgemisch (1,5 µl) wurde über ein Polyacrylamidgel in einem Sequenzierer (ABI Prism 377 DNA Sequenzierer, Applied Biosystems) getrennt. Anhand der Fluoreszenzsignale lässt sich die Basensequenz der DNA-Matrize ablesen.

II.7.7 Phylogenetische Einordnung der 16S rRNA-Gensequenzen

Die Rohsequenzdaten (Elektropherogramme) wurden mit dem Programm Seqman II (DNASTAR, Madison, WI, USA) bearbeitet. Teilsequenzen wurden zusammengefügt und die Vektorsequenzen entfernt. Ein erster phylogenetischer Vergleich der Sequenzen erfolgte in einer öffentlich verfügbaren Datenbank durch das Programm „BLAST“ (http://www.ncbi.nlm.nih.gov/blast/). Nah verwandte Sequenzen wurden heruntergeladen und zur weiteren phylogenetischen Analyse mitverwendet.

Die Phylogenetische Verrechnung und Darstellung der 16S rDNA-Sequenzdaten erfolgte mit der Phylogenie-Software ARB (http://www.arb-home.de/; (Ludwig et al., 2004)). Die Klonsequenzen, sowie nah verwandte Umweltsequenzen („BLAST“-Suche) wurden importiert und mit der in ARB enthaltenen „FAST-Aligner“-Funktion mit bereits vorhandenen Sequenzen in ein Alignment gebracht (Ludwig, 1995). Dabei wurden die jeweiligen homologen Positionen einander gegenübergestellt, was eine weitgehend korrekte Zuordnung in den hypervariablen Regionen der 16S rRNA-Gene ermöglichte (Gutell et al., 1994). Anschließend wurde das Alignment manuell überprüft und gegebenenfalls korrigiert, sowie die Primersequenzen entfernt. Unter Anwendung des Parsimony-Algorithmus (Fitch, 1971) wurden die aufgearbeiteten Sequenzdaten in den „Gesamtbaum“ der ARB-Datenbank eingebracht. Mit dieser Funktion wird die zu analysierende Sequenz einer Sequenz im Stammbaum zugeordnet, zu der die geringste Anzahl an Nukleotidsubstitutionen besteht. Für diese Berechnung wurden keine evolutiven Korrekturfaktoren berücksichtigt, und die eingerechnete Sequenz hat hierbei keinen Einfluss auf die Topologie des Stammbaums. Zur Identifizierung von chimären Sequenzen, d.h. Mischprodukten aus Sequenzen phylogenetisch verschiedener Organismen, die als Artefakte während der PCR entstehen können, wurde ein sog. *fractional treeing* (Ludwig et al., 1997) durchgeführt; ergab sich unter Berücksichtung der vorderen Hälfte einer Sequenz eine signifikant andere phylogenetische Einordnung als unter Berücksichtigung der zweiten Hälfte, so deutete dies auf eine chimäre Sequenz hin, die verworfen wurde.

Mit dem so erhaltenen Baum wurden die klonierten 16S rRNA-Sequenzen archaeellen Gruppen zugeordnet und Verwandtschaftsverhältnisse zu ähnlichen 16S rRNA-Sequenzen bestimmt. Zur Bestimmung der TRFs der einzelnen Klonsequenzen wurde das in ARB integrierte TRF-CUT Werkzeug (Ricke et al., 2005) verwendet und damit ein *in silico* Verdau mit *Taq*I durchgeführt. Somit konnten die in der T-RFLP-Analyse erhaltenen Peaks phylogenetischen Gruppen zugeordnet werden.

III. Ergebnisse

III.1. Kohlenstoffisotopeneffekte bei der gemischten Säuregärung von Sacchariden durch *Clostridium papyrosolvens*

Holger Penning und Ralf Conrad

Zusammenfassung:

Die Fermentation ist der erste Schritt des anaeroben Abbaus organischer Materie und liefert die Substrate nachfolgender Prozesse. Erstmals wurde in dieser Arbeit die Kohlenstoffisotopenfraktionierung bei der anaeroben Fermentation untersucht. Während des linearen Abbauweges zum Intermediat Pyruvat wurden lösliche Saccharide (Glucose und Cellobiose) fraktioniert, das Polysaccharid Cellulose jedoch nicht. Das Ausbleiben der Fraktionierung bei Cellulose war durch den vorangehenden geschwindigkeits-begrenzenden Schritt der Hydrolyse bestimmt. Im verzweigten Teil des Fermentationsweges war am Verzweigungspunkt Pyruvat die Isotopenfraktionierung zu Lactat stärker als zu Acetyl-CoA. Von Acetyl-CoA ausgehend, welches der zweite Verzweigungspunkt im Katabolismus von *C. papyrosolvens* ist, wurde ^{12}C stärker für die Bildung von Ethanol als von Acetat bevorzugt. Dieses Muster wurde sowohl in Batch- als auch in Chemostatkulturen unabhängig vom metabolisierten Saccharid gefunden. Verschiebungen im relativen katabolischen Kohlenstofffluss durch geänderte Wachstumsbedingungen waren alleinig für Änderungen der $\delta^{13}C$-Werte der Produkte verantwortlich und folgten somit theoretischen Prinzipien. Die hier erhaltenen Ergebnisse können zur Berechnung der $\delta^{13}C$-Werte von Fermentationsprodukten wie Acetat oder Ethanol genutzt werden, deren direkte Messung auf Grund sehr geringer Konzentrationen in der Umwelt meist nicht möglich ist.

Carbon isotope effects associated with mixed-acid fermentation of saccharides by *Clostridium papyrosolvens*

(eingereicht bei Geochimica & Cosmochimica Acta)

Holger Penning and Ralf Conrad

Max Planck Institute for Terrestrial Microbiology, Karl-von-Frisch-Str., 35043 Marburg, Germany

Abstract — In anoxic environments microbial fermentation is the first metabolic process in the path of organic matter degradation. Since little is known about carbon isotope fractionation during microbial fermentation, we studied mixed-acid fermentation of different saccharides (glucose, cellobiose, cellulose) in *Clostridium papyrosolvens*. The bacterium was grown anaerobically in batch under different growth conditions, both in pure culture and in coculture with *Methanobacterium bryantii* utilizing H_2/CO_2 or *Methanospirillum hungatei* utilizing both H_2/CO_2 and formate. Major fermentation products were acetate, lactate, ethanol, formate, H_2, and CO_2 (and CH_4 in methanogenic coculture), with acetate becoming dominant at low H_2 partial pressures. Incomplete fermentation of saccharides was associated with fractionation of C isotopes during formation of pyruvate from glucose (α = 1.019) and cellobiose (α = 1.005), but not from cellulose. After complete conversion of the saccharides, acetate was ^{13}C-enriched ($\alpha_{sacc/ac}$ = 0.992 - 0.997), whereas lactate ($\alpha_{sacc/lac}$ = 1.002 - 1.007), ethanol ($\alpha_{sacc/etoh}$ = 1.009 – 1.013), and formate ($\alpha_{sacc/form}$ = 1.007 - 1.011) were ^{13}C-depleted. The total inorganic carbon (TIC) produced was only slightly enriched in ^{13}C, but was more enriched, when formate was produced in large amounts, as $^{12}CO_2$ was preferentially converted with H_2 to formate. Carbon isotope fractionation during biomass formation was slightly normal ($\alpha_{sacc/biom} \approx 1.002$). The observations in batch culture were confirmed in glucose-limited chemostat culture at dilution rates of 0.02 - 0.15 h^{-1} at both low and high hydrogen partial pressure. Our experiments showed that the carbon flow at metabolic branch points in the fermentation path governed carbon isotope fractionation to the accumulated products. The first branch point is the conversion of pyruvate to either acetyl-CoA + CO_2 or lactate. Formation of acetyl-CoA exhibited a stronger preference for ^{12}C than formation of lactate

with 4.9 - 8.7‰. The second branch point is the conversion of acetyl-CoA to either acetate or ethanol. Formation of ethanol exhibited a stronger preference of ^{12}C than formation of acetate with 15.3 - 17.8‰. At low hydrogen partial pressures, as normally observed under environmental conditions, fermentation of saccharides should mainly result in the production of acetate that is only slightly enriched in ^{13}C (< 3‰). These results might be useful to calculate isotopic signatures of the fermentation products, if these cannot be measured directly, and thus help constraining biogeochemical models of C-flux in anoxic environments.

Introduction

In the anaerobic degradation of organic matter, low-molecular-weight organic compounds are important intermediates (Ward and Winfrey, 1985; Zinder, 1993). They are products of fermentation and serve as substrates for the terminal mineralization of carbon to CO_2 and CH_4. Acetate, which in nature is usually present at only very low concentrations, plays a key role as substrate for methanogenesis, iron reduction and sulfate reduction (Lovley, 1993; Ward and Winfrey, 1985; Zinder, 1993). Primary fermenting microorganisms seem to be the major producers of acetate (Chidthaisong and Conrad, 2000), whereas secondary fermenting (Krylova et al., 1997) and chemolithotrophic homoacetogenic bacteria (Lovley and Klug, 1983) produce much smaller amounts. In anaerobic soils and sediments, analysis of stable carbon isotopes has been used for tracing and quantifying carbon flow (Hornibrook et al., 2000; Sugimoto and Wada, 1993). The extent, to which the lighter isotope is preferred, is characteristic for distinct biogeochemical processes. With knowledge of the fractionation factors of the individual processes, it is possible to determine the dominant processes, simply by measuring the isotopic composition of a few key compounds. Fractionation factors of homoacetogenesis (Gelwicks et al., 1989; Preuss et al., 1989), acetoclastic methanogenesis (Gelwicks et al., 1994; Krzycki et al., 1987) and hydrogenotrophic methanogenesis (Balabane et al., 1987; Botz et al., 1996) have been determined in pure microbial culture. However, for the calculation of the fraction of methane produced by acetoclastic methanogenesis, the $\delta^{13}C$ of acetate needs to be known. Since acetate usually cannot be measured directly due to its low steady state concentration under natural conditions, the fractionation associated with acetate production by primary fermentation is important information.

During fermentation carbon atoms are channeled through a metabolic network with branch points (e.g. pyruvate, acetyl-CoA), at which the carbon flow is divided into different branches (Fig. 1). At these branch points one reactant is consumed by two or more competing reactions, each reaction having its own kinetic isotope effect. Generally $^{12}k/^{13}k > 1$, so that in linear reactions the product is always depleted in ^{13}C or has the same isotope ratio as the initial reactant, when the reaction is run to completion. Therefore, ^{13}C depletion of the product with respect to the substrate is called normal fractionation, whereas ^{13}C enrichment is called inverse fractionation. While inverse carbon isotope fractionation does not occur in linear reactions, it is obligatory at branch points, if the substrate is completely consumed and the fractionation factors (α) of the competing reactions differ. At the branch points, the carbon isotope flow is divided and ^{12}C preferentially flows into the product generated by the reaction with the larger α. Because of conservation of mass the other product must be enriched in ^{13}C. In most of our experiments the substrate was quantitatively converted to the different products. This had the advantage that the isotope ratios of the products were not influenced by the fractionation associated with saccharide uptake into the cell. Hence, isotope effects at the branch points of the saccharide fermentation path could be examined. In addition, difficulties linked to intra-molecular carbon specific fractionation of incomplete reactions were avoided. Such difficulties emerge for example during the incomplete oxidation of pyruvate to acetyl-CoA by pyruvate dehydrogenase, where the ^{13}C depletion of acetyl CoA is concentrated in the carbonyl carbon atom while only a minor effect is seen in the methyl carbon (De Niro and Epstein, 1977). Quantitative substrate conversion does not allow expression of such linear isotope effects within the metabolic network and thus does not bias the analysis of branch points.

Nevertheless, the intra-molecular isotopic composition of the saccharides is important. Early studies assumed homogeneity (Blair et al., 1985; De Niro and Epstein, 1977), but Rossmann et al. (1991) found that glucose from both maize and beet sugar had a similar intra-molecular distribution of ^{13}C that was non-statistical. Carbon positions 3 and 4 of glucose were found to be enriched in ^{13}C, whereas the other positions were depleted relative to the average $\delta^{13}C$ of the glucose. In the Emden-Meyerhoff-Parnas (EMP) pathway carbon positions 3 and 4 of glucose form the carboxyl group of pyruvate. Since pyruvate is a branch point, where both lactate and acetyl-CoA can be formed, knowledge

of the positional isotope distribution is helpful for interpretation of carbon isotope fractionation.

Knowledge of the fractionation factors involved in the formation of acetate and other fermentation products and their dependency on growth parameters is a prerequisite for modeling the later reactions in the mineralization of organic matter. So far, carbon stable isotope fractionation during saccharide fermentation has been studied only once using *Escherichia coli* (Blair et al., 1985). Therein, *E. coli* fermented glucose under aerobic conditions, so that the thus obtained fractionation factors cannot be applied reliably to the carbon flow in anaerobic systems. In addition, *E. coli* is an intestinal bacterium, which plays no role in outdoor environments. Therefore, we chose the bacterium *Clostridium papyrosolvens*, which is cellulolytic and was first isolated from an anaerobic estuarine sediment (Madden et al., 1982), later from freshwater swamps (Leschine and Canaleparola, 1983; Pohlschroder et al., 1994), and from rice field soil (Chin et al., 1998). *C. papyrosolvens* ferments saccharides in a mixed-acid fermentation via the EMP-pathway producing acetate, CO_2, ethanol, formate, lactate, and H_2 (Fig. 1). In the present study we investigated the stable carbon isotope fractionation associated with the fermentation of different saccharides (glucose, cellobiose, and cellulose) under batch and continuous growth conditions and tested the effect of environmental conditions like temperature, substrate concentration, and hydrogen partial pressure.

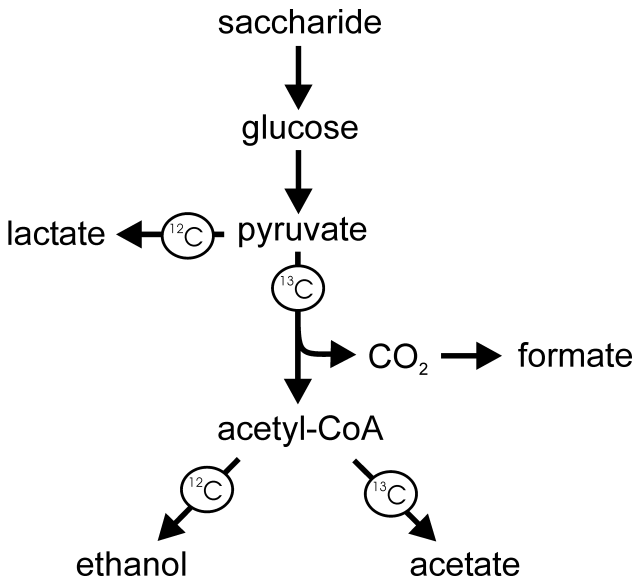

Figure 1: Catabolic carbon flow during fermentation of saccharides by *C. papyrosolvens*. At branch points (pyruvate and acetyl-CoA) the reactions with a stronger preference of ^{12}C are indicated by ^{12}C on the arrow; ^{13}C on the arrow indicates a less pronounced ^{12}C preference.

Materials and Methods

Cultures and growth conditions

Clostridium papyrosolvens (DSM 2782), *Methanobacterium bryantii* (DSM 863), and *Methanospirillum hungatei* (DSM 864) were obtained from the Deutsche Sammlung von Mikroorganismen (Braunschweig, Germany). The microorganisms were grown on phosphate-buffered mineral medium under N_2. The composition was (in grams liter^{-1} unless otherwise indicated): KH_2PO_4, 1.9; Na_2HPO_4*2 H_2O, 6.4; NH_4Cl, 0.3; $MgCl_2$*6 H_2O, 0.1; NaCl, 0.3; KCl, 0.15; $CaCl_2$*2H_2O, 0.055; Na_2S*9H_2O, 0.24; trace element solution, 2 mL (Chin et al., 1998); alkaline trace element solution 1 mL (Stams et al., 1993); vitamin solution, 1 mL (Wolin et al., 1963); resazurine at 0.5% (wt/vol), 1mL; pH adjusted to 7.2. Glucose (Merck, Frankfurt, Germany), cellobiose (Fluka, Taufkirchen, Germany), and cellulose (Fluka, Taufkirchen, Germany; concentrations expressed as anhydroglucose; Mw = 162 g/mol) were used as substrate. Isotope fractionation after complete conversion of saccharides was investigated in cultures of *C. papyrosolvens* (pure culture) and *C. papyrosolvens* with methanogenic partner (coculture). Pure and coculture experiments with glucose or cellobiose, in which the influence of temperature and substrate concentration was tested, were conducted in 120-mL serum vials with 50 mL of culture volume. Each combination of temperature and concentration was carried out in triplicate. Pure culture experiments with cellulose were performed only at 30°C in 1000 mL glass bottles with 500 ml culture volume. After complete substrate consumption, gas and liquid samples were taken for analysis of concentration and carbon isotopic composition. In addition, the coculture of *C. papyrosolvens* and *M. bryantii* was grown on cellulose in triplicate (500 mL glass bottles; 250 mL culture volume) and continuously sampled during the course of growth. Isotope fractionation during growth was investigated at 30°C in 1000 mL glass bottles with 500 mL culture volume in three replicate pure cultures with glucose (2.78 mM), cellobiose (1.46 mM), and cellulose (2.81 mM), respectively. Samples were taken continuously until complete fermentation of the saccharides. In the mass calculations corrections were made for the influence of sampling regarging masses and gas phase-liquid phase ratio.

Chemostat cultures were performed in 600-mL fermenter vessels with a working volume of 290 mL (headspace flushed with N_2; low hydrogen setup) or 270 mL (non-flushed headspace; high hydrogen setup). The mineral medium described above was used,

but with half the concentration of phosphate. *C. papyrosolvens* was grown under glucose limitation (10 mM), and steady-state conditions were maintained for at least ten volume changes, before gas and liquid samples were taken. Cultures were kept at a temperature of 30°C and stirred with 200 rpm. The pH was kept constant at pH 7.2 by automatic titration with NaOH solution. The biomass density was measured as optical density (OD_{600}) using a photometer at 600 nm.

Liquid samples for HPLC and isotopic analysis were filtered through 0.2-µm membrane filters (REZIST 13/0.2 PTFE, Schleicher & Schuell, Dassel, Germany) and stored at –20°C until analysis. For $\delta^{13}C$ analysis of biomass, cells were harvested by centrifugation (26,000 x g, 15 min, 4°C), washed two times with phosphate buffer (50 mM, pH 7.2), and dried to constant weight at 105°C.

Chemical and isotopic analysis.

CH_4 and CO_2 were analyzed by gas chromatography using a flame ionization detector (Shimadzu, Kyoto, Japan). CO_2 was detected after conversion to CH_4 with a methanizer (Ni-catalyst at 350°C, Chrompack, Middelburg, Netherlands). H_2 was analyzed by gas chromatography using a thermal conductivity detector (Shimadzu, Kyoto, Japan). Acetate, ethanol, formate, and fatty acids were measured by HPLC (Sykam, Gilching, Germany) with a refraction index and UV-detector, having a detection limit of 3-5 µM (Krumböck and Conrad, 1991). Glucose concentration was measured photometrically (Bergmeyer et al., 1974).

Stable isotope analysis of $^{13}C/^{12}C$ in gas samples was performed using a gas chromatograph combustion isotope ratio mass spectrometer (GC-C-IRMS) system that was purchased from Thermoquest (Bremen, Germany). The principle operation was described (Brand, 1996). The isotope ratios were detected with a Finnigan MAT delta plus IRMS. The CH_4 and CO_2 in the gas samples (40-400 µL) were first separated in a Hewlett Packard 6890 gas chromatograph using a Pora Plot Q column (27.5 m length, 0.32 mm i.d.; 10 µm film thickness; Chrompack, Frankfurt, Germany) at 30°C and He (99.996% purity; 2.6 mL min^{-1}) as carrier gas. After conversion of CH_4 to CO_2 in the Finnigan Standard GC Combustion Interface III the $^{13}C/^{12}C$ was analyzed in the IRMS.

To measure the $\delta^{13}C$ of acetate (mean of both C atoms), 0.5-2 mL liquid sample was freeze-dried (Alpha 1-4, Christ, Osterode, Germany) and thereafter redissolved in 20-50 µL formic acid (0.1 M) in propanol. The analysis of acetate samples (1 µL) was carried

out with the same gas chromatograph using a FFAP column (30 m length, 0.32 mm i.d., 0.25 µm film thickness, J&W Scientific, Folsom, USA). The oven temperature was kept at 80°C for 4 min and then increased by 20°C/min to 240°C. Reference gas was CO_2 (99.998% purity; Messer-Griessheim, Düsseldorf, Germany) calibrated with the working standard methylstearate (Merck). The latter was intercalibrated at the Max-Planck-Institut für Biogeochemie, Jena, Germany (courtesy of Dr. W.A. Brand) against NBS22 and USGS 24, and reported in the delta notation versus V-PDB: $\delta^{13}C = 10^3 (R_{sa}/R_{st}-1)$ with $R = {}^{13}C/{}^{12}C$ of sample (sa) and standard (st), respectively. The precision of repeated analysis was ± 0.2‰ when 1.3 nmol CH_4 was injected.

Isotopic measurement of formate, lactate, ethanol, and acetate were performed on a HPLC system (Spectra System P1000, Thermo Finnigan, San Jose, CA, USA; Mistral, Spark, Emmen, The Netherlands) equipped with an ion-exclusion column (Aminex HPX-87-H, Biorad) and coupled to Finnigan LC IsoLink (Thermo Electron Corporation, Bremen, Germany) as described by Krummen et al. (2004). Isotope ratios were detected on Finnigan MAT delta plus advantage IRMS. Reference gas was CO_2 calibrated as described above. The analysis of $\delta^{13}C$ of biomass and the saccharides was carried out at the Max-Planck-Institute for Biogeochemistry, Jena, Germany, with a EA-IRMS system consisting of an autosampler (AS 128, CE Instruments, Rodano, Italy), an elemental analyser (NA 1110 CN, CE Instruments) and an isotope ratio mass spectrometer (IRMS Delta^{plus} XL, Finnigan MAT, Bremen, Germany), coupled via a home-built interface (”ConFlo III”; Werner et al. (1999)) modified and supplemented as described in Brooks et al. (2003)).

The samples and the laboratory reference compounds (acetanilide and caffeine) were applied in solid samples tin capsules (Lüdi, purchased from IVA, Meerbusch, Germany). The standardisation scheme of the EA-IRMS measurements as well as the measurement strategy and the calculations for assigning the final $\delta^{13}C$-values on the V-PDB scale was analogous to that described by Werner and Brand (2001) on an elemental-analyzer-IRMS.

Calculations

Fractionation factors for a reaction A → B are defined after Hayes (1993):

$$\alpha_{A/B} = (\delta_A + 1000)/(\delta_B + 1000) \quad (1)$$

sometimes expressed as $\varepsilon \equiv 10^3 (1 - \alpha)$. Because total oxidized carbon was distributed among different carbon species (gaseous CO_2, dissolved CO_2, HCO_3^-, and CO_3^{2-}), $\delta^{13}C$ of total inorganic carbon (δ_{TIC}) could not be determined directly. This value was calculated by the following mass-balance equation:

$$\delta_{TIC} = X_g\delta_g + X_d\delta_d + X_b\delta_b + X_c\delta_c \quad (2)$$

where X = mole fraction and δ = isotopic composition of the C of *g* = gaseous CO_2, *d* = dissolved CO_2, *b* = HCO_3^-, and *c* = CO_3^{2-}. The distribution of carbon among these species was calculated using solubility and equilibrium constants (Stumm and Morgan, 1995). δ_g was measured directly, the remaining isotopic compositions were calculated from the from relevant equilibrium isotopic fractionation factors at 15 and 30°C (Deines et al., 1974; Mook et al., 1974):

$$\delta_d = \alpha_{d/g}\delta_g + (\alpha_{d/g} - 1)1000 \quad (3)$$

$$\delta_b = \alpha_{b/g}\delta_g + (\alpha_{b/g} - 1)1000 \quad (4)$$

$$\delta_c = \alpha_{c/g}\delta_g + (\alpha_{c/g} - 1)1000 \quad (5)$$

Fractionation at branch points in the fermentation path was calculated based on the conservation of mass and the difference in fractionation observed between the two products, which is a valid approach for systems at equilibrium and under kinetic control. The following approximations – that are appropriate for carbon isotope fractionation – were used (Hayes, 2001; Hayes, 2002):

$$\delta_p = \delta_r + (1 - f_p)\,\Omega_d \quad (6)$$

$$\delta_q = \delta_r - f_p\,\Omega_d \quad (7)$$

where r = reactant; p, q = products of the reaction at the branch point; f_p = fractional yield of p; $\Omega = [(\alpha_{r/p} / \alpha_{r/q}) - 1]10^3$, and d = designation of the branch point (e.g. pyruvate). In the corresponding diagram, where f_p is plotted against the isotopic composition of p and q, the straight lines represent the isotopic compositions of the C flow branching into p and q, and are vertically separated by Ω (equ. 8), the difference between the isotope effects.

$$\Omega = -\Delta\delta_q / f_p = \Delta\delta_p / (1 - f_p) = \delta_p - \delta_q \quad (8)$$

where $\Delta\delta_q = (\delta_q - \delta_r)$ and $\Delta\delta_p = (\delta_p - \delta_r)$.

Values of Ω can alternatively be determined by the slope of the regression line of each product. Disagreement between the differently calculated values of Ω would imply

that the C-flow might not be as simple as assumed (e.g. more than two branches). The fractional yields are defined as the follows:

$$f_{ac} = \frac{n(acetate)}{n(acetate) + n(ethanol)} \quad (9)$$

$$f_{lac} = \frac{n(lactate)}{n(lactate) + n(acetate) + n(ethanol)} \quad (10)$$

where n = moles of the accumulated products.

An equation presented by Mariotti et al. (1981) was used to calculate the isotopic effect (ε) associated with the uptake and fermentation of saccharides to pyruvate:

$$\delta_p = \delta_{si} - \varepsilon(1-f)\left[\ln(1-f)\right]/f \quad (11)$$

where δ_{si} = isotope composition of the saccharide at the beginning; δ_p = isotope composition of the pooled products at the instance, when f was determined; and f = fractional yield of the products based on consumption of the saccharide ($0 < f < 1$). Linear regression of δ_p against $(1-f)[\ln(1-f)]/f$ gives ε as the slope. For fermentation, where several products are formed, δ–values of the products other than acetate were not measured directly but were calculated using the fractionation factors derived from the branch point analysis ($\Omega_{ac\text{-}CoA}$ = 17; Ω_{pyr} = 3). Average isotope composition of the products was calculated using equation 12 and 13 based on mass balance equation:

$$\delta_{ac-CoA} = f_{ac}\delta_{ac} + (1-f_{ac})(\delta_{ac} - \Omega_{ac-CoA}) \quad (12)$$

$$\delta_{pyr} = (1-f_{lac})\delta_{ac-CoA} + f_{lac}(\delta_{ac-CoA} - \Omega_{pyr}) \quad (13)$$

Results

Batch experiments

Clostridium papyrosolvens converted the saccharides (sacc) glucose (gluc), cellobiose, and cellulose in a mixed-acid fermentation to the major products acetate (ac), ethanol (etoh), H_2 and CO_2 (Table 1). Additional minor fermentation products were formate (form) and lactate (lac). Carbon recoveries were 108.8 ± 4.1%, 68.7 ± 1.9%, and 64.3 ± 0.5% for glucose, cellobiose, and cellulose, respectively. Since the saccharides were completely consumed, the residual carbon must have been converted into microbial biomass (biom). This biomass yield was apparently higher with cellobiose and cellulose, which is consistent with carbon recoveries in *Clostridium thermocellum* (Strobel, 1995) and *Ruminococcus albus* (Thurston et al., 1993), where cell yields were 30% higher for

cellobiose than for glucose as substrate. In *Clostridium cellulolyticum*, which is closely related to *C. papyrosolvens* (96.6% 16S rDNA gene similarity), cell yields were found to be higher with cellulose than with cellobiose (Desvaux et al., 2000). The increased biomass yield is explained by the expense of less ATP per hexose unit when cellulose or cellobiose rather than glucose are the substrate (Lynd et al., 2002).

Table 1: Product formation and carbon recovery during fermentation of different saccharides by *C. papyrosolvens* in batch pure cultures and cocultures with hydrogenotrophic methanogenic archaea.

substrate	organisms	T [°C]	saccharide [mM]	Lactate [mmol]	Formate [mmol]	Acetate [mmol]	Ethanol [mmol]	TIC [mmol]	Hydrogen [mmol]	Methane [mmol]	Carbon recovery [%]
glucose ($\delta^{13}C$ = -10.67‰)	*C. papyrosolvens*	15	2.22	0.002 ± 0.000	0.017 ± 0.001	0.187 ± 0.006	0.064 ± 0.003	0.282 ± 0.010	0.309 ± 0.004		121.1
			4.44	0.001 ± 0.001	0.015 ± 0.003	0.357 ± 0.018	0.098 ± 0.004	0.575 ± 0.040	0.651 ± 0.035		112.8
			8.88	0.001 ± 0.001	0.010 ± 0.000	0.602 ± 0.001	0.158 ± 0.014	1.044 ± 0.027	1.132 ± 0.002		98.0
	C. papyrosolvens	30	2.22	0.000 ± 0.000	0.039 ± 0.001	0.143 ± 0.004	0.092 ± 0.001	0.284 ± 0.006	0.217 ± 0.002		119.0
			4.44	0.000 ± 0.000	0.084 ± 0.001	0.238 ± 0.002	0.166 ± 0.002	0.447 ± 0.017	0.368 ± 0.003		100.7
			8.88	0.010 ± 0.001	0.168 ± 0.001	0.407 ± 0.005	0.336 ± 0.006	0.907 ± 0.032	0.635 ± 0.010		101.1
cellobiose ($\delta^{13}C$ = -25.11‰)	*C. papyrosolvens*	30	1.17	0.006 ± 0.000	0.020 ± 0.002	0.140 ± 0.001	0.070 ± 0.001	0.143 ± 0.006	0.160 ± 0.001		68.7
			2.34	0.022 ± 0.001	0.073 ± 0.002	0.357 ± 0.001	0.089 ± 0.002	0.254 ± 0.005	0.287 ± 0.003		73.2
			4.67	0.090 ± 0.004	0.151 ± 0.005	0.522 ± 0.013	0.155 ± 0.017	0.432 ± 0.017	0.482 ± 0.004		64.0
cellulose ($\delta^{13}C$ = -25.23‰)	*C. papyrosolvens*	30	2.81	0.014 ± 0.003	ND	1.344 ± 0.005	0.587 ± 0.023	1.540 ± 0.010	3.787 ± 0.050		64.3
glucose ($\delta^{13}C$ = -10.67‰)	*C. papyrosolvens*/ *M. hungatei*	30	2.22	0.031 ± 0.002	ND	0.119 ± 0.005	0.037 ± 0.001	0.271 ± 0.006	0.00 ± 0.000	0.07 ± 0.003	84.9
			4.44	0.074 ± 0.024	ND	0.221 ± 0.003	0.069 ± 0.008	0.370 ± 0.008	0.00 ± 0.000	0.13 ± 0.003	80.9
			8.88	0.191 ± 0.017	ND	0.470 ± 0.021	0.133 ± 0.017	0.600 ± 0.056	0.00 ± 0.001	0.26 ± 0.014	89.3
	C. papyrosolvens/ *M. bryantii*	30	2.22	0.026 ± 0.011	0.055 ± 0.006	0.130 ± 0.003	0.038 ± 0.004	0.492 ± 0.019	0.00 ± 0.000	0.06 ± 0.004	105.3
			4.44	0.089 ± 0.024	0.072 ± 0.031	0.230 ± 0.012	0.044 ± 0.015	0.582 ± 0.052	0.00 ± 0.000	0.12 ± 0.017	92.7
			8.88	0.211 ± 0.015	0.162 ± 0.007	0.407 ± 0.001	0.099 ± 0.008	0.631 ± 0.017	0.00 ± 0.000	0.22 ± 0.004	89.3
cellobiose ($\delta^{13}C$ = -25.11‰)	*C. papyrosolvens*/ *M. hungatei*	30	1.17	0.024 ± 0.009	ND	0.113 ± 0.004	0.035 ± 0.001	0.264 ± 0.006	0.00 ± 0.000	0.06 ± 0.002	73.3
			2.34	0.013 ± 0.007	ND	0.193 ± 0.002	0.092 ± 0.004	0.356 ± 0.006	0.00 ± 0.000	0.13 ± 0.002	62.5
			4.67	0.033 ± 0.005	ND	0.381 ± 0.020	0.203 ± 0.012	0.600 ± 0.005	0.00 ± 0.000	0.24 ± 0.007	62.6
	C. papyrosolvens/ *M. bryantii*	30	1.17	0.007 ± 0.004	0.019 ± 0.005	0.116 ± 0.006	0.036 ± 0.004	0.506 ± 0.014	0.00 ± 0.000	0.07 ± 0.003	80.7
			2.34	0.012 ± 0.008	0.066 ± 0.013	0.192 ± 0.005	0.086 ± 0.002	0.567 ± 0.005	0.00 ± 0.000	0.11 ± 0.003	69.8
			4.67	0.041 ± 0.005	0.164 ± 0.023	0.341 ± 0.009	0.183 ± 0.015	0.686 ± 0.006	0.00 ± 0.000	0.19 ± 0.006	66.9

ND: not detected

In Table 1, the patterns of product formation for the different substrates and different growth conditions illustrate the metabolic flexibility of *C. papyrosolvens*. Fermentation of glucose resulted in lower amounts of H_2 at 30°C versus 15°C at all substrate concentrations, and instead resulted in the accumulation of increased amounts of formate. Ethanol was a relatively important product on glucose, but lactate on cellobiose. Different saccharide concentrations did not influence the pattern of product formation on glucose, but on cellobiose f_{lac} increased with the saccharide concentration (Table 2). The fermentation pattern on cellulose was similar as on glucose, but no formate was produced.

In addition to the pure culture experiments, *C. papyrosolvens* was also grown in methanogenic coculture with either *M. hungatei* or *M. bryantii* (Table 1). *M. hungatei* and *M. bryantii* are both hydrogenotrophic methanogens, i.e. they produce CH_4 from H_2/CO_2. *M. hungatei* also uses formate as alternative substrate for CH_4 production. However, they do not use acetate for CH_4 production and assimilate only small amounts of it into biomass. To be able to generate a carbon mass balance for *C. papyrosolvens*, total inorganic carbon (TIC) produced during fermentation was calculated as the sum of produced methane and remaining TIC at the end of the incubation. Methane produced by methanogenic archaea increased with saccharide concentration in both cocultures. Methane yields were lower in the cocultures with *M. bryantii* compared to those with *M. hungatei*, because formate was not metabolized by *M. bryantii*. Carbon recoveries were 90.4 ± 3.4% and 69.3 ± 2.8% for glucose and cellobiose, respectively, showing the same trend as in pure culture (Table 1).

Although the same cultures were used for inoculation, the product patterns were strongly different between the different saccharides. With glucose, lactate was a major fermentation product and increased with substrate concentration to more than 20% of initial glucose carbon at the highest concentration. The f_{ac} and f_{lac} in the coculture experiments were larger than those in the pure culture experiments indicating that the electron flow was preferentially into lactate rather than ethanol (Table 2). The larger f_{ac}, in particular, is remarkable, since acetate formation allows ATP production by substrate level phosphorylation (Gottschalk, 1986). Increased f_{ac} is characteristic for a fermentation balance, in which H_2 partial pressures are kept at low values (Dolfing, 1988). With cellobiose, the fermentation pattern in coculture was similar as in pure culture. Lower yields of formate in the coculture with *M. bryantii* were due to the consumption of produced H_2 and the concomitantly lower conversion of $H_2 + CO_2$ to formate.

Table 2: Isotope ratios and fractionation factors of products of fermentation of different saccharides by *C. papyrosolvens* in batch pure cultures and cocultures with hydrogenotrophic methanogenic archaea. f_{ac} and f_{lac} are calculated from Table 1 using equations (9) and (10).

substrate	organisms	T [°C]	saccharide [mM]	f_{ac}	f_{lac}	pH	δ_{ac} [‰]	δ_{TIC} [‰]	δ_{biom} [‰]	$\alpha_{sacc/ac}$	$\alpha_{sacc/TIC}$	$\alpha_{sacc/biom}$
glucose ($\delta^{13}C$ = -10.67‰)	*C. papyrosolvens*	15	2.22	0.74	0.01	7.02 ± 0.01	-6.72 ± 1.87	-9.78 ± 1.02	-14.06 ± 0.16	0.996	0.999	1.003
			4.44	0.79	0.00	6.86 ± 0.01	-4.98 ± 0.27	-9.54 ± 0.23	-16.09 ± 0.13	0.994	0.999	1.006
			8.88	0.79	0.00	6.66 ± 0.01	-4.27 ± 0.11	-10.91 ± 0.35	-16.52 ± 0.16	0.994	1.000	1.006
	C. papyrosolvens	30	2.22	0.61	0.00	7.02 ± 0.01	-4.17 ± 0.43	-8.43 ± 0.14	-14.67 ± 1.35	0.993	0.998	1.004
			4.44	0.59	0.00	6.86 ± 0.01	-2.69 ± 0.3	-7.30 ± 0.31	-12.10 ± 0.14	0.992	0.997	1.001
			8.88	0.55	0.01	6.66 ± 0.01	-4.21 ± 0.22	-7.30 ± 0.14	-12.09 ± 0.04	0.994	0.997	1.001
cellobiose ($\delta^{13}C$ = -25.11‰)	*C. papyrosolvens*	30	1.17	0.66	0.03	7.04 ± 0.01	-16.32 ± 0.86	-19.70 ± 0.31	-25.17 ± 0.15	0.991	0.994	1.000
			2.34	0.80	0.05	6.93 ± 0.01	-18.45 ± 0.55	-18.89 ± 0.11	-26.24 ± 0.00	0.993	0.994	1.001
			4.67	0.77	0.12	6.64 ± 0.02	-20.58 ± 0.52	-18.34 ± 0.09	-26.80 ± 0.11	0.995	0.993	1.002
cellulose ($\delta^{13}C$ = -25.23‰)	*C. papyrosolvens*	30	2.81	0.70	0.01	6.950 ± 0.020	-22.46 ± 0.25	-22.61 ± 0.03		0.997	0.997	
glucose ($\delta^{13}C$ = -10.67‰)	*C. papyrosolvens/ M. hungatei*	30	2.22	0.76	0.17	7.07 ± 0.00	-12.23 ± 1.39	-3.63 ± 0.07		1.002		
			4.44	0.76	0.20	6.92 ± 0.02	-10.70 ± 0.35	-1.23 ± 0.22		1.000		
			8.88	0.78	0.24	6.62 ± 0.01	-10.67 ± 0.41	1.10 ± 0.83		1.000		
	C. papyrosolvens/ M. bryantii	30	2.22	0.77	0.13	7.07 ± 0.03	-10.78 ± 0.54	-4.77 ± 0.66		1.000		
			4.44	0.84	0.25	6.93 ± 0.01	-11.97 ± 0.88	-2.53 ± 0.65		1.001		
			8.88	0.80	0.29	6.72 ± 0.01	-12.05 ± 0.04	4.36 ± 0.3		1.001		
cellobiose ($\delta^{13}C$ = -25.11‰)	*C. papyrosolvens/ M. hungatei*	30	1.17	0.76	0.14	7.04 ± 0.01	-20.22 ± 0.27	-10.59 ± 0.62		0.995		
			2.34	0.68	0.05	6.92 ± 0.01	-21.59 ± 0.12	-10.98 ± 0.27		0.996		
			4.67	0.65	0.05	6.64 ± 0.01	-21.10 ± 0.27	-9.68 ± 0.7		0.996		
	C. papyrosolvens/ M. bryantii	30	1.17	0.76	0.05	7.13 ± 0.01	-21.40 ± 0.74	-10.61 ± 0.18		0.996		
			2.34	0.69	0.04	6.99 ± 0.01	-21.10 ± 0.56	-12.55 ± 1.6		0.996		
			4.67	0.65	0.07	6.72 ± 0.02	-20.09 ± 0.50	-9.60 ± 1.23		0.995		

Cocultures on cellulose were only performed with *M. bryantii* and were not run to completion (Figure 2). Even at the relatively higher cellulose concentration (22.47 mM expressed as hexose equivalent) in the coculture than the pure culture, formation of formate was almost not observed. In the beginning (< 600 h), H_2 accumulated and the fermentation pattern was similar as observed in pure culture. Later on, the H_2 partial pressure (p_{H2}) decreased and f_{ac} increased from 0.68 to values larger than 0.8 (Figure 2). This effect of p_{H2} on f_{ac} was also observed in pure culture (relation included in Fig. 3A).

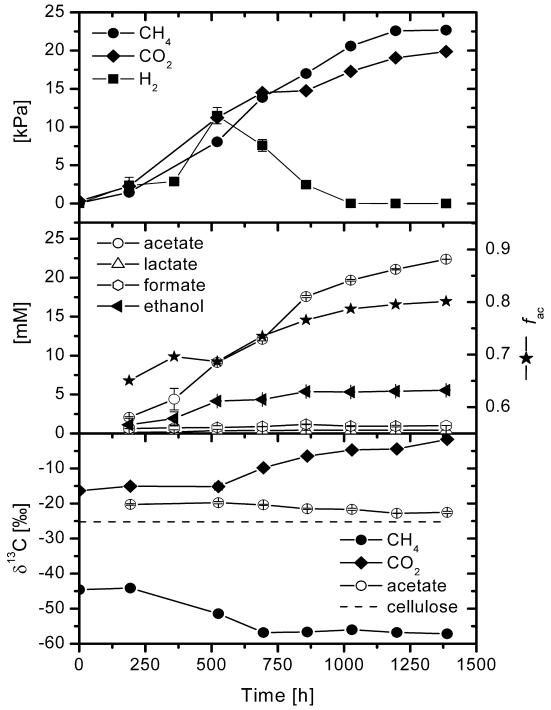

Figure 2: Coculture of *C. papyrosolvens* and *M. bryantii* growing on cellulose as the only substrate. After a lag phase hydrogen formed by *C. papyrosolvens* was consumed by *M. bryantii* leading to a shift of the fermentation pattern to acetate (increasing f_{ac}) concomitant with a decrease in δ_{ac}. Strong fractionation of methanogenesis causes ^{13}C enrichment of CO_2; mean ± SE, n = 3.

In pure cultures of *C. papyrosolvens*, acetate was generally enriched in ^{13}C ($\alpha_{sacc/ac}$ = 0.992 – 0.997), with the smallest fractionation on cellulose (Table 2). Temperature did not influence the fractionation factor, whereas increasing cellobiose concentrations resulted in decreasing fractionation ($\alpha_{sacc/ac}$ increased from 0.991 to 0.995). The TIC formed from glucose was slightly enriched in ^{13}C or was not fractionated, while that from cellobiose exhibited a stronger enrichment in ^{13}C (Table 2). Fractionation into biomass was normal and slightly stronger for glucose than for cellobiose. In the methanogenic cocultures, only the fractionation of saccharide into acetate could be

evaluated, since TIC was enriched in ^{13}C due to the strong isotope effect associated with hydrogenotrophic methanogenesis (Table 2). Independent of the methanogenic partner and the saccharide concentration, a normal ($\alpha_{sacc/ac}$ = 1.000 – 1.002) and an inverse ($\alpha_{sacc/ac}$ = 0.995 – 0.996) fractionation was observed for glucose and cellobiose, respectively. In the methanogenic cocultures grown on cellulose, δ_{ac} was initially similar to that observed in pure culture, but eventually decreased with increasing f_{ac}, becoming close to that of $\delta_{cellulose}$ (Fig. 2).

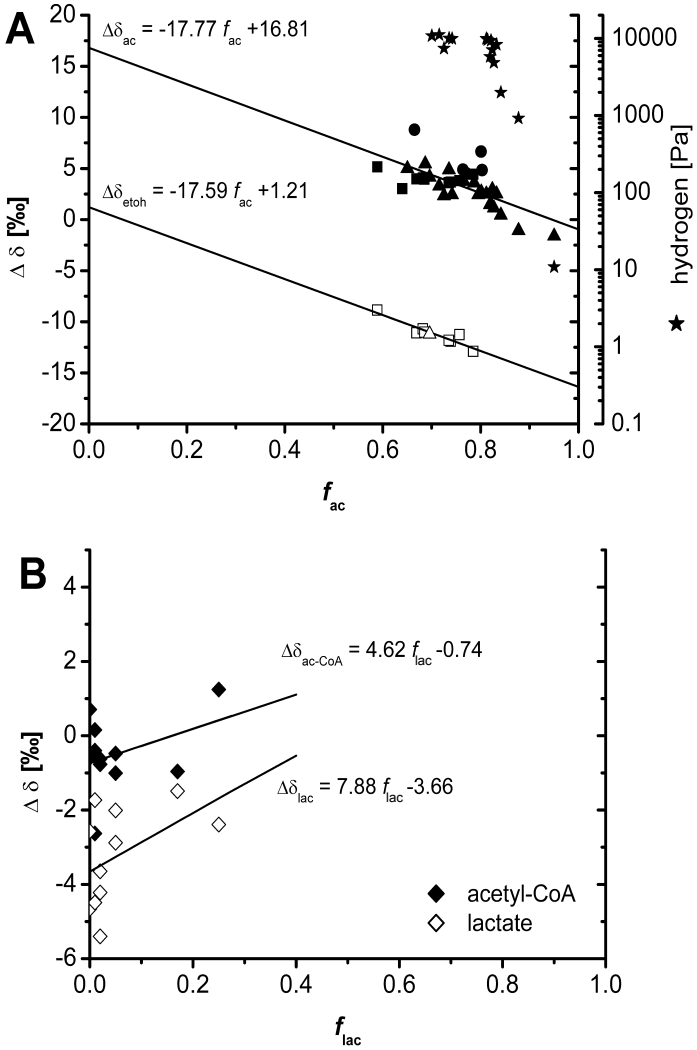

Figure 3: Split of isotope carbon flow at the branch points (A) acetyl-CoA and (B) pyruvate (see scheme in Fig.1). Fractionation is shown by the slope and the vertical difference between the product regression lines. (A) Strong isotope fractionation occurred between acetate and ethanol, where acetate was the ^{13}C-enriched product. f_{ac} increased with decreasing p_{H2} for *C. papyrosolvens* grown on cellulose. Δδ–values of acetate and ethanol are shown for the different saccharides: ■, acetate from glucose; □, ethanol from glucose; ●, acetate from cellobiose; ▲, acetate from cellulose; △, ethanol from cellulose. (B) Small isotope fractionation between acetyl-CoA and lactate, where lactate was the ^{13}C-depleted product.

Chemostat experiments

C. papyrosolvens was grown in glucose-limited chemostat culture under a relatively high (64.10 ± 5.12%) and a relatively low p_{H2} (0.59 ± 0.18%). Concentration and isotopic composition of the fermentation products, turbidity of the culture (OD_{600}), and fractionation factors are shown form for $0.02 \leq D \leq 0.25$ h^{-1} in Fig. 4 and Table 3. To be able to generate a carbon mass balance (Table 3), TIC produced during fermentation was calculated by

$$n(TIC) = \frac{n(glucose) - n(lactate)}{3} - n(formate) \tag{14}$$

where n is given as mol of carbon.

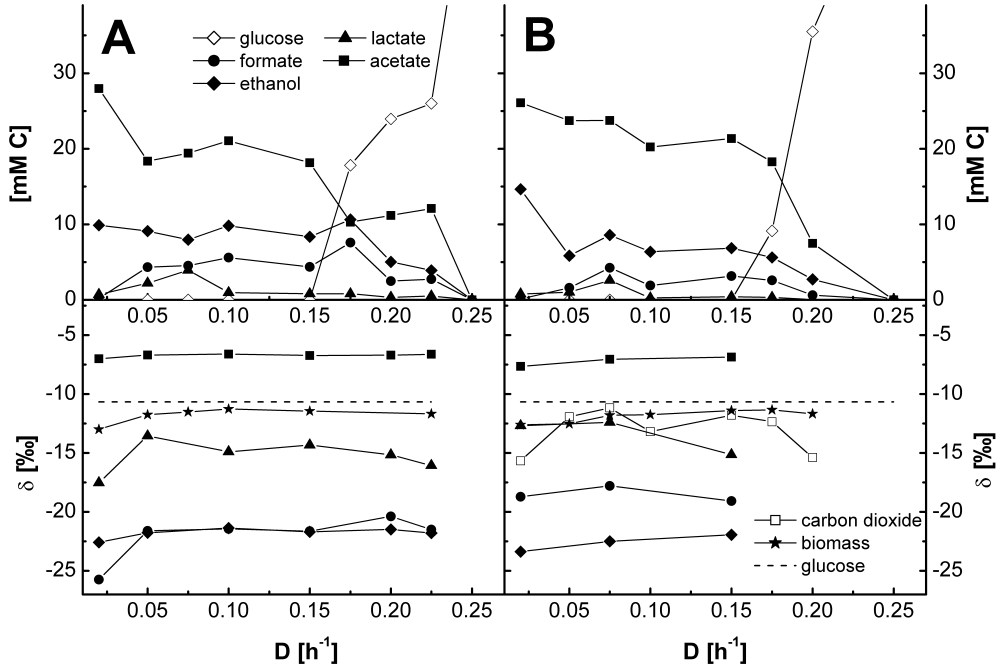

Figure 4: Glucose-limited chemostat culture of *C. papyrosolvens* at $0.02 < D < 0.25$ h^{-1}. Upper panels show steady state concentrations of glucose and dissolved products in the chemostat, lower panels show the carbon isotope composition of biomass and products. (A) high hydrogen setup, (B) low hydrogen setup; growth rate (= D) did not influence carbon isotope fractionation, if glucose was completely consumed ($D \leq 0.15$ h^{-1}).

Table 3: Growth and isotope fractionation recorded in glucose-limited chemostat cultures of *C. papyrosolvens*.

p_{H2} [%]	dilution rate [h^{-1}]	OD_{600}	carbon recovery [%]	$\alpha_{gluc/ac}$	$\alpha_{gluc/lac}$	$\alpha_{gluc/etoh}$	$\alpha_{gluc/CO2}$	$\alpha_{gluc/biom}$
high	0.020	0.333	97.6	0.996	1.007	1.012	1.005	1.002
(64.1 ± 5.12)	0.050	0.481	82.8	0.996	1.003	1.011	1.000	1.001
	0.075	0.701	85.5				0.998	1.001
	0.100	0.840	86.4	0.996	1.004	1.011	0.997	1.001
	0.150	0.660	78.8	0.996	1.004	1.011	0.998	1.001
	0.175	0.536	89.3					
	0.200	0.556	87.5	0.996	1.005	1.011	0.997	1.001
	0.225	0.544	89.7	0.996	1.005	1.011	0.998	
low	0.020	0.367	102.5	0.997	1.002	1.013	1.005	1.002
(0.59 ± 0.18)	0.050	0.400	84.2				1.001	1.002
	0.075	0.692	91.5	0.996	1.002	1.012	1.000	1.001
	0.100	0.644	78.1				1.003	1.001
	0.150	0.810	81.0	0.996	1.005	1.012	1.001	1.001
	0.175	0.800	83.8				1.002	1.001
	0.200	0.316	89.9				1.005	1.001

At $D \leq 0.15$ h^{-1}, glucose was completely fermented, whereas at higher D the bacteria were not able to completely consume glucose (neither under high nor low p_{H2}), which finally resulted in washout of the cells at D = 0.25 h^{-1}. The product pattern was similar as in the batch cultures with glucose and did not significantly change with D. Absolute amounts of the products, however, varied with the chemostat setup. Slightly higher amounts of ethanol, lactate, and formate were observed at the higher p_{H2} (Fig. 4A), indicating an increased electron flow into reduced fermentation products rather than into acetate. The fractionation to biomass was independent of growth rate and extent of glucose consumption, and was slightly normal ($\alpha_{sacc/biom}$ = 1.001 – 1.002).

At dilution rates ≤ 0.15 h^{-1} (complete consumption of glucose), acetate was generally ^{13}C-enriched giving a narrow range of $\alpha_{sacc/ac}$ = 0.996 – 0.997 (Table 3). The reduced products lactate and ethanol showed normal fractionation ($\alpha_{sacc/lac}$ = 1.002 - 1.007; $\alpha_{sacc/etoh}$ = 1.011 – 1.013). At low p_{H2}, fractionation of glucose to carbon dioxide (here δ_{CO2} rather than δ_{TIC} was used, since equilibrium between the inorganic carbon species did not establish) was normal ($\alpha_{sacc/CO2}$ = 1.000 – 1.005). At high p_{H2}, δ_{CO2} steadily increased with time, and did not stabilize within ten volume changes. Therefore we tested this increase over an extended period. Equilibrium was finally reached after 180 volume changes. The delayed adjustment of the equilibrium was probably due to equilibration between CO_2 and formate and was properly described by a logarithmic function of δ_{CO2} with volume changes

(Fig. 5). Fractionation between CO_2 and formate was calculated from the last three data points in Fig. 5 ($\alpha_{CO2/form} = 1.015$). At dilution rates > 0.15 h^{-1} (incomplete consumption of glucose) and at high p_{H2}, fractionation of ^{13}C was similar as in the other experiments.

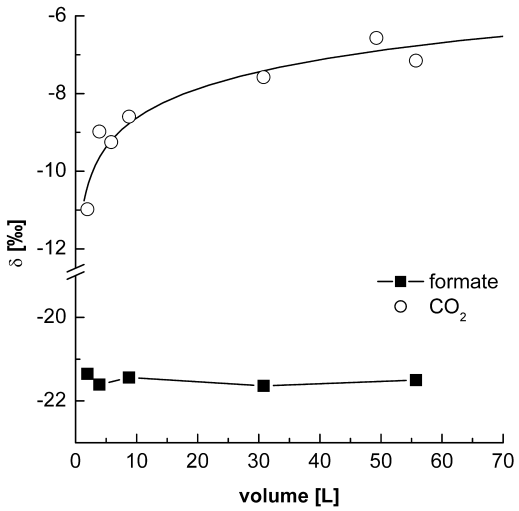

Figure 5: Establishment of isotopic equilibrium between CO_2 and formate in the non-flushed headspace chemostat (high hydrogen setup). Non steady state conditions in the headspace versus steady state conditions in the liquid phase allows ^{13}C enrichment of CO_2 until equilibrium, which is described by a logarithmic curve.

Data analysis

The analysis of isotopic behavior at the branch points (Fig. 1) of the fermentation pathway was based on the equations (6) and (7) (Hayes, 2001). The data are plotted for the branch point acetyl-CoA (ac-CoA) and pyruvate (pyr), respectively (Fig. 3). The fractional yield (*f*) of one of the formed products is plotted against the difference of the isotopic values of product and substrate ($\Delta\delta$). A negative slope indicates that *f* represents the fraction of the product enriched in ^{13}C and vice versa. For the branch point acetyl-CoA, $\delta_r = \delta_{ac\text{-}CoA}$, the ^{13}C-enriched product was acetate and the ^{13}C-depleted product was ethanol. In these experiments, in which only a small fraction of the carbon flow branched into lactate at the upstream branch point pyruvate (Fig. 1), it can be assumed that $\delta_{ac\text{-}CoA} = \delta_{sacc}$. Therefore, we considered for the data analysis only experiments, in which $f_{lac} < 0.05$ (Fig. 3A). We also assumed that the branching of carbon to anabolic reactions had a negligible effect on carbon isotope fractionation since $\alpha_{sacc/biom} \approx 1$ (Table 2 and 3). The value of $\Omega_{ac\text{-}CoA}$ at the branch point acetyl-CoA is given by the difference between δ_{ac} and

δ_{etoh} (equ. 8) resulting in $\Omega_{ac\text{-}CoA}$= 15.31 ± 0.86 (average ± SD). Alternatively, $\Omega_{ac\text{-}CoA}$ was computed from the slope of the regression lines in Fig. 3 (equ. 7), giving:

$$\Delta\delta_{ac} = (\delta_{ac-CoA} - \delta_{ac}) = -17.77 f_{ac} + 16.81 \qquad (r^2 = 0.68;\ SD = 1.48) \tag{15}$$

$$\Delta\delta_{etoh} = (\delta_{ac-CoA} - \delta_{etoh}) = -17.59 f_{ac} + 1.21 \qquad (r^2 = 0.93;\ SD = 0.45) \tag{16}$$

$\Omega_{ac\text{-}CoA}$ determined from the slopes of equations (15) and (16) agrees well, and was only slightly higher than the $\Omega_{ac\text{-}CoA}$ determined by difference.

For saccharide fermentation via the EMP pathway the carbon atoms in acetyl-CoA correspond to positions 1, 2, 5 and 6 in the glucose-units. Thus, the difference in $\delta_{C1,2,5,6}$ and δ_{sacc} can theoretically be seen as the intercept of the regression line at f_{ac} = 1. However, the accuracy of the data was too low for interpretation of the intramolecular composition of the saccharides and its effect on isotope fractionation.

For the branch point pyruvate (Fig. 1), lactate and acetyl-CoA were the alternative products, with $\delta_r = \delta_{sacc}$, $\delta_p = \delta_{lac}$, and $\delta_q = \delta_{ac\text{-}CoA}$. $\delta_{ac\text{-}CoA}$ was calculated by the following mass balance equation:

$$\delta_{ac-CoA} = f_{ac}\delta_{ac} + (1 - f_{ac})\delta_{etoh} \tag{17}$$

Lactate was depleted in ^{13}C in comparison to acetyl-CoA, so that $\Delta\delta_{lac}$ and $\Delta\delta_{ac\text{-}CoA}$ increased with increasing f_{lac} (Fig. 3B). The value of $\Omega_{pyruvate}$ at the branch point was obtained from the difference between $\delta_{ac\text{-}CoA}$ and δ_{lac} (equ. 8), giving Ω_{pyr} = 2.78 ± 1.57 (average ± SD), and alternatively from the slope of the regression lines (equ. 7):

$$\Delta\delta_{ac-CoA} = (\delta_{pyr} - \delta_{ac-CoA}) = 4.62 f_{lac} - 0.74 \qquad (r^2 = 0.37;\ SD = 1.22) \tag{18}$$

$$\Delta\delta_{lac} = (\delta_{pyr} - \delta_{lac}) = 7.88 f_{lac} - 3.66 \qquad (r^2 = 0.48;\ SD = 0.98) \tag{19}$$

Since only a limited number of incubations exhibited a sufficiently large f_{lac} (only cocultures grown on glucose had high f_{lac}; Table 2), Ω_{pyr} was not well constrained. Since Ω_{pyr} was relatively small, the experimental and analytical error had a stronger influence on Ω_{pyr} than in the case of $\Omega_{ac\text{-}CoA}$ at the downstream branch point. However the isotopic depletion of lactate was consistent throughout the different experiments and the intercept of the regression line of $\delta_{ac\text{-}CoA}$ was close to zero, which is in agreement with the assumption of no change in isotopic composition from the saccharide to pyruvate. The preferential isotope flow through the fermentation network of *C. papyrosolvens* is schematically summarized in Fig. 1.

To address the question, whether there is a potential fractionation associated with the linear reactions involved in uptake of saccharide and catabolism to pyruvate, the first branch point, we evaluated those data, in which the saccharide substrate was not completely consumed, using equation (11) derived by Mariotti et al. (1981). For this purpose δ_{pyr} was calculated using equation (12) and (13), based on the mass balance equation and the fractionation factors (Ω) determined at the branch points.

In Fig. 6, δ_{pyr} is plotted as a function of $(1-f)[\ln(1-f)]/f$, with f = fraction of saccharide-glucose consumed. The slope of the regression gives $-\varepsilon$ ($\varepsilon_{glucose}$ = -18.46 ± 2.99‰ and $\varepsilon_{cellobiose}$ = -5.94 ± 1.88‰; mean ± SD), which can be transformed to α–values. The thus determined $\alpha_{sacc/pyr}$ were 1.018 and 1.006 for glucose and cellobiose, respectively (Fig. 6). After quantitative conversion of the saccharide (i.e. $f = 1$; $(1-f)[\ln(1-f)]/f = 0$), the δ_{pyr} was –10.70‰ and – 25.82‰ for glucose and cellobiose, respectively, as determined by the regression line. This is in good agreement with the δ_{si} (δ_{gluc} = -10.67; $\delta_{cellobiose}$ = -25.11). For cellulose as substrate, δ_{pyr} did not change with f, which means that no fractionation occurred during uptake and catabolism to pyruvate.

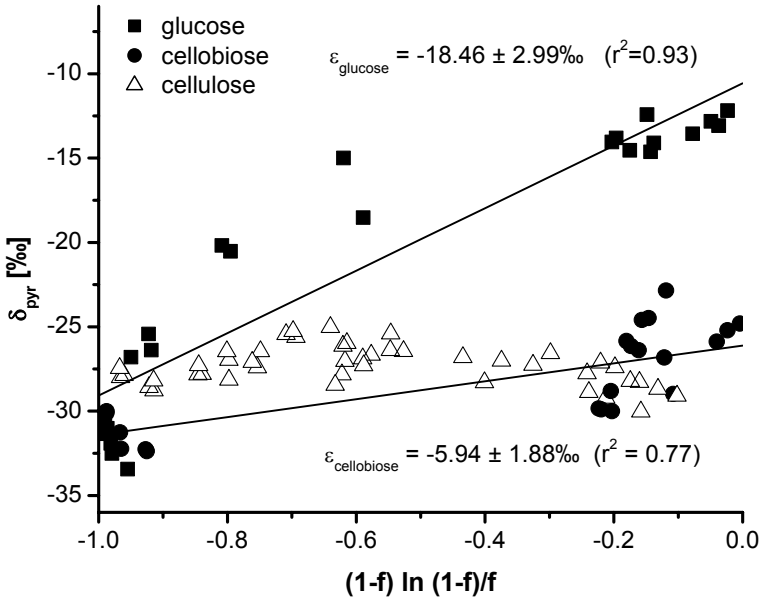

Figure 6: Isotope fractionation during the course of fermentation to pyruvate for different saccharides by *C. papyrosolvens* fitted to the equation derived by Mariotti et al. (1981). The soluble substrates glucose and cellobiose exhibited fractionation, whereas no fractionation occurred with the polysaccharide cellulose. δ_{pyr} is the isotope ratio of all products, calculated by equations (12) and (13).

Discussion

Stable carbon isotope fractionation during fermentation of saccharides was studied in *C. papyrosolvens*. Isotope fractionation can occur in linear reactions, such as substrate uptake, if the substrate is not completely consumed. More importantly, however, isotope fractionation generally occurs at branch points in the metabolic path.

Isotope fractionation during the linear part of the metabolic pathway

Saccharides are linearly metabolized in *C. papyrosolvens* to the first branch point of the fermentation path, i.e. pyruvate (Fig. 1). Fractionation between saccharide and pyruvate was found for the soluble saccharides glucose and cellobiose, but not for insoluble cellulose (Fig. 6). Fractionation was stronger for glucose than for cellobiose. The observed fractionation during utilization of glucose and cellobiose was likely due to the fractionation occurring during uptake of the saccharides into the bacterial cell. No fractionation was observed for cellulose utilization (Fig. 6). Cellulose is hydrolyzed at the cellulosome by expenditure of ATP (Lynd et al., 2002), and the resulting oligomers and glucose are then transported into the cell. We assume, that after cellulose hydrolysis the products are taken up before a larger pool of molecules establishes, so that uptake happens quantitatively without fractionation. A rather fast uptake appears to be a reasonable strategy for the microbial cell, as it avoids giving competitors access to the easily degradable hydrolysis products. In natural anaerobic systems glucose is usually present at only very low concentrations (Chidthaisong and Conrad, 2000; King and Klug, 1982), so that quantitative uptake of the products of polysaccharide hydrolysis without isotope fractionation may be the rule. Indeed, hydrolysis of polysaccharides has been found to be the rate-limiting step in the degradation of complex organic matter (Billen, 1982; Degens and Mopper, 1975; Fey and Conrad, 2003). Therefore, it is reasonable to assume that fractionation during uptake of saccharides does not occur in natural environments. Consequently, experiments with quantitative conversion of saccharides are adequate for investigation of the stable carbon isotope fractionation associated with the branch points in the fermentation path.

Division of carbon isotopes at branches in the metabolic pathway

Since in *C. papyrosolvens* the fermentation path of saccharides is linear until the formation of pyruvate, δ_{pyr} - integrated over the complete fermentation - equals δ_{sacc}. At the first branch point pyruvate, the carbon flow is channeled to the products lactate,

acetyl-CoA + CO_2, and biomass. Lactate was generally ^{13}C-depleted with respect to acetyl-CoA, indicating a stronger preference for ^{12}C by the lactate dehydrogenase than the pyruvate ferredoxin oxidoreductase (Fig. 3B). The saccharides were assumed to have a homogenous intramolecular isotopic composition. Yet for maize and sugar beet, the isotopic difference between total glucose and the carbon positions (i.e., C-1, 2, 5, 6) forming acetyl-CoA ($\delta_{sacc} - \delta_{C1,2,5,6}$) was found to be 2.1 and 4.1‰, respectively (Rossmann et al., 1991). If the saccharides used in our experiments had a similar intramolecular isotope distribution, the Ω_{pyr} determined by the vertical difference between δ_{lac} and $\delta_{ac\text{-}CoA}$ or the slope of the regression line of $\delta_{ac\text{-}CoA}$ in Fig. 3B would be affected. However, the slope determined from the regression line of $\Delta\delta_{lac}$ should still represent the true Ω_{pyr}, since lactate contains all the 3 carbon atoms of pyruvate. Although the slope of the regression line of δ_{lac} suggested a larger Ω_{pyr} (i.e., 7.9‰), than the slope of the regression line of $\delta_{ac\text{-}CoA}$ (i.e., 4.6‰), both regressions were only weak ($r^2 < 0.5$) and thus, the values of Ω_{pyr} not very accurate. If we consider the depletion in ^{13}C (i.e., 2.1 - 4.1‰) at the positions in the glucose that are later converted to acetyl-CoA and the vertical difference between the regression lines of $\Delta\delta_{lac}$ and $\Delta\delta_{ac\text{-}CoA}$ in Fig. 3b, the true Ω_{pyr} may range between 4.9 and 8.7‰.

Carbon dioxide is produced by decarboxylation of pyruvate and should retain the isotopic composition of positions C-3 and C-4 of glucose, being enriched in ^{13}C relative to the other positions. Therefore, the isotopic composition of TIC should reflect that of C-3 and C-4 of glucose in those experiments, in which only small amounts of lactate were formed and the CO_2 was not further converted to formate. In the pure cultures with glucose at 15°C, in which lactate and formate formation was very low (Table 1), δ_{TIC} indicates slight ^{13}C enrichment at C-3 and C-4 of glucose (Table 2). At these low f_{lac} (i.e. 0.00 - 0.01) $\delta_{ac\text{-}CoA}$ was slightly depleted in ^{13}C with respect to δ_{gluc} (Fig 3B). This is in agreement with the relative ^{13}C depletion of $\delta_{C1,2,5,6}$ in glucose. Production of formate and lactate in the other pure culture experiments resulted, as expected, in a decrease of $\alpha_{sacc/TIC}$ because of the fractionation at the branch point pyruvate and the incomplete conversion of TIC to formate.

At the second branch point acetyl-CoA (Fig. 1), carbon flow splits to the formation of acetate (via acetyl-phosphate), ethanol (via acetaldehyde), and biomass. Ethanol was generally ^{13}C-depleted, resulting in a relatively high $\Omega_{ac\text{-}CoA}$, which was consistently

determined by both the vertical difference and the slopes of the regression lines of $\Delta\delta_{etoh}$ and $\Delta\delta_{ac}$ (Fig. 3A).

Acetyl-CoA as well as pyruvate is also a precursor of biomass. The carbon flow to biomass at these two branch points was not quantified in this study, so that the relative significance of isotopic change caused by this additional branch could not be considered. Moreover, knowledge on fractionation to the different cell components is limited. For fungi grown on different sugars slight fractionation against ^{12}C was found during the synthesis of amino acids (Abraham and Hesse, 2003), but no research of this kind has been done in bacteria. Fatty acids exhibit in general a slight depletion in ^{13}C with respect to the substrate (Abraham et al., 1998). Since the $\alpha_{sacc/biom}$ observed in our experiments was only small and since in anaerobic microorganisms the carbon flow into anabolic versus catabolic reactions is also relatively small, the error introduced by ignoring biomass formation for calculation of Ω_{pyr} and $\Omega_{ac\text{-}CoA}$ should be relatively small.

Hydrogen formate lyase reversibly catalyzes the conversion of $H_2 + CO_2$ to formate. The formation of formate observed in our experiments was probably caused by CO_2 reduction. The reaction of $H_2 + CO_2$ to formate is not quantitative, so that CO_2 was still present. Since ^{12}C is generally preferred in reactions with primary isotope effects, the direction, in which the reaction occurs, could be confirmed by the following observations. Formation of formate was increased at 30°C, and well correlated with a slight decrease in $\alpha_{sacc/TIC}$ (Table 1). In chemostat cultures at high p_{H2}, δ_{CO2} increased with time until a stable value was reached (Fig. 5). The non-flushed headspace created a non-steady state situation for gaseous CO_2, while all dissolved fermentation products were at steady state. Due to the preferential formation of formate from $^{12}CO_2$, CO_2 in the headspace became enriched in ^{13}C. Isotopic equilibrium of the reversible reaction was not established before 180 changes in the culture volume.

Carbon flow determines isotope fractionation to the products

In our experiments we found that variations in temperature, type of substrate, and initial substrate concentration did not directly influence the carbon isotope fractionation (Table 1), but resulted in strong shifts in the carbon flow at the branch points, which in turn affected the isotopic composition of the products. The metabolic flexibility of *C. papyrosolvens* allowed these relative changes in carbon flow, so that the isotopic

composition of the products varied to some extent, although the fractionation factors to the products at the branch points were constant (Hayes, 2001).

Growth rate is often considered as an important variable affecting the intrinsic isotope fractionation of an organism (Henn et al., 2002; Londry and Des Marais, 2003). However, little is known about the effect of growth rate, since it is difficult to control in batch culture. Here, using chemostat cultures, fractionation by *C. papyrosolvens* was found to be independent of growth rate in the range investigated (Fig. 4). An effect would actually be expected only if a change of the metabolic pathway was associated with a change in growth rate, or if different enzymes (isoenzymes) catalyzed the same reactions at the different growth rates and had different fractionation characteristics. From our experiments we conclude that if there were isoenzymes involved, they did not differ in their discrimination of carbon isotopes.

We also tested the influence of the p_{H2}, e.g. by running chemostat cultures at high and low p_{H2} (Fig. 4; Table 2) and by growing cocultures with H_2-consuming methanogens (Fig.2; Table 1). The H_2 partial pressure had a strong effect on carbon flow in *C. papyrosolvens* and thus also on carbon isotope fractionation. The strong effect of p_{H2} is a general feature for carbon flow in fermenting microorganisms and anoxic environments (Dolfing, 1988; Schink, 1997; Stams, 1994; Zeikus, 1983). In *C. papyrosolvens*, pyruvate is decarboxylated by pyruvate-ferredoxin oxidoreductase. During this reaction ferredoxin is reduced, which has a very low redox potential ($E^{o\prime}$ = -0.41 V) that allows the formation of hydrogen even at high p_{H2} (Gottschalk, 1986). Our experiments confirmed that formation of H_2 occurred up to very high partial pressures as expected. Furthermore, we observed an increase in acetate formation at low p_{H2}. This change is only slightly expressed in the different chemostat setups, but in the cocultures growing on cellulose acetate was the almost exclusive product as soon as a low p_{H2} was reached. Removal of H_2 thus channeled the carbon flow into acetate, which is a preferred fermentation product, since it allows generation of additional ATP by substrate chain phosphorylation (Gottschalk, 1986). It is well known from various culture experiments that removal of H_2 results in preferential production of acetate (Dolfing, 1988; Schink, 1997; Stams, 1994; Zeikus, 1983).

A low p_{H2} is also characteristic for natural conditions in anoxic environments. This characteristic allows us to narrow down the isotopic composition of acetate produced by primary fermentation in the environment. Considering the carbon flow at the two branch points (Fig. 1), very low amounts of lactate should be produced, yielding acetyl-CoA

isotopically similar to pyruvate, so that the $\delta^{13}C$ of the produced acetate will almost exclusively be determined by the branching of carbon flow at acetyl-CoA. There, p_{H2} determines f_{ac} and in the following δ_{ac} (p_{H2} included in Fig. 3A for *C. papyrosolvens* grown on cellulose). Since hydrogen is only present at very low amounts in most anoxic soils and sediments, we may expect a high f_{ac} (> 0.85). Consequently, δ_{ac} should be only slightly enriched (< 3‰) in ^{13}C with respect to the substrate used in fermentation, e.g. polysaccharide.

Our study addressed the fractionation of stable carbon isotopes during anaerobic fermentation of different saccharides using *C. papyrosolvens* as model organism. Though this bacterium is a typical fermenting bacterium in anoxic rice field soil and other outdoor environments, other fermenting microorganisms with different metabolic pathways may be more important in other environments. Therefore additional work on other types of microorganisms, e.g. propionate-producing fermenting bacteria, is required. Beside the fractionation factors to the individual fermentation products, we were able to elucidate the fractionation patterns at the metabolic branch points of *C. papyrosolvens*. These branch points are also part of metabolic pathways of other groups of microorganisms, so that the fractionation observed for *C. papyrosolvens* should allow predicting carbon isotope fractionation in other organisms.

Biogeochemical implications

Our results contribute to the understanding of the biogeochemical cycling of $^{13}C/^{12}C$ in carbohydrates, acetate, lactate and ethanol in anoxic environments. Acetate is one of the most important intermediates in anoxic soils and sediments. It is the precursor of 25-50% and 60-70% of methane in organic rich marine and freshwater sediments, respectively (Blair and Carter, 1992). For modeling of isotopic fractionation by acetate-consuming or producing processes in anoxic habitats δ_{ac} must be known. For example, δ_{ac} may be used for determining the contribution of acetoclastic and hydrogenotrophic methanogenesis to methane production (Conrad, 2005) or the relative consumption of acetate in sulfate reduction versus methanogenesis (Blair and Carter, 1992). Despite the importance of δ_{ac}, it can hardly be measured directly in natural environments, since acetate-consuming reactions, like sulfate reduction or acetoclastic methanogenesis, decrease acetate concentrations to steady state values that are usually too low for analysis. Therefore information on the isotope ratio of acetate in natural environments is generally

rare. Only a limited number of studies measured δ_{ac} in the field (Blair et al., 1987; Blair and Carter, 1992) or in incubations (Conrad et al., 2002; Sugimoto and Wada, 1993). Calculation of δ_{ac} from the $\delta^{13}C$ value of total organic carbon (δ_{TOC}) would overcome these analytical problems, if the isotope fractionation during fermentation of TOC is known. Our study presents experimental evidence for only a slight (<3‰) ^{13}C enrichment of acetate with respect of δ_{TOC} at low p_{H2}, which is typical for natural environments at steady state. This confirms earlier assumptions (Blair and Carter, 1992; Gelwicks et al., 1989), now allowing the estimation of δ_{ac} from δ_{TOC} with more confidence.

Compared to acetate, fermentation products such as lactate or ethanol are usually considered to be of less importance in natural environments. However, recent studies indicate that ethanol may be an important intermediate in methanogenic peat mires (Horn et al., 2003; Metje and Frenzel, 2005), which cover a large area in the Northern Latitudes and play an important role in the global methane budget (Harriss et al., 1993). According to our results, a high carbon flow to ethanol would result in production of acetate that is relatively strongly (<17‰) enriched in ^{13}C compared to TOC. Hence, our results might be relevant for interpreting carbon flow and isotope discrimination in anoxic peat.

TOC is the ultimate source of primary fermentation products like acetate and ethanol. The degradable part of TOC mostly consists of polysaccharides. For example, plant material, such as rice straw, is composed of 32-37% cellulose and 29-37% hemicellulose, which are relatively easily degradable, and only 5-15% lignin, which is hardly degraded under anoxic conditions (Shen et al., 1998; Tsutsuki and Ponnamperuma, 1987; Watanabe et al., 1993). We found, that the isotope ratio of the fermentation products of cellulose did not change during the course of fermentation. Similarly, δ_{TOC} was stable with depth in the sediment of Cape Lookout Bight, although the TOC content decreased by up to 30% (Blair and Carter, 1992). The lack of isotope discrimination during the degradation of cellulose in anoxic soils and sediments is probably due to the fact that hydrolysis of polysaccharides is usually the rate-limiting step (Billen, 1982), so that the hydrolysis products (e.g., glucose, cellobiose) are metabolized quantitatively without an isotope effect. However, during fermentation of soluble carbohydrates (e.g., glucose, cellobiose) the isotopically lighter molecules are preferentially selected, as shown in the present study. In summary, we can assume that δ_{TOC} in the environment stays unchanged during its degradation, if it consists primarily of polysaccharides. Then, it is straightforward to calculate the isotope ratio of fermentation products using experimentally

determined fractionation data, such as provided in our study. The δ_{TOC} in sediments and soils is originally that of the TOC of dead plants and algae. δ_{TOC} derived from C_3 plants usually has values around –28‰, whereas from C_4 plants it is about –14‰ (O'Leary, 1988). In this study we found that the isotope fractionation during fermentation to acetate was the same both for saccharides derived from C_3 and C_4 plants, as the ^{13}C isotopic signatures of cellulose and cellobiose were characteristic for C_3 plants and that of glucose for C_4 plants, respectively.

In conclusion, the fractionation characteristics determined for the fermentation of carbohydrates might be useful to calculate from δ_{TOC} the isotopic signatures of the fermentation products, if these cannot be measured directly, and thus help constraining biogeochemical models of C-flux in anoxic environments, such as wetland soils, freshwater and ocean sediments. As an immediate result, we propose to use δ_{TOC} (+ 0 to 3‰) as proxy for δ_{ac} if the latter cannot be measured directly.

Acknowledgements. We thank P. Claus for excellent technical assistance during analysis of ^{13}C data, and W. A. Brand and R. Werner for isotopic analysis of biomass and the carbohydrates. The study was financially supported by the Fonds der Chemischen Industrie.

Reference List

Abraham W. R. and Hesse C. (2003) Isotope fractionations in the biosynthesis of cell components by different fungi: a basis for environmental carbon flux studies. *FEMS Microbiol. Ecol.* **46**, 121-128.

Abraham W. R., Hesse C., and Pelz O. (1998) Ratios of carbon isotopes in microbial lipids as an indicator of substrate usage. *Appl. Environ. Microbiol.* **64**, 4202-4209.

Balabane M., Galimov E., Hermann M., and Letolle R. (1987) Hydrogen and carbon isotope fractionation during experimental production of bacterial methane. *Organic Geochemistry* **11**, 115-119.

Bergmeyer H. U., Bernt E., Schmidt F., and Stork H. (1974) D-glucose. In *Methods of Enzymatic Analysis, vol. 3* (ed. H. U. Bergmeyer). Vol. 3. pp. 1196-1201. Academic Press.

Billen G. (1982) Modelling the processes of organic matter degradation and nutrients recycling in sedimentary systems. In *Sediment Microbiology* (ed. D. B. Nedwell and C. M. Brown). pp. 15-52. Academic Press.

Blair N., Leu A., Munoz E., Olsen J., Kwong E., and Desmarais D. (1985) Carbon isotopic fractionation in heterotrophic microbial metabolism. *Appl. Environ. Microbiol.* **50**, 996-1001.

Blair N. E. and Carter W. D. (1992) The carbon isotope biogeochemistry of acetate from a methanogenic marine sediment. *Geochim. Cosmochim. Acta* **56**, 1247-1258.

Blair N. E., Martens C. S., and Desmarais D. J. (1987) Natural abundances of carbon isotopes in acetate from a coastal marine sediment. *Science* **236**, 66-68.

Botz R., Pokojski H. D., Schmitt M., and Thomm M. (1996) Carbon isotope fractionation during bacterial methanogenesis by CO_2 reduction. *Org. Geochem.* **25**, 255-262.

Brand W. A. (1996) High precision isotope ratio monitoring techniques in mass spectrometry. *J. Mass Spectrom.* **31**, 225-235.

Brooks P. D., Geilmann H., Werner R. A., and Brand W. A. (2003) Improved precision of coupled $\delta^{13}C$ and $\delta^{15}N$ measurements from single samples using an elemental analyser/isotope ratio mass spectrometer combination with a post-column 6-port valve and selective CO_2 trapping; improved halide. *Rapid Commun. Mass Spectrom.* **17**, 1924-1926.

Chidthaisong A. and Conrad R. (2000) Turnover of glucose and acetate coupled to reduction of nitrate, ferric iron and sulfate and to methanogenesis in anoxic rice field soil. *FEMS Microbiol. Ecol.* **31**, 73-86.

Chin K. J., Rainey F. A., Janssen P. H., and Conrad R. (1998) Methanogenic degradation of polysaccharides and the characterization of polysaccharolytic clostridia from anoxic rice field soil. *Syst. Appl. Microbiol.* **21**, 185-200.

Conrad R. (2005) Quantification of methanogenic pathways using stable carbon isotopic signatures: a review and a proposal. *Org. Geochem.* **36**, 739-752.

Conrad R., Klose M., and Claus P. (2002) Pathway of CH_4 formation in anoxic rice field soil and rice roots determined by ^{13}C-stable isotope fractionation. *Chemosphere* **47**, 797-806.

De Niro M. J. and Epstein S. (1977) Mechanism of carbon isotope fractionation associated with lipid-synthesis. *Science* **197**, 261-263.

Degens E. T. and Mopper K. (1975) Early diagenesis of organic matter in marine salts. *Soil Sci.* **119**, 65-72.

Deines P., Langmuir D., and Harmon R. S. (1974) Stable carbon isotope ratios and existence of a gas-phase in evolution of carbonate ground waters. *Geochim. Cosmochim. Acta* **38**, 1147-1164.

Desvaux M., Guedon E., and Petitdemange H. (2000) Cellulose catabolism by *Clostridium cellulolyticum* growing in batch culture on defined medium. *Appl. Environ. Microbiol.* **66**, 2461-2470.

Dolfing J. (1988) Acetogenesis. In *Biology of Anaerobic Microorganisms* (ed. A. J. B. Zehnder). pp. 417-468. Wiley.

Fey A. and Conrad R. (2003) Effect of temperature on the rate limiting step in the methanogenic degradation pathway in rice field soil. *Soil Biol. Biochem.* **35**, 1-8.

Gelwicks J. T., Risatti J. B., and Hayes J. M. (1989) Carbon isotope effects associated with autotrophic acetogenesis. *Org. Geochem.* **14**, 441-446.

Gelwicks J. T., Risatti J. B., and Hayes J. M. (1994) Carbon isotope effects associated with aceticlastic methanogenesis. *Appl. Environ. Microbiol.* **60**, 467-472.

Gottschalk G. (1986) *Bacterial Metabolism*. Springer-Verlag.

Harriss R., Bartlett K., Frolking S., and Crill P. (1993) Methane emissions from northern high-latitude wetlands. In *Biogeochemistry of Global Change. Radiatively Active Trace Gases* (ed. R. S. Oremland). pp. 449-486. Chapman & Hall.

Hayes J. M. (1993) Factors controlling ^{13}C contents of sedimentary organic compounds - Principles and evidence. *Mar. Geol.* **113**, 111-125.

Hayes J. M. (2001) Fractionation of carbon and hydrogen isotopes in biosynthetic processes. *Rev. Mineral. Geochem.* **43**, 225-277.

Hayes, J. M. (2002) Practice and Principles of Isotopic Measurements in Organic Geochemistry.

http://www.gps.caltech.edu/~als/Library/Other%20Stuff/Practice%20and%20Principles.pdf

Henn M. R., Gleixner G., and Chapela I. H. (2002) Growth-dependent stable carbon isotope fractionation by basidiomycete fungi: $\delta^{13}C$ pattern and physiological process. *Appl. Environ. Microbiol.* **68**, 4956-4964.

Horn M. A., Matthies C., Küsel K., Schramm A., and Drake H. L. (2003) Hydrogenotrophic methanogenesis by moderately acid-tolerant methanogens of a methane-emitting acidic peat. *Appl. Environ. Microbiol.* **69**, 74-83.

Hornibrook E. R. C., Longstaffe F. J., and Fyfe W. S. (2000) Evolution of stable carbon isotope compositions for methane and carbon dioxide in freshwater wetlands and other anaerobic environments. *Geochim. Cosmochim. Acta* **64**, 1013-1027.

King G. M. and Klug M. J. (1982) Glucose metabolism in sediments of a eutrophic lake: tracer analysis of uptake and product formation. *Appl. Environ. Microbiol.* **44**, 1308-1317.

Krumböck M. and Conrad R. (1991) Metabolism of position-labeled glucose in anoxic methanogenic paddy soil and lake sediment. *FEMS Microbiol. Ecol.* **85**, 247-256.

Krummen M., Hilkert A. W., Juchelka D., Duhr A., Schluter H. J., and Pesch R. (2004) A new concept for isotope ratio monitoring liquid chromatography/mass spectrometry. *Rapid Commun. Mass Spectrom.* **18**, 2260-2266.

Krylova N. I., Janssen P. H., and Conrad R. (1997) Turnover of propionate in methanogenic paddy soil. *FEMS Microbiol. Ecol.* **23**, 107-117.

Krzycki J. A., Kenealy W. R., De Niro M. J., and Zeikus J. G. (1987) Stable carbon isotope fractionation by *Methanosarcina barkeri* during methanogenesis from acetate, methanol, or carbon dioxide-hydrogen. *Appl. Environ. Microbiol.* **53**, 2597-2599.

Leschine S. B. and Canaleparola E. (1983) Mesophilic cellulolytic clostridia from freshwater environments. *Appl. Environ. Microbiol.* **46**, 728-737.

Londry K. L. and Des Marais J. D. (2003) Stable carbon isotope fractionation by sulfate-reducing bacteria. *Appl. Environ. Microbiol.* **69**, 2942-2949.

Lovley D. R. (1993) Dissimilatory metal reduction. *Ann. Rev. Microbiol.* **47**, 263-290.

Lovley D. R. and Klug M. J. (1983) Methanogenesis from methanol and methylamines and acetogenesis from hydrogen and carbon dioxide in sediments of a eutrophic lake. *Appl. Environ. Microbiol.* **45**, 1310-1315.

Lynd L. R., Weimer P. J., van Zyl W. H., and Pretorius I. S. (2002) Microbial cellulose utilization: Fundamentals and biotechnology. *Microbiol. Mol. Biol. R.* **66**, 506-577.

Madden R. H., Bryder M. J., and Poole N. J. (1982) Isolation and characterization of an anaerobic, cellulolytic bacterium, *Clostridium papyrosolvens* sp.nov. *Int. J. Syst. Bacteriol.* **32**, 87-91.

Mariotti A., Germon J. C., Hubert P., Kaiser P., Letolle R., Tardieux A., and Tardieux P. (1981) Experimental determination of nitrogen kinetic isotope fractionation - Some principles - Illustration for the denitrification and nitrification processes. *Plant Soil* **62**, 413-430.

Metje M., and Frenzel P. (2005) The effect of temperature on anaerobic ethanol oxiodation and methanogenesis in an acid peat from a northern wetland. *Appl. Environ. Microbiol.*, in revision.

Mook W. G., Bommerso J. C., and Staverma W. H. (1974) Carbon isotope fractionation between dissolved bicarbonate and gaseous carbon dioxide. *Earth Planet. Sc. Lett.* **22**, 169-176.

O'Leary M. H. (1988) Carbon Isotopes in Photosynthesis. *Bioscience* **38**, 328-336.

Pohlschroder M., Leschine S. B., and Canaleparola E. (1994) Multicomplex cellulase xylanase system of *Clostridium papyrosolvens* C7. *J. Bacteriol.* **176**, 70-76.

Preuss A., Schauder R., Fuchs G., and Stichler W. (1989) Carbon isotope fractionation by autotrophic bacteria with 3 different CO_2 fixation pathways. *Z. Naturforsch. C.* **44**, 397-402.

Rossmann A., Butzenlechner M., and Schmidt H. L. (1991) Evidence for a nonstatistical carbon isotope distribution in natural glucose. *Plant Physiol.* **96**, 609-614.

Schink B. (1997) Energetics of syntrophic cooperation in methanogenic degradation. *Microbiol. Mol. Biol. R.* **61**, 262-&.

Shen H. S., Ni D. B., and Sundstol F. (1998) Studies on untreated and urea-treated rice straw from three cultivation seasons: 1. Physical and chemical measurements in straw and straw fractions. *Animal Feed Sci. Technol.* **73**, 243-261.

Stams A. J. M. (1994) Metabolic interactions between anaerobic bacteria in methanogenic environments. *Ant. Leeuwenhoek* **66**, 271-294.

Stams A. J. M., Vandijk J. B., Dijkema C., and Plugge C. M. (1993) Growth of syntrophic propionate-oxidizing bacteria with fumarate in the absence of methanogenic bacteria. *Appl. Environ. Microbiol.* **59**, 1114-1119.

Strobel H. J. (1995) Growth of the thermophilic bacterium *Clostridium thermocellum* in continuous culture. *Curr. Microbiol.* **31**, 210-214.

Stumm W. and Morgan J. J. (1995) *Aquatic Chemistry*. Wiley-Interscience.

Sugimoto A. and Wada E. (1993) Carbon isotopic composition of bacterial methane in a soil incubation experiment - Contributions of acetate and CO_2/H_2. *Geochim. Cosmochim. Acta* **57**, 4015-4027.

Thurston B., Dawson K. A., and Strobel H. J. (1993) Cellobiose versus glucose-utilization by the ruminal bacterium *Ruminococcus albus*. *Appl. Environ. Microbiol.* **59**, 2631-2637.

Tsutsuki K. and Ponnamperuma F. N. (1987) Behavior of anaerobic decomposition products in submerged soils . Effects of organic material amendment, soil properties, and temperature. *Soil Sci. Plant Nutr.* **33**, 13-33.

Ward D. M. and Winfrey M. R. (1985) Interactions between methanogenic and sulfate-reducing bacteria in sediments. *Adv. Aquat. Microbiol.* **3**, 141-179.

Watanabe A., Katoh K., and Kimura M. (1993) Effect of rice straw application on CH_4 emission from paddy fields. 2. contribution of organic constituents in rice straw. *Soil Sci. Plant Nutr.* **39**, 707-712.

Werner R. A. and Brand W. A. (2001) Referencing strategies and techniques in stable isotope ratio analysis. *Rapid Commun. Mass Spectrom.* **15**, 501-519.

Werner R. A., Bruch B. A., and Brand W. A. (1999) ConFlo III - An interface for high precision delta C-13 and delta N-15 analysis with an extended dynamic range. *Rapid Commun. Mass Spectrom.* **13**, 1237-1241.

Wolin E. A., Wolin M. J., and Wolfe R. S. (1963) Formation of methane by bacterial extracts. *J. Biol. Chem.* **238**, 2882-&.

Zeikus J. G. (1983) Metabolic communication between biodegradative populations in nature. In *Microbes in their Natural Environments* (ed. J. H. Slater, R. Whittenbury, and J. W. T. Wimpenny). pp. 423-462. Cambridge University Press.

Zinder S. H. (1993) Physiological ecology of methanogens. In *Methanogenesis. Ecology, Physiology, Biochemistry and Genetics* (ed. J. G. Ferry). pp. 128-206. Chapman & Hall.

III.2. Änderung der Kohlenstoffisotopenfraktionierung bei unterschiedlichen thermodynamischen Bedingungen in hydrogenotrophen methanogenen mikrobiellen Kulturen und Umweltproben

Holger Penning, Caroline M. Plugge, Pierre E. Galand und Ralf Conrad

Zusammenfassung:

Kohlenstoffisotopenfraktionierungsfaktoren methanbildender Prozesse sind wichtige Kenngrößen, die die Quantifizierung methanbildender Prozesse in Böden und Sedimenten ermöglichen. Ursachen für die Variation der Isotopenfraktionierung während der Methanogenese von H_2/CO_2 wurden in dieser Arbeit in syntrophen und obligat syntrophen Kokulturen von *Methanobacteriaceae* und *Methanomicrobiaceae* unter unterschiedlichen thermodynamischen Wachstumsbedingungen untersucht. Die Isotopenfraktionierung korrelierte mit der Änderung der Gibbs freien Energie (ΔG) der Methanbildung von H_2/CO_2 und wurde durch eine halbe Gauss-Kurve beschrieben. Anoxisch inkubierte Umweltproben folgten nicht dieser Korrelation, da H_2-Gradienten die exakte Bestimmung von ΔG beeinflussten. Jedoch konnte aus der Korrelation der Kokulturexperimente über die Isotopenfraktionierung auf die freie Energie *in situ* geschlossen werden. Dies zeigte, dass hydrogenotrophe methanogene *Archaea* unter weitaus günstigeren energetischen Bedingungen leben, als das durch die Bestimmung von ΔG über Gasmessungen bisher angenommen wurde.

Variation of carbon isotope fractionation in hydrogenotrophic methanogenic microbial cultures and environmental samples at different energy status

(akzeptiert bei Global Change Biology)

Holger Penning[1], Caroline M. Plugge[2], Pierre E. Galand[3], Ralf Conrad[1*]

[1] Max Planck Institute for Terrestrial Microbiology, Karl-von-Frisch-Str., 35043 Marburg, Germany

[2] Wageningen University, Laboratory of Microbiology, Hesselink-van-Suchtelenweg 4, NL-6703 CT Wageningen, The Netherlands

[3] University of Helsinki, Department of Biological and Environmental Sciences, General Microbiology, POB 56, FIN-00014 Helsinki, Finland

Abstract

Methane is a major product of anaerobic degradation of organic matter and an important greenhouse gas. Its stable carbon isotope composition can be used to reveal active methanogenic pathways, if associated isotope fractionation factors are known. To clarify the causes that lead to the wide variation of fractionation factors of methanogenesis from H_2 plus CO_2 ($\alpha_{CO2\text{-}CH4}$), pure cultures and various cocultures were grown under different thermodynamic conditions. In syntrophic and obligate syntrophic cocultures thriving on different carbohydrate substrates fermentative bacteria were coupled to three different species of hydrogenotrophic methanogens of the families *Methanobacteriaceae* and *Methanomicrobiaceae*. We found that C-isotope fractionation was correlated to the Gibbs free energy change (ΔG) of CH_4-formation from H_2 plus CO_2 and that the relation can be described by a semi-Gauss curve. The derived relationship was used to quantify the average ΔG that is available to hydrogenotrophic methanogenic archaea in their habitat, thus avoiding the problems encountered with measurement of low H_2 concentrations on a microscale. Boreal peat, rice field soil and rumen fluid, which represent major sources of atmospheric CH_4, exhibited increasingly smaller $\alpha_{CO2\text{-}CH4}$, indicating that thermodynamic conditions for hydrogenotrophic methanogens became increasingly more favorable. Vice versa, we hypothesize that environments with similar energetic conditions will also exhibit

similar isotope fractionation. Our results, thus provide a mechanistic constraint for modelling the ^{13}C flux from microbial sources of atmospheric CH_4.

Introduction

Anoxic environments such as natural wetlands and flooded rice fields contribute approximately a third to the CH_4 budget of the atmosphere (Cicerone and Oremland, 1988). In these systems microbes almost exclusively produce CH_4 from acetate and H_2/CO_2. Hydrogenotrophic methanogenesis ($4\ H_2 + CO_2 \rightarrow CH_4 + 2\ H_2O$; $\Delta G^o = -130.7\ kJ\ mol^{-1}$) strongly prefers the isotopically lighter carbon, whereas the isotope effect is less expressed in acetoclastic methanogenesis. This difference in isotope fractionation can be used for modelling of C-flux in methanogenic environments (Conrad, 2005). In addition, measurements of carbon stable isotope ratios of CH_4 have been proven to be useful for constraining individual atmospheric CH_4 sources and sinks, and in interpreting the atmospheric CH_4 budget (Gupta *et al.* 1996; Lowe *et al.* 1994; Bräunlich *et al.* 2001; Fletcher *et al.* 2004). Although the $^{13}C/^{12}C$-isotopic composition of CH_4 produced from CO_2 reduction has a characteristic signature, the magnitude of fractionation is usually considerably different between many natural systems and methanogenic microbial cultures (Conrad, 2005; Fey *et al.* 2004; Valentine *et al.* 2004). The wide variation of magnitude of fractionation (i.e. fractionation factor α) is a problem for modelling of C-fluxes (Conrad, 2005). Several authors observed this discrepancy, and assumed it being due to microbial culturing conditions, which often strongly differ from those in the natural environment (Sugimoto and Wada, 1993; Burke, 1993; Whiticar, 1999). However, the factors determining the wide range of α-values are basically unknown. Recently, Valentine *et al.* (2004) found that the fractionation of C-isotopes was affected by the supply of H_2 to a CO_2-reducing culture of *Methanothermobacter marburgensis*, and explained the observation by the differential reversibility hypothesis. They proposed that isotope fractionation in multistep enzymatic processes depends on enzymatic reversibility, which in turn depends on the Gibbs free energy of catabolism. So far, this is the only study measuring both H_2 partial pressures (p_{H2}) and C-isotope fractionation explicitly, and only two data points exist (Valentine *et al.* 2004). To control p_{H2} and rigorously study its effect on C-isotope fractionation, we grew cocultures of different H_2-producing fermenting bacteria and H_2-consuming methanogenic archaea covering a broad range of p_{H2}. This experimental approach was used to test, whether a

general function of methanogenic carbon isotope fractionation vs. p_{H2} exists. We found that such a relationship indeed existed, such that α changed with the Gibbs free energy (ΔG) available to hydrogenotrophic methanogens, and that this relationship was generally valid for the different methanogenic microbial species studied.

Furthermore, we tested whether it is possible to predict α from p_{H2} measured in samples from natural methanogenic environments. Our results indicate that this is not a reliable option, since the measured values of p_{H2} hardly represent the Gibbs free energy (ΔG) available to hydrogenotrophic methanogens *in situ*. Such a determination has been problematic, since methanogens typically live within micro-aggregates involving steep gradients of p_{H2} (Hoehler *et al.* 2001; Krylova and Conrad, 1998; Conrad *et al.* 1985), preventing the exact analysis of energetically relevant H_2 concentrations *in situ*. Instead, we propose that measurement of α gives a more reliable value of the *in situ* ΔG than the measurement of p_{H2}, and show that more free energy is available to the hydrogenotrophic methanogens than suggested by measurement of p_{H2}.

Material and Methods

Archaeal and bacterial strains

Methanobacterium bryantii (DSM 863), *Methanobacterium formicicum* (DSM 1535), *Methanospirillum hungatei* (DSM 864), *Methanothermobacter marburgensis* (DSM 2133), *Acetobacterium woodii* (DSM 1030), and *Clostridium papyrosolvens* (DSM 2782) were obtained from Deutsche Sammlung für Mikroorganismen und Zellkulturen. *Syntrophobacter fumaroxidans* (DSM 10017) was from our own culture collection (Laboratory of Microbiology, Wageningen University, The Netherlands).

Cultivation

Cocultures of the fermenting organisms *C. papyrosolvens* and *A. woodii* were each grown with methanogenic partner organisms (*M. bryantii* or *M. hungatei*) in glass bottles (500 ml; Müller and Krempel, Bülach, Switzerland) with 250 ml as culture volume on phosphate buffered mineral medium with defined bicarbonate concentrations (0.16-2.8 mM) under N_2. The composition was (in grams liter^{-1} unless otherwise indicated): KH_2PO_4, 1.9; $Na_2HPO_4 \times 2\ H_2O$, 6.4; NH_4Cl, 0.3; $MgCl_2 \times 6\ H_2O$, 0.1; NaCl, 0.3; KCl, 0.15; $CaCl_2 \times 2H_2O$, 0.055; $Na_2S \times 9H_2O$, 0.24; trace element solution, 2 ml (Chin *et al.* 1998); alkaline trace element solution 1 ml (Stams *et al.* 1993); vitamin solution, 1 ml (Wolin *et*

al. 1963); resazurine at 0.5% (wt/vol), 1 ml; pH adjusted to 7.2. Concentrations of glucose, cellobiose, and cellulose (expressed as anhydroglucose; Mw = 162 g mol^{-1}) were 4.44, 2.34, and 4.94 mM, respectively. Cocultures of *S. fumaroxidans* and *M. hungatei* or *M. formicicum* were grown in glass bottles (1000 ml; Müller and Krempel) under N_2 on the medium described by Stams *et al.* (1993) containing 38 mM bicarbonate and 30 mM propionate. *M. marburgensis* was grown in a flow-through batch reactor on mineral medium with $H_2/CO_2/N_2$ gas mixtures of 80/20/0% and 5/20/75%, respectively (Schönheit *et al.* 1980). Rapid gas flow guaranteed that ≤3% of the CO_2 supplied was converted to CH_4. This assured, that inflow and outflow of CO_2 had nearly the same isotope composition and proper calculation of $\alpha_{CO2\text{-}CH4}$ was possible. Cultures were grown at 30°C, except those with *S. fumaroxidans* at 37°C, and *M. marburgensis* at 65°C.

Environmental samples

Rice field soil samples were collected from rice fields of the Italian Rice Research Institute in Vercelli, Italy. Soil slurries, which represent the water-saturated conditions after flooding in rice fields, were prepared at a weight ratio of 1:1 with addition of 4 mg rice straw g^{-1} soil and anoxically incubated at 30°C. The peat was sampled at the Lakkasuo mire complex in central Finland (61°48´N, 24°19'E, ca. 150 m altitude), from a mesotrophic fen (MES), an oligotrophic fen (OLI) and an ombrotrophic bog (OMB) and anoxically incubated at 10°C (Galand *et al.* 2005). Methanogenesis from acetate was inhibited with CH_3F (Janssen *et al.* 1997). The concentration of CH_3F was optimized as described (Conrad and Klose, 1999), applying 1% in rice field soil and 2% in peat soil. Selective inhibition by CH_3F was earlier confirmed by stoichiometrical correlation of accumulated acetate with the deficit in CH_4 production (Conrad and Klose, 1999; Frenzel and Bosse, 1996). At higher CH_3F concentration also hydrogenotrophic methanogenesis is partially inhibited (Conrad and Klose, 1999), but not changing its carbon isotope fractionation (Conrad, 2005). Rumen fluid was sampled at the slaughterhouse of Marburg and immediately afterwards incubated under N_2 at 30°C or H_2/CO_2 (4:1) at 25°C.

Analytical methods

CH_4 and CO_2 were analyzed by GC-FID (Shimadzu, Kyoto, Japan). CO_2 was detected upon conversion to CH_4 with a methanizer (Ni-catalyst at 350°C, Chrompack, Middelburg, Netherlands). H_2 was analyzed by GC-TCD (Shimadzu, Kyoto, Japan) and a HgO-to-Hg conversion detector (RGD2; Trace Analytical, Menlo Park, CA) (Seitz *et al.*

1990). Stable isotope analysis of $^{13}C/^{12}C$ in gas samples was performed using a gas chromatograph combustion isotope ratio mass spectrometer (GC-C-IRMS) system (Thermoquest, Bremen, Germany). For principle operation see Brand (1996). Briefly, after conversion of CH_4 to CO_2 in the Finnigan Standard GC Combustion Interface III isotope ratios were detected with the IRMS (Finnigan MAT model delta plus) (Fey *et al.* 2004). Reference gas was CO_2 (99.998% purity; Messer-Griessheim, Düsseldorf, Germany), calibrated with the working standard methylstearate (Merck). The latter was intercalibrated at the Max-Planck-Institut für Biogeochemie, Jena, Germany (courtesy of Dr. W.A. Brand) against NBS22 and USGS 24, and reported in the delta notation versus V-PDB:
$\delta^{13}C = 10^3 (R_{sa}/R_{st}-1)$ with $R = {}^{13}C/{}^{12}C$ of sample (sa) and standard (st), respectively. The precision of repeated analysis was ± 0.2‰ when 1.3 nmol CH_4 was injected.

Calculations

Fractionation factors for methanogenesis from H_2/CO_2 are defined according to Hayes (1993):

$$\alpha_{CO_2-CH_4} = (\delta^{13}C_{CO_2} + 1000)/(\delta^{13}C_{CH_4} + 1000) \quad (1)$$

The isotopic signature for a newly formed CH_4 (δ_n) was calculated from the isotopic signatures at two time points t =1 (δ_1) and t = 2 (δ_2) by the following mass balance equation:

$$\delta_2 = f_n\delta_n + (1- f_n)\,\delta_1 \quad (2)$$

with f_n being the fraction of the newly formed CH_4 relative to the total at t = 2.

Gibbs free energies for methanogenesis in the methanogenic system were calculated from the standard Gibbs free energies of formation (Thauer *et al.* 1977) and the Nernst equation:

$$\Delta G = \Delta G^\circ + RT \ln \frac{p_{CH_4}}{p_{H_2}^4 p_{CO_2}} \quad (3)$$

ΔG^o was corrected for a temperature of 25°C using the Van´t Hoff equation. α was corrected following an the algorithm given by Whiticar et al. (1986), which is based on carbon isotope exchange equilibria (Richet *et al.* 1977):

$$10^2 \ln \alpha_T = 2.92\,(10^3/T) - 2.96 \quad (4)$$

where T is the formation temperature in K. Correction was then made by the difference between the α_T calculated for 25°C and the growth temperatures of the cultures (adjustment of $\alpha_{CO2\text{-}CH4}$ was 0.0017 for 30°C, 0.0041 for 37 °C, and 0.0123 for 65°C).

Results

Pure culture experiments

Pure cultures of *Methanothermobacter marburgensis* were grown in a flow-through batch bioreactor on different $H_2/CO_2/N_2$ gas mixtures (80/20/0% and 5/20/75%; Fig. 1). Almost parallel increase of optical density and CH_4 concentration indicated non-limited growth conditions in the high-H_2 reactor (Fig. 1 A), whereas in the low-H_2 reactor (Fig. 1 B) two phases of exponential growth were displayed. In the first 30 h the CH_4 production rate and OD_{600} increased exponentially (non-limited growth). After that, however, the growth rate decreased, and the increase in CH_4 production rate declined and stabilized at 5 ml min^{-1} (l of $H_2/CO_2/N_2)^{-1}$. Such behaviour is typical for hydrogenotrophic growth of methanogens, which uncouple CH_4 production from biomass production when the supply of H_2 is not limiting (Schönheit *et al.* 1980). During transition of the CH_4 production rate to a stable value the H_2 partial pressures (p_{H2}) measured in the gas exhaust decreased and stabilized after 30 h (data not shown), demonstrating that H_2 limited growth conditions established. Values of $\alpha_{CO2\text{-}CH4}$ ranged between 1.034 and 1.039 under non-limited conditions (Fig. 1 A,B), and increased in the reactor with low H_2 concentration (Fig. 1 B) to constant values between 1.062 and 1.064, when H_2 became limiting.

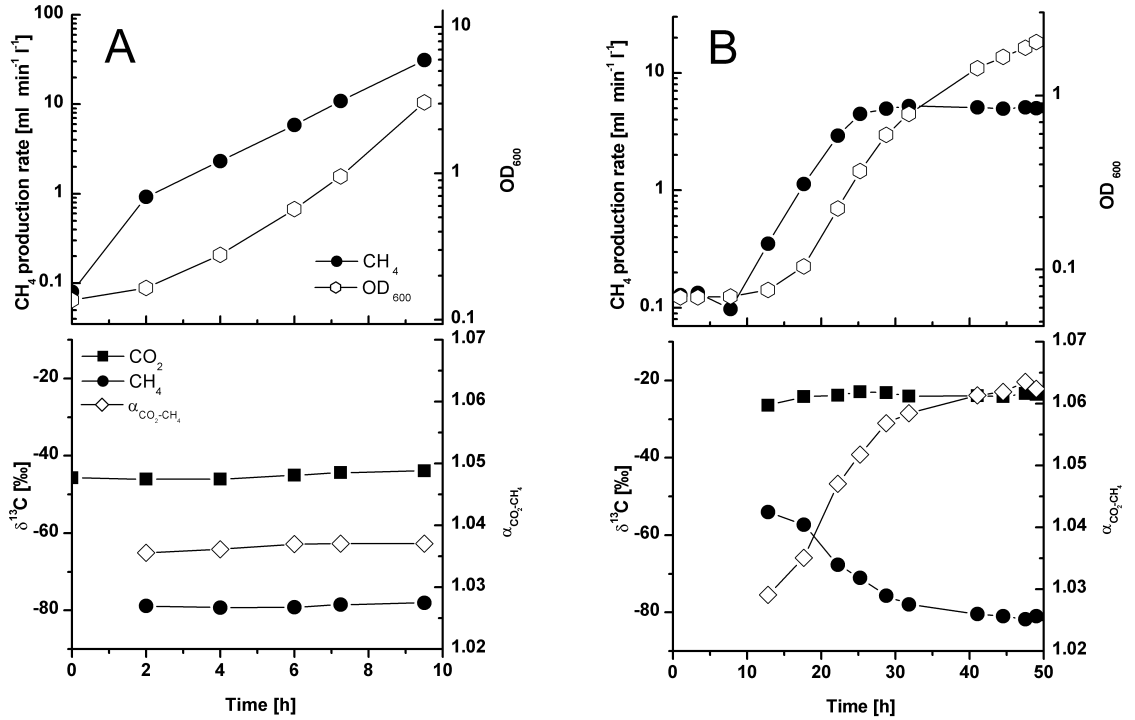

Figure 1: Growth curve and CH_4 production of *M. marburgensis* in flow-through bioreactor experiments with $H_2/CO_2/N_2$ gas mixtures of (A) 80/20/0% and (B) 5/20/75% (upper diagrams). Time course of $\delta^{13}CH_4$, $\delta^{13}CO_2$ and α is shown in the lower diagrams of (A) and (B). Rapid gas flow guaranteed that ≤3% of the CO_2 supplied was converted to CH_4. Unlimited availability of H_2 (A) resulted in low and stable α-values, whereas limitation of H_2 (B), as indicated by slow growth and stagnant CH_4 production rate during the late growth phase, resulted in high α-values.

Coculture experiments

Influence of p_{H2} on carbon isotope fractionation was then tested in closed system, where equilibrium of gases between headspace and liquid phase establishes. To create different p_{H2} growth conditions for hydrogenotrophic methanogens, syntrophic (wide range of p_{H2}) and obligate syntrophic cocultures (narrow p_{H2} range) were chosen for our experiments. In syntrophic cocultures of *Clostridium papyrosolvens* and *Methanobacterium bryantii* glucose and cellobiose were completely fermented by *C. papyrosolvens* within 200 h to acetate, lactate, ethanol, formate, H_2, and CO_2. Only H_2 and CO_2 were further converted to CH_4 by the methanogenic archaeon *M. bryantii* and accumulated exponentially in the system (Fig. 2). Partial pressures of the intermediate H_2 increased transiently to more than 2.5 kPa (Fig. 2). Cellulose, by contrast, allowed only a relatively low fermentation rate limited by the hydrolysis of cellulose. In these cultures, hydrogenotrophic CH_4 production kept the p_{H2} low ($p_{H2} < 0.1$ kPa) and CH_4 was linearly produced. Carbon isotope composition of CO_2 and newly formed CH_4 (equ. 2), from which

$\alpha_{CO2\text{-}CH4}$ was calculated (equ. 1), is shown in Figure 2. Calculation of $\delta^{13}C$ of CH_4 was made evaluating each data point separately, since the determination is very sensitive, if changes of the measured $\delta^{13}C$ of CH_4 (accumulated) and of the CH_4 partial pressure are small. Changes of isotope ratio and concentration that were close to the analytical error of GC-C-IRMS or GC-FID measurement were therefore not included in the data evaluation. In the cocultures growing on glucose or cellobiose, CH_4 formed by *M. bryantii* at high p_{H2} exhibited low carbon isotope fractionation ($\alpha_{CO2\text{-}CH4} < 1.04$), whereas at low p_{H2} α-values increased. In contrast on cellulose, α-values were relatively high from the beginning on ($\alpha_{CO2\text{-}CH4} = 1.044$) and stabilized after 500 h at $\alpha_{CO2\text{-}CH4} = 1.076$ with $p_{H2} = 10$ Pa (Fig. 2).

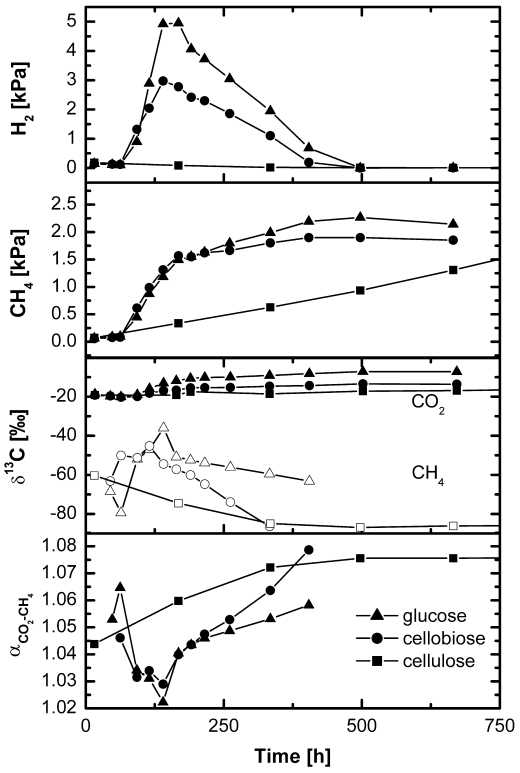

Figure 2: Change of fractionation factor α, $\delta^{13}CH_4$, $\delta^{13}CO_2$, and partial pressures of H_2 and CH_4 in a coculture of *C. papyrosolvens* and *M. bryantii.* High p_{H2} correspond to low α and vice versa. With cellulose, *M. bryantii* operated close to its threshold for H_2 exhibiting very high isotope fractionation.

Additional syntrophic cocultures (*C. papyrosolvens* with *Methanospirillum hungatei*, *Acetobacterium woodii* with *M. bryantii*, and *A. woodii* with *M. hungatei*) were analyzed the same way. Trends in these cocultures were the same as shown in Fig. 2 for *C. paprosolvens* and *M. bryantii* and are, therefore, not shown individually, but are later

included in the data analysis. Isotope fractionation at very low p_{H2} was investigated with the obligate syntrophic cocultures of *Syntrophobacter fumaroxidans* coupled to either *M. hungatei* or *Methanobacterium formicicum*. Propionate oxidation by *S. fumaroxidans* was only possible at low p_{H2} equivalent to a ΔG of about -15 kJ mol^{-1}, similarly as observed before (Scholten and Conrad, 2000). This low p_{H2} was maintained by the methanogen, which in turn, was also only provided with little free energy ($\Delta G \approx$ -40 to -20 kJ mol^{-1}). In contrast, the cocultures, which were not obligate syntrophic, operated at a higher p_{H2} and thus allowed generally more free energy ($\Delta G \approx$ -100 to -50 kJ mol^{-1}) to the methanogenic partner.

Data analysis of cocultures

Although each individual coculture showed a good correlation between the values of p_{H2} and $\alpha_{CO2\text{-}CH4}$ measured during the course of growth ($r^2 > 0.82$), there was no general relationship between p_{H2} and $\alpha_{CO2\text{-}CH4}$ across all the different coculture experiments. Instead, a good correlation was found between the catabolic ΔG of the methanogenic reaction and the $\alpha_{CO2\text{-}CH4}$ of the reaction determined in the same incubation (Fig. 3, 4). Values of $\alpha_{CO2\text{-}CH4}$ were calculated for the actual conditions using measured p_{H2}, p_{CH4}, and p_{CO2}, and the Nernst equation (equ. 3). Figure 3 shows the relation for the coculture of *C. papyrosolvens* and *M. bryantii* (Fig. 2). After inoculation ΔG for the coculture was -70 kJ mol^{-1}. During the course of the experiment ΔG decreased in cocultures with glucose and cellobiose to -100 kJ mol^{-1} concomitant with a decrease in $\alpha_{CO2\text{-}CH4}$ (1.02 – 1.03). With decrease of p_{H2} and therefore increase in ΔG also $\alpha_{CO2\text{-}CH4}$ increased again. In the coculture with cellulose, where ΔG steadily increased with time, $\alpha_{CO2\text{-}CH4}$ increased simultaneously to values up to 1.08.

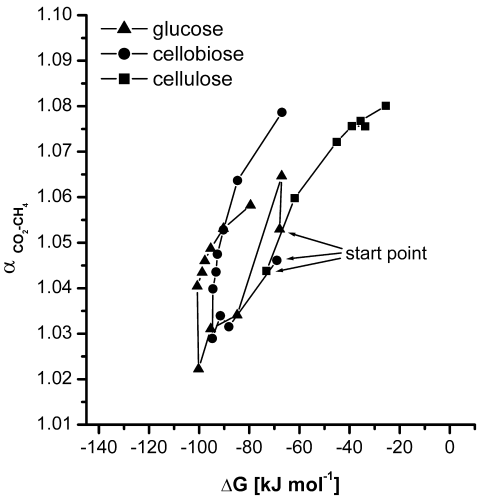

Figure 3: α–ΔG relation in coculture of *C. papyrosolvens* and *M. bryantii* growing on different substrates, of which process and isotope data are shown in Figure 2. ΔG and $\alpha_{CO2\text{-}CH4}$ well correlate and show a decrease and later increase for glucose and cellobiose, whereas for cellulose there is a steady increase.

Figure 4 summarizes the results of all the different syntrophic and obligate syntrophic cocultures tested. We calculated the values of $\alpha_{CO2\text{-}CH4}$ and ΔG separately for each replicate of the cocultures to increase precision. Syntrophic cocultures (with *C. papyrosolvens* or *A. woodii* as fermenting partner) were active within a wide range of ΔG, as well as $\alpha_{CO2\text{-}CH4}$, whereas obligate syntrophic cocultures (*S. fumaroxidans* as fermenting partner) could only operate within a narrow range of ΔG (-45 to -17 kJ mol^{-1}). Both, *M. bryantii* and *M. hungatei*, displayed the relation over a wide range of ΔG and $\alpha_{CO2\text{-}CH4}$. *M. formicicum* was only used in the obligate syntrophic cocultures and was, therefore, restricted to the high ΔG values, characteristic for these cultures. Pure culture data of *M. marburgensis* (Fig.1) could not be included in the figure due to lack of the *in situ* p_{H2} in the flow-through system necessary for calculation of ΔG. Yet, two data points from Valentine *et al.* (2004) are included and well fit the observed α–ΔG relation. A Gauss function (equ. 5) was used to fit the data (justification see Discussion) and resulted in a goodness of fit of $r^2 = 0.77$:

$$y = y_0 + A \exp[-(x-x_c)^2/(2w^2)] \quad (5)$$

with $y_0 = 1$; $A = 0.0919 \pm 0.0104$; $x_c = 11.8376 \pm 23.5222$; $w = 78.0067 \pm 14.1127$.

Due to the individual treatment of replicates no errors bars can be shown for the data points, but we calculated the 95% confidence range for the α–ΔG relation (included in Fig. 4).

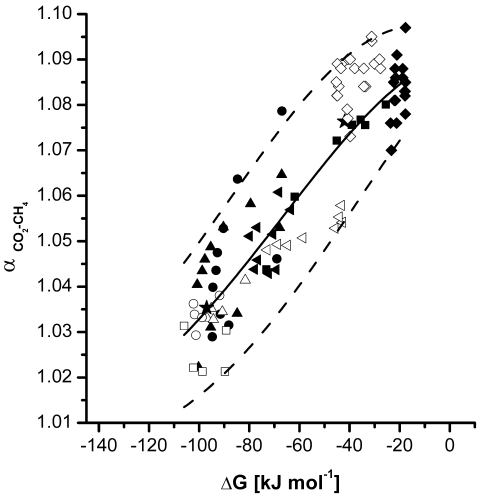

Figure 4: α–ΔG relation in cocultures of H_2-producing fermenting and H_2-consuming methanogenic microorganisms; the line is a fit (using Origin Microcal^{TM}) to the Gauss function ($y = y_0 + A \exp[-(x-x_c)^2/(2w^2)] = 1 + 0.0919 \exp[-(x-11.8376)^2/12170]$).
▲ *C. papyrosolvens*/*M bryantii* (glucose); ● *C. papyrosolvens*/*M. bryantii* (cellobiose); ■ *C. papyrosolvens*/*M. bryantii* (cellulose); ◄ *A. woodii*/*M. bryantii* (glucose); △ *C. papyrosolvens*/*M. hungatei* (glucose); ○ *C. papyrosolvens*/*M. hungatei* (cellobiose); □ *C. papyrosolvens*/*M. hungatei* (cellulose); ◁ *A. woodii*/*M. hungatei* (glucose); ◆ *S. fumaroxidans*/*M. formicicum* (propionate); ◇ *S. fumaroxidans*/*M. hungatei* (propionate); ★ *M. marburgensis* (H_2/CO_2; data from Valentine et al. (2004))

Incubations of environmental samples

To test the implication of the observed α–ΔG relation for natural methanogenic systems, samples from different environments were incubated under anoxic conditions. As in the cocultures only time points with active methanogenesis were used in the data analysis, which was performed as described for the cocultures. In the α–ΔG relation diagrams of the environmental incubations (Fig. 5) also the regression curve of the culture experiments and its 95% confidence lines are included. In incubations of rice field soil and peat, acetoclastic methanogenesis was inhibited with methyl fluoride (Janssen and Frenzel, 1997) to avoid changes of the $\delta^{13}C$ of CH_4 by CH_4 produced from acetate (Fig. 5 A). This approach has recently been proposed for determination of $\alpha_{CO2\text{-}CH4}$ (Conrad, 2005) and successfully tested in eutrophic lake sediment (Chan *et al.* 2005) and rice field soil (unpublished data). In rice field soil, ΔG (-54 to -30 kJ mol^{-1}) and $\alpha_{CO2\text{-}CH4}$ (1.043 to 1.053) increased simultaneously with time. The peat incubations plotted over a wide range of $\alpha_{CO2\text{-}CH4}$ (1.045 to 1.087) and at high ΔG (-37 to -7 kJ mol^{-1}). In the rice field soil and peat system, data followed the α–ΔG relation only for $\alpha_{CO2\text{-}CH4} > 1.065$, whereas for

$\alpha_{CO2\text{-}CH4} < 1.065$, data were on the right side of the α–ΔG relation. Using the α–ΔG relation and the p_{H2} measured in the environmental samples would thus predict (via ΔG that decreases with p_{H2}) much higher α than actually measured. On the other hand, the α–ΔG relation and the measured α would predict much lower (more negative) values of ΔG than calculated from measured p_{H2}.

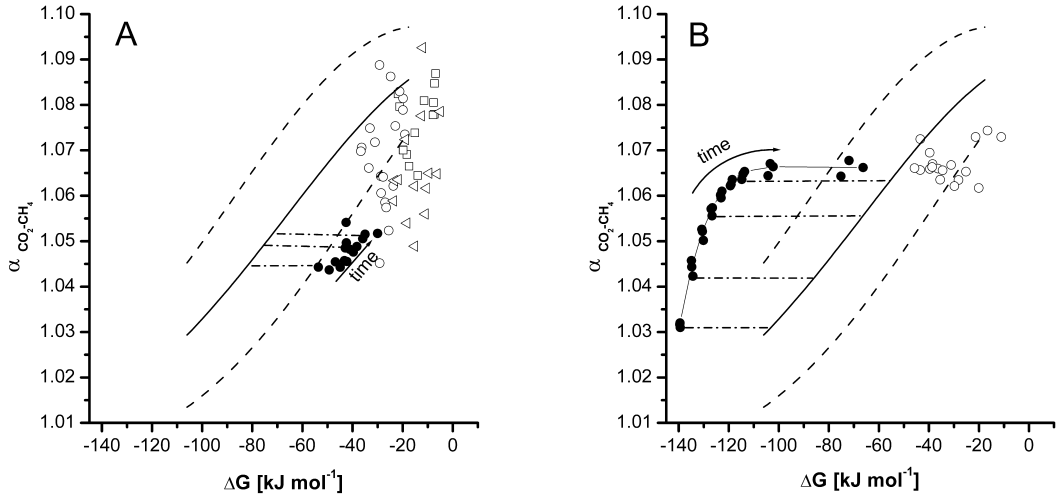

Figure 5: α–ΔG relation in different environmental samples including regression curve and confidence lines from Fig. 4; arrows indicate the time course of incubation, dash-dotted lines show the difference between the apparent ΔG (symbols) and the actual ΔG (regression curve) of hydrogenotrophic methanogenesis. The actual ΔG available to methanogens in their environmental habitat was up to 60 kJ mol^{-1} more negative than suggested from the apparent ΔG determined from bulk measurement of p_{H2} (difference shown by horizontal dash-dotted lines). However, in rumen fluid incubated under H_2/CO_2 it was more positive. (A) rice field soil and peat (● rice field soil; □ peat OLI; ○ peat MES; ◁ peat OMB). (B) rumen fluid (○ rumen (N_2); ● rumen (H_2/CO_2)).

We also used rumen fluid, since in this environment CH_4 is almost exclusively produced from H_2/CO_2 (Sharp *et al.* 1998) and thus, inhibition of acetoclastic methanogenesis with methyl fluoride is not necessary. Incubation of rumen fluid was conducted under N_2 and H_2/CO_2 headspace (Fig. 5 B). For incubations under N_2 headspace data clustered in a relatively confined area (ΔG = -11 to -46 kJ mol^{-1}; $\alpha_{CO2\text{-}CH4}$ = 1.061 to 1.074) within the 95% confidence limit of the α–ΔG relation. In contrast, the H_2/CO_2 headspace created very low ΔG values at the beginning (-140 kJ mol^{-1}), which continuously decreased, when CH_4 was produced by hydrogenotrophic archaea. Values of $\alpha_{CO2\text{-}CH4}$ strongly increased initially (1.032 to 1.067) and stabilized at a similar $\alpha_{CO2\text{-}CH4}$ as observed in the incubation under N_2. Simultaneously, bulk p_{H2} decreased so that the

measured ΔG gradually changed from -145 to -75 kJ mol^{-1}, similarly as observed in rumen fluid incubated under a N_2 atmosphere. Hence, for rumen incubated under H_2/CO_2 data first plotted on the left side of the α–ΔG relation curve, but later approached and finally crossed the curve reaching the cluster of the rumen incubation under N_2. Again, the α–ΔG relation together with the measured p_{H2} did not allow prediction of α. However, using the α–ΔG relation together with the α measured after stabilization would predict a reasonable value of ΔG available to the hydrogenotrophic methanogens.

Discussion

Pure and coculture experiments

Different hydrogenotrophic methanogenic archaea were grown under varying growth conditions to elucidate the factors causing the fractionation of carbon isotopes during CH_4 production from H_2/CO_2. In pure cultures of *M. marburgensis* (Fig. 1) we could show, that $\alpha_{CO2\text{-}CH4}$ depended on the p_{H2}. $\alpha_{CO2\text{-}CH4}$ increased with decreasing p_{H2}, confirming the results by Valentine *et al.* (2004). To quantify the observed correlation we used cocultures in closed systems, where partial pressures of the gases involved in the methanogenic reaction could be quantified with a high precision. $\alpha_{CO2\text{-}CH4}$ produced from *M. bryantii* in coculture with *C. papyrosolvens* at high p_{H2} was similar as reported for pure cultures of *Methanobacterium spp.* (Belyaev *et al.* 1983) when grown on H_2/CO_2 at a ratio of 4:1 as required for stoichiometric conversion to CH_4. However, with decreasing p_{H2}, as for *M. marburgensis* in the flow-through reactor, $\alpha_{CO2\text{-}CH4}$ strongly increased. The cocultures demonstrated, that the relation of α to p_{H2} was not specific to pure culture data, and that the coculture experiments were not biased by the different mode of H_2/CO_2 gas transfer (i.e. between different microbes within the culture medium or between the gas phase and the culture medium). In addition, we found that the different isotopic composition of glucose and cellobiose, $\delta^{13}C$ = -10.85 ± 0.05‰ and -25.23 ± 0.47‰, respectively, resulted in a different isotopic composition of the pool of CO_2, but did not influence the value of $\alpha_{CO2\text{-}CH4}$ (Fig. 2). This observation shows that isotopic equilibrium was reached between the CO_2 produced by fermentation and the CO_2 in the medium.

α–ΔG relation

Although we found a good correlation of $\alpha_{CO2\text{-}CH4}$ from p_{H2} for the single cocultures, the lack of a general dependency across the different coculture experiments indicated, that p_{H2} was not the only factor determining $\alpha_{CO2\text{-}CH4}$. The catabolic ΔG, however, did yield for all data a good correlation ($r^2 = 0.77$). Valentine *et al.* (2004) recently observed that a culture of *M. marburgensis* exhibited a larger fractionation ($\alpha_{CO2\text{-}CH4} = 1.064$) at low (310 Pa) and a lower fractionation ($\alpha_{CO2\text{-}CH4} = 1.031$) at high (80,000 Pa) p_{H2} (data points included in Fig. 4), and proposed that this difference is due to the extent of enzymatic reversibility that is controlled by the ΔG of the methanogenic reaction. They further suggested that the differential reversibility would act in concert with the intracellular availability of CO_2. High metabolic rates would decrease the intracellular concentration of CO_2, effectively creating an irreversible flux of CO_2 to CH_4. If then CO_2 was quantitatively consumed, consequently, no fractionation occurs by methanogenesis ($\alpha_{CO2\text{-}CH4} = 1.0$) and only a slight fractionation by transport into the cell would be observed.

Our results are consistent with this hypothesis demonstrating that α is indeed a function of the ΔG. With respect to energetics of methanogenesis, it is important to note that methanogens activate CO_2 by forming formyl methanofuran. This reaction is endergonic under standard conditions and becomes exergonic only when coupled to the late reaction steps that conserve energy (e.g. methyl transferase and heterodisulfide reductase; Thauer, 1998). A low value of the ΔG (large negative values) of methanogenesis from $H_2 + CO_2$ thus facilitates activation of CO_2 by lowering also the ΔG of this single reaction, decreases reversibility and results in low $\alpha_{CO2\text{-}CH4}$. A high value of the ΔG (low negative values), on the other hand, impedes activation of CO_2, increases ΔG of this reaction and results in high $\alpha_{CO2\text{-}CH4}$. For activation of CO_2 a certain amount of free energy is always required, since methanogenesis can only proceed, if this step is made exergonic. With increase of ΔG, less free energy will be available to drive each step of the multi-reaction process, further increasing the reversibility and, therefore, the fractionation of the reactions. Finally a maximum of α is reached at the thermodynamic limit of the microorganisms (Fig. 4), which in theory is equivalent to ¼ - ⅓ ATP or about -15 to -25 kJ mol^{-1} for mesophilic methanogens (Yao and Conrad, 1999; Hoehler *et al.* 2001; Schink and Stams, 2003; Müller, 2004). Since methanogenesis cannot proceed above

$\Delta G = 0$, a semi-Gauss curve was used for correlation. The maximum fractionation is solely determined by ΔG, since isotopic equilibrium of the CO_2 pools outside and inside the cell can be assumed at the low metabolic rates associated with high ΔG. However, irreversible CO_2 flow becomes more important with decreasing ΔG and the concomitant increase of the metabolic rate, and finally governs the $\alpha-\Delta G$ relation. At very low ΔG the hypothetical limit of zero fractionation ($\alpha_{CO2\text{-}CH4} = 1.0$) will be reached, if all CO_2 entering the cell is quantitatively metabolized. The semi-Gauss curve accounts for this boundary condition predicted by irreversible CO_2 flow.

As explained above, the observed relation (Fig. 4) is partly explained by the reversibility hypothesis depending on the free energy of the reaction (Valentine *et al.* 2004). For H-isotopes a similar correlation (i.e. a free-energy dependence of the kinetic isotope effect) was found, showing a bell-shaped curve with its maximum at $\Delta G = 0$ (Sühnel, 1990; Cook, 1991). There, the experimentally observed correlations in proton-transfer reactions could be theoretically explained both by the Marcus and quantum-statistical mechanical model. To our knowledge similar investigations on carbon isotopes have not been performed yet, so this interesting finding for H-isotopes should be evaluated for the element carbon. In addition, methanogenesis is a multi reaction process. This further complicates the calculation of carbon isotope fractionation, since concentrations of reactants and products of each single reaction of methanogenesis have to be known to determine ΔG. Therefore, we have to point out that the similarity between the theoretical free energy dependence of the kinetic isotope effect observed for H-isotopes and the $\alpha-\Delta G$ relation observed for hydrogenotrophic methanogenesis in our study is probably only circumstantial. However, the observed relationship between $\alpha_{CO2\text{-}CH4}$ and ΔG presented here appeared to be valid for all the four different methanogenic microbial species (from three genera and two families) tested (Fig. 4), emphasizing that it is a general feature of C-isotope fractionation in hydrogenotrophic methanogenesis. Although two of the tested methanogens (*M. bryantii* and *M. hungatei*) follow the $\alpha-\Delta G$ relation over the whole range of $\alpha_{CO2\text{-}CH4}$ and ΔG observed, it cannot be dismissed, that specifics of enzymes - like individual binding sites and activation energies - are different in other hydrogenotrophic methanogens and might change the $\alpha-\Delta G$ relation to a certain extent. This could be the case, if for example K- and r-strategists had developed differently fractionating sets of enzymes depending on p_{H2}. However, regarding carbon isotope fractionation none of this has been reported yet and the archaea tested in this study are also typical representatives of

hydrogenotrophic methanogens in natural environments (Grosskopf *et al.* 1998; Chan *et al.* 2005; Koizumi *et al.* 2004).

Application of the α–ΔG relation to environmental systems

Studies determining ΔG in natural systems from measurements of p_{H2}, p_{CH4} and p_{CO2} have indicated that hydrogenotrophic methanogens operate at the thermodynamic limit (ΔG = -15 and -25 kJ mol^{-1}). Although CH_4 formation may be active at ΔG ≈ 0 (Jackson and McInerney, 2002), such activity does not support growth, which in chemostat culture required ΔG ≈ -36 kJ mol^{-1} (Seitz *et al.* 1990). The severe energetic limitation in natural systems is in contrast to observations that the composition of methanogenic communities in the environment can change with time implying growth (Peters and Conrad, 1996; Krüger *et al.* 2005; Lueders and Friedrich, 2002). Determination of *in situ* ΔG is dependent on the measurement of realistic p_{H2}. The actual *in situ* p_{H2} is at the microsite where the methanogens live, which, however, may not be represented by the p_{H2} that is typically measured in the bulk fluid or in the equilibrated gas phase of the whole environmental sample. In natural environments, methanogens are closely associated with H_2-forming bacteria so that interspecies-H_2-transfer can occur between juxtaposed partners (Hoehler *et al.* 2001; Krylova and Conrad, 1998; Conrad *et al.* 1985). Hence, methanogens may experience higher p_{H2} (i.e. more negative ΔG) than deduced from bulk measurements, which may overestimate the effective ΔG (i.e. less negative).

Having an alternative way to determine ΔG (i.e. the α–ΔG relation), we tested the hypothesis that the ΔG effective for the methanogens in natural systems may be lower than expected from p_{H2} measurements. During incubation of rumen fluid the p_{H2} experienced by the methanogens is probably different than that measured in the headspace, since microbial aggregates are formed (see above) and rumen methanogens to a large part intimately associate with protozoa (Sharp *et al.* 1998) creating p_{H2} gradients. p_{H2} gradients lead to a measured p_{H2} that does not agree with the p_{H2} experienced by the methanogenic organism. In the case of H_2/CO_2 in the headspace, a lower p_{H2} was present in close proximity to the methanogens, which consumed H_2. In the case of a N_2 headspace, it was the opposite, since the products of fermentation, which are the substrates of methanogenesis, were produced by fermenting organisms next to the methanogenic archaea. The methanogens, therefore, had already depleted the p_{H2} before it could be quantified in the bulk fluid or the headspace in equilibrium with the bulk liquid. An exception to this rule were some of the peat

samples (Fig. 5 B; $\alpha_{CO2\text{-}CH4} > 1.065$), in which degradable organic substrates and thus H_2 production rates were presumably low. In these incubations metabolic activity of methanogens kept the p_{H2} close to the threshold of hydrogenotrophic methanogenesis, that the ΔG determined from bulk p_{H2} measurements approached the α–ΔG relation close to the maximum α (i.e. a gradient between the p_{H2} experienced by the archaea and the p_{H2} measured in the headspace was reduced to a minimum; Fig. 5 A). Collectively, these results are consistent with our hypothesis that $\alpha_{CO2\text{-}CH4}$ is a good predictor of the ΔG available to the methanogens *in situ*. The values of ΔG determined the conventional way (equ. 3) and using the α–ΔG relation are exemplarily shown by horizontal dash-dotted lines for the incubation of rumen under H_2/CO_2 headspace and rice field soil and show a difference of up to 60 kJ mol^{-1}(Fig. 5). We propose that the more reliable ΔG values were those extrapolated from the α–ΔG relation, and that a large fraction of the methanogens actually experienced a more negative ΔG than indicated by measurement of bulk p_{H2}.

The α–ΔG relation found in our coculture experiments may overcome the problem of biased p_{H2} measurements in natural methanogenic environments, since the average ΔG available to the hydrogenotrophic methanogenic community can now be constrained by the C-isotope fractionation. The resulting *in situ* ΔG values show that hydrogenotrophic methanogens often thrive at ΔG of -40 to -100 kJ mol^{-1}. These ΔG values are lower than those derived from measurements of p_{H2} in the bulk of environmental samples (i.e. about -20 kJ mol^{-1} in anoxic rice field soil; Yao and Conrad, 1999), and are sufficient for the synthesis of ½ to 1 ATP per reaction. Thus, there is a chance to solve the dilemma of earlier observations where relatively high ΔG values, hardly sufficient for active growth of methanogenic populations, were associated with changes in community composition or even net growth of methanogenic populations (Peters and Conrad, 1996; Krüger *et al.* 2005; Lueders and Friedrich, 2002).

Conclusions

We have shown that the fractionation of stable C-isotopes during hydrogenotrophic methanogenesis is related to the Gibbs free energy of catabolism, thus confirming the differential reversibility hypothesis of Valentine *et al.* (2004). The existence of a α–ΔG relation that is common to all species of H_2/CO_2-consuming methanogens implies that the mechanistic basis for stable C-isotope fractionation is the same. This implication is quite

likely, since the enzymology of hydrogenotrophic methanogenesis is rather uniform (Thauer, 1998), but should be confirmed by more detailed research.

We have also shown that the α–ΔG relation can be used to determine the free energy available for hydrogenotrophic methanogenesis *in situ* without need to measure the notoriously low H_2 partial pressures, which may be biased. Comparison of ΔG calculated from the α–ΔG relation and by the traditional way may be used to interpret the microenvironment of methanogenic microbial consortia with respect to the H_2 gradient experienced by the microbiota. Such a knowledge, even when approximate, helps judging the *in situ* living conditions of the methanogenic microbiota, a metabolic microbial group with high impact on global atmospheric chemistry and physics in the past (Kasting, 1993), the present (Lelieveld and Crutzen, 1992) and the future (Wang *et al.* 2004).

Accepting a common α–ΔG relation for hydrogenotrophic methanogenesis, this would have implications for the interpretation of stable isotope signatures measured in natural environments. Values of $\delta^{13}C$ in environmental CH_4 and CO_2 are frequently interpreted with respect to the predominant path of CH_4 formation. Calculating an apparent α ($\alpha_c = (\delta^{13}CO_2 + 10^3)/(\delta^{13}CH_4 + 10^3)$) it is generally assumed that low $\alpha_c < 1.055$ and high $\alpha_c > 1.065$ are indicative for the predominant operation of acetotrophic and hydrogenotrophic methanogenesis, respectively (Whiticar *et al.* 1986; Whiticar, 1999). However, hydrogenotrophic methanogenesis may also cause low α_c, if the methanogens operate in a micro-environment with plenty of free energy available (e.g. eutrophic anoxic systems), in which H_2 production by fermenting bacteria is high. Hence, one should be more cautious when interpreting $\delta^{13}C$ values without determining the fractionation factor of hydrogenotrophic methanogenesis separately.

In addition, the α–ΔG relation explains the wide variation of $\alpha_{CO2\text{-}CH4}$ in the environment. Although we cannot use the relation to precisely quantify C-isotope fractionation, we can better predict $\alpha_{CO2\text{-}CH4}$ in different types of environments. We tested three environments (peat, rice field soil, and rumen), which are important for global CH_4 showing that the relatively narrow range of energy conditions in these environments determines the observed range of α–values. These findings agree with environmental studies, where low values of $\alpha_{CO2\text{-}CH4}$ were found in the high-p_{H2} environment rumen ($\alpha_{CO2\text{-}CH4} = 1.031$; Levin *et al.* 1993), whereas under energy-limiting conditions as in bogs values of $\alpha_{CO2\text{-}CH4}$ were close to 1.07 (Lansdown *et al.* 1992; AveryJr *et al.* 1999). Due to

the relatively favourable energy conditions for hydrogenotrophic methanogens in rice field soils, values of α there usually show intermediate isotope fractionation ($\alpha_{CO2\text{-}CH4}$ = 1.045 – 1.060; Bilek *et al.* 1999; Sugimoto and Wada, 1993; Tyler *et al.* 1997). With the α–ΔG relation as theoretical background in combination with experimental data from methanogenic environments we may better predict values of $\alpha_{CO2\text{-}CH4}$ for CH_4-producing environments for which no detailed isotope studies exist. Our results thus provide a mechanistic constraint for modelling the ^{13}C flux from microbial sources of atmospheric CH_4.

Acknowledgements

We thank P. Claus for excellent technical assistance during analysis of ^{13}C data and W. A. Brand for isotopic analysis of the carbohydrate substrates. This work was supported by the Research Council for Earth and Life Sciences (ALW) with financial aid from the Netherlands Organization for Scientific Research (NWO).

References

AveryJr GB, Shannon RD, White JR, Martens CS, Alperin MJ (1999) Effect of seasonal changes in the pathways of methanogenesis on the $\delta^{13}C$ values of pore water methane in a Michigan peatland. *Global Biogeochemical Cycles* **13** 475-484.

Belyaev SS, Wolkin R, Kenealy WR, Deniro MJ, Epstein S, Zeikus JG (1983) Methanogenic Bacteria from the Bondyuzhskoe Oil-Field - General Characterization and Analysis of Stable-Carbon Isotopic Fractionation. *Applied and Environmental Microbiology* **45** 691-697.

Bilek RS, Tyler SC, Sass RL, Fisher FM (1999) Differences in CH_4 oxidation and pathways of production between rice cultivars deduced from measurements of CH_4 flux and $\delta^{13}C$ of CH_4 and CO_2. *Global Biogeochemical Cycles* **13** 1029-1044.

Brand WA (1996) High precision isotope ratio monitoring techniques in mass spectrometry. *Journal of Mass Spectrometry* **31** 225-235.

Bräunlich M, Aballain O, Marik T *et al.* (2001) Changes in the global atmospheric methane budget over the last decades inferred from ^{13}C and D isotopic analysis of Antarctic firn air. *Journal of Geophysical Research* **106** 20465-20481.

Burke RA (1993) Possible Influence of hydrogen concentration on microbial methane stable hydrogen isotopic composition. *Chemosphere* **26** 55-67.

Chan OC, Claus P, Casper P, Ulrich A, Lueders T, Conrad R (2005) Vertical distribution of structure and function of the methanogenic archaeal community in Lake Dagow sediment. *Environmental Microbiology* **7** 1139-1149.

Chin KJ, Rainey FA, Janssen PH, Conrad R (1998) Methanogenic degradation of polysaccharides and the characterization of polysaccharolytic clostridia from anoxic rice field soil. *Systematic and Applied Microbiology* **21** 185-200.

Cicerone RJ, Oremland RS (1988) Biogeochemical aspects of atmospheric methane. *Global Biogeochemical Cycles* **2** 299-327.

Conrad R (2005) Quantification of methanogenic pathways using stable carbon isotopic signatures: a review and a proposal. *Organic Geochemistry* **36** 739-752.

Conrad R, Klose M (1999) How specific is the inhibition by methyl fluoride of acetoclastic methanogenesis in anoxic rice field soil? *FEMS Microbiology Ecology* **30** 47-56.

Conrad R, Phelps TJ, Zeikus JG (1985) Gas metabolism evidence in support of the juxtaposition of hydrogen-producing and methanogenic bacteria in sewage-sludge and lake-sediments. *Applied and Environmental Microbiology* **50** 595-601.

Cook PF (1991) Enzyme mechanism from isotope effects. CRC Press.

Fey A, Claus P, Conrad R (2004) Temporal change of ^{13}C isotope signatures and methanogenic pathways in rice field soil incubated anoxically at different temperatures. *Geochimica et Cosmochimica Acta* **68** 293-306.

Fletcher SEM, Tans PP, Bruhwiler LM, Miller JB, Heimann M (2004) CH_4 sources estimated from atmospheric observations of CH_4 and its $^{13}C/^{12}C$ isotopic ratios: 1. Inverse modeling of source processes. *Global Biogeochemical Cycles* **18** B4004-doi:10.1029/2004GB002223.

Frenzel P, Bosse U (1996) Methyl fluoride, an inhibitor of methane oxidation and methane production. *FEMS Microbiology Ecology* **21** 25-36.

Galand PE, Fritze H, Conrad R, Yrjälä K (2005) Pathways for methanogenesis and diversity of methanogenic archaea in three boreal peatland ecosystems. *Applied and Environmental Microbiology* **71** 2195-2198.

Grosskopf R, Janssen PH, Liesack W (1998) Diversity and structure of the methanogenic community in anoxic rice paddy soil microcosms as examined by cultivation and direct 16S rRNA gene sequence retrieval. *Applied and Environmental Microbiology* **64** 960-969.

Gupta M, Tyler S, Cicerone R (1996) Modeling atmospheric $\delta^{13}CH_4$ and the causes of recent changes in atmospheric CH_4 amounts. *Journal of Geophysical Research* **101** 22923-22932.

Hayes JM (1993) Factors controlling ^{13}C contents of sedimentary organic compounds - Principles and evidence. *Marine Geology* **113** 111-125.

Hoehler TM, Alperin MJ, Albert DB, Martens CS (2001) Apparent minimum free energy requirements for methanogenic Archaea and sulfate-reducing bacteria in an anoxic marine sediment. *FEMS Microbiology Ecology* **38** 33-41.

Jackson BE, McInerney MJ (2002) Anaerobic microbial metabolism can proceed close to thermodynamic limits. *Nature* **415** 454-456.

Janssen PH, Frenzel P (1997) Inhibition of methanogenesis by methyl fluoride: Studies of pure and defined mixed cultures of anaerobic bacteria and archaea. *Applied and Environmental Microbiology* **63** 4552-4557.

Kasting JF (1993) Earth's early atmosphere. *Science* **259** 920-926.

Koizumi Y, Takii S, Fukui M (2004) Depth-related change in archaeal community structure in a freshwater lake sediment as determined with denaturing gradient gel electrophoresis of amplified 16S rRNA genes and reversely transcribed rRNA fragments. *FEMS Microbiology Ecology* **48** 285-292.

Krüger M, Frenzel P, Kemnitz D, Conrad R (2005) Activity, structure and dynamics of the methanogenic archaeal community in a flooded Italian rice field. *FEMS Microbiology Ecology* **51** 323-331.

Krylova NI, Conrad R (1998) Thermodynamics of propionate degradation in methanogenic paddy soil. *FEMS Microbiology Ecology* **26** 281-288.

Lansdown JM, Quay PD, King SL (1992) CH_4 production via CO_2 reduction in a temperate bog: A source of ^{13}C-depleted CH_4. *Geochimica et Cosmochimica Acta* **56** 3493-3503.

Lelieveld J, Crutzen PJ (1992) Indirect chemical effects of methane on climate warming. *Nature* **355** 339-342.

Levin I, Bergamaschi P, Dorr H, Trapp D (1993) Stable isotopic signature of methane from major sources in Germany. *Chemosphere* **26** 161-177.

Lowe DC, Brenninkmeijer CAM, Brailsford GW, Lassey KR, Gomez AJ, Nisbet EG (1994) Concentration and ^{13}C records of atmospheric methane in New Zealand and Antarctica: Evidence for changes in methane sources. *Journal of Geophysical Research* **99** 16913-16925.

Lueders T, Friedrich MW (2002) Effects of amendment with ferrihydrite and gypsum on the structure and activity of methanogenic populations in rice field soil. *Applied and Environmental Microbiology* **68** 2484-2494.

Müller V (2004) An exceptional variability in the motor of archaeal A(1)A(0) ATPases: From multimeric to monomeric rotors comprising 6-13 ion binding sites. *Journal of Bioenergetics and Biomembranes* **36** 115-125.

Peters V, Conrad R (1996) Sequential reduction processes and initiation of CH_4 production upon flooding of oxic upland soils. *Soil Biology & Biochemistry* **28** 371-382.

Richet P, Bottinga Y, Javoy M (1977) Review of hydrogen, carbon, nitrogen, oxygen, sulfur, and chlorine stable isotope fractionation among gaseous molecules. *Annual Review of Earth and Planetary Sciences* **5** 65-110.

Schink B, Stams AJM (2003) Syntrophism among prokaryotes. In:The Prokaryotes: An evolving electronic resource for the microbiological community (ed Dworkin M), p. http://link.springer-ny.com/link/service/books/10125/. Springer, New York.

Scholten JCM, Conrad R (2000) Energetics of syntrophic propionate oxidation in defined batch and chemostat cocultures. *Applied and Environmental Microbiology* **66** 2934-2942.

Schönheit P, Moll J, Thauer RK (1980) Growth-Parameters (K_s, μ_{max}, Y_s) of *Methanobacterium thermoautotrophicum*. *Archives of Microbiology* **127** 59-65.

Seitz HJ, Schink B, Pfennig N, Conrad R (1990) Energetics of syntrophic ethanol oxidation in defined chemostat cocultures. 1. Energy requirement for H_2 production and H_2 oxidation. *Archives of Microbiology* **155** 82-88.

Sharp R, Ziemer CJ, Stern MD, Stahl DA (1998) Taxon-specific associations between protozoal and methanogen populations in the rumen and a model rumen system. *FEMS Microbiology Ecology* **26** 71-78.

Stams AJM, Vandijk JB, Dijkema C, Plugge CM (1993) Growth of syntrophic propionate-oxidizing bacteria with fumarate in the absence of methanogenic bacteria. *Applied and Environmental Microbiology* **59** 1114-1119.

Sugimoto A, Wada E (1993) Carbon isotopic composition of bacterial methane in a soil incubation experiment - Contributions of acetate and CO_2/H_2. *Geochimica et Cosmochimica Acta* **57** 4015-4027.

Sühnel J (1990) The kinetic deuterium-isotope effect of proton-transfer reactions in solution - comparison of the marcus and the quantum-statistical mechanical models. *Journal of Physical Organic Chemistry* **3** 62-68.

Thauer RK (1998) Biochemistry of methanogenesis: a tribute to Marjory Stephenson. *Microbiology-UK* **144** 2377-2406.

Thauer RK, Jungermann K, Decker K (1977) Energy conservation in chemotropic anaerobic bacteria. *Bacteriological Reviews* **41** 100-180.

Tyler SC, Bilek RS, Sass RL, Fisher FM (1997) Methane oxidation and pathways of production in a Texas paddy field deduced from measurements of flux, $\delta^{13}C$, and δD of CH_4. *Global Biogeochemical Cycles* **11** 323-348.

Valentine DL, Chidthaisong A, Rice A, Reeburgh WS, Tyler SC (2004) Carbon and hydrogen isotope fractionation by moderately thermophilic methanogens. *Geochimica et Cosmochimica Acta* **68** 1571-1590.

Wang JS, Logan JA, McElroy MB, Duncan BN, Megretskaia IA, Yantosca RM (2004) A 3-D model analysis of the slowdown and interannual variability in the methane growth rate from 1988 to 1997 [Review]. *Global Biogeochemical Cycles* **18** B3011-doi:10.1029/2003GB002180.

Whiticar MJ (1999) Carbon and hydrogen isotope systematics of bacterial formation and oxidation of methane. *Chemical Geology* **161** 291-314.

Whiticar MJ, Faber E, Schoell M (1986) Biogenic methane formation in marine and freshwater environments: CO_2 reduction vs. acetate fermentation - Isotope evidence. *Geochimica et Cosmochimica Acta* **50** 693-709.

Wolin EA, Wolin MJ, Wolfe RS (1963) Formation of methane by bacterial extracts. *Journal of Biological Chemistry* **238** 2882-&.

Yao H, Conrad R (1999) Thermodynamics of methane production in different rice paddy soils from China, the Philippines and Italy. *Soil Biology & Biochemistry* **31** 463-473.

III.3. Einfluss der Hemmung der acetoklastischen Methanogenese auf das Wachstum archaeeller Populationen in einem anoxischen Umweltmodellsystem

Holger Penning und Ralf Conrad

Zusammenfassung:

Die Isotopenfraktionierung der Methanogenese aus H_2/CO_2 kann in Umweltinkubationen über die Hemmung des zweiten methanliefernden Prozesses, der acetoklastischen Methanogenese, bestimmt werden. Hier wurde erstmals der Einfluss des Hemmstoffs Methylfluorid (CH_3F) auf die archaeelle Gemeinschaft untersucht und damit die spezifische Wirkung auf die Zielorganismen evaluiert. Die Dynamik archaeeller Gruppen im Reiswurzel-Modellsystem wurde über die Kombination von *Fingerprint*- (Terminale-Restriktionsfragment-Längen-Polymorphismusanalyse) und quantitativer Analyse (*real time* PCR) des phylogenetischen 16S rRNA-Marker-Gens verfolgt. Während CH_3F die Methanbildung von Acetat verhinderte, war spezifisch das Wachstum der einzigen acetoklastischen methanogenen Gruppe, der *Methanosarcinaceae*, gehemmt. Hingegen wurden die anderen archaeellen Gruppen nicht direkt gehemmt. Somit ist die Hemmung mit CH_3F in der Tat eine geeignete Methode um die Methanproduktion aus Acetat und die Isotopenfraktionierung während der Methanogenese aus H_2/CO_2 zu bestimmen. Weiterhin zeigte diese Arbeit, dass die experimentell bestimmte Populationsgröße der methanogenen *Archaea* mit der aus der Erhaltungsenergie theoretisch bestimmten übereinstimmte.

Effect of inhibition of acetoclastic methanogenesis on growth of archaeal populations in an anoxic model environment

(akzeptiert bei Applied and Environmental Microbiology)

Holger Penning and Ralf Conrad

Max Planck Institute for Terrestrial Microbiology, Karl-von-Frisch-Str., 35043 Marburg, Germany

Abstract

Methyl fluoride is frequently used to specifically inhibit acetoclastic methanogenesis thus allowing determination of the relative contribution of acetate versus H_2/CO_2 to total CH_4 production in natural environments. However, the effect of the inhibitor on growth of the target archaeal population has not yet been studied. Therefore, we incubated rice roots as environmental model system under anoxic conditions in the presence and absence of CH_3F, measured activity and Gibbs free energy (ΔG) of CH_4 production, and determined the abundance of individual archaeal populations using a combination of quantitative (real time) PCR and analysis of terminal restriction fragment length polymorphism (T-RFLP) targeting the 16S rRNA gene. It was shown that CH_3F did not only specifically inhibit acetoclastic methanogenic activity, but also the proliferation of *Methanosarcina* spp, which were the prevalent acetoclastic methanogens in our environmental model system. Therefore, inhibition experiments with CH_3F seem to be a suitable method for quantifying acetoclastic CH_4 production. It is furthermore shown that growth and final population size of methanogens were consistent with energetic conditions that at least covered the maintenance requirements of the population.

Introduction

Atmospheric CH_4 significantly contributes to global warming (4,35). Among the dominant sources of CH_4 are wetlands and flooded rice fields, which are responsible for a third of the atmospheric CH_4 budget (4). To understand the processes responsible for methane production and consumption in anoxic environments, it is useful to study the flow of carbon and electrons. Here, metabolic inhibitors are frequently used to allow quantification of single processes (31). Methyl fluoride (CH_3F), when applied at the appropriate concentration, was found to be a rather specific inhibitor of acetoclastic methanogenesis while the operation of CH_4 production from H_2/CO_2 was unaffected (8,16). Consequently, CH_3F has been used to follow changes in carbon flow in methanogenic systems (9). However, a crucial requirement for unbiased application of inhibitors is specificity, meaning that they must not influence any other process or reaction, while the target reaction or process must be completely inactivated. Methyl fluoride is known to affect other processes than acetoclastic methanogenesis, too. For example, it also inhibits aerobic oxidation of CH_4 and to less extent also oxidation of ammonia (32,33). With respect to CH_4 production, the optimized concentration of CH_3F for complete inhibition of acetoclastic methanogenesis must not be exceeded, since at too high concentrations hydrogenotrophic methanogenesis can also be partially inhibited (16). On the other hand, CH_3F is apparently not inhibitory for acetotrophic sulfate reducers (e.g., *Desulfotomaculum* spp) and for acetogenic fermenting bacteria (e.g., *Acetobacterium* spp) (16). However, many archaeal and bacterial phylogenetic clusters that are found in natural environments are yet uncultured, so that inhibiting effects on them cannot be excluded. Although the inhibition of acetoclastic methanogenesis by CH_3F in anoxic environments has been well established (1,20), the effect of the inhibitor on the metabolically active microbial community has not yet been investigated.

Here we tested the effect of CH_3F on a natural archaeal community using molecular techniques. For our study we chose anoxically incubated rice roots, which are a well studied model system with respect to the archaeal community structure (2,22,38) and biogeochemical processes (7). Growth of archaeal populations was followed by a combination of quantitative PCR and T-RFLP analysis and compared to the maximum population densities that are feasible applying maintenance theory.

Materials and Methods

Growth and incubation conditions. Rice plants (*Oryza sativa*, var. Roma, type japonica) were grown in the greenhouse as described by Lehmann-Richter et al. (22) using soil obtained from the rice fields in Vercelli, Italy (15). After 90 days the plants were removed from the growth container and roots were carefully washed maintaining anoxic conditions (22). Freshly collected and washed rice roots (30 g per incubation) were placed into glass bottles (1000 ml; Müller and Krempel, Bülach, Switzerland) filled with 500 ml anoxic deionized water and 50 g marble grains giving a neutral carbonate-buffered aqueous phase. The bottles were closed with latex stoppers and gassed with N_2. Acetoclastic methanogenesis was inhibited by addition of 1.3% methyl fluoride (CH_3F; 99%; ABCR Karlsruhe, Germany). Methyl fluoride treatments and controls without inhibitor were incubated in triplicate at 25°C in the dark.

Extraction of RNA/DNA and PCR amplification of archaeal 16S rRNA genes. The incubation vessels were shaken vigorously to detach microorganisms from the roots before taking liquid samples from each replicate. Nucleic acids were extracted from 10 ml of the liquid phase. After centrifugation (26,000 × g, 15 min, 4°C), the cell pellets were re-suspended in 0.5 ml sterile distilled water and extracted according to a cell lysis protocol involving bead beating in the presence of the denaturant sodium dodecyl sulfate, phenol-chloroform-isoamyl alcohol (PCI) extraction, and polyethylene glycol precipitation as previously described (30).

For DNA analysis (targeting 16S rRNA genes) 5 µl was removed from the primary extract of each replicate of control and inhibition incubations. The remaining nucleic acid extracts of the control and the inhibition experiment were pooled and subsequently used for preparation of ribosomal RNA. The RNA in the two composite extracts was purified by digestion of co-extracted DNA with RQ1 RNase free DNase (Promega, Hilden, Germany) according to the manufacturer's instructions and subsequent re-extraction with PCI (see above). Aliquots of raw nucleic acid extracts and RNA preparations were visualized by standard agarose gel electrophoresis to verify the quality of extracted total nucleic acids and RNA preparations. First strand synthesis of cDNA from RNA was done as follows. 8.5 µl RNA extract, 1 µl of 10× Hexanucleotide Mix (diluted 1:50; Roche, Mannheim, Germany), and 20 U of RNasin® Ribonuclease Inhibitor (Promega) were incubated for 10 min at 70°C. After cooling on ice M-MLV RT 5× Reaction Buffer, 100 pmol of each

deoxynucleoside triphosphate (Amersham Pharmacia Biotech, Freiburg, Germany), and 200 U M-MLV RT (Promega) were added to a final volume of 25 µl and incubated at 37°C for 1 h.

Archaeal 16S rRNA genes were amplified using the forward primer A109f (5'-ACKGCTCAGTAACACGT-3'; (12)) and the FAM-labeled (= 5-carboxyfluorescein, 5' terminal) backward primer A915b (5'- GTGCTCCCCCGCCAATTCCT-3'; (40)). In a total volume of 50 µl, PCR reaction contained 10 × PCR buffer (Invitrogen GmbH, Karlsruhe, Germany), 1.25 U of *Taq* DNA-Polymerase (Invitrogen GmbH), 2.5 nmol of each deoxynucleoside triphosphate (Amersham Pharmacia Biotech), 75 nmol $MgCl_2$, 4 µg of bovine serum albumin (Roche), and 16.5 pmol of each primer (MWG Biotech, Ebersberg, Germany). A volume of 1 µl DNA or cDNA solution was added as template. Amplification was performed by using Gene Amp System 9700 (Applied Biosystems, Weiterstadt, Germany) with an initial denaturation step (4 min, 94°C) followed by 30 cycles of denaturation (45 s, 94°C), annealing (1 min, 55°C) and extension (1 min, 72°C), and terminal extension step (7 min, 72°C).

Real-time PCR. The archaeal 16S rRNA gene copy number in DNA extracts was determined by quantitative PCR (qPCR) assays based on real-time PCR previously described (36,42). PCR was carried out in an iCycler IQ thermocycler (Bio-Rad, München, Germany) using the primer pair A109f/A915b described above. Each 25 µl PCR reaction contained 12.25 µl SYBR Green Jumpstart™ *Taq* Ready Mix (Sigma-Aldrich, Taufkirchen, Germany), 37.5 nmol $MgCl_2$, (Invitrogen GmbH), 8.25 pmol of each primer (MWG Biotech), and 5 µl of DNA or H_2O as a negative control. The assay was performed with the following thermo-profile: DNA denaturation (40 s, 94°C), primer annealing (30 s, 55°C) and elongation (90 s, 72°C). Fluorescence data were collected during the elongation step. Quantification of archaeal templates was done with a serial dilution of a cloned 16S rRNA gene sequence amplified with vector primers (17). The standard DNA was fluorimetrically quantified using the PicoGreen dsDNA quantitation kit (Molecular Probes, Invitrogen). iCycler software (version 3.0a; Bio-Rad) was used for data analysis, calculation of target molecules (16S rRNA gene copies) was done as described earlier (19,41).

Terminal – Restriction Fragment Length Polymorphism (T-RFLP) analysis. The principle of the T-RFLP analysis has been described by Liu et al. (23). Fluorescently labeled SSU rRNA gene amplicons were purified by use of the QIAquick PCR Purification

Kit (Quiagen GmbH, Hilden, Germany) according to the instructions of the manufacturer. DNA concentrations of purified SSU rRNA gene fragments were determined by standard UV photometry (Biophotometer; Eppendorf, Hamburg, Germany). Restriction digest was performed in a total volume of 10 µl containing ≈80 ng of SSU rRNA gene amplicons. SSU rRNA gene amplicons were restricted with 5 U of enzyme *Taq*I (Fermentas, St. Leon-Rot, Germany) and 1 µl of the appropriate incubation buffer and incubated for 3 h at 65°C. The digested amplicons were mixed with an internal lane standard and analyzed with polyacrylamide gel electrophoresis as previously described (3). Analysis was performed for the DNA extract of each replicate. The relative abundance of a detected T-RF within a given T-RFLP pattern was calculated as the respective signal area of the peak divided by the peak area of all peaks of the T-RFLP pattern starting from a fragment size of 56 bp to exclude T-RFs caused by primers. Standard errors for averaged relative abundances of T-RFs were ≤ 2% of total or 10% of the relative abundance of the particular peak. Changes in absolute 16S rRNA gene copy numbers of each T-RF were calculated by multiplication of its relative abundance with the total 16S rRNA gene copy number from that particular time point. Note, that the same primer set was used for both T-RFLP analysis and qPCR.

Cloning and sequencing. Three clone libraries of archaeal 16S rRNA or 16S rRNA gene amplicons were created using samples from day 28 of the incubation (cDNA and DNA from the control, and DNA from the CH_3F treatment). Amplicons (A109f/A915b) were cloned in *Escherichia coli* JM109 using the pGEM-T Vector System II cloning kit (Promega) according to the manufacturer's instructions. Clones were selected randomly and checked for correct insert size by vector-targeted PCR and agarose gel electrophoresis. DNA sequences were determined on an ABI Prism 377 DNA sequencer with Big Dye terminator chemistry as specified by the manufacturer (Applied Biosystems).

Sequence data and phylogenetic analysis. Sequences were assembled and checked with the Lasergene software package (DNASTAR, Madison, WI, USA). 16S rRNA gene sequences (approx. 800 bp) were compared with a BLAST search to sequences of the EMBL database (www.ebi.ac.uk). Sequence alignment (Fast Aligner tool version 1.03), calculation of distance matrices and construction of phylogenetic trees were accomplished with the ARB software package (version Linux Beta 030822; http://www.arb-home.de; (26)). Sequences closely related to the cloned 16S rRNA gene sequences were obtained from the GenBank database (http://www.ncbi.nih.gov/Genbank) and integrated into the 16S rRNA gene database (released June 2002, ARB).

The terminal sequence positions at the 5′ and 3′ends of the 16S rRNA gene sequences (300 bp for partial sequences and 500 bp for full length sequences) were also subjected to a separate treeing analysis ("fractional treeing" (25)) to identify chimeric sequences. Differences in the phylogenetic placement of a fragment pair were considered indicative of chimera formation. For *in silico* determination of T-RFs the ARB-implemented TRF-CUT tool was used (37).

Nucleotide sequence accession numbers. The 16S rRNA gene sequences generated from the control (CRR: control rice root) and from the CH_3F incubation (IRR: inhibition rice root) were deposited in the EMBL database under AM050403 to AM050425.

Quantification of gaseous and dissolved compounds. Liquid samples (2.5 ml) were taken with a sterile syringe, membrane-filtered (0.2 µm) and stored frozen (-20°C) until analysis. Gas samples (0.25-1.0 ml) were taken with a gas-tight pressure lock syringe (Dynatech, Baton Rouge, LA, USA) after the bottles were vigorously shaken by hand, and analyzed immediately by gas chromatography. CH_4 and CO_2 were analyzed by gas chromatography using a flame ionization detector (Shimadzu, Kyoto, Japan). CO_2 was detected after conversion to CH_4 with a methanizer (Ni-catalyst at 350°C, Chrompack, Middelburg, Netherlands). H_2 was analyzed by gas chromatography using a thermal conductivity detector (Shimadzu) and a HgO-to-Hg conversion detector (RGD2; Trace Analytical, Menlo Park, CA) (39). Acetate, ethanol, formate, and fatty acids were measured by HPLC (Sykam, Gilching, Germany) with a refraction index and UV-detector, having a detection limit of 3-5 µM (21).

Calculations. Gibbs free energies (ΔG) of the production of CH_4 were calculated from the respective standard Gibbs free energies (ΔG°) and the actual concentrations of reactants and products using Nernst's equation. The values of ΔG° were calculated from the standard Gibbs energies of formation (44) using the following reactions:

$$4H_2 + CO_2 \rightarrow CH_4 + 2\,H_2O \qquad \Delta G° = -130.7\ kJ\ mol^{-1} \qquad (1)$$

$$CH_3COO^- + H^+ \rightarrow CH_4 + CO_2 \qquad \Delta G° = -75.7\ kJ\ mol^{-1} \qquad (2)$$

The potential capacity for maintaining a particular population size (N) of methanogens was calculated from the thermodynamic data and from the CH_4 production rates measured in the experiment using the following equation (5):

$$N_{mc} = -\Delta G\, v_{CH4}\, m_E^{-1}\, \gamma^{-1} \quad (3)$$

with N_{mc} = number of (hydrogenotrophic or acetoclastic) methanogenic archaea (cells ml^{-1}); ΔG = Gibbs free energy (kJ mol^{-1}) of the (hydrogenotrophic or acetoclastic) methanogenic reaction determined for the particular incubation condition; v_{CH4} = rate of (hydrogenotrophic or acetoclastic) methanogenesis (mol CH_4 h^{-1} ml^{-1}); m_E = maintenance energy (kJ h^{-1} (C-mol of methanogenic biomass)$^{-1}$); γ = molar mass of a methanogenic cell (C-mol). The value of γ was assumed to be 8×10^{-15} C-mol, using the equivalence of 25 g microbial dry mass for 1 C-mol biomass (45) and assuming that a microbial cell had a mass of about 2×10^{-13} g (34,46). The value of m_E was reported to be constant for anaerobic microorganisms, amounting to 3.3 kJ h^{-1} C-mol^{-1} biomass at 25°C (45). The v_{CH4} for hydrogenotrophic and acetoclastic methanogenesis was calculated from the measured rates of total CH_4 production (v_{tot}) times f_{mc} and (1-f_{mc}), respectively, f_{mc} being the fraction of methane formed from H_2/CO_2. Values of f_{mc} were determined from measurement of $\delta^{13}C$ in CH_4, CO_2, and acetate as described by (6). Detailed results of the measurements will be presented elsewhere. The calculation of N is not very sensitive to the accuracy of f_{mc}, but is linearly influenced by the other parameters, i.e. ΔG, m_E, v_{tot} and γ.

Results

Process data of rice root incubations. During the anoxic incubation of excised rice roots CO_2 and CH_4 accumulated steadily, whereas H_2, acetate, and propionate accumulated only transiently and later decreased again (Fig. 1; H_2 and CO_2 not shown). In the control incubations, CH_4 production started immediately albeit at low rate, and strongly increased on day 14 (Fig. 1A). Similar activity patterns have been observed before (7,38). In the CH_3F incubations, on the other hand, CH_4 accumulated very little until day 24, while acetate accumulated linearly reaching about 10 mM (Fig. 1B), indicating that acetoclastic methanogenesis was inhibited. Complete inhibition of acetoclastic methanogenesis was confirmed by stoichiometric calculations. Until day 24 the sum of the rate of acetate production in the CH_3F incubation and the rate of acetate consumption in the control equaled the difference of methane production rates between control and CH_3F incubation.

After day 24, accumulation of acetate ceased, and turned into net decrease after day 33, while CH_4 production rate increased, indicating resumption of acetoclastic methanogenesis. This resumption was due to the decrease of the CH_3F concentration below the threshold (about 1.0-1.2%) of inhibition (Fig. 1A). The loss of CH_3F was accounted for by gas and liquid sampling.

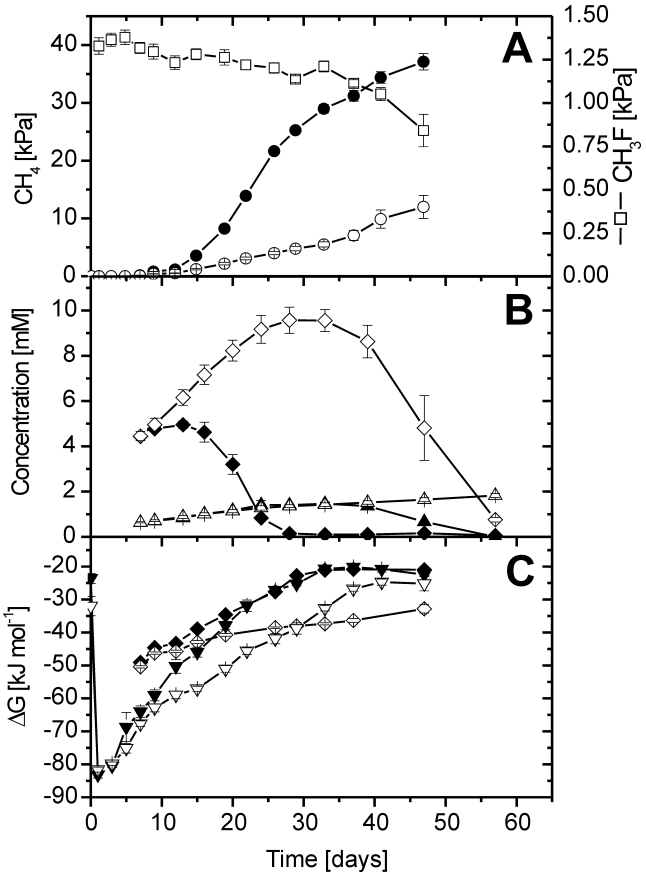

Figure 1: Change in gas partial pressures, concentrations and Gibbs free energies of control (full symbols) and CH_3F (open symbols) rice root incubations: (A) CH_4 (●,○), CH_3F (□); (B) acetate (◆,◇), propionate (▲,△); (C) Gibbs free energies of the conversion of CO_2 and H_2 to CH_4 (▼,▽), of the conversion of acetate to CH_4 and CO_2 (◆,◇). Mean ± SE; n=3.

Propionate accumulated to 1.45 mM in both control and CH_3F treatment until day 33 (Fig. 1B). Thereafter propionate further increased in the CH_3F incubation, while it was completely consumed in the control. Low concentrations of ethanol (≤ 150 µM), butyrate (≤ 70 µM), valerate (≤ 50 µM), and caproate (≤ 30 µM) were also detected. Although their maximum concentrations were comparable in the control and CH_3F incubation, the compounds accumulated in the CH_3F incubation until the end, whereas none of them was detectable in the control after day 33.

In the control, Gibbs free energies for CH_4 production from H_2/CO_2 and acetate were strongly exergonic in the beginning but then increased with incubation time, and finally reached about –20 kJ mol^{-1} after day 40 (Fig. 1C). These values are close to the thermodynamic threshold of methanogenic activity (14,39,47). In the CH_3F treatments, ΔG of hydrogenotrophic methanogenesis was relatively more negative throughout the experiment, since H_2 partial pressures were always slightly higher in the CH_3F treatments than in the control, but finally also reached relatively high values of –25 kJ mol^{-1}, close to the thermodynamic threshold (Fig. 1C). Acetoclastic methanogenesis, on the other hand, was always thermodynamically feasible in the CH_3F-treated incubations.

Diversity of Archaea in rice root incubations. T-RFLP analysis targeting the 16S rRNA gene was done using samples collected from control and CH_3F treatments over the entire incubation time. The T-RFLP patterns of the control were similar as observed before (2), revealing a dynamic change of the different phylogenetic groups of archaea. The T-RFLP patterns are not shown explicitly, but were used in calculation of 16S rRNA gene copy numbers for the individual archaeal populations as described below.

Three clone libraries of archaeal 16S rRNA fragments were constructed from samples taken on day 28: (1) 16S rRNA (RNA-based) from the control, (2) 16S rRNA gene (DNA-based) from the control, and (3) 16S rRNA gene (DNA-based) from the CH_3F incubation. From a total of 90 clones, no chimera were identified. Phylogenetic analysis of clones showed that all sequences were affiliated with the same eury- and crenarchaeotal lineages described before (2). These included the methanogenic families of *Methanobacteriaceae* and *Methanosarcinaceae*, as well as uncultured *Archaea* designated as Rice Clusters I, III, IV, and V (3,13). The sequence dissimilarities of *Methanosarcinaceae*- and *Methanobacteriaceae*-related sequences were < 3 and < 2% to *Methanosarcina barkeri* and *Methanobacterium bryantii*, respectively. Rice cluster I (RC-I) clone sequences were >97% similar to clone AS08-16 from rice field soil (28), RC-III sequences were >97% similar to ARR16 from rice roots (13) and AS08-11 from rice field soil (28), and RC-IV sequences were >94% similar to AS01-06 and AS08-25 from rice field soil (28). Clones from RC-V were >82% similar to the closest relatives UniArc49 (43) and WCHD3-30 (10).

The relative abundance of the different lineages on day 28 of incubation differed between the different clone libraries (Table 1). In the control *Methanosarcinaceae* strongly dominated on rRNA gene level, and were the exclusive archaea on rRNA level. By

contrast, the clone library of 16S rRNA genes from the CH_3F incubation was much more diverse, representing all detected groups. RC-V accounted for the largest number of clones (25%), RC-I and RC-III represented 17.5% each, followed by the other groups. *In silico* determination of T-RFs of the archaeal 16S rRNA fragments using *Taq*I (37) yielded uniform and specific lengths for each archaeal lineage (Table 1), indicating that the combination of the chosen primer set and restriction enzyme was suitable for differentiating the individual T-RF as phylogenetic lineages. We compared the relative abundance of archaeal T-RFs in the clone library with the T-RFLP pattern of the same replicate, from which the clone library was constructed (Table 1). The relative abundances were in fairly good agreement, indicating that all major T-RFs could be phylogenetically assigned and that cloning bias did not play a serious role.

Table 1: Relative abundances (%) of phylogenetic groups in rice root incubations on day 28, based on frequencies of 16S rRNA or 16S rRNA genes in clone libraries and T-RFLP analysis.

Phylogenetic group (T-RF length)	Control (rRNA gene; n=24)		CH_3F (rRNA gene; n=35)		Control (rRNA; n=31)	
	Clone library	T-RFLP[§]	Clone library	T-RFLP[§]	Clone library	T-RFLP[§]
MB (92)		0.9	5.0	1.8		
MS (186)	87.5	92.8	12.5	14.0	100.0	99.2
RC-I (393)		2.7	17.5	21.5		
RC-III (381)		0.7	17.5	9.0		0.8
RC-V (689)	4.2	1.3	25.0	35.7		
RC-IV (810)	8.3	1.0	10.0	11.0		

MB, *Methanobacteriaceae*; MS, *Methanosarcinaceae*; RC, Rice Cluster; [§] same replicate as for construction of the clone library was used.

T-RFLP analysis of 16S rRNA (RNA-based) was only performed for day 20, 24, and 28 and is shown together with the relative abundance pattern of the 16S rRNA gene (DNA-based) at the same time points (Fig. 2). Comparing the course of T-RF on RNA- and DNA-level shows that the 186-bp T-RF always had a higher relative abundance on RNA-level, whereas the other T-RFs had either a similar or lower relative abundance. The 689-bp T-RF was even not detected on RNA-level. The relative increase of the 186-bp T-RF and the relative decrease of the other T-RFs on RNA-level was seen about eight days earlier than on DNA-level in the control and the CH_3F treatment.

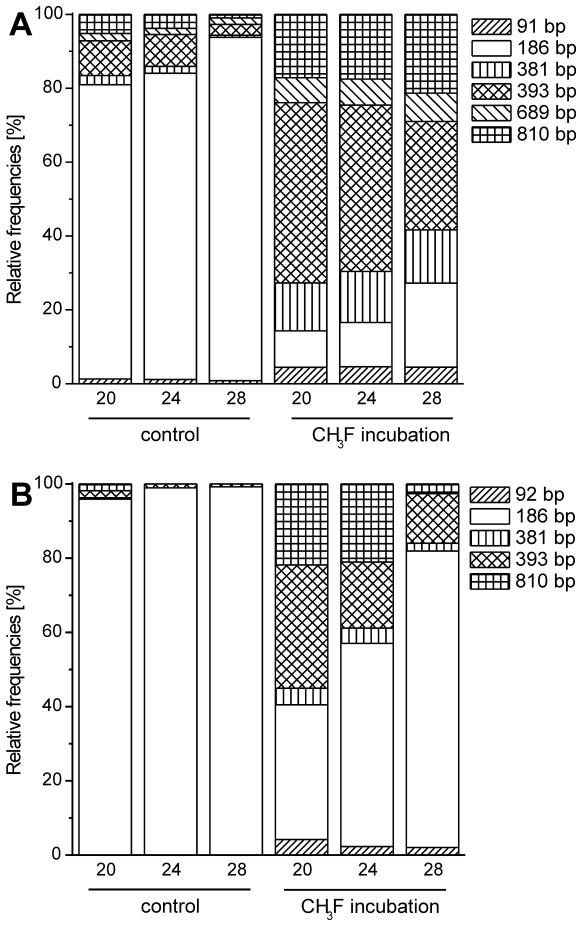

Figure 2: Course of archaeal population dynamics determined by (A) 16S rRNA gene-targeted and (B) 16S rRNA-targeted T-RFLP analysis for incubation days 20, 24, 28 for control and CH_3F incubation. Numbers in the legend indicate the fragment length of the T-RF; (A) average values of triplicate incubations; (B) single value from three pooled replicates.

Population dynamics of *Archaea*. To address the dynamics of archaeal groups, we performed T-RFLP analysis and qPCR targeting 16S rRNA genes (DNA level).

Numbers of 16S rRNA gene copies (N_{copy}) determined by qPCR increased rapidly in the control until day 24, and then stabilized at 10^8 ml^{-1} (Fig. 3A). In the CH_3F incubation, on the other hand, N_{copy} reached only 1.5×10^7 ml^{-1} at day 20 to 28, but then increased further reaching 4×10^7 ml^{-1} at day 47.

Experiments by Lueders and Friedrich (29) showed, that our T-RFLP assay allows the determination of the relative abundance of the individual T-RF within the total archaeal population. However, even if the amplification efficiency between the investigated archaeal groups would be different, this would not affect our interpretation, since the inhibition effects are compared within the same archaeal groups and not among them.

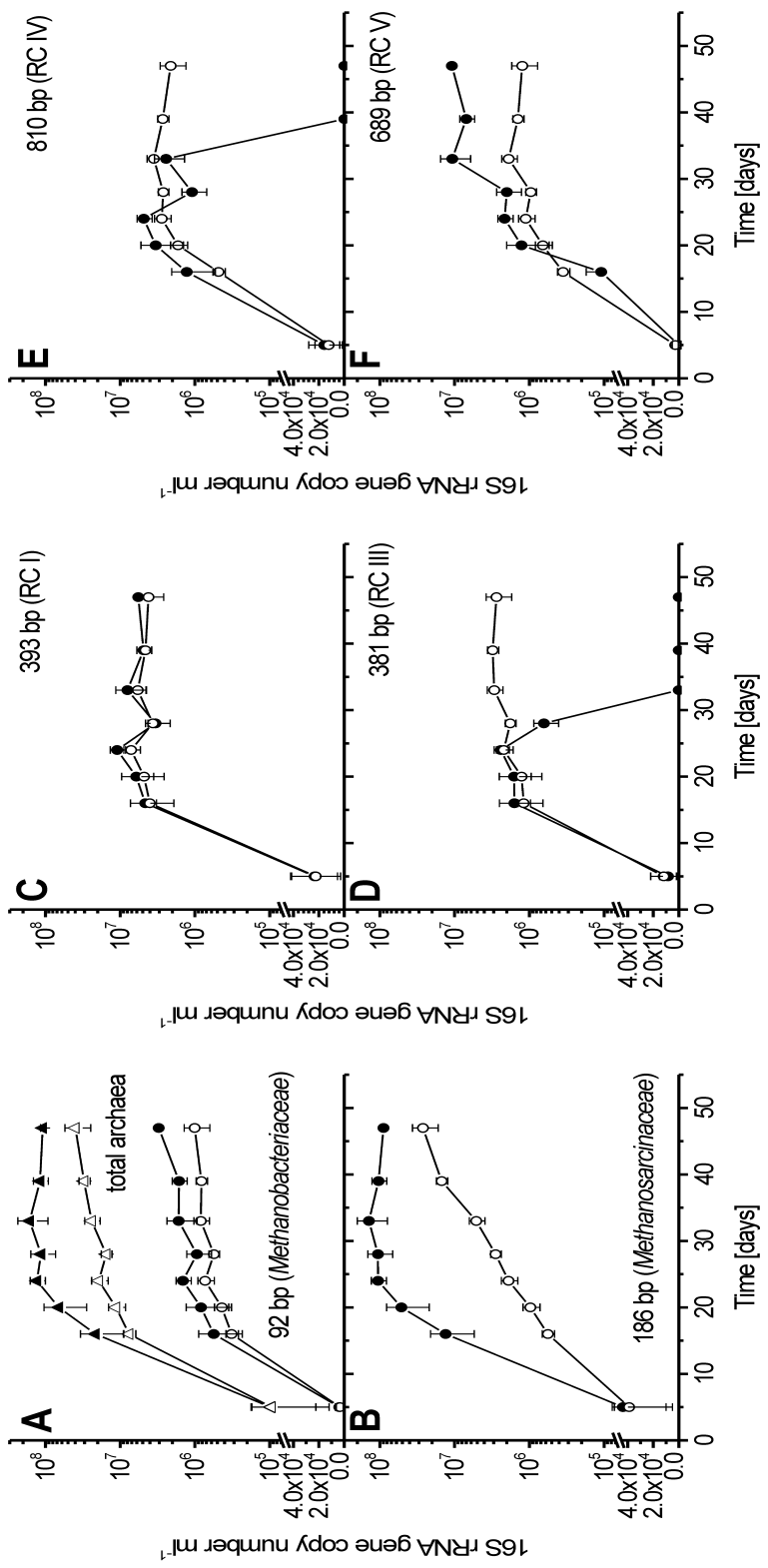

Figure 3: Temporal change of archaeal 16S rRNA gene copy numbers (N_{copy}) per ml ; (A) total archaea (triangles) and the 92-bp T-RF (circles), (B) 186-bp T-RF, (C) 393-bp T-RF, (D) 381-bp T-RF, (E) 810-bp T-RF, and (F) 689-bp T-RF. All panels show temporal changes of control (full symbols) and CH_3F (open symbols) incubations (mean ± SD; n=3).

The qPCR assay, which applies the same primers and PCR conditions, quantifies the total 16S rRNA gene copy numbers of the archaeal population. Combination of both data sets thus allows the determination of the temporal change of the 16S rRNA gene copy numbers of individual archaeal lineages (Fig. 3). The 92-bp T-RF, representing *Methanobacteriaceae*, steadily increased with incubation time both in the control and the CH_3F incubation, while absolute numbers were slightly higher in the control (significant only on day 39 and 47) (Fig. 3A). Maximum copy numbers were 3×10^6 and 1×10^6 ml^{-1} in control and CH_3F incubation, respectively. The 186-bp T-RF, representing *Methanosarcinaceae*, exponentially increased in the control until day 28 and then stayed at about $N_{copy} = 1\times10^8$ ml^{-1} until the end (Fig. 3B). By contrast in the CH_3F incubation, the N_{copy} was always much lower than in the control and increased much slower. The 393-bp T-RF, representing methanogenic RC-I, initially increased, but reached a constant level of about $N_{copy} = 5\times10^6$ ml^{-1} after about 20 days in both control and CH_3F incubation (Fig. 3C). A different time course was observed for the 381-bp T-RF, representing euryarchaeotal RC-III (Fig. 3D), and the 810-bp T-RF, representing crenarchaeotal RC IV (Fig. 3E). The copy numbers of both T-RF increased in the control as well as in the CH_3F incubation until day 24. Thereafter, N_{copy} stabilized in the CH_3F incubations (3×10^6 ml^{-1}), but decreased to zero in the control. A value of zero means, that no peak of the particular T-RF was detected in the T-RFLP analysis. The 689-bp T-RF, representing euryarchaeotal RC-V, showed a similar increase in both incubations until day 24 with a slightly higher N_{copy} in the control (Fig. 3F). Then, however, it increased further in the control (reaching about 10^7 ml^{-1}), but remained constant in the CH_3F incubation (about 10^6 ml^{-1}).

Number of theoretically maintained cells. The CH_4 production rates and Gibbs free energies of methanogenesis (Fig. 1) were used to calculate the number of methanogens (N_{mc}; equ. 3) that can be maintained at steady state by the respective energy conditions (Fig. 4). Values of N_{mc} were in a range of 2×10^7 to 6×10^7 ml^{-1} and compared fairly well with the measured numbers (N_{mm}). Values of N_{mm} were determined using16S rRNA gene copy numbers (N_{copy}) of methanogenic *Methanobacteriaceae* (T-RF = 92 bp), *Methanosarcinaceae* (T-RF = 186 bp) and RC-I (T-RF = 393 bp), which increased with time from $< 10^5$ ml^{-1} to about 10^8 ml^{-1}. Since *Methanosarcina* spp., the dominant methanogenic population, have three rRNA gene copies per genome (18), final values of N_{mm} were around 4×10^7 ml^{-1}, i.e. similar to N_{mc} (Fig. 4).

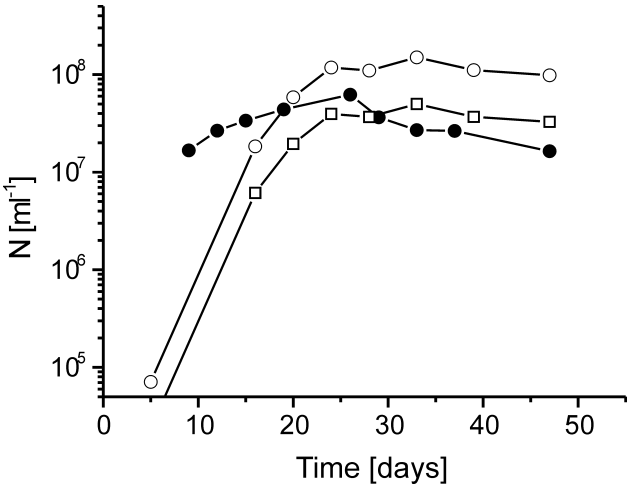

Figure 4: Comparison of experimentally determined 16S rRNA gene copy numbers (N_{copy}; ○) and derived cell numbers (N_{mm}; □) with the theoretically derived maximum number (N_{mc}; ●) of methanogenic archaea in the control incubation.

Discussion

Our experiments with rice roots as model system confirmed that CH_3F inhibited acetoclastic CH_4 production and resulted in the accumulation of acetate (8). The inhibition was released around day 24, when the CH_3F concentration decreased below a threshold of 1.0-1.2%, resulting in resumption of methanogenic acetate utilization. Simultaneous T-RFLP analysis and qPCR of archaeal 16S rRNA genes showed that CH_3F specifically inhibited proliferation of acetoclastic methanogenic *Methanosarcinaceae*. In the uninhibited control, *Methanosarcinaceae* grew exponentially mainly on transiently produced acetate and reached titers compatible with maintenance theory.

The temporal change of the population size (i.e., 16S rRNA copy numbers) of six prevalent archaeal groups was quantified (Fig. 3). The presumed target organisms for the inhibitor CH_3F are the archaea performing acetoclastic methanogenesis, i.e. *Methanosarcinaceae* and *Methanosaetaceae*. We did neither detect a clone sequence of *Methanosaetaceae* nor a T-RF characteristic for this group, which is in agreement with earlier rice root studies, where this group was hardly detectable (2,13). *Methanosarcinaceae* (186-bp T-RF), on the other hand, were abundant and active as shown by the T-RFLP patterns based on rRNA genes (abundance) and ribosomal RNA (activity) (Fig.2). The abundance and activity of *Methanosarcinaceae* was strongly decreased in the CH_3F versus the control incubation. Instead, RC-I methanogens became

relatively more abundant and active (Fig. 2) confirming previous experiments by Lu et al. (24). Nevertheless, growth of *Methanosarcinaceae* was not completely abolished in the CH_3F treatment (Fig. 3B). Although the acetoclastic methanogenic pathway was inhibited, *Methanosarcinaceae* were probably able to gain energy from conversion of H_2/CO_2 to CH_4. After cessation of inhibition by CH_3F, growth could again be sustained by acetoclastic in addition to or instead of hydrogenotrophic methanogenesis. The stop of growth in the control after day 24 was probably due to energetic limitation, as the Gibbs free energy of both hydrogenotrophic and acetoclastic methanogenesis approached the thermodynamic threshold. This threshold is believed to be around –20 kJ mol^{-1}, equivalent to synthesis of about 1/3 ATP (14,39,47). By contrast in the CH_3F incubation, the *Methanosarcinaceae* population also grew after day 28, when the CH_3F inhibition ceased, since acetate was still available to provide sufficient energy.

Methanobacteriaceae (92-bp T-RF) and RC-I methanogens (393-bp T-RF) are the hydrogenotrophic methanogenic archaeal groups found in the rice root incubations. RC-I does not yet exist in pure culture, but genomic information on the methanogenic operons already exists (11,27). Both groups are unable to perform acetoclastic methanogenesis and should therefore not be influenced directly by CH_3F. Indeed, RC-I as the dominant hydrogenotrophic methanogenic group was not affected, and *Methanobacteriaceae*-16S rRNA gene copy numbers were only slightly decreased in the CH_3F incubation. Hence, our study demonstrates that CH_3F specifically inhibited the proliferation of acetoclastic methanogens in a natural model environment, but did not affect hydrogenotrophic methanogens.

However, we observed an effect of CH_3F on other non-methanogenic archaeal populations present in our model environment. Thus, 16S rRNA gene copy numbers of RC-III (381-bp T-RF) and RC-IV (810-bp T-RF) decreased in the control after day 24 finally reaching zero, but remained at a constant number in the CH_3F treatment. An enrichment culture of RC-III archaea, which are distantly related to *Thermoplasmatales*, was recently shown to grow anaerobically on yeast extract, peptone and tryptone (17). However, nothing is known about the physiology of the crenarcheotal lineage RC-IV. The prevention of decrease of RC-III and RC-IV populations by CH_3F might be a secondary effect of the inhibition, e.g. due to the higher concentrations of acetate and H_2 in the presence compared to the absence of CH_3F. Analogously, ethanol and the fatty acids butyrate, valerate and caproate were still detectable at the late phase of the CH_3F

incubation, whereas in the control they were below the detection limit. We speculate, that CH_3F inhibition leads to prolongation of favorable conditions for RC-III and RC-IV due such secondary effects of inhibition.

The 16S rRNA gene copy numbers of the euryarchaeotal lineage RC-V (689-bp T-RF), of which the physiology is unknown, still increased after day 24 in the control, but not in the CH_3F treatment. We do not know the mechanism behind this observation, but it is noteworthy that the T-RF of RC-V could not be detected in the T-RFLP pattern generated from the ribosomal fraction (RNA-based) (Fig. 2B), suggesting that RC-V was not very active, at least not between day 20 and 28.

In the rice root environmental system CH_4 was produced from acetate and H_2/CO_2 by three different phylogenetic groups of methanogenic archaea (*Methanobacteriaceae*, RC-I, and *Methanosarcinaceae*). The numbers of methanogenic organisms that can be maintained by the Gibbs free energy and the CH_4 production rate under the actual incubation conditions were found to be consistent to those actually observed (Fig. 4). The accuracy of the calculation depends linearly on the uncertainty of the input values. Values of Gibbs free energies and CH_4 production rates were determined from measured values and introduced only a relatively small error. However, the coefficient γ, which represents the C-mass of a single cell, is highly uncertain and may vary within an order of magnitude. For our calculations we used a value of 2×10^{-13} g C per cell (34,46). A larger cell mass would result in lower theoretical numbers of methanogens, and vice versa. The calculated number is the maximum of cells sustained without net growth at steady state. Our determinations showed that energetic conditions in the control incubation were permissive for net growth until about day 20 to 30, but then could not maintain more than about 2×10^7 to 4×10^7 methanogenic cells ml^{-1}. At this time, the most prevalent methanogenic populations (i.e., *Methanosarcinaceae* and RC-I) had stopped growth (Fig.3), and the numbers of methanogenic cells observed were similar to those calculated from maintenance theory (Fig. 4). This observation for the first time shows that the maintenance energy requirement of the cells is possibly important for determining microbial population size in a natural environment.

Acknowledgements. We thank Dr. Gesche Braker for helpful discussions and technical advice and the Fonds der Chemischen Industrie, Deutschland, for financial support.

References

1. **Chan, O. C., P. Claus, P. Casper, A. Ulrich, T. Lueders, and R. Conrad**. 2005. Vertical distribution of structure and function of the methanogenic archaeal community in Lake Dagow sediment. Environmental Microbiology **7**:1139-1149.

2. **Chin, K. J., T. Lueders, M. W. Friedrich, M. Klose, and R. Conrad**. 2004. Archaeal community structure and pathway of methane formation on rice roots. Microb. Ecol. **47**:59-67.

3. **Chin, K. J., T. Lukow, and R. Conrad**. 1999. Effect of temperature on structure and function of the methanogenic archaeal community in an anoxic rice field soil. Appl. Environ. Microbiol. **65**:2341-2349.

4. **Cicerone, R. J. and R. S. Oremland**. 1988. Biogeochemical aspects of atmospheric methane. Global Biogeochem. Cy. **2**:299-327.

5. **Conrad, R.** 1999. Soil microorganisms oxidizing atmospheric trace gases (CH_4, CO, H_2, NO). Ind. J. Microbiol. **39**:193-203.

6. **Conrad, R.** 2005. Quantification of methanogenic pathways using stable carbon isotopic signatures: a review and a proposal. Org. Geochem. **36**:739-752.

7. **Conrad, R. and M. Klose**. 1999. Anaerobic conversion of carbon dioxide to methane, acetate and propionate on washed rice roots. FEMS Microbiol. Ecol. **30**:147-155.

8. **Conrad, R. and M. Klose**. 1999. How specific is the inhibition by methyl fluoride of acetoclastic methanogenesis in anoxic rice field soil? FEMS Microbiol. Ecol. **30**:47-56.

9. **Conrad, R. and M. Klose**. 2000. Selective inhibition of reactions involved in methanogenesis and fatty acid production on rice roots. FEMS Microbiol. Ecol. **34**:27-34.

10. **Dojka, M. A., P. Hugenholtz, S. K. Haack, and N. R. Pace**. 1998. Microbial diversity in a hydrocarbon- and chlorinated-solvent-contaminated aquifer undergoing intrinsic bioremediation. Appl. Environ. Microbiol. **64**:3869-3877.

11. **Erkel, C., D. Kemnitz, M. Kube, P. Ricke, K. J. Chin, S. Dedysh, R. Reinhardt, R. Conrad, and W. Liesack**. 2005. Retrieval of first genome data for rice cluster I methanogens by a combination of cultivation and molecular techniques. FEMS Microbiol. Ecol. **53**:187-204.

12. **Grosskopf, R., P. H. Janssen, and W. Liesack**. 1998. Diversity and structure of the methanogenic community in anoxic rice paddy soil microcosms as examined by cultivation and direct 16S rRNA gene sequence retrieval. Appl. Environ. Microbiol. **64**:960-969.

13. **Grosskopf, R., S. Stubner, and W. Liesack**. 1998. Novel euryarchaeotal lineages detected on rice roots and in the anoxic bulk soil of flooded rice microcosms. Appl. Environ. Microbiol. **64**:4983-4989.

14. **Hoehler, T. M., M. J. Alperin, D. B. Albert, and C. S. Martens**. 2001. Apparent minimum free energy requirements for methanogenic Archaea and sulfate-reducing bacteria in an anoxic marine sediment. FEMS Microbiol. Ecol. **38**:33-41.

15. **Holzapfel-Pschorn, A. and W. Seiler**. 1986. Methane emission during a cultivation period from an Italian rice paddy. J. Geophys. Res. **91**:11803-11814.

16. **Janssen, P. H. and P. Frenzel**. 1997. Inhibition of methanogenesis by methyl fluoride: Studies of pure and defined mixed cultures of anaerobic bacteria and archaea. Appl. Environ. Microbiol. **63**:4552-4557.

17. **Kemnitz, D., S. Kolb, and R. Conrad**. 2005. Phenotypic characterization of Rice Cluster III archaea without prior isolation by applying quantitative polymerase chain reaction to an enrichment culture. Environ. Microbiol. **7**:553-565.

18. **Klappenbach, J. A., P. R. Saxman, J. R. Cole, and T. M. Schmidt**. 2001. rrndb: the Ribosomal RNA Operon Copy Number Database. Nucleic Acids Res. **29**:181-184.

19. **Kolb, S., C. Knief, S. Stubner, and R. Conrad**. 2003. Quantitative detection of methanotrophs in soil by novel pmoA-targeted real-time PCR assays. Appl. Environ. Microbiol. **69**:2423-2429.

20. **Krüger, M., G. Eller, R. Conrad, and P. Frenzel**. 2002. Seasonal variation in pathways of CH_4 production and in CH_4 oxidation in rice fields determined by stable carbon isotopes and specific inhibitors. Glob. Change Biol. **8**:265-280.

21. **Krumböck, M. and R. Conrad**. 1991. Metabolism of position-labeled glucose in anoxic methanogenic paddy soil and lake sediment. FEMS Microbiol. Ecol. **85**:247-256.

22. **Lehmann-Richter, S., R. Grosskopf, W. Liesack, P. Frenzel, and R. Conrad**. 1999. Methanogenic archaea and CO_2-dependent methanogenesis on washed rice roots. Environ. Microbiol. **1**:159-166.

23. **Liu, W. T., T. L. Marsh, H. Cheng, and L. J. Forney**. 1997. Characterization of microbial diversity by determining terminal restriction fragment length polymorphisms of genes encoding 16S rRNA. Appl. Environ. Microbiol. **63**:4516-4522.

24. **Lu, Y. H., T. Lueders, M. W. Friedrich, and R. Conrad**. 2005. Detecting active methanogenic populations on rice roots using stable isotope probing. Environ. Microbiol. **7**:326-336.

25. **Ludwig, W., S. H. Bauer, M. Bauer, I. Held, G. Kirchhof, R. Schulze, I. Huber, S. Spring, A. Hartmann, and K. H. Schleifer**. 1997. Detection and in situ identification of representatives of a widely distributed new bacterial phylum. FEMS Microbiol. Lett. **153**:181-190.

26. **Ludwig, W., O. Strunk, R. Westram, L. Richter, H. Meier, Yadhukumar, A. Buchner, T. Lai, S. Steppi, G. Jobb, W. Forster, I. Brettske, S. Gerber, A. W. Ginhart, O. Gross, S. Grumann, S. Hermann, R. Jost, A. Konig, T. Liss, R. Lussmann, M. May, B. Nonhoff, B. Reichel, R. Strehlow, A. Stamatakis, N. Stuckmann, A. Vilbig, M. Lenke, T. Ludwig, A. Bode, and K. H. Schleifer**. 2004. ARB: a software environment for sequence data. Nucleic Acids Res. **32**:1363-1371.

27. **Lueders, T., K. J. Chin, R. Conrad, and M. Friedrich**. 2001. Molecular analyses of methyl-coenzyme M reductase alpha-subunit (mcrA) genes in rice field soil and enrichment cultures reveal the methanogenic phenotype of a novel archaeal lineage. Environ. Microbiol. **3**:194-204.

28. **Lueders, T. and M. Friedrich**. 2000. Archaeal population dynamics during sequential reduction processes in rice field soil. Appl. Environ. Microbiol. **66**:2732-2742.

29. **Lueders, T. and M. W. Friedrich**. 2003. Evaluation of PCR amplification bias by terminal restriction fragment length polymorphism analysis of small-subunit rRNA and mcrA genes by using defined template mixtures of methanogenic pure cultures and soil DNA extracts. Appl. Environ. Microbiol. **69**:320-326.

30. **Lueders, T., M. Manefield, and M. W. Friedrich**. 2004. Enhanced sensitivity of DNA- and rRNA-based stable isotope probing by fractionation and quantitative analysis of isopycnic centrifugation gradients. Environ. Microbiol. **6**:73-78.

31. **Oremland, R. S. and D. G. Capone**. 1988. Use of "specific" inhibitors in biogeochemistry and microbial ecology. Adv. Microb. Ecol. **10**:285-383.

32. **Oremland, R. S. and C. W. Culbertson**. 1992. Evaluation of methyl fluoride and dimethyl ether as inhibitors of aerobic methane oxidation. Appl. Environ. Microbiol. **58**:2983-2992.

33. **Oremland, R. S. and C. W. Culbertson**. 1992. Importance of methane-oxidizing bacteria in the methane budget as revealed by the use of a specific inhibitor. Nature **356**:421-423.

34. **Paul, E. A. and F. E. Clark**. 1989. Soil microbiology and biochemistry. Academic, New York.

35. **Prinn, R. G.** 1994. Global atmospheric-biospheric chemistry, p. 1-18. *In* R. G. Prinn (ed.), Global Atmospheric-Biospheric Chemistry. Plenum, New York.

36. **Raeymaekers, L.** 2000. Basic principles of quantitative PCR. Molecular Biotechnology **15**:115-122.

37. **Ricke, P., S. Kolb, and G. Braker**. 2005. Application of a newly developed ARB software-integrated tool for in silico terminal restriction fragment length polymorphism analysis reveals the dominance of a novel pmoA cluster in a forest soil. Appl. Environ. Microbiol. **71**:1671-1673.

38. **Scheid, D., S. Stubner, and R. Conrad**. 2003. Effects of nitrate- and sulfate-amendment on the methanogenic populations in rice root incubations. FEMS Microbiol. Ecol. **43**:309-315.

39. **Seitz, H. J., B. Schink, N. Pfennig, and R. Conrad**. 1990. Energetics of syntrophic ethanol oxidation in defined chemostat cocultures. 1. Energy requirement for H_2 production and H_2 oxidation. Arch. Microbiol. **155**:82-88.

40. **Stahl, D. A. and R. Amann**. 1991. Development and application of nucleic acid probes, p. 205-248. *In* E. Stackebrandt and M. A. Goodfellow (eds.), Nucleic acid techniques in bacterial systematics. Wiley, New York.

41. **Stubner, S.** 2002. Enumeration of 16S rDNA of Desulfotomaculum lineage 1 in rice field soil by real-time PCR with SybrGreen (TM) detection. J. Microbiol. Meth. **50**:155-164.

42. **Suzuki, M. T., L. T. Taylor, and E. F. Delong**. 2000. Quantitative analysis of small-subunit rRNA genes in mixed microbial populations via 5 '-nuclease assays. Appl. Environ. Microbiol. **66**:4605-4614.

43. **Takai, K. and K. Horikoshi**. 1999. Genetic diversity of archaea in deep-sea hydrothermal vent environments. Genetics **152**:1285-1297.

44. **Thauer, R. K., K. Jungermann, and K. Decker**. 1977. Energy-Conservation in Chemotropic Anaerobic Bacteria. Bacteriol. Rev. **41**:100-180.

45. **Tijhuis, L., M. C. M. VanLoosdrecht, and J. J. Heijnen**. 1993. A thermodynamically based correlation for maintenance Gibbs energy requirements in aerobic and anaerobic chemotrophic growth. Biotechnol. Bioeng. **42**:509-519.

46. **Whitman, W. B., D. C. Coleman, and W. J. Wiebe**. 1998. Prokaryotes: The unseen majority. PNAS **95**:6578-6583.

47. **Yao, H. and R. Conrad**. 1999. Thermodynamics of methane production in different rice paddy soils from China, the Philippines and Italy. Soil Biol. Biochem. **31**:463-473.

III.4. Geochemische Charakterisierung des anoxischen Reiswurzel-Modellsystems durch Thermodynamik, stabile Kohlenstoffisotopie und Hemmung der acetoklastischen Methanogenese

Holger Penning, Stanley C. Tyler und Ralf Conrad

Zusammenfassung:

Anoxisch inkubierte Reiswurzeln sind auf Grund der hohen Dynamik geochemischer Prozesse und ihrer mikrobiellen Gemeinschaft ein gutes Modellsystem zur Untersuchung prinzipieller Fragen in anoxischen Systemen. Hier wurde der Ablauf geochemischer Prozesse in Reiswurzelinkubationen mit und ohne Hemmung der acetoklastischen Methanogenese durch Methylfluorid (CH_3F) untersucht. Die effektive Hemmung der Methanproduktion aus Acetat konnte präzise über die Isotopensignatur der Methylgruppe des sich akkumulierenden Acetats nachgewiesen werden. Diese Arbeit zeigte erstmals, dass dieses Modellsystem nicht von H_2-Gradienten beeinflusst ist. Somit war es auch bei H_2-abhängigen Reaktionen möglich, durch Vergleich der Prozessdaten mit den errechneten thermodynamischen Bedingungen, die Hemmwirkung von CH_3F zu beurteilen. In der Tat hemmte CH_3F spezifisch die acetoklastische Methanogenese. Zudem wurde die Isotopenfraktionierung der acetoklastischen Methanproduktion von *Methanosarcinaceae* unter *steady state*- und nicht-*steady sta*te-Bedingungen bestimmt. Die Fraktionierungsfaktoren lagen im Bereich der bereits früher in Reinkulturen bestimmten Werte, so dass für *Methanosarcinaceae* Reinkulturwerte in Umweltsystemen zur Modellierung verwendet werden können. Mit Hilfe der hier bestimmten Fraktionierungsfaktoren wurde der Anteil der hydrogenotrophen Methanogenese modelliert und stimmte mit den gemessenen Prozessdaten überein.

Geochemical characterization of the anoxic model system rice roots using thermodynamics, carbon stable isotopes, and specific inhibition of acetoclastic methanogenesis

(eingereicht bei Geobiology)

Holger Penning[1], Stanley C. Tyler[2], and Ralf Conrad[1]*

[1]Max Planck Institute for Terrestrial Microbiology, Karl-von-Frisch-Str., 35043 Marburg, Germany

[2]Department of Earth Systems Science, University of California, Irvine, California 92697-3100, USA

Abstract

Methanogenic processes can be quantified by stable carbon isotopes, if necessary modeling parameters, especially fractionation factors, are known. Anoxically incubated rice roots are a model system with a dynamic microbial community and thus suitable to investigate principal geochemical processes in anoxic natural systems. Here we applied an inhibitor of acetoclastic methanogenesis (methyl fluoride), calculated the thermodynamics of the involved processes, and analyzed the carbon stable isotope signatures of products and intermediates to characterize the carbon flow during anaerobic degradation of rice roots to the final products CO_2 and CH_4. Using a comprehensive stable isotope approach we show that this model system is not affected by H_2 gradients and confirm that methyl fluoride is a specific inhibitor of acetoclastic methanogenesis. Complete inhibition of acetoclastic methanogenesis was confirmed by four different approaches based on both compound specific and intramolecular stable carbon isotope signatures and on process data. During the inhibition phase, we quantified the fractionation factor of CH_4 production from H_2/CO_2. The fractionation factor of acetoclastic methanogenesis was experimentally determined at non-steady state and steady state conditions, of which the latter was used for successfully modelling the carbon flow. The model results were in agreement with the measured process data. Our study clearly demonstrates that stable carbon isotope

signatures are a proper tool to quantify carbon flow, if fractionation factors are determined experimentally.

Introduction

Atmospheric CH_4 significantly contributes to global warming (Cicerone and Oremland, 1988; Prinn, 1994). Among the dominant sources of CH_4 are wetlands and flooded rice fields, which are responsible for a third of the CH_4 emissions to the atmosphere (Cicerone and Oremland, 1988). Different functional groups of microorganisms catalyze the reactions in anaerobic degradation of organic matter to the final products CO_2 and CH_4. To understand the processes responsible for CH_4 production and consumption in anoxic environments, it is useful to study the flow of carbon and electrons. Thermodynamics, specific inhibitors and stable isotopes help to characterize such systems. Thermodynamic conditions determine the feasibility of reactions and are therefore a good tool to narrow down the total number of anaerobic processes to the ones that are potentially active. Further simplification of the complex anoxic system is attained by the use of metabolic inhibitors, which may even permit one to quantify a single target process (Oremland and Capone, 1988). Under anoxic conditions methyl fluoride (CH_3F) was found to be a specific inhibitor of acetoclastic methanogenesis while allowing the operation of CH_4 production from H_2/CO_2 (Conrad and Klose, 1999; Penning and Conrad, 2005b; Janssen and Frenzel, 1997). Later CH_3F was used to follow changes in the carbon flow and Gibbs free energies (Conrad and Klose, 2000; Conrad *et al.* 2002). Besides thermodynamics and inhibitors, stable carbon isotopes, which are naturally occurring tracers, are also useful to constrain the carbon flow. Isotope signatures have been used to identify active methane formation and oxidation in marine sediments (Alperin *et al.* 1992; Whiticar, 1999) and rice paddies (Tyler *et al.* 1997; Chanton *et al.* 1997). This is feasible, since important microbial reactions involved in the degradation of organic matter like homoacetogenesis (Gelwicks *et al.* 1989), and methanogenesis from H_2/CO_2 (Botz *et al.* 1996; Fuchs *et al.* 1979) or acetate (Gelwicks *et al.* 1994; Krzycki *et al.* 1987) imprint characteristic isotope signatures in their products, which allow one to quantify their participation in carbon flow. Here the quantification of the pathways forming the greenhouse gas CH_4 are of special interest. Since in most terrestrial anoxic environments CH_4 is only produced from H_2/CO_2 or acetate, their relative contribution to methanogenesis can be determined with knowledge of the isotope fractionation factors for

their reactions. In contrast to the slightly varying fractionation factor of acetoclastic methanogenesis (Gelwicks *et al.* 1994; Zyakun *et al.* 1988; Krzycki *et al.* 1987), the fractionation factor of hydrogenotrophic methanogenesis varies within a wide range (Fey *et al.* 2004). Fortunately, it can be determined in incubation experiments using the inhibitor CH_3F , so that the methanogenic pathways contributing to the total CH_4 production can be quantified (reviewed by Conrad, 2005).

To investigate anaerobic reactions geochemically, we chose anoxically incubated rice roots. The rice root system is an important source for the global CH_4 budget, since around 30% of the total CH_4 emission from rice fields originates from plant photosynthesized carbon (Minoda *et al.* 1996). Furthermore it is a well studied model system with respect to the archaeal community structure (Chin *et al.* 2004; Lu and Conrad, 2005; Chidthaisong *et al.* 2002) and biogeochemical processes (Conrad *et al.* 2002). Because it is relatively homogeneous and its natural community of microorganisms belongs to an important anoxic environment, this model system is highly valuable to investigate general questions related to biogeochemical processes in anoxic environments.

Therefore, we used this model to study the anaerobic degradation of root organic carbon by measuring the concentrations and $^{13}C/^{12}C$ isotopic signatures of the main metabolites (i.e. CH_4, CO_2, acetate and propionate) and calculating the Gibbs free energies of conceivable processes. We showed that CH_3F was indeed a specific inhibitor of acetoclastic methanogenesis and could be used to discriminate isotopic fractionation during acetoclastic versus hydrogenotrophic methanogenesis. Furthermore, we measured the intramolecular isotope signature of acetate, the key intermediate in CH_4 production from rice roots at non-steady state and steady-state conditions, supplying useful information for quantifying the path of carbon in methanogenesis.

Materials and Methods

Growth and incubation conditions. Rice plants (*Oryza sativa*, var. Roma, type japonica) were grown in the greenhouse as described by Conrad et al. (2002) using soil obtained from the rice fields in Vercelli, Italy (Holzapfel-Pschorn and Seiler, 1986). After 90 days the plants were removed from the growth container and roots were carefully washed keeping anoxic conditions (Conrad *et al.* 2002). Incubations were performed in glass bottles (1000 ml; Müller and Krempel, Bülach, Switzerland) closed with latex

stoppers. Bottles were filled with 500 ml anoxic deionized water containing 50 g of marble grains ($\delta^{13}C$ of marble = 1.65‰; Merck, Darmstadt, Germany) as a buffer and autoclaved one week before start of the incubation. Dry-blotted rice roots (30 g) were added to the bottles and then gassed with N_2. Washing and preparation of roots was done within three hours after harvest of the plants. Inhibition of acetoclastic methanogenesis was accomplished by addition of 1.3% of methyl fluoride (CH_3F; 99%; ABCR Karlsruhe, Germany). The methyl fluoride treatment and control incubation were both conducted in triplicate at 25°C under dark conditions to avoid the growth of algae.

Quantification of gaseous and dissolved compounds. Liquid samples (12.5 ml) were taken with a sterile syringe, membrane-filtered (0.2 µm) and stored frozen (-20°C) until analysis. Gas samples (0.25-1.0 ml) were taken with a gas-tight pressure lock syringe (Dynatech, Baton Rouge, LA, USA) after the bottles were vigorously shaken by hand, and analyzed immediately by gas chromatography. CH_4 and CO_2 were analyzed by gas chromatography using a flame ionization detector (Shimadzu, Kyoto, Japan). CO_2 was detected after conversion to CH_4 with a methanizer (Ni-catalyst at 350°C, Chrompack, Middelburg, Netherlands). H_2 was analyzed by gas chromatography, depending on H_2 concentration either with a thermal conductivity detector (Shimadzu, Kyoto, Japan) or a HgO-to-Hg conversion detector (RGD2; Trace Analytical, Menlo Park, CA, USA) (Seitz *et al.* 1990). Acetate, ethanol, formate, and fatty acids were measured by HPLC (Sykam, Gilching, Germany) with a refraction index and UV-detector, having a detection limit of 3-5 µM (Krumböck and Conrad, 1991).

Carbon isotope analysis. Stable isotope analysis of $^{13}C/^{12}C$ in gas samples was performed using a gas chromatograph combustion isotope ratio mass spectrometer (GC-C-IRMS) system (Thermoquest, Bremen, Germany). Its principle operation is described by Brand (1996). The CH_4 and CO_2 in the gas samples (40-400 µl) were first separated in a Hewlett Packard 6890 gas chromatograph using a Pora Plot Q column (27.5 m length, 0.32 mm i.d.; 10 µm film thickness; Chrompack, Frankfurt, Germany) at 30°C with He (99.996% purity; 2.6 ml min^{-1}) as carrier gas. After conversion of CH_4 to CO_2 in the Finnigan Standard GC Combustion Interface III, the $^{13}C/^{12}C$ was analyzed by the IRMS instrument (Finnigan MAT model delta plus).

The isotope reference gas was CO_2 (99.998% purity; Messer-Griessheim, Düsseldorf, Germany) calibrated with the working standard methylstearate (Merck). The

latter was intercalibrated at the Max-Planck-Institut für Biogeochemie, Jena, Germany (courtesy of Dr. W.A. Brand) against NBS 22 and USGS 24, and reported in the delta notation versus V-PDB: $\delta^{13}C = 10^3 (R_{sa}/R_{st}-1)$ with $R = {}^{13}C/{}^{12}C$ of sample (sa) and standard (st), respectively. The precision of repeated analysis was ± 0.2‰, when 1.3 nmol CH_4 was injected.

Isotopic measurements of lactate, formate, acetate, propionate, and ethanol were performed on a HPLC system (Spectra System P1000, Thermo Finnigan, San Jose, CA, USA; Mistral, Spark, Emmen, The Netherlands) equipped with an ion-exclusion column (Aminex HPX-87-H, Biorad, München, Germany) and coupled to Finnigan LC IsoLink (Thermo Electron Corporation, Bremen, Germany) as described by Krummen et al. (2004). Isotope ratios were detected on an IRMS (Finnigan MAT delta plus advantage). Isotope reference gas was CO_2 calibrated as described above.

An off-line pyrolysis was conducted to determine $\delta^{13}C$ of the methyl group of acetate ($\delta_{ac\text{-}methyl}$). Acetate in the liquid sample was purified using HPLC by collecting the acetate fraction from each run. The purified sample was added to a strong NaOH solution and dried in a Pyrex tube under vacuum. The dried reactants were pyrolyzed under vacuum at 400°C, converting the carboxyl carbon to CO_2 and the methyl carbon to CH_4 (Blair *et al.* 1985). Gas samples were taken and then analyzed by GC-C-IRMS as above.

Calculations. Fractionation factors for a reaction A → B are defined after Hayes (1993):

$$\alpha_{A/B} = (\delta_A + 1000)/(\delta_B + 1000) \quad (1)$$

sometimes expressed as $\varepsilon \equiv 10^3 (1 - \alpha)$.

The isotopic signature for a newly formed CH_4 (δ_n) was calculated from the isotopic signatures at two time points t =1 (δ_1) and t = 2 (δ_2) by the following mass balance equation:

$$\delta_2 = f_n\delta_n + (1- f_n)\, \delta_1 \quad (2)$$

with f_n being the fraction of the newly formed C-compound relative to the total at t = 2.

Relative contribution of acetate- and CO_2-derived CH_4 to total CH_4 was determined using the following mass balance equation (Conrad, 2005):

$$f_{mc} = (\delta_{CH4} - \delta_{ma})/(\delta_{mc} - \delta_{ma}) \quad (3)$$

where f_{mc} is the fraction of CH_4 formed from H_2/CO_2, δ_{CH4} the $\delta^{13}C$ of total produced methane, and δ_{ma} and δ_{mc} are the isotope ratios of CH_4 either derived from acetate or

H_2/CO_2. δ_{ma} was calculated from $\delta_{ac\text{-}methyl}$ using α_{ma} (experimentally determined in this study and from literature data) until day 26, thereafter $\alpha = 1.00$ assuming $\delta_{ac\text{-}methyl} = -32‰$. δ_{mc} was calculated using the α experimentally determined from hydrogenotrophic methanogenesis ($\alpha_{CO2/CH4}$), when acetoclastic methanogenesis was completely inhibited. After ceasing of inhibition $\alpha_{CO2/CH4} = 1.072$ was used.

An equation presented by Mariotti et al. (1981) was used to calculate the isotopic effect (ε) associated with acetoclastic methanogenesis. Determination was done from the residual reactant (equ. 9):

$$\delta_r = \delta_{ri} + \varepsilon[\ln(1-f)] \quad (4)$$

where δ_{ri} is the isotope composition of the reactant (ac-methyl) at the beginning, which in our case is the maximum accumulation of acetate in the incubation; δ_r is the isotope composition of the residual reactant at the instant, when f was determined; and f = fractional yield of the products based on the consumption of acetate ($0 < f < 1$). Linear regression of δ_r against ln(1-f) gives ε as the slope. We are aware, that acetate is still being produced by fermentation, even as acetoclastic methanogenesis begins. This causes the value of $\delta_{ac\text{-}methyl}$ to decrease somewhat due to the continuously produced isotopically light acetate. To lessen this effect we only used $0.0 < f < 0.5$ for the analysis thereby significantly reducing the effect on $\delta_{ac\text{-}methyl}$.

Gibbs free energies (ΔG) of CH_4 production of, propionate production from precursors, and propionate oxidation were calculated from the respective standard Gibbs free energies ($\Delta G°$) and the actual concentrations of reactants and products. The $\Delta G°$ were calculated from the standard Gibbs free energies of formation (Thauer *et al.* 1977).

$$4\ H_2 + CO_2 \rightarrow CH_4 + 2\ H_2O \qquad \Delta G° = -130.7\ kJ\ mol^{-1} \quad (5)$$

$$4\ H_2 + 2\ CO_2 \leftrightarrows\ CH_3COO^- + H^+ + 2\ H_2O \qquad \Delta G° = -55.1\ kJ\ mol^{-1} \quad (6)$$

$$CH_3COO^- + H^+ \rightarrow CH_4 + CO_2 \qquad \Delta G° = -75.7\ kJ\ mol^{-1} \quad (7)$$

$$3\ H_2 + CH_3COO^- + CO_2 \leftrightarrows\ CH_3CH_2COO^- + 2\ H_2O \qquad \Delta G° = -71.7\ kJ\ mol^{-1} \quad (8)$$

$$7\ H_2 + 3\ CO_2 \leftrightarrows\ CH_3CH_2COO^- + H^+ + 4\ H_2O \qquad \Delta G° = -126.8\ kJ\ mol^{-1} \quad (9)$$

Results

Process data of rice root incubations

During anoxic incubation of excised rice roots from *Oryza sativa*, CO_2 and CH_4 accumulated, whereas H_2, acetate, and propionate accumulated transiently and later decreased (Fig. 1, 2a, 3a). In the control, CH_4 production started at a low rate on day one, strongly increased on day 14, and then slowed down (Fig. 1a). In contrast in the CH_3F incubation, where acetoclastic methanogenesis was inhibited, CH_4 accumulated to less extent until day 33, while after that the CH_4 production rate increased. Acetate accumulated in the control to 5 mM until day 13, whereas in the CH_3F incubation acetate accumulated until day 28 to 10 mM before it was consumed to steady state values around 100 µM (Fig. 2a). This steady state concentration is approximately the threshold concentration typical for *Methanosarcinaceae* (Jetten *et al.* 1990), the dominant acetoclastic methanogenic group in the rice root system (Chin *et al.* 2004). Consumption of acetate (Fig. 2a) and increase of the CH_4 production rate (Fig. 1a) occurred later in the CH_3F incubation. This indicated the cessation of inhibition of acetoclastic methanogenesis, which was due to the decline of the concentration of the inhibitor CH_3F. The decline of CH_3F was mostly caused by gas and liquid sampling (Fig. 1a). Because of the relatively high Bunsen coefficient of 0.99 for CH_3F (Frenzel and Bosse, 1996), liquid sampling contributed significantly the decrease of the CH_3F concentration.

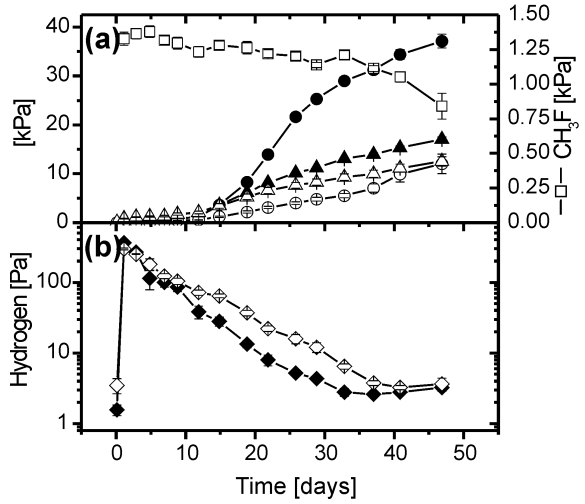

Figure 1: Change in gas partial pressures in the headspace of control (full symbols) and CH_3F (open symbols) rice root incubations. (a) Accumulated CH_4 (●,○), CO_2 (▲,△), and the inhibitor CH_3F (□). (b) Hydrogen accumulated transiently in the system (◆,◇). Mean ± SE; n=3.

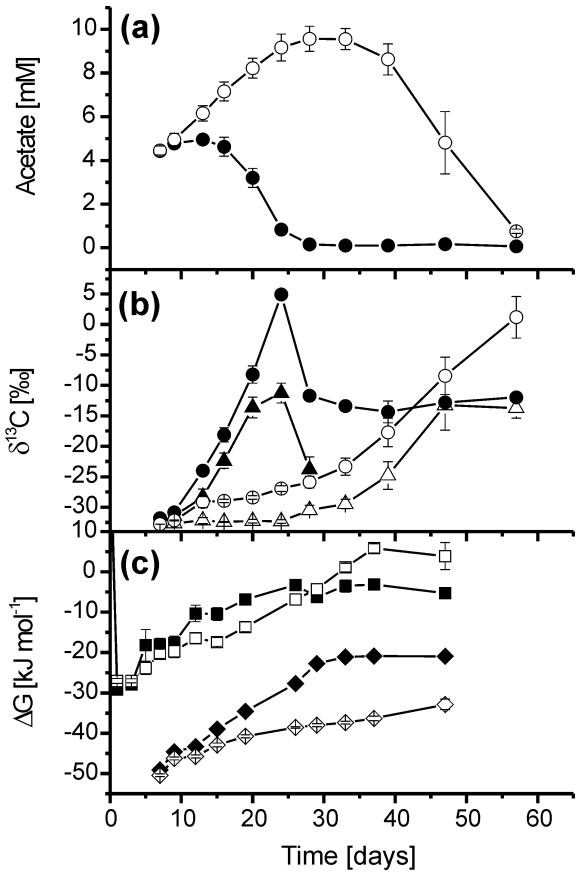

Figure 2: Changes in (a) acetate concentrations, and isotope ratios of (b) methyl-acetate ($\delta_{ac\text{-}methyl}$; ▲,△) and total acetate (δ_{ac}; ●,○). (c) Gibbs free energy for acetate production from H_2/CO_2 (■,□) and CH_4 production form acetate (◆,◇). All panels show temporal changes of control (full symbols) and CH_3F (open symbols) incubations (mean ± SE; n=3).

The threshold of inhibition for the rice root incubation was approximately 1.1 kPa CH_3F. The partial H_2 pressure (pH_2) reached a maximum of 350 Pa after 24 h and then decreased throughout the experiment, stabilizing around 3 Pa after day 37 (Fig. 1b). The value of pH_2 was generally elevated in the CH_3F incubation (differences from day 9 to 26 were between 10 and 36 Pa). The slight increase of pCO_2 within the first ten days was followed by an increased CO_2 production rate in both setups with a higher rate in the control. The fatty acid propionate accumulated in both setups until day 33 reaching 1.45 mM (Fig. 3a). After that propionate further increased in the CH_3F incubation, while it was completely consumed in the control until day 57. Low concentrations of ethanol (max. 150 µM), butyrate (max. 70 µM), valerate (max. 50 µM), and caproate (max. 30 µM) were also detected. Although their maximum concentrations were comparable in the control and CH_3F incubation, the compounds accumulated in the CH_3F incubation until the end, whereas none of them was detectable in the control after day 33.

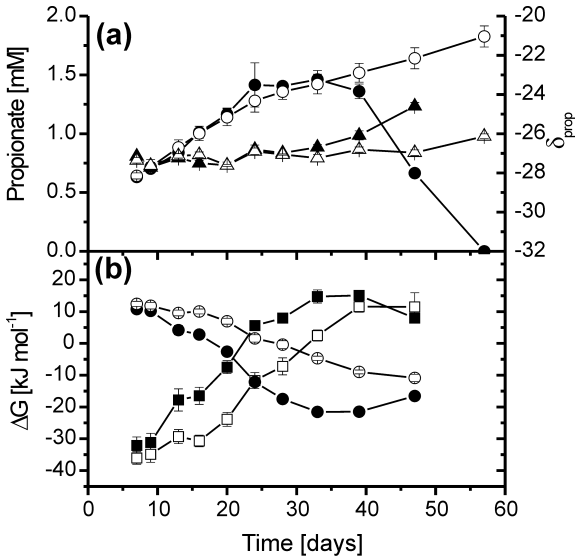

Figure 3: Propionate formation and consumption in control (full symbols) and CH_3F (open symbols) incubations. (a) Propionate concentration (●,○) and isotope composition (▲,△). (b) Gibbs free energies for the formation of propionate from CO_2 (equ. 8; ■,□) and conversion of propionate to acetate + CO_2 (equ. 7; ●,○). Mean ± SE; n=3.

Thermodynamics

The Gibbs free energies for CH_4 production from H_2/CO_2 (equ. 5) were strongly exergonic from day one on and increased with incubation time (Fig. 4a). Stable values close to the thermodynamic limit of hydrogenotrophic methanogenic activity, which is around --20 kJ mol^{-1} (Yao and Conrad, 1999; Hoehler *et al.* 2001), were reached after day 40 (-20 and -25 kJ mol^{-1} for the control and CH_3F incubation, respectively). As expected from the difference in pH_2, ΔG was higher in the control than in the CH_3F treatment by a difference of up to 15 kJ mol^{-1}. Acetoclastic methanogenesis, the second pathway of methane formation, was highly exergonic (ΔG = -50 to -20 kJ mol^{-1}) at any time in both setups (equ. 7; Fig. 2c). The ΔG of homoacetogenesis (equ. 6) was negative until day 29 in the CH_3F incubation, whereas in the control it was negative throughout the experiment albeit with ΔG > -11 kJ mol^{-1} after day 10. Other than from fermentation, propionate can be produced from H_2 + acetate + CO_2 (equ. 8) or from H_2 + CO_2 (equ. 9). Both processes are reversible and therefore could consume propionate, if ΔG of propionate production reaches positive values. Propionate formation from these two processes was thermodynamically possible until around day 17 and day 30 in the control and CH_3F incubation, respectively. After that, oxidation of propionate became thermodynamically

favored. The ΔG of propionate formation from CO_2 and of propionate oxidation to H_2 + acetate + CO_2 are shown in Fig. 3b.

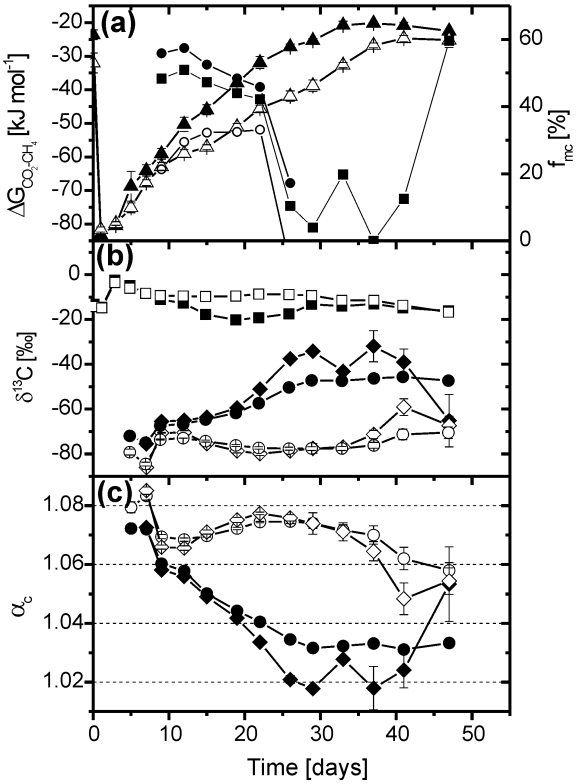

Figure 4: (a) Temporal change of Gibbs free energies of the conversion of CO_2 and H_2 to CH_4 (▲,△) and calculated fraction of hydrogenotrophic methanogenesis (f_{mc}) in the control using $\alpha_{ac\text{-}methyl/CH4}$ = 1.020 (■). Before day 29 f_{mc} is also given by using $\alpha_{ac\text{-}methyl/CH4}$ = 1.015 (●) or $\alpha_{ac\text{-}methyl/CH4}$ = 1.030 (○) for calculation. (b) Changes of measured δ_{CO2} (■,□) and $\delta_{CH4\text{-}acc}$ (●,○), and the calculated $\delta_{CH4\text{-}new}$ (◆,◇). (c) Fractionation factors $\alpha_{c\text{-}new}$ (◆,◇) and $\alpha_{c\text{-}acc}$ (●,○). All panels show temporal changes of control (full symbols) and CH_3F (open symbols) incubations (mean ± SE; n=3).

Carbon isotope geochemistry

Microbially mediated reactions characteristically change the isotope composition of key intermediates and final products of carbon flow. We measured carbon isotope ratios of the involved compounds to follow the course of the reactions. δ_{CH4} is reported as accumulated CH_4 ($\delta_{CH4\text{-}acc}$), which is the measured value, and as $\delta_{CH4\text{-}new}$, which is the calculated isotope composition of CH_4 formed since previous sampling (equ. 2). $\delta_{CH4\text{-}new}$ is a stronger indicator for changes in the dominant methanogenic pathway, since it shows changes also in the late phase of the incubation, where a different isotope ratio of newly formed CH_4 might be overseen in $\delta_{CH4\text{-}acc}$ due to the dilution effect (for comparison, both

$\delta_{CH4\text{-}acc}$ and $\delta_{CH4\text{-}new}$ are shown in Fig. 4b). In the control a small decrease in $\delta_{CH4\text{-}new}$ at day seven was followed by a steady increase to values ≈ -35‰ after day 26 (Fig. 4b). Yet in the CH_3F incubation, $\delta_{CH4\text{-}new}$ stayed at -77 ± 2‰ from day 15 to 33, and then increased. In both setups the increase of $\delta_{CH4\text{-}new}$ was correlated to pronounced acetate consumption (Fig. 2a). δ_{CO2} decreased in the CH_3F incubation from an initial maximum on day three to stable values of -16 ± 2‰ from day 15 to 33, followed by a slight decrease to the end of the experiment. In the control δ_{CO2} stronger decreased until day 19 and then again increased to values similar as in the CH_3F incubation.

The apparent carbon isotope fractionation during hydrogenotrophic methanogenesis (α_c; equ. 1) was calculated for $\delta_{CH4\text{-}new}$ ($\alpha_{c\text{-}new}$) and $\delta_{CH4\text{-}acc}$ ($\alpha_{c\text{-}acc}$)(Fig. 4). The fractionation is termed "apparent", since the isotope signature of CH_4 in the system might be determined by acetoclastic and hydrogenotrophic methanogenesis, while for the calculation only the isotope signature of the methanogenic substrate CO_2 is used. Yet, if acetoclastic methanogenesis is completely inhibited by CH_3F and methane is exclusively produced from H_2/CO_2, α_c becomes equal to $\alpha_{CO2/CH4}$. $\alpha_{c\text{-}new}$ decreased in the control due to CH_4 production from acetate and stayed at low values (≈ 1.02), except of the increase at the end of the incubation. In the CH_3F incubation, on the other hand, $\alpha_{c\text{-}new}$ stayed between 1.071 and 1.077 from day 15 to 33, and then decreased with the onset of acetoclastic methanogenesis.

The carbon isotope ratios of the sum of the two C-atoms of acetate (δ_{ac}) as well as of only the methyl group of acetate ($\delta_{ac\text{-}methyl}$) were experimentally determined (Fig. 2b). The value of $\delta_{ac\text{-}methyl}$ is of particular interest, since the methyl-group of acetate is converted to CH_4 in acetoclastic methanogenesis (Weimer and Zeikus, 1978; deGraaf *et al.* 1996). In the control, $\delta_{ac\text{-}methyl}$ increased from -31 to -11‰ from day nine to 24 simultaneously with a decrease in acetate concentration. At day 28, when acetate had declined to 150 µM, $\delta_{ac\text{-}methyl}$ had again decreased to -24‰. In the CH_3F incubation, $\delta_{ac\text{-}methyl}$ stayed constant at -32 ‰ until day 24 and then increased to –13‰ with decreasing acetate concentration, showing the same correlation as observed in the control. Values of δ_{ac} followed the same trend as $\delta_{ac\text{-}methyl}$, but were isotopically enriched in ^{13}C compared to $\delta_{ac\text{-}methyl}$ with exception of day seven and nine. $\delta_{ac\text{-}carboxyl}$ ($\delta_{ac\text{-}carboxyl} = 2\,\delta_{ac} - \delta_{ac\text{-}methyl}$) became further isotopically enriched relative to $\delta_{ac\text{-}methyl}$ until day 24 and day 39 in the control and CH_3F incubation, respectively (Table 1). The difference in isotope ratios

between the methyl and carboxyl group of acetate was highest, when acetate was almost depleted to the steady state concentration and was isotopically most ^{13}C-enriched. In the control, δ_{ac} stabilized at –13‰ after day 28 at acetate concentrations of about 100 µM.

Table 1: Isotope composition of acetate, methyl-acetate, carboxyl-acetate, CO_2, $CH_{4\text{-new}}$, the difference of CO_2 and carboxyl-acetate, and the difference of methyl-acetate and CH_4 (values are means of triplicates).

		$\delta^{13}C$ [‰]					
	time [days]	ac	ac-methyl	ac-carboxyl*	CO_2	$CH_{4\text{-new}}$	$\Delta(CO_2$ - ac-carboxyl)§
control	9	-30.83	-31.43	-30.23	-11.15	-65.52	19.08
	13	-24.02	-28.29	-19.74	-12.72	-65.04	7.03
	16	-18.11	-22.37	-13.86	-17.74	-63.67	-3.88
	20	-8.22	-13.64	-2.80	-20.22	-59.50	-17.43
	24	4.93	-11.25	21.11	-19.21	-51.06	-40.32
	28	-11.69	-23.77	0.39	-17.09	-34.25	-17.48
	33	-13.40	nd		-16.63	-43.17	
	39	-14.36	nd		-14.71	-38.97	
	47	-12.78	nd		-15.59	-65.13	
	57	-11.98	nd				
CH_3F	9	-32.16	-32.62	-31.70	-9.35	-70.60	22.35
	13	-29.15	-32.18	-26.12	-9.52	-70.48	16.60
	16	-28.95	-32.40	-25.51	-9.76	-75.44	15.75
	20	-28.39	-32.27	-24.51	-9.52	-78.73	14.99
	24	-26.94	-32.31	-21.58	-8.67	-79.87	12.92
	28	-25.89	-30.46	-21.32	-9.34	-77.52	11.98
	33	-23.32	-29.45	-17.20	-11.43	-77.05	5.77
	39	-17.70	-24.78	-10.62	-11.46	-59.12	-0.83
	47	-8.43	-13.25	-3.60	-16.69	-67.36	-13.09
	57	1.18	-13.73	16.08			-16.08

*$\delta_{ac\text{-}carboxyl} = 2\ \delta_{ac} - \delta_{ac\text{-}methyl}$; §$\Delta(CO_2$ - ac-carboxyl) $= \delta_{CO2} - \delta_{ac\text{-}carboxyl}$; nd: not determined.

Using equ. 4 derived by Mariotti et al. (1981) we determined the fractionation factor for $0.0 < f < 0.5$ in the control and CH_3F incubation to be $\varepsilon = 29.7$ ($r^2 = 0.94$) or expressed as $\alpha_{ac\text{-}methyl/CH4} = 1.030$ (Fig. 5). This value is probably slightly underestimated, since the ongoing production of acetate by fermentation decreased the ^{13}C content of acetate during its consumption. Steady state conditions established in the control at the late phase of the experiment for the concentration and isotope ratio of acetate. There, fractionation of acetoclastic methanogenesis ($\alpha_{ac\text{-}methyl/CH4}$) was determined by a second

method. The fractionation factor ε of acetoclastic methanogenesis was given by the difference of the measured isotope ratio of acetate at steady state concentration ($\delta_{ac\text{-}ss}$ = -13 ± 1‰; average signature of both C atoms; Fig. 2b at late phase in the control) and of acetate formed by fermentation ($\delta_{ac\text{-}methyl\text{-}ferm}$ = -32‰; signature of the methyl group C; early phase of CH_3F incubation in Fig. 2b) (described in principle by Hayes, 2001). Hereby, we assumed that the acetate with the isotope signature of $\delta_{ac\text{-}ferm}$ was identical to that accumulating in the presence of CH_3F, i.e., when acetate consumption by acetoclastic methanogenesis was inhibited. $\delta_{ac\text{-}methyl\text{-}ss}$ was calculated from $\delta_{ac\text{-}ferm}$ and $\delta_{ac\text{-}ss}$ using a ^{13}C depletion of the methyl group of 4‰, which was a typical difference during acetate accumulation and initial consumption (Table 1).

$$\varepsilon = \delta_{ac\text{-}methyl\text{-}ss} - \delta_{ac\text{-}methyl\text{-}ferm} = (-13 - 4) - (-32)\ ‰ = 15‰ (\equiv \alpha_{ac\text{-}methyl/CH4} = 1.015) \quad (10)$$

The fatty acid propionate accumulated in the CH_3F incubation with a stable $\delta^{13}C$ of propionate (δ_{prop} = -27‰). In contrast in the control, where propionate oxidation was energetically favored and thus the propionate concentration decreased from day 33 on, δ_{prop} slightly increased (propionate was under the detection limit of HPLC-IRMS on day 57; Fig. 3a).

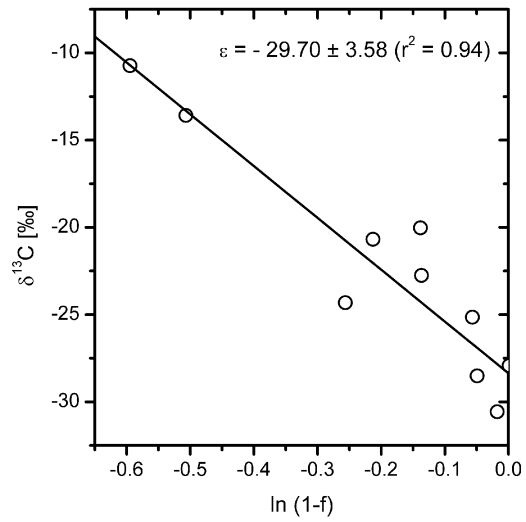

Figure 5: Isotope fractionation by acetoclastic methanogenesis during consumption of accumulated acetate in rice root incubations based on methyl carbon of acetate substrate.

Calculated values of the relative contribution of hydrogenotrophic methanogenesis (equ. 3) in the control are included in Fig. 4a. δ_{mc}, required for the calculation, was calculated using $\alpha_{CO2/CH4\text{-}new}$ of the CH_3F-inhibition (see Fig. 4c) until day 26 then $\alpha_{CO2/CH4}$ = 1.072. Before day 29, when $\alpha_{ac\text{-}methyl/CH4}$ was required for modeling due to non-

steady-state conditions, f_{mc} was calculated using the values of $\alpha_{ac\text{-}methyl/CH4}$ that we determined in our study (1.015 and 1.030; see discussion for details) and the value from pure culture data (1.020; (Gelwicks *et al.* 1994)). Using $\alpha_{ac\text{-}methyl/CH4}$ = 1.020, until day 15, f_{mc} was initially about 50% and then decreased to minimum values at days 28 and 36. Thereafter f_{mc} increased to about 60% at day 47.

To determine, whether the calculated free energy for methanogenesis from H_2/CO_2 (equ. 4) agreed with the *in situ* energy conditions, $\alpha_{CO2/CH4}$ was plotted against $\Delta G_{CO2/CH4}$ (equ. 5) for the CH_3F incubation from day nine to 26 (Fig. 6), during which time acetoclastic methanogenesis was completely inhibited by CH_3F. A α-ΔG correlation, which was found for cocultures of fermenting and hydrogenotrophic methanogens (Penning *et al.* 2005), is included in Fig. 6. Penning et al. (2005) found that incubations of environmental samples only follow this correlation, if no H_2 gradients between the site of H_2 production and the site of measurement exist. The relatively good agreement of the incubation data with the α-ΔG correlation thus means that thermodynamic calculations that are based on H_2 gas measurements well reflect the actual *in situ* ΔG. Values of $\alpha_{CO2/CH4}$ (1.064 to 1.078) and $\Delta G_{CO2/CH4}$ (-65 to -39 kJ mol^{-1}) increased with incubation time and clearly followed the α-ΔG relation observed for defined cocultures of fermenting bacteria and hydrogenotrophic methanogens (Penning *et al.* 2005).

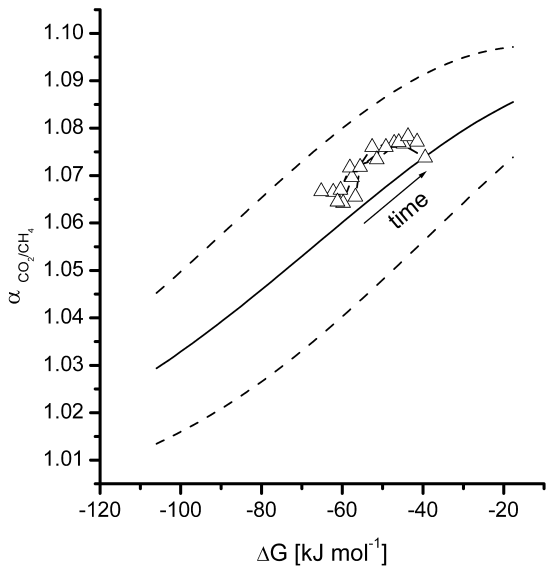

Figure 6: α-ΔG relation of hydrogenotrophic methanogenesis for the individual CH_3F incubations. Data follow the relation found for defined cocultures (Penning *et al.* 2005), indicating lack of hydrogen gradient between the microenvironment of methanogens and the headspace.

Discussion

Lack of H_2 gradients

Agreement of our incubation data with the correlation of hydrogenotrophic cocultures (Fig. 6) demonstrated, that in the rice root model system no H_2 gradient existed for CH_4 production from H_2/CO_2. This result is different from those in many environmental systems, where H_2 gradients are frequently present between the microsite of the organism and the site of measurement (Hoehler *et al.* 2001). Since the thermodynamics of many anaerobic reactions are governed by the concentration of the important intermediate H_2, process data often disagree with the energetic feasibility of reactions (Conrad and Klose, 1999). With the observed lack of a H_2 gradient for hydrogenotrophic methanogenesis in rice root incubations, it is reasonable to assume that this gradient does also not exist for other H_2-dependent reactions. This should result in good agreement between thermodynamic calculations and observed process data, which was indeed earlier reported for rice root incubations (Conrad and Klose, 2000). The unbiased thermodynamic calculations enabled us to assess inhibition of anaerobic processes by comparing thermodynamics and process data. If a thermodynamically favored reaction is not detected, it indicates that the presence of CH_3F indeed inhibited this reaction. Prerequisite of this approach is that the evaluated reaction was observed in the control (no CH_3F), proving that the required specific microorganisms necessary for the reaction were present in the rice root system. Particular processes are discussed below.

In the CH_3F incubation, pH_2 was constantly higher in comparison to the control (Fig. 1). This phenomenon was earlier observed in incubations of rice field soil, where a difference of 1-2 Pa was observed (Conrad and Klose, 1999). In our study the difference was more pronounced (differences from day 9 to 26 were between 10 and 36 Pa), but showed the same trend. The elevated pH_2 in the CH_3F incubation can be explained either by an increased H_2 production or a decreased H_2 consumption. Increased H_2-production from fermentation is unlikely, since isotope signatures and concentrations of other products of fermentation did not show differences between the inhibited and control setups (δ_{prop} during the time of complete inhibition; δ_{ac} at day 7, when acetoclastic methanogenesis was not active yet). Of the H_2-consuming processes, homoacetogenesis tested with *Acetobacterium woodii* was earlier found not to be inhibited by CH_3F (Janssen and Frenzel, 1997). We therefore assume that CH_3F might affect the efficiency of H_2

consumption by hydrogenotrophic methanogens, which determine the threshold of H_2 in anaerobic systems depleted in other terminal electron acceptors, e.g., sulfate. Although it is known, that hydrogenotrophic methanogenesis is partially inhibited at higher CH_3F concentrations (Janssen and Frenzel, 1997), the influence of CH_3F on pH_2 has not explicitly been tested. However, inhibition experiments of acetoclastic methanogenesis showed that CH_3F-concentrations up to 3 kPa did not change the value of $\alpha_{CO2/CH4}$ in anoxic incubations (Chan *et al.* 2005), suggesting that isotope fractionation is not affected.

Evaluation of complete inhibition of acetoclastic methanogenesis

Decreased CH_4 production and accumulation of acetate are commonly used to assess the successful inhibition of acetoclastic methanogenesis (Janssen and Frenzel, 1997; Conrad and Klose, 1999). Complete inhibition of acetoclastic methanogenesis was confirmed by stoichiometric calculations (data not shown explicitly). Until day 24 the sum of the rate of acetate production in the CH_3F incubation and the rate of acetate consumption in the control equaled the difference of methane production rates between control and CH_3F incubation. However this indicator is not appropriate under all conditions, since changes in CH_4 production rates also depend on substrate availability and thermodynamic constraints. Acetate accumulation, on the other hand, does reflect the difference between production and consumption and not exclusively the absence of consumption. Due to these limitations, CH_4 production and acetate accumulation cannot always be used to precisely determine the cessation of inhibition.

Carbon isotope signatures of CO_2, CH_4 and acetate alternatively can be used as indicators of active acetoclastic methanogenesis, since they are sensitive to relative changes in the methanogenic pathways. The decrease of δ_{CO2} between day 12 and 29 in the control was caused by isotopically relatively light CO_2 produced from acetate (Fig. 4b). This correlation would also be expected to start at cessation of the CH_3F inhibition and indeed was seen when $\delta_{CO2\text{-}new}$ (calculated using equ. 2) was determined (data not shown), suggesting the ending of the inhibition around day 30. For CH_4 it is expected, that $\delta_{CH4\text{-}new}$ increases when inhibition ends, since δ_{ma} is less negative than δ_{mc} (Conrad, 2005; Krzycki *et al.* 1987). This occurred in the CH_3F incubation at day 36 and indicated active acetoclastic methanogenesis. A drawback of using $\delta_{CH4\text{-}new}$ to identify ongoing acetoclastic methanogenesis is, that $\alpha_{CO2/CH4}$ can vary over a range from at least 1.03 to 1.08 (Fey *et al.* 2004). An increase of $\delta_{CH4\text{-}new}$ could therefore also be explained by a decrease of $\alpha_{CO2/CH4}$.

However, this is not expected here, since $\alpha_{CO2/CH4}$ was shown to decrease with $\Delta G_{CO2/CH4}$ (Penning *et al.* 2005) and the opposite trend was observed here.

A further indicator for cessation of inhibition of acetoclastic methanogenesis is the isotope ratio of accumulated acetate. $\delta_{ac\text{-}methyl}$ is a more suitable indicator than δ_{ac}, because $\delta_{ac\text{-}methyl}$ is unaffected by the exchange of the carboxyl group of acetate with dissolved CO_2 (deGraaf *et al.* 1996; Gelwicks *et al.* 1989). The value of $\delta_{ac\text{-}methyl}$ of the accumulated acetate is stable, if acetate is produced with a constant isotope signature and is not consumed. The quality of this indicator therefore depends on the activity of reactions involved in acetate consumption and production. Fermentation is the dominant acetate-producing process in the rice root system. Pure culture studies predict that during mixed-acid fermentation under similar conditions as in our incubations, acetate has a stable isotope ratio close to that of the substrate (Penning and Conrad, 2005a). Besides fermentation, a minor part of acetate was previously found in rice root incubations to be produced by homoacetogenesis (Conrad and Klose, 2000), which is a strongly fractionating process ($\alpha_{CO2/Ac}$ = 1.058; (Gelwicks *et al.* 1989)). Homoacetogenesis was thermodynamically favored at all times in the control ($\Delta G < 0$; Fig. 2c). Yet this does not mean that the process was active, since in organisms ΔG has to be sufficiently negative to drive anabolic reactions. When the homoacetogen *A. woodii* was grown in chemostat culture on H_2/CO_2, it could thrive at $\Delta G \leq$ -30 kJ mol^{-1} (calculated from data of Peters *et al.* 1998), the minimum energy determined by Seitz et al. (1990) was $\Delta G \leq$ -20 kJ mol^{-1}. In our experiments ΔG of homoacetogenesis was > -20 kJ mol^{-1} after day seven in the CH_3F treatment, and therefore unlikely to be active. The stable value of $\delta_{ac\text{-}methyl}$ until day 24 indicates that acetate produced from homoacetogenesis, which might have occurred in the initial phase of the incubation (before day 9), was not sufficient to decrease the value of $\delta_{ac\text{-}methyl}$ typical for primary fermentation. Therefore homoacetogenesis apparently did not operate and thus did not influence the determination of cessation of inhibition of acetoclastic methanogenesis. For acetate production via propionate oxidation, growth was sustained in a chemostat at ΔG as high as $\approx$ -10 kJ mol^{-1} (Scholten and Conrad, 2000). Therefore propionate oxidation was not permissive until day 47 in the CH_3F treatment (Fig. 3b). Consumption of acetate via assimilation by microorganisms involves only minute amounts of acetate and was therefore not considered. With the reasonable assumption that acetate is only produced by fermentation with a constant stable isotope

signature close to that of the substrate and that acetoclastic methanogenesis is the only acetate-consuming process, the cessation of inhibition is depicted by the increase in $\delta_{ac\text{-}methyl}$ caused by isotope fractionation of acetoclastic methanogenesis on day 28. Comparing the time points of cessation of inhibition (Table 2), it seems that methods that use products of acetoclastic methanogenesis yield later time points, whereas acetate-based methods yield earlier time points. This is a reasonable result, since changes in the substrate happen earlier and changes in isotope signatures of the accumulated gases (CH_4, CO_2) are not so rapidly seen due to the high background. Thus we suggest to rather use substrate-based indicators to determine the end point of inhibition of acetoclastic methanogenesis. In the following discussion we will therefore use the time range between day 24 and 28 as cessation of inhibition.

Table 2: Indicators used to determine the cessation of inhibition of acetoclastic methanogenesis by CH_3F.

indicator	based on		time of cessation [days]
	substrate	product	
mass balance*	+	+	24 – 28
δ_{CO2}	-	+	29 – 33
δ_{CH4}	-	+	33 – 36
$\delta_{ac\text{-}methyl}$	+	-	24 – 28

* comparing the difference of methane production rates between control and CH_3F incubation with of the rate of acetate production in the CH_3F incubation

Effect of CH_3F on fermentation processes

Acetoclastic methanogenesis was thermodynamically favored throughout the incubation in the presence of CH_3F (Fig. 2c). The organisms catalyzing the reaction were present in the system as confirmed by active acetoclastic methanogenesis in the control. Despite these favorable conditions, the lack of ongoing acetoclastic methanogenesis demonstrated that acetoclastic methanogenesis was indeed inhibited by the presence of CH_3F. The Gibbs free energies of anaerobic reactions other than acetoclastic methanogenesis were also compared with their activity as indicated by conversion of

substrates to products. As reported earlier (Conrad and Klose, 2000), CH_3F did not change the pattern of propionate accumulation during complete inhibition of acetoclastic methanogenesis (Fig. 3a). Values of δ_{prop} in the control and CH_3F treatment were not significantly different and therefore indicated that propionate formation was unaffected by CH_3F. Propionate was probably produced both from fermentation of organic matter and reduction of CO_2, whereas formation from acetate + CO_2 was, if at all, only of minor importance, since its ΔG was >-13 kJ mol^{-1} on day seven and then increased. Acetate is also produced by fermentation and might be subject to inhibition. Its isotope signatures and concentrations could only be evaluated for day seven and nine, when acetoclastic methanogenesis was not yet active in either set of conditions. On those days, no inhibition effect could be observed. The influence of CH_3F on propionate oxidation could not be evaluated in this study, since conditions that allowed the growth of propionate oxidizing bacteria (ΔG < -10 kJ mol^{-1}; (Scholten and Conrad, 2000)) were only reached at day 47 in the CH_3F incubation (Fig. 3). From this analysis we can conclude, that beside acetoclastic methanogenesis, no other reaction seemed to be affected by the inhibitor CH_3F.

Isotope fractionation associated with turnover of acetate and propionate

Acetoclastic methanogenesis and the exchange of the carboxyl group of acetate with dissolved CO_2 (Gelwicks *et al.* 1989; deGraaf *et al.* 1996) govern the variation of isotope composition of acetate. The exchange reaction was found to rapidly occur in cell suspensions of *Methanobacterium barkeri* (Eikmanns and Thauer, 1984) being due to the reversible exchange of the carbonyl carbon of acetyl-CoA and CO_2 (Fischer and Thauer, 1990). Although the molecular target of CH_3F and the inhibition mechanism are not yet known, we found that the exchange reaction was not affected by CH_3F. Therefore we assume that the carbon monoxide dehydrogenase (CODH), which catalyzes this reaction was also not affected by CH_3F. This is supported by results of experiments with *A. woodii* (Janssen and Frenzel, 1997), which uses the CODH pathway, if grown on H_2/CO_2 (Diekert and Wohlfarth, 1994). There, growth of *A. woodii* was not inhibited by 1 kPa CH_3F. Thus, we could observe the isotope effect of the exchange reaction during complete inhibition of acetoclastic methanogenesis (before day 28), although acetoclastic methanogenesis was not active. There the exchange decreased the difference in the isotope ratios of the carboxyl group of acetate and CO_2 ($\Delta\delta_{CO2\text{-}ac\text{-}carboxyl}$), while $\delta_{ac\text{-}methyl}$ stayed stable (Table 1). Although the inhibition of acetoclastic methanogenesis allows us to look at the exchange reaction

separately, it might also alter the kinetics of the exchange reaction, which most probably depends on the metabolic rate of the methanogens. Therefore the exchange may occur at different rates in inhibited and control incubations.

During acetate consumption by acetoclastic methanogenesis the carboxyl-group recorded both the isotope effect of the exchange reaction and of acetoclastic methanogenesis, whereas in the methyl group only the fractionation caused by the latter reaction was seen. The fractionation determined from methyl-acetate by a closed system approach ($\alpha_{ac\text{-}methyl/CH4}$ = 1.030; Fig. 5) was larger than earlier reported values of pure cultures of *Methanosarcina spp.* (1.021 to 1.027) (Gelwicks *et al.* 1994; Zyakun *et al.* 1988; Krzycki *et al.* 1987), which are the almost exclusive acetoclastic methanogens in the rice root system (Chin *et al.* 2004). At steady state conditions, which were established in the control at the late phase of the experiment for the concentration and isotope ratio of acetate, the fractionation of acetoclastic methanogenesis was determined by a second method, resulting in $\alpha_{ac\text{-}methyl/CH4}$ = 1.015. Although for both determinations assumptions have to be made, the values are in proximity to pure culture determinations and suggest that for *Methanosarcinaceae* no strong difference in fractionation behavior at environmental and pure culture conditions exist.

Propionate was also isotopically fractionated during consumption. From day 33 on, when propionate was oxidized in the control, δ_{prop} slightly increased with decreasing propionate concentration. Due to the lack of sufficient data no quantification of the fractionation factor was done. The data suggest, however, that it is lower than for acetoclastic methanogenesis.

Quantification of H_2/CO_2-derived CH_4

In the one-source-one-sink situation of acetate in the rice root incubation, i.e. fermentation is the only acetate-producing and acetoclastic methanogenesis the only acetate-consuming process, steady-state conditions of acetate (not-changing stable isotope composition of acetate at the steady state acetate concentration) imply that all the freshly produced acetate by fermentation was converted to CH_4. Thus the isotope ratio of acetate-derived CH_4 (δ_{ma}) has the same value as the acetate produced by fermentation. For modeling purposes the acetate flow can then be followed in two ways. Either $\delta_{ac\text{-}ss}$ and a fractionation factor $\alpha_{ac\text{-}methyl\text{-}ss/CH4} \approx 1.020$, or $\delta_{ac\text{-}methyl\text{-}ferm}$ and no fractionation

($\alpha_{ac\text{-}methyl\text{-}ferm/CH4}$ = 1.00) can be used. Calculation with $\delta_{ac\text{-}methyl\text{-}ferm}$ is only valid, however, if a one-source-one-sink situation for acetate is valid.

The fraction of CH_4 produced from H_2/CO_2 (f_{mc}) calculated for the control (equ. 3; Fig. 4a) agreed well with thermodynamic and process data. Using $\alpha_{ac\text{-}methyl/CH4}$ = 1.02, the decrease of f_{mc} after day 22 occurred shortly after onset of acetate consumption. After consumption of accumulated acetate to threshold values (day 33), f_{mc} again increased correlating with a decreasing overall CH_4 production rate, which was caused by less thermodynamically favorable conditions for acetoclastic methanogenesis due to low acetate concentrations. The experimentally determined value of $\alpha_{ac\text{-}methyl/CH4}$ at steady-state ($\alpha_{ac\text{-}methyl/CH4}$ = 1.015) yielded reasonable values of f_{mc}, whereas the fractionation factor determined at non-steady state conditions ($\alpha_{ac\text{-}methyl/CH4}$ = 1.030) was obviously too large, even resulting in a negative f_{mc}. Since the $\alpha_{ac\text{-}methyl/CH4}$ of 1.030 is probably still an underestimation due to ongoing production of acetate, we conclude that at least in this system the determination of $\alpha_{ac\text{-}methyl/CH4}$ using a closed system approach (Fig. 5) is not appropriate, although we cannot present an explanation. Yet, using $\alpha_{ac\text{-}methyl/CH4}$ of 1.020 or 1.015 allowed to correctly model the carbon flow, demonstrating that isotope modeling together with the specific inhibitor CH_3F is a proper tool to determine f_{mc}.

Conclusions

Rice roots have been proven to be an useful model system to test the specificity of CH_3F, since the influence of the inhibitor on environmental relevant microbial groups can be evaluated with a combination of thermodynamics and process data. Here we have shown that CH_3F completely blocked acetoclastic methanogenesis, whereas no inhibition of other processes could be found. This method might be useful also to test the specificity of other frequently used inhibitors in anoxic systems. Hereby, the rice root model system has the advantage that it is not affected by a H_2-gradient so that also the thermodynamic conditions for H_2-dependent reactions are properly calculated.

Given the specificity of CH_3F, we could confidently quantify the isotope fractionation of hydrogenotrophic methanogenesis, which is an essential modeling parameter for determination of the carbon flow to methane. The complete inhibition of acetoclastic methanogenesis that is required for this purpose was confirmed by four different methods mostly based on carbon isotope signatures. The isotope fractionation from acetoclastic methanogenesis, the other methane-producing process, was determined

by two methods and roughly agreed with the values determined in pure cultures. Yet only the fractionation determined under steady-state conditions did well fit to the data. Overall, modeling the carbon flow to methane from isotope signatures agreed with thermodynamic and process data.

The inhibition of the only acetate consuming process demonstrated that the isotope ratio of acetate stayed constant and was close to the fermentation substrate (rice roots), only influenced by exchange reactions involving its carboxyl-group but not the methyl-group. This agrees with the isotope flow in the fermenting bacterium *Clostridium papyrosolvens*, where an δ_{ac} close to the substrate is expected, when acetate is the predominant fermentation product (Penning and Conrad, 2005a).

In summary, the application of an inhibitor, thermodynamics, and carbon isotope signatures allowed a comprehensive understanding of the rice root model system especially with respect to fermentation and methanogenesis. This strategy should be used to evaluate other anaerobic processes, e.g. propionate oxidation, which could be only touched here. Further understanding of isotope fractionation could allow in the future also to model the initial reactions in the anaerobic degradation of organic matter.

Acknowledgements

We thank P. Claus for excellent technical assistance during analysis of ^{13}C data and the Fonds der Chemischen Industrie for financial support.

Reference List

Alperin MJ, Blair NE, Albert DB, Hoehler TM, Martens CS (1992) Factors that control the stable carbon isotopic composition of methane produced in an anoxic marine sediment. *Global Biogeochemical Cycles* **6** 271-291.

Blair N, Leu A, Munoz E, Olsen J, Kwong E, Desmarais D (1985) Carbon isotopic fractionation in heterotrophic microbial metabolism. *Applied and Environmental Microbiology* **50** 996-1001.

Botz R, Pokojski HD, Schmitt M, Thomm M (1996) Carbon isotope fractionation during bacterial methanogenesis by CO2 reduction. *Organic Geochemistry* **25** 255-262.

Brand WA (1996) High precision isotope ratio monitoring techniques in mass spectrometry. *Journal of Mass Spectrometry* **31** 225-235.

Chan OC, Claus P, Casper P, Ulrich A, Lueders T, Conrad R (2005) Vertical distribution of structure and function of the methanogenic archaeal community in Lake Dagow sediment. *Environmental Microbiology* **7** 1139-1149.

Chanton JP, Whiting GJ, Blair NE, Lindau CW, Bollich PK (1997) Methane emission from rice: Stable isotopes, diurnal variations, and CO2 exchange. *Global Biogeochemical Cycles* **11** 15-27.

Chidthaisong A, Chin KJ, Valentine DL, Tyler SC (2002) A comparison of isotope fractionation of carbon and hydrogen from paddy field rice roots and soil bacterial enrichments during CO2/H2 methanogenesis. *Geochimica et Cosmochimica Acta* **66** 983-995.

Chin KJ, Lueders T, Friedrich MW, Klose M, Conrad R (2004) Archaeal community structure and pathway of methane formation on rice roots. *Microbial Ecology* **47** 59-67.

Cicerone RJ, Oremland RS (1988) Biogeochemical aspects of atmospheric methane. *Global Biogeochemical Cycles* **2** 299-327.

Conrad R (2005) Quantification of methanogenic pathways using stable carbon isotopic signatures: a review and a proposal. *Organic Geochemistry* **36** 739-752.

Conrad R, Klose M (1999) How specific is the inhibition by methyl fluoride of acetoclastic methanogenesis in anoxic rice field soil? *Fems Microbiology Ecology* **30** 47-56.

Conrad R, Klose M (2000) Selective inhibition of reactions involved in methanogenesis and fatty acid production on rice roots. *Fems Microbiology Ecology* **34** 27-34.

Conrad R, Klose M, Claus P (2002) Pathway of CH_4 formation in anoxic rice field soil and rice roots determined by ^{13}C-stable isotope fractionation. *Chemosphere* **47** 797-806.

deGraaf W, Wellsbury P, Parkes RJ, Cappenberg TE (1996) Comparison of acetate turnover in methanogenic and sulfate-reducing sediments by radiolabeling and stable isotope labeling and by use of specific inhibitors: Evidence for isotopic exchange. *Applied and Environmental Microbiology* **62** 772-777.

Diekert G, Wohlfarth G (1994) Metabolism of Homoacetogens. *Antonie Van Leeuwenhoek International Journal of General and Molecular Microbiology* **66** 209-221.

Eikmanns B, Thauer RK (1984) Catalysis of an isotopic exchange between CO_2 and the carboxyl group of acetate by *Methanosarcina barkeri* grown on acetate. *Archives of Microbiology* **138** 365-370.

Fey A, Claus P, Conrad R (2004) Temporal change of ^{13}C isotope signatures and methanogenic pathways in rice field soil incubated anoxically at different temperatures. *Geochimica et Cosmochimica Acta* **68** 293-306.

Fischer R, Thauer RK (1990) Methanogenesis from acetate in cell extracts of *Methanosarcina barkeri*: Isotope exchange between CO_2 and the carbonyl group of acetyl-CoA, and the role of H_2. *Archives of Microbiology* **153** 156-162.

Frenzel P, Bosse U (1996) Methyl fluoride, an inhibitor of methane oxidation and methane production. *Fems Microbiology Ecology* **21** 25-36.

Fuchs G, Thauer R, Ziegler H, Stichler W (1979) Carbon isotope fractionation by *Methanobacterium thermoautotrophicum*. *Archives of Microbiology* **120** 135-139.

Gelwicks JT, Risatti JB, Hayes JM (1989) Carbon isotope effects associated with autotrophic acetogenesis. *Organic Geochemistry* **14** 441-446.

Gelwicks JT, Risatti JB, Hayes JM (1994) Carbon isotope effects associated with aceticlastic methanogenesis. *Applied and Environmental Microbiology* **60** 467-472.

Hayes JM (1993) Factors controlling C-13 contents of sedimentary organic compounds - Principles and evidence. *Marine Geology* **113** 111-125.

Hayes JM (2001) Fractionation of carbon and hydrogen isotopes in biosynthetic processes. *Stable Isotope Geochemistry* **43** 225-277.

Hoehler TM, Alperin MJ, Albert DB, Martens CS (2001) Apparent minimum free energy requirements for methanogenic Archaea and sulfate-reducing bacteria in an anoxic marine sediment. *Fems Microbiology Ecology* **38** 33-41.

Holzapfel-Pschorn A, Seiler W (1986) Methane emission during a cultivation period from an Italian rice paddy. *Journal of Geophysical Research* **91** 11803-11814.

Janssen PH, Frenzel P (1997) Inhibition of methanogenesis by methyl fluoride: Studies of pure and defined mixed cultures of anaerobic bacteria and archaea. *Applied and Environmental Microbiology* **63** 4552-4557.

Jetten MSM, Stams AJM, Zehnder AJB (1990) Acetate threshold and acetate activating enzymes in methanogenic bacteria. *Fems Microbiology Ecology* **73** 339-344.

Krumböck M, Conrad R (1991) Metabolism of position-labeled glucose in anoxic methanogenic paddy soil and lake sediment. *Fems Microbiology Ecology* **85** 247-256.

Krummen M, Hilkert AW, Juchelka D, Duhr A, Schluter HJ, Pesch R (2004) A new concept for isotope ratio monitoring liquid chromatography/mass spectrometry. *Rapid Communications in Mass Spectrometry* **18** 2260-2266.

Krzycki JA, Kenealy WR, De Niro MJ, Zeikus JG (1987) Stable carbon isotope fractionation by *Methanosarcina barkeri* during methanogenesis from acetate, methanol, or carbon dioxide-hydrogen. *Applied and Environmental Microbiology* **53** 2597-2599.

Lu Y, Conrad R (2005) In situ stable isotope probing of methanogenic *Archaea* in the rice rhizosphere. *Science* **309** 1088-1090.

Mariotti A, Germon JC, Hubert P, Kaiser P, Letolle R, Tardieux A, Tardieux P (1981) Experimental determination of nitrogen kinetic isotope fractionation - Some principles - Illustration for the denitrification and nitrification processes. *Plant and Soil* **62** 413-430.

Minoda T, Kimura M, Wada E (1996) Photosynthates as dominant source of CH_4 and CO_2 in soil water and CH_4 emitted to the atmosphere from paddy fields. *Journal of Geophysical Research* **101** 21091-21097.

Oremland RS, Capone DG (1988) Use of "specific" inhibitors in biogeochemistry and microbial ecology. *Adv.Microb.Ecol.* **10** 285-383.

Oremland RS, Culbertson CW (1992a) Evaluation of methyl fluoride and dimethyl ether as inhibitors of aerobic methane oxidation. *Applied and Environmental Microbiology* **58** 2983-2992.

Oremland RS, Culbertson CW (1992b) Importance of methane-oxidizing bacteria in the methane budget as revealed by the use of a specific inhibitor. *Nature* **356** 421-423.

Penning H, Conrad R (2005a) Carbon isotope effects associated with mixed-acid fermentation of saccharides by *Clostridium papyrosolvens*. *Geochimica et Cosmochimica Acta* **submitted**.

Penning H, Conrad R (2005b) Effect of inhibition of acetoclastic methanogenesis on growth of archaeal populations in an anoxic model environment. *Applied and Environmental Microbiology* **in press**.

Penning H, Plugge CM, Galand PE, Conrad R (2005) Variation of carbon isotope fractionation in hydrogenotrophic methanogenic microbial cultures and environmental samples at different energy status. *Global Change Biology* **in press**.

Peters V, Janssen PH, Conrad R (1998) Efficiency of hydrogen utilization during unitrophic and mixotrophic growth of Acetobacterium woodii on hydrogen and lactate in the chemostat. *Fems Microbiology Ecology* **26** 317-324.

Prinn RG (1994) Global atmospheric-biospheric chemistry. In:Global Atmospheric-Biospheric Chemistry (ed Prinn RG), pp. 1-18. Plenum, New York.

Scholten JCM, Conrad R (2000) Energetics of syntrophic propionate oxidation in defined batch and chemostat cocultures. *Applied and Environmental Microbiology* **66** 2934-2942.

Seitz HJ, Schink B, Pfennig N, Conrad R (1990) Energetics of syntrophic ethanol oxidation in defined chemostat cocultures. 1. Energy requirement for H_2 production and H_2 oxidation. *Archives of Microbiology* **155** 82-88.

Thauer RK, Jungermann K, Decker K (1977) Energy conservation in chemotropic anaerobic bacteria. *Bacteriological Reviews* **41** 100-180.

Tyler SC, Bilek RS, Sass RL, Fisher FM (1997) Methane oxidation and pathways of production in a Texas paddy field deduced from measurements of flux, $\delta^{13}C$, and δD of CH_4. *Global Biogeochemical Cycles* **11** 323-348.

Weimer PJ, Zeikus JG (1978) Acetate metabolism in *Methanosarcina barkeri*. *Archives of Microbiology* **119** 175-182.

Whiticar MJ (1999) Carbon and hydrogen isotope systematics of bacterial formation and oxidation of methane. *Chemical Geology* **161** 291-314.

Yao H, Conrad R (1999) Thermodynamics of methane production in different rice paddy soils from China, the Philippines and Italy. *Soil Biology & Biochemistry* **31** 463-473.

Zyakun AM, Bondar VA, Laurinavichus KS, Shipin OV, Belyaev SS, Ivanov MV (1988) Fractionation of carbon isotopes under the growth of methane-producing bacteria on various substrates. *Mikrobiologiceskij Zhurnal* **50** 16-22.

IV. Zusammenfassende Diskussion

Nach der Umsetzung alternativer Elektronenakzeptoren wie Nitrat und Sulfat werden beim anaeroben Abbau organischer Materie die Endprodukte Kohlendioxid und Methan in einem Netzwerk anaerober Prozesse gebildet. Hierbei variiert der jeweilige Anteil eines Prozesses am Gesamtkohlenstofffluss in Abhängigkeit von biologischen und physikochemischen Parametern. Die stabile Kohlenstoffisotopensignatur der umgesetzten Substrate und Intermediate ermöglicht es, relative Anteile bestimmter Prozesse am Kohlenstofffluss zu bestimmen. Für die erfolgreiche Modellierung ist allerdings die genaue Kenntnis der Isotopen-Fraktionierungsfaktoren erforderlich.

Ziel dieser Arbeit war es, Isotopen-Fraktionierungsfaktoren für die primäre Fermentation und die hydrogenotrophe Methanogenese in mikrobiellen Kulturen zu bestimmen, und diese in anoxischen Modellsystemen zur Quantifizierung des Kohlenstoffflusses einzusetzen. Bei der experimentellen Bestimmung wurde besonderer Wert auf unterschiedliche Wachstumsbedingungen gelegt, um deren Einfluss auf die Fraktionierung im natürlichen System beurteilen zu können. Neben der Kohlenstoffflussmodellierung wurde im Reiswurzel-Modellsystem der Einfluss eines Hemmstoffs der acetoklastischen Methanogenese auf archaeelle Gruppen untersucht.

IV.1. Einfluss des Hemmstoffs Methylfluorid auf die archaeelle Gemeinschaft

Durch Hemmung der acetoklastischen Methanogenese mit Methylfluorid (CH_3F) kann der Fraktionierungsfaktor der hydrogenotrophen Methanogenese bestimmt werden, der ein Schlüsselparameter für die Kohlenstoffflussmodellierung ist (Conrad, 2005). Voraussetzung für diese Methode ist, dass CH_3F spezifisch die acetoklastische Methanogenese hemmt und gleichzeitig andere anaerobe Prozesse nicht beeinflusst. Zwar ergaben Reinkulturversuche keine Hinweise auf eine Unspezifität von CH_3F (Janssen und Frenzel, 1997), jedoch ist derzeit nur ein kleiner Teil der natürlichen archaeellen Diversität in Stammsammlungen repräsentiert (DeLong, 2003), so dass eine Hemmung unkultivierter archaeeller Linien durch CH_3F nicht ausgeschlossen werden kann. Daher wurde in dieser Arbeit mit molekularbiologischen und geochemischen Methoden der Einfluss von CH_3F auf die archaeelle Gemeinschaft im Reiswurzel-Modellsystem untersucht.

In den Inkubationsexperimenten wurde die vollständige Hemmung der acetoklastischen Methanogenese dadurch bestätigt, dass das unter gehemmten Bedingungen akkumulierte Acetat der Differenz an gebildetem Methan in der Kontroll-

und CH_3F-Inkubation entsprach (Prinzip nach Conrad und Klose, 1999b). Das Ende der Hemmwirkung von CH_3F auf Grund der Erniedrigung der CH_3F-Konzentration durch Probenahme wurde präzise über die Isotopensignatur der Methylgruppe von Acetat detektiert. Die Spezifität von CH_3F wurde geochemisch mit Hilfe der zur Verfügung stehenden Gibbs freien Energie getestet. Ein Prozess wurde als gehemmt angesehen, wenn bei thermodynamisch günstigen Bedingungen ($\Delta G < 0$ kJ mol^{-1}) das Substrat nicht zum jeweiligen Produkt umgesetzt wurde. Diese Methode konnte nur für Prozesse angewendet werden, die im Kontrollexperiment abliefen und für die somit sichergestellt war, dass die Mikroorganismen, die diesen Prozess katalysieren, in der Inkubation vorhanden waren. Da im Reiswurzel-Modellsystem kein H_2-Gradient vorhanden ist (siehe IV.3), war es auch möglich H_2-abhängige Prozesse zu untersuchen. Die Auswertung dieses Versuchs ergab, dass die acetoklastische Methanogenese eindeutig inhibiert wurde. Jedoch, wurde die Propionatbildung über Fermentation oder aus H_2/CO_2, wie in einer früheren Studie, nicht beeinflusst (Conrad und Klose, 2000). Ebenfalls wurde die Bildung von Acetat, welche durch Fermentation oder Homoacetogenese bedingt gewesen sein kann, nicht durch CH_3F beeinflusst. Es konnten somit keine geochemischen Anhaltspunkte für eine unspezifische Hemmung durch CH_3F gefunden werden.

Die archaeelle Gemeinschaft im Reiswurzel-Modellsystem wurde von sechs archaeellen Gruppen dominiert, die bereits zuvor für dieses System beschrieben worden waren (Chin et al., 2004). Die methanogenen Vertreter waren *Methanosarcinaceae* (hydrogenotroph und acetoklastisch), *Methanobacteriaceae* (hydrogenotroph) und Rice Cluster (RC)-I (hydrogenotroph; (Erkel et al., 2005)). Weitere archaeelle Linien waren RC-III, RC-IV und RC-V (Chin et al., 1999; Grosskopf et al., 1998b). Das Wachstum der acetoklastischen methanogenen *Methanosarcinaceae* wurde bei vollständiger Hemmung stark reduziert, allerdings nicht gänzlich gestoppt, da *Methanosarcinaceae* auch über hydrogenotrophe Methanogenese Energie gewinnen können (Thauer, 1998). Nicht gehemmt hingegen waren methanogene Gruppen, die Acetat nicht zur Energiegewinnung nutzen können (*Methanobacteriaceae* und RC-I). Ebenfalls unbeeinflusst war das Wachstum von RC-III, RC-IV und RC-V. Erst nach Ende der Hemmung verlief das Wachstum dieser drei Gruppen in der Kontroll- und CH_3F-Inkubation unterschiedlich. Diese späte Entwicklung ist wahrscheinlich auf Sekundäreffekte der CH_3F-Hemmung wie z.B. den verspäteten Abbau von Fettsäuren und Ethanol auf Grund des erhöhten p_{H2} zurückzuführen, nicht aber auf die direkte Hemmwirkung von CH_3F. Von den

unkultivierten archaeellen Linien RC-III, RC-IV und RC-V sind nur für das weitläufig mit den *Thermoplasmatales* verwandte RC-III Hinweise auf die Physiologie aus Anreicherungskulturen verfügbar (Kemnitz et al., 2005). Diese Gruppe ist nicht methanogen und wächst bevorzugt auf Hefeextrakt, Pepton und Trypton. Über die Physiologie der anderen Gruppen ist noch nichts bekannt. Daher ist zu diesem Zeitpunkt eine Interpretation des unterschiedlichen Wachstumsverhaltens am Ende der Reiswurzelinkubation nicht möglich. Zusammenfassend ergab sowohl die geochemische als auch die molekularbiologische Untersuchung keine Hinweise auf eine unspezifische Hemmung durch CH_3F. Somit kann die Hemmung der acetoklastischen Methanogenese durch den spezifischen Inhibitor CH_3F in der Tat genutzt werden, um die Methanproduktion aus Acetat und, wie von Conrad (2005) vorgeschlagen, die für die Modellierung wichtigen Parameter α_{mc} und δ_{ac} zu bestimmen.

IV.2. Fermentation

Der Abbau organischer Materie beginnt mit der Primärfermentation, deren Produkte die Reaktanden für nachfolgende Abbaureaktionen sind (Schink, 1997). Die Gärung unterscheidet sich von den meisten anderen Prozessen, an denen die Kohlenstoff-Isotopenfraktionierung untersucht wurde (z.B. Homoacetogenese, hydrogenotrophe Methanogenese) dadurch, dass sich im Katabolismus der Kohlenstofffluss verzweigt und mehrere Produkte gebildet werden. An den Verzweigungspunkten findet eine zusätzliche Isotopenfraktionierung statt (Blair et al., 1985; Hayes, 2001). Zu Beginn des Abbauwegs, vom Saccharid bis zum Intermediat Pyruvat, ist der Kohlenstofffluss jedoch linear (Abbildung IV-1). Diese Arbeit zeigt, dass in *C. papyrosolvens* bei der Umsetzung zu Pyruvat ^{12}C-Glucose und ^{12}C -Cellobiose bevorzugt umgesetzt wurden. Dagegen trat bei Cellulose keine Fraktionierung auf, da Cellulose vor der Aufnahme in die Zelle von Gluconasen hydrolysiert wird (Lynd et al., 2002) und dieser Vorgang geschwindigkeitsbestimmend ist (Billen, 1982; Degens und Mopper, 1975; Fey und Conrad, 2003). Die gebildeten Glucose-Oligomere oder -Monomere werden direkt nach der Freisetzung quantitativ aufgenommen und ohne Fraktionierung zu Pyruvat umgesetzt. Im Gegensatz dazu wird bei der Umsetzung von Glucose und Cellobiose der Isotopeneffekt exprimiert, da bei deren Aufnahme und weiteren Umsetzung in der Zelle aus einem großen Substratpool selektiert werden kann (Hayes, 2002). Unter Umweltbedingungen sind lösliche Substrate wie Glucose nur in sehr geringen

Konzentrationen vorhanden (Chidthaisong und Conrad, 2000; King und Klug, 1982) und es werden fast ausschließlich Polymere fermentiert. Dort sollte daher Pyruvat – wie es hier für Cellulose gezeigt wurde – dieselbe Isotopensignatur wie das Substrat aufweisen.

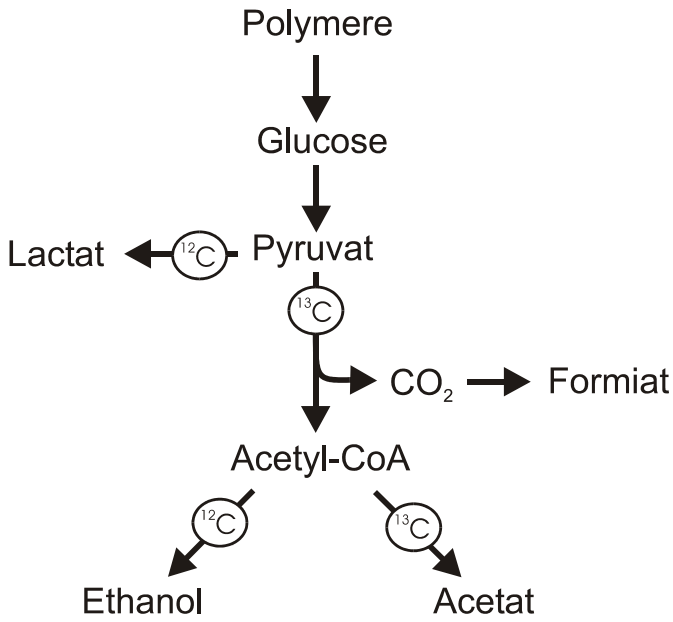

Abbildung IV-1. Katabolischer Kohlenstoffffluss während der gemischten Säuregärung durch *C. papyrosolvens*. An den Verzweigungspunkten ist die stärker ^{12}C-bevorzugende Reaktion durch einen ^{12}C-Pfeil gekennzeichnet. Die weniger ^{12}C-bevorzugende Reaktion ist durch einen ^{13}C-Pfeil dargestellt.

Zur Untersuchung der Isotopenfraktionierung im nicht-linearen Abbauweg, d.h. an den Verzweigungspunkten Pyruvat und Acetyl-CoA, wurde in den Versuchen das jeweilige Substrat vollständig umgesetzt. Somit wurde der oben erwähnte Isotopeneffekt auch bei löslichen Substraten nicht exprimiert und eine isolierte Betrachtung des verzweigten Abbauwegs war möglich. Am Verzweigungspunkt Pyruvat wurde ^{12}C bevorzugt in Lactat eingebaut, während Acetyl-CoA im Vergleich zu Pyruvat an ^{12}C abgereichert war. Die Differenz in der Isotopensignatur beider Produkte war zwischen 4,9 und 8,7 ‰. Das ^{12}C-abgereicherte Acetyl-CoA ist ebenfalls ein Verzweigungspunkt, an dem sich der Kohlenstoffffluss zur Bildung von Acetat (über Acetylphosphat) und Ethanol (über Acetaldehyd) teilt. Hier wurde ^{12}C bevorzugt zur Bildung von Ethanol verwendet, so dass Ethanol 15,3 bis 17,8 ‰ isotopisch leichter war. An beiden Verzweigungspunkten war die Differenz der Isotopensignatur der gebildeten Produkte konstant und korrelierte nicht mit dem Verhältnis der Produkte, was sich im parallelen Verlauf der Regressionsgeraden für die Isotopensignatur der Produkte zeigt (siehe z.B. Abbildung IV-2). Das bedeutet, dass sich die Fraktionierungsfaktoren der einzelnen Reaktionen nicht ändern (Hayes, 2002).

Ändert sich jedoch das Verhältnis der gebildeten Produkte zueinander, so variiert auch ihre Isotopensignatur den theoretischen Prinzipien der Isotopenfraktionierung folgend (Hayes, 2001). Beispielhaft soll dies für den Verzweigungspunkt Acetyl-CoA erläutert werden (Abbildung IV-2), wobei Cellulose einer C_3-Pflanze ($\delta_{cellulose}$ = -28 ‰; (O'Leary, 1988)) fermentiert wird und keine Lactatbildung stattfindet ($f_{lac} = 0$; d.h. $\delta_{acetyl\text{-}CoA} = \delta_{cellulose}$). Weiterhin wurde ein Unterschied der Stärke der Fraktionierung zu Ethanol und Acetat (Ω) von 16 ‰ gewählt (y-Differenz der parallel verlaufenden Linien von δ_{ac} und $\delta_{ethanol}$). Wird nur wenig Ethanol gebildet (5 % aus Acetyl-CoA = $f_{ac} = 0{,}95$), wie es für anoxischen Reisfeldboden typisch ist, hätte das gebildete Acetat einen Wert von -27,2 ‰ und Ethanol von -43,2 ‰. Nimmt man jedoch einen erhöhten Ethanol-Anteil an, wie es für Moore berichtet wurde (Horn et al., 2003; Metje und Frenzel, 2005), so hätte bei einem $f_{ac} = 0{,}5$ Acetat einen Wert von -18 ‰ und Ethanol von -36 ‰. Die hier vorgestellten Ergebnisse der Reiswurzelinkubationen stimmen mit diesem Modell überein. Als Acetat nur durch Fermentation gebildet wurde und nicht verbraucht wurde (bei $f_{ac} = 0{,}99$ und $f_{lac} = 0{,}00$), war $\delta_{ac} \approx$ -30 ‰. Die Acetatisotopensignatur war somit wie erwartet im Bereich der Isotopensignatur des Substrats, dem organischen Kohlenstoff der Reiswurzel (≈ -28 ‰).

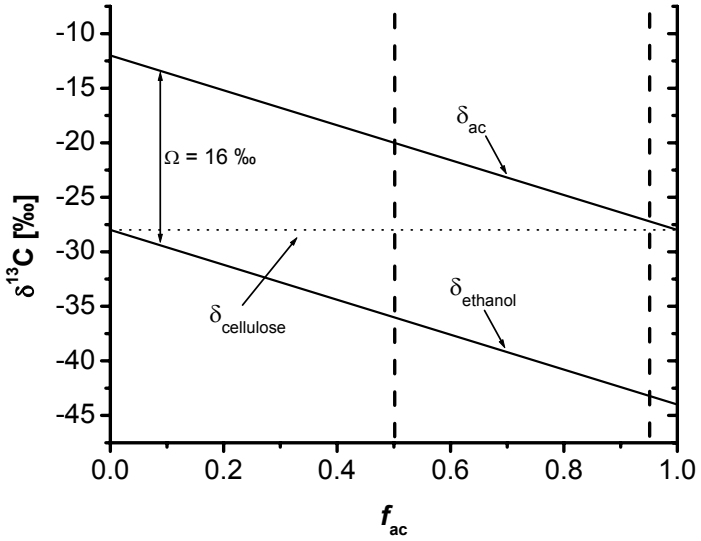

Abbildung IV-2. Kohlenstoffisotopie der Produkte Acetat und Ethanol am Verzweigungspunkt Acetyl-CoA in Abhängigkeit des relativen Kohlenstoffflusses zu Acetat (f_{ac}). Hier gezeigt für ein Substrat mit Isotopensignatur einer C_3-Pflanze ($\delta_{cellulose}$ = -28 ‰; gepunktete Linie) und ohne Lactatproduktion (f_{lac} = 0). Für f_{ac} = 0,5 und f_{ac} = 0,95 (gestrichelte Linien) wird der Einfluss von f_{ac} auf die Isotopensignatur von Ethanol und Acetat im Text erläutert. Die y-Differenz der Linien von δ_{ac} und $\delta_{ethanol}$ ist durch den Unterschied der Stärke der Fraktionierung zu Acetat und Ethanol bestimmt (Ω = 16 ‰).

Grundsätzlich darf also nicht immer der gleiche Fraktionierungsfaktor zur Berechnung der Isotopensignatur der einzelnen Produkte verwendet werden. Hingegen muss der Fraktionierungsfaktor ausgehend vom Kohlenstoffffluss zu den Produkten (f_{ac}, f_{lac}) berechnet werden, da er sich wie in obigem Beispiel gezeigt in dessen Abhängigkeit ändert. Die Bestimmung von f_{ac} und f_{lac} in Umweltsystemen kann sich als schwierig erweisen, da Produkte der Fermentation nicht akkumulieren, sondern von nachfolgenden Prozessen verbraucht werden. Daher wäre eine Korrelation zu einem leicht zu messenden Parameter hilfreich. In einigen Experimenten mit *C. papyrosolvens* korrelierte f_{ac} mit abnehmendem p_{H2}, wie dies zuvor bereits für *C. papyrosolvens* in Reinkultur und methanogener Kokultur gezeigt wurde (Chin et al., 1998). Offensichtlich ermöglichte der geringere p_{H2} die Bildung eines erhöhten Anteils des bevorzugten Produkts Acetat, bei dessen Bildung ein zusätzliches ATP über Substratphosphorylierung generiert werden kann (Gottschalk, 1986). Der Einfluss des p_{H2} sollte daher genauer auf seine Funktion als Indikator für den Kohlenstoffffluss untersucht werden. Jedoch ist unter Umweltbedingungen ein Zusammenspiel unterschiedlicher zusätzlicher Parameter (z.B.

pH; Mikroorganismus) zu vermuten, so dass im Moment noch keine generellen Annahmen gemacht werden können.

In dieser Arbeit wurde erstmals die Kohlenstoff-Isotopenfraktionierung bei der anaeroben Fermentation untersucht. Zusammenfassend erlauben die gewonnenen Erkenntnisse die Isotopensignatur von Produkten der Fermentation vorauszusagen, wenn die Isotopensignatur des Substrats und der relative Kohlenstofffluss zu den Produkten der Fermentation bekannt sind. Während des Abbaus des Polysaccharids Cellulose fand keine Isotopenfraktionierung statt. Damit war das Verhalten ähnlich wie in Sedimenten, wo trotz des Abbaus organischer Materie dessen Isotopensignatur (δ_{org}) konstant blieb (Blair und Carter, 1992). Da organisches Material großteils aus Polysacchariden besteht (Tsutsuki und Ponnamperuma, 1987), ist anzunehmen, dass dort ebenfalls die Hydrolyse der geschwindigkeitsbestimmende Schritt ist und somit keine Isotopenfraktionierung beim linearen Abbauweg der Fermentation auftritt. Damit wäre δ_{org} stabil und könnte als Ausgangsgröße ($\delta_{Substrat}$) zur Berechnung der Isotopensignatur der Produkte mit den hier bestimmten Fraktionierungsfaktoren verwendet werden.

IV.3. Methanogenese

Beim anoxischen Abbau organischer Substanz ist die Methanogenese der letzte Mineralisierungsschritt. In den meisten terrestrischen Systemen wird Methan dabei fast ausschließlich acetoklastisch und hydrogenotroph gebildet (Conrad und Claus, 2005). Die Kohlenstoff-Isotopenfraktionierung der methanbildenden Prozesse in mikrobiellen Kulturen und Umweltmodellsystemen sollen Gegenstand der folgenden Diskussion sein.

Allein die archaeellen Familien der *Methanosaetaceae* und *Methanosarcinaceae* sind in der Lage aus Acetat Methan zu produzieren. Für *Methanosarcina* spp. wurden bereits in früheren Reinkulturversuchen Fraktionierungsfaktoren ($1.021 \leq \alpha \leq 1.027$) bestimmt (Gelwicks et al., 1994; Krzycki et al., 1987; Zyakun et al., 1988). Die Überprüfung dieser Werte in Umweltsystemen ist schwierig, da meist beide acetoklastische Familien vorhanden sind und somit keine gruppenspezifischen Informationen gewonnen werden können. Eine Ausnahme ist das Reiswurzel-Modellsystem, in dem fast ausschließlich *Methanosarcinaceae* vorhanden sind (Chin et al., 2004; die vorliegende Arbeit). In diesem System wurde die Fraktionierung der acetoklastischen Methanogenese unter *steady state*- ($\alpha = 1.015$) und nicht-*steady state*-Bedingungen ($\alpha = 1.030$) über die Acetatisotopie bestimmt. Obwohl für diese Bestimmung Annahmen bei der intramolekularen Isotopenverteilung in Acetat und bei der Acetatakkumulation getroffen wurden, liegen die für das Modellsystem erhaltenen Werte im Bereich der Werte für Reinkulturen. Man kann somit annehmen, dass die für *Methanosarcinaceae* in Reinkulturen bestimmten Werte auf Umweltsysteme übertragen werden können.

Für die hydrogenotrophe Methanogenese unterscheiden sich die Fraktionierungsfaktoren in der Umwelt und in Reinkulturen stark. In den meisten Fällen sind die α-Werte unter natürlichen Bedingungen viel höher als für Reinkulturen (Fey et al., 2004). Es wurde vermutet, dass nicht den natürlichen Bedingungen entsprechende Kultivierungsbedingungen, insbesondere hohe Wasserstoffpartialdrücke, für diese Diskrepanz verantwortlich sind (Valentine et al., 2004). Um dieses Phänomen detailliert zu untersuchen, wurden in dieser Arbeit syntrophe und obligat syntrophe Kokulturen von hydrogenotrophen Methanogenen unterschiedlicher archaeeller Familien kultiviert. Dies ermöglichte die Isotopenfraktionierung bei unterschiedlichem p_{H2} zu bestimmen. Obwohl

für die einzelnen Versuche α mit p_{H2} korrelierte, war eine solche Korrelation nicht für alle Experimente möglich und zeigte an, dass p_{H2} nicht der alleinige Steuerungsfaktor ist. Jedoch korrelierte für alle Kokulturen und Wachstumsbedingungen die Änderung der Gibbs freien Energie (ΔG) der hydrogenotrophen Methanogenese mit α (Kurve mit 95 % Vertrauensbereichen in Abbildung IV-3).

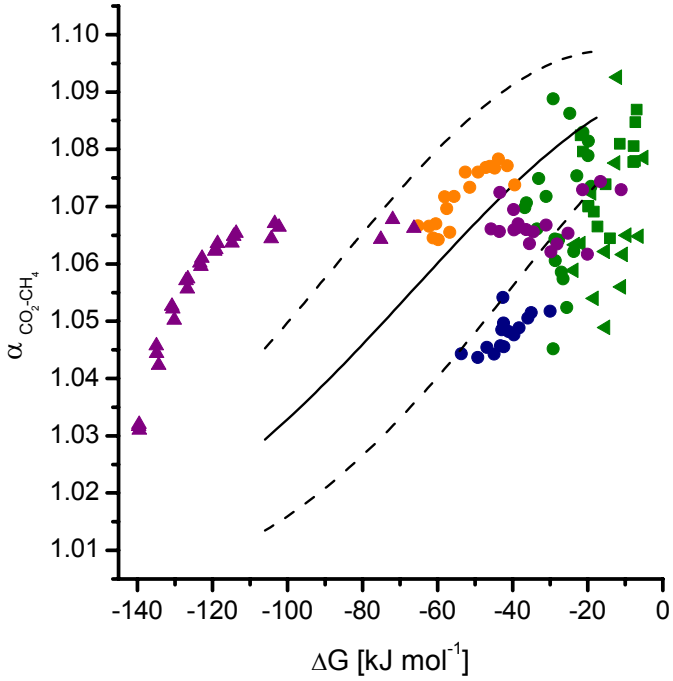

Abbildung IV-3. α-ΔG Korrelation von methanogenen Kokulturen und anoxisch inkubierten Umweltproben. Die durchgezogene Kurve ist die Regression aus den Kokulturversuchen (gestrichelte Linien: Ränder der 95 % Vertrauensbereiche). Acetoklastische Methanogenese, falls vorhanden, wurde in Umweltinkubationen mit Methylfluorid gehemmt. ● Reiswurzeln, ● Reisfeldboden; Hochmoor (■, oligotroph; ●, mesotroph; ◀, ombrotroph); Pansen (▲, unter H_2/CO_2; ●, unter N_2).

Der Anstieg von α mit ΔG wurde durch eine halbe Gauss-Kurve (r^2 = 0,77) modelliert. Die Regression durch eine Gaussfunktion wurde auf Grund der im Folgenden beschriebenen Grenzbedingungen gewählt. Bei stark negativem ΔG (viel freie Energie steht zur Verfügung), steigt die Methanbildungsrate an, so dass der CO_2-Pool innerhalb der Zelle immer kleiner wird und sich kein isotopisches Gleichgewicht zwischen dem extra- und intrazellulären CO_2 mehr einstellt. Im Extremfall ist der CO_2-Transport in die Zelle der limitierende Schritt der Methanogenese, wobei die CO_2-Konzentration in der Zelle gegen null geht und CO_2 quantitativ zu Methan umgesetzt wird. Dies entspräche einer

Fraktionierung von $\alpha = 1$ und wird durch die halbe Gausskurve beschrieben. Mit zunehmendem ΔG nimmt die Reversibilität der Einzelreaktionen der Methanogenese zu, so dass es zu einem Anstieg der Fraktionierung kommt. Die stärkste Fraktionierung in Kokulturen erfolgte am thermodynamischen Limit der methanogenen *Archaea*, das theoretisch bei -15 bis -25 kJ mol^{-1} bzw. ¼ bis ⅓ ATP liegt (Conrad, 1999; Müller, 2004; Schink und Stams, 2003; Yao und Conrad, 1999). Theoretisch wäre die maximale Fraktionierung bei $\Delta G = 0$ zu erwarten, wenn die Reversibilität der Reaktion am höchsten ist. Diese Grenzbedingung wird ebenfalls durch die Gaussfunktion beschrieben.

Die $\alpha-\Delta G$ Korrelation war für die vier untersuchten Spezies (aus den Familien der *Methanobacteriaceae* und *Methanomicrobiaceae*) gültig. Ein Artefakt durch art- bzw. gruppenspezifische unveränderliche Fraktionierungsfaktoren ist auszuschließen, da *M. bryantii* und *M. hungatei* der Korrelation über den gesamten Bereich folgten. Obwohl die Ergebnisse eine generelle Gültigkeit der Korrelation für alle hydrogenotrophen *Archaea* vermuten lassen, kann nicht ausgeschlossen werden, dass Enzyme hier nicht untersuchter Gruppen sich so weit unterscheiden (z.B. an Bindestellen oder in der Aktivierungsenergie), dass sie eine veränderte Isotopenfraktionierung zeigen. Jedoch sind die Enzyme hydrogenotropher Methanogener weitestgehend konserviert (Thauer, 1998) und die untersuchten Arten sind in der Natur von großer Bedeutung (Grosskopf et al., 1998a; Nüsslein et al., 2001), so dass zum jetzigen Zeitpunkt kein starkes Argument gegen die Übertragung der $\alpha-\Delta G$ Korrelation auf die Umwelt spricht.

In dieser Arbeit wurde für mehrere Umweltsysteme getestet, ob auch dort die für Kokulturen beschriebene $\alpha-\Delta G$ Korrelation gilt. Dies war aus zwei Gründen von Interesse: Wäre die Korrelation ebenfalls in Umweltsystemen vorhanden, so wäre es möglich, über das aus den gemessenen Partialdrücken errechnete ΔG den Fraktionierungsfaktor α für die hydrogenotrophe Methanogenese zu bestimmen. Andererseits könnte mit dieser Korrelation das Vorhandensein von H_2-Gradienten in Umweltsystemen aufgezeigt werden. H_2-Gradienten beeinflussen das über Gaspartialdrücke berechnete ΔG und können daher zu einer fehlerhaften Berechnung von ΔG in natürlichen Systemen führen (Hoehler et al., 2001). H_2-produzierende und -konsumierende Mikroorganismen sind häufig eng miteinander assoziiert, um einen effektiven H_2-Transfer zu ermöglichen (Conrad et al., 1985; Conrad et al., 1989; Hoehler et al., 2001; Krylova und Conrad, 1998) (Abbildung IV-4). Dies hat zur Folge, dass

H_2-Konsumenten den p_{H2} bereits in der Nähe der Produzenten verringern und im Porenwasser von Böden und Sedimenten weitaus geringere H_2-Konzentrationen vorhanden sind. Die Messung von H_2 erfolgt jedoch entweder im Porenwasser oder in der mit dem Porenwasser im Gleichgewicht stehenden Gasphase, da technisch eine H_2-Messung zwischen den Mikroorganismen unmöglich ist. Dies bedeutet, dass sich der Messwert und die Konzentration, die dem Organismus zur Verfügung steht, unterscheiden können. H_2-Gradienten verursachen folglich systematische Fehler bei der Berechnung von ΔG für H_2-abhängige Reaktionen. Tatsächlich folgten die Reisfeldboden- und Moorinkubationen nicht der für Kokulturen beschriebenen Korrelation und wiesen auf einen vorhandenen H_2-Gradienten hin (Abbildung IV-3). Das Reiswurzel-Modellsystem folgte der Korrelation und besitzt offensichtlich keinen H_2-Gradienten. Für Pansenflüssigkeit konnte ein H_2-Gradient durch eine 80%ige H_2-Atmosphäre erzeugt werden, jedoch ist dieser unter N_2 Atmosphäre nur gering ausgeprägt.

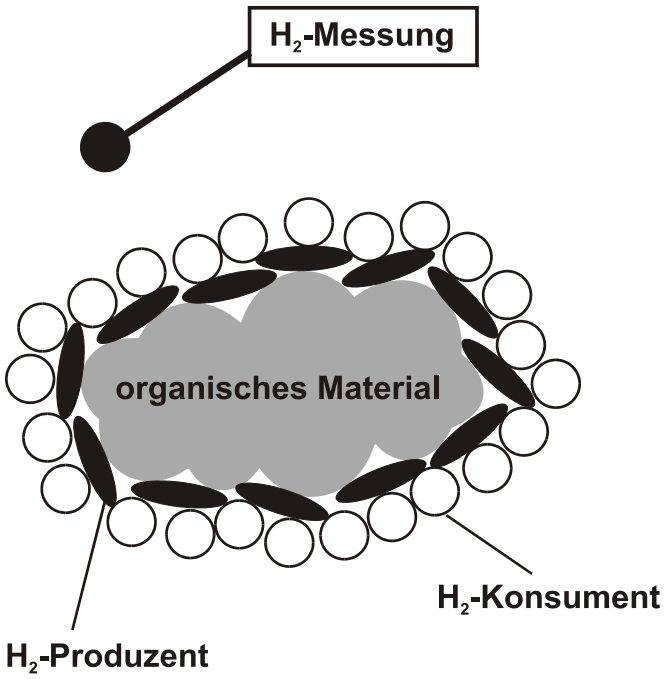

Abbildung IV-4. Modell der räumlichen Organisation H_2-produzierender und H_2-konsumierender Mikroorganismen in Boden- und Sedimentsystemen. Produzierter H_2 wird in direkter Nähe von Konsumenten teilweise verbraucht. Die gemessene Konzentration entspricht daher nicht derjenigen, die dem H_2-Konsumenten zur Verfügung steht (nach Hoehler et al., 2001).

Generell scheint bei höherer Heterogenität des Systems und damit wahrscheinlich vermehrter Aggregatbildung von Mikroorganismen, wie sie für Böden und Sedimente typisch ist, auch der H_2-Gradient größer zu werden. In Systemen mit H_2-Gradienten erlaubt

die α–ΔG Korrelation über Isotopensignatur von Methan das *in situ*-ΔG zu bestimmen. Vergleicht man die über die zwei Methoden bestimmten ΔG-Werte, zeigt sich, dass das über Gaspartialdrücke bestimmte ΔG meist größer als das über die α–ΔG Korrelation bestimmte ΔG ist. Das bedeutet, dass den Organismen mehr Energie zur Verfügung steht als zuvor vermutet (Conrad, 1999). Über die Partialdrücke waren in anderen Studien sehr hohe ΔG-Werte bestimmt worden, die die beobachtete Änderung methanogener Populationen bzw. deren Wachstum nicht erlauben würden (Krüger et al., 2005; Lueders und Friedrich, 2002; Peters und Conrad, 1996). Dieser Widerspruch kann nun mit der Bestimmung von ΔG über die α–ΔG Korrelation aufgeklärt werden. Da die *in situ* Gibbs freie Energie für hydrogenotrophe Methanogene in H_2-Gradienten beeinflussten Systemen bestimmt werden kann, ist es zusätzlich möglich die Zellzahl methanogener *Archaea*, die über die Gibbs freie Energie erhalten werden kann, zu berechnen. In dieser Arbeit wurde für das nicht durch H_2-Gradienten beeinflusste Reiswurzel-Modellsystem gezeigt, dass diese Berechnung gut mit der durch molekularbiologische Methoden bestimmten Zellzahl übereinstimmte. Dieselbe Strategie kann nun in H_2-Gradienten beeinflussten Systemen angewendet werden, um zu testen, ob die Größe methanogener Populationen hauptsächlich durch thermodynamische Zwänge gesteuert ist.

Diese Arbeit zeigt, dass der Fraktionierungsfaktor eines linearen Reaktionsweges nicht notwendigerweise eine feste Größe sein muss. Für die hydrogenotrophe Methanogensese korrelierte die Isotopenfraktionierung mit der Änderung der Gibbs freien Energie der Reaktion. Auch wenn der kausale Zusammenhang noch nicht völlig geklärt ist, ermöglicht die α–ΔG Korrelation einen völlig neuen Einblick in die energetischen Wachstumsbedingungen hydrogenotropher methanogener *Archaea* unter Umweltbedingungen. Die Bestimmung von α über die α–ΔG Korrelation ist aber auf Systeme ohne H_2-Gradienten (z.B. Reiswurzel-Modellsystem) begrenzt.

IV.4. Schlussbetrachtung und Ausblick

Die in dieser Dissertation vorgelegten Arbeiten erweitern das Wissen über den Fluss der stabilen Kohlenstoffisotope ^{13}C und ^{12}C in anaeroben Prozessen. Die gewonnenen Einblicke ermöglichen unter weit weniger Annahmen als zuvor, den relativen Kohlenstofffluss von Acetat und CO_2 zu CH_4 durch Isotopenmodellierung zu quantifizieren, was beispielhaft für das Reiswurzel-Modellsystem gezeigt wurde.

Auf die Bedeutung der $\alpha-\Delta G$ Korrelation zur Bestimmung des *in situ* ΔG und des Fraktionierungsfaktors wurde bereits hingewiesen. Für Berechnungen des globalen Methan-Haushalts wurden bisher relativ hohe Fraktionierungsfaktoren für Methanbildung aus CO_2 angenommen. Diese Arbeit zeigt, dass auch in Umweltsystemen relativ niedrige Werte bei stark negativem ΔG (entspricht hohem p_{H2}) möglich sind. Daher sollten zur Berechnung von $\delta^{13}C_{CH4}$ aus Bereichen mit hohem p_{H2} entsprechend niedrigere Faktoren verwendet werden. Zusätzlich zeigte die Korrelation, dass Isotopenfraktionierungsfaktoren in linearen Reaktionen nicht konstant sein müssen. Sicherlich ist die CO_2-Poolgröße eine Ursache für den beobachteten Effekt, jedoch muss sie nicht der alleinige Grund sein. Die Reaktionsraten der Isotope (^{13}k, ^{12}k) sind zwar *per definitionem* konstant, doch könnte die Fraktionierung von ΔG abhängen, ähnlich wie es für die Temperatur der Fall ist. Eine Abhängigkeit der Isotopenfraktionierung von ΔG wurde bereits über die Marcus Theorie und das Quantum-statistisch mechanische Modell vorhergesagt (Sühnel, 1990) und experimentell für das Element Wasserstoff gefunden (Kresge, 1980). Graphisch entspricht die vorhergesagte Beziehung einer Glockenkurve mit Maximum bei $\Delta G = 0$. Dieses Phänomen wurde für das Element Kohlenstoff noch nicht erforscht und sollte daher Thema weiterer Untersuchungen sein. Ein besseres Verständis der physikalischen Prinzipien, die die Isotopenfraktionierung steuern, könnte zudem neue Anwendungsbereiche stabiler Isotope aufzeigen.

Um eine umfassende Modellierung des Kohlenstoffflusses in anaeroben Systemen zu ermöglichen, sollte in Zukunft bei der Bestimmung von Fraktionierungsfaktoren der Schwerpunkt auf die fermentativen Prozesse gelegt werden. In dieser Arbeit wurde mit der gemischten Säuregärung ein Anfang gemacht. Arbeiten zu anderen primären (z.B. Propionatfermentation) und sekundären (z.B. Propionatoxidation, Ethanoloxidation) fermentativen Abbauwegen sollten folgen. Hierbei ist von besonderem Interesse, ob an analogen Verzweigungspunkten in unterschiedlichen Organismen eine ähnliche Isotopenverteilung zu den Produkten vorliegt. Falls solche Analogien vorhanden sind, wäre es möglich das Fraktionierungsverhalten noch nicht untersuchter Organismen an den analogen Verzweigungspunkten vorherzusagen.

V. Literatur

Billen G. (1982) Modelling the processes of organic matter degradation and nutrients recycling in sedimentary systems. In *Sediment Microbiology* (ed. D. B. Nedwell and C. M. Brown). 15-52. Academic Press.

Blair N., Leu A., Munoz E., Olsen J., Kwong E., und Desmarais D. (1985) Carbon isotopic fractionation in heterotrophic microbial metabolism. *Appl. Environ. Microbiol.* **50**, 996-1001.

Blair N. E. und Carter W. D. (1992) The carbon isotope biogeochemistry of acetate from a methanogenic marine sediment. *Geochim. Cosmochim. Acta* **56**, 1247-1258.

Brand W. A. (1996) High precision isotope ratio monitoring techniques in mass spectrometry. *J. Mass Spectrom.* **31**, 225-235.

Chan O. C., Claus P., Casper P., Ulrich A., Lueders T., und Conrad R. (2005) Vertical distribution of structure and function of the methanogenic archaeal community in Lake Dagow sediment. *Environmental Microbiology* **7**, 1139-1149.

Chidthaisong A. und Conrad R. (2000) Turnover of glucose and acetate coupled to reduction of nitrate, ferric iron and sulfate and to methanogenesis in anoxic rice field soil. *FEMS Microbiol. Ecol.* **31**, 73-86.

Chin K. J., Lueders T., Friedrich M. W., Klose M., und Conrad R. (2004) Archaeal community structure and pathway of methane formation on rice roots. *Microb. Ecol.* **47**, 59-67.

Chin K. J., Lukow T., und Conrad R. (1999) Effect of temperature on structure and function of the methanogenic archaeal community in an anoxic rice field soil. *Appl. Environ. Microbiol.* **65**, 2341-2349.

Chin K. J., Rainey F. A., Janssen P. H., und Conrad R. (1998) Methanogenic degradation of polysaccharides and the characterization of polysaccharolytic clostridia from anoxic rice field soil. *Syst. Appl. Microbiol.* **21**, 185-200.

Cicerone R. J. und Oremland R. S. (1988) Biogeochemical aspects of atmospheric methane. *Global Biogeochem. Cy.* **2**, 299-327.

Conrad R. (1999) Contribution of hydrogen to methane production and control of hydrogen concentrations in methanogenic soils and sediments [review]. *FEMS Microbiol. Ecol.* **28**, 193-202.

Conrad R. (2005) Quantification of methanogenic pathways using stable carbon isotopic signatures: a review and a proposal. *Org. Geochem.* **36**, 739-752.

Conrad R. und Klose M. (1999a) Anaerobic conversion of carbon dioxide to methane, acetate and propionate on washed rice roots. *FEMS Microbiol. Ecol.* **30**, 147-155.

Conrad R. und Klose M. (1999b) How specific is the inhibition by methyl fluoride of acetoclastic methanogenesis in anoxic rice field soil? *FEMS Microbiol. Ecol.* **30**, 47-56.

Conrad R. und Klose M. (2000) Selective inhibition of reactions involved in methanogenesis and fatty acid production on rice roots. *FEMS Microbiol. Ecol.* **34**, 27-34.

Conrad R., Klose M., und Claus P. (2002) Pathway of CH_4 formation in anoxic rice field soil and rice roots determined by ^{13}C-stable isotope fractionation. *Chemosphere* **47**, 797-806.

Conrad R., Mayer H. P., und Wüst M. (1989) Temporal change of gas metabolism by hydrogen-syntrophic methanogenic bacterial associations in anoxic paddy soil. *FEMS Microbiol. Ecol.* **62**, 265-274.

Conrad R., Phelps T. J., und Zeikus J. G. (1985) Gas metabolism evidence in support of juxtapositioning between hydrogen producing and methanogenic bacteria in sewage sludge and lake sediments. *Appl. Environ. Microbiol.* **50**, 595-601.

Conrad R. und Claus P. (2005) Contribution of methanol to the production of methane and its ^{13}C-isotopic signature in anoxic rice field soil. *Biogeochem.* **73**, 381-393.

de Vries J. J. (2005) Volume I: Introduction - theory, methods, review. In *Environmental isotopes in the hydrological cycle: Principles and applications* (ed. W. G. Mook). http://www.iaea.org/programmes/ripc/ih/volumes/volume1.htm. International Atomic Energy Agency.

Degens E. T. und Mopper K. (1975) Early diagenesis of organic matter in marine salts. *Soil Sci.* **119**, 65-72.

Deines P., Langmuir D., und Harmon R. S. (1974) Stable carbon isotope ratios and existence of a gas-phase in evolution of carbonate ground waters. *Geochim. Cosmochim. Acta* **38**, 1147-1164.

DeLong E. F. (2003) Oceans of *Archaea*. *ASM News* **69**, 503-511.

Erkel C., Kemnitz D., Kube M., Ricke P., Chin K. J., Dedysh S., Reinhardt R., Conrad R., und Liesack W. (2005) Retrieval of first genome data for rice cluster I methanogens by a combination of cultivation and molecular techniques. *FEMS Microbiol. Ecol.* **53**, 187-204.

Fey A., Claus P., und Conrad R. (2004) Temporal change of ^{13}C isotope signatures and methanogenic pathways in rice field soil incubated anoxically at different temperatures. *Geochim. Cosmochim. Acta* **68**, 293-306.

Fey A. und Conrad R. (2003) Effect of temperature on the rate limiting step in the methanogenic degradation pathway in rice field soil. *Soil Biol. Biochem.* **35**, 1-8.

Fitch W. M. (1971) Toward defining course of evolution - minimum change for a specific tree topology. *Systematic Zoology* **20**, 406-&.

Frenzel P. und Bosse U. (1996) Methyl fluoride, an inhibitor of methane oxidation and methane production. *FEMS Microbiol. Ecol.* **21**, 25-36.

Gelwicks J. T., Risatti J. B., und Hayes J. M. (1989) Carbon isotope effects associated with autotrophic acetogenesis. *Org. Geochem.* **14**, 441-446.

Gelwicks J. T., Risatti J. B., und Hayes J. M. (1994) Carbon isotope effects associated with aceticlastic methanogenesis. *Appl. Environ. Microbiol.* **60**, 467-472.

Gottschalk G. (1986) *Bacterial Metabolism*. Springer-Verlag.

Grosskopf R., Janssen P. H., und Liesack W. (1998a) Diversity and structure of the methanogenic community in anoxic rice paddy soil microcosms as examined by cultivation and direct 16S rRNA gene sequence retrieval. *Appl. Environ. Microbiol.* **64**, 960-969.

Grosskopf R., Stubner S., und Liesack W. (1998b) Novel euryarchaeotal lineages detected on rice roots and in the anoxic bulk soil of flooded rice microcosms. *Appl. Environ. Microbiol.* **64**, 4983-4989.

Gutell R. R., Larsen N., und Woese C. R. (1994) Lessons from an evolving rRNA - 16S and 23S rRNA structures from a comparative perspective. *Microbiol. Rev.* **58**, 10-26.

Hayes J. M. (1993) Factors controlling ^{13}C contents of sedimentary organic compounds - Principles and evidence. *Mar. Geol.* **113**, 111-125.

Hayes J. M. (2001) Fractionation of carbon and hydrogen isotopes in biosynthetic processes. *Stable Isotope Geochemistry* **43**, 225-277.

Hayes, J. M. (2002) Practice and principles of isotopic measurements in organic geochemistry. http://www.gps.caltech.edu/~als/Library/Other%20Stuff/Practice%20and%20Principles.pdf

Hobson P. N. (1997) *The rumen microbial ecosystem*. Blackie Academic & Professional.

Hoehler T. M., Alperin M. J., Albert D. B., und Martens C. S. (2001) Apparent minimum free energy requirements for methanogenic Archaea and sulfate-reducing bacteria in an anoxic marine sediment. *FEMS Microbiol. Ecol.* **38**, 33-41.

Horn M. A., Matthies C., Küsel K., Schramm A., und Drake H. L. (2003) Hydrogenotrophic methanogenesis by moderately acid-tolerant methanogens of a methane-emitting acidic peat. *Appl. Environ. Microbiol.* **69**, 74-83.

Janssen P. H. und Frenzel P. (1997) Inhibition of methanogenesis by methyl fluoride: Studies of pure and defined mixed cultures of anaerobic bacteria and archaea. *Appl. Environ. Microbiol.* **63**, 4552-4557.

Kemnitz D., Kolb S., und Conrad R. (2005) Phenotypic characterization of Rice Cluster III archaea without prior isolation by applying quantitative polymerase chain reaction to an enrichment culture. *Environ. Microbiol.* **7**, 553-565.

King G. M. und Klug M. J. (1982) Glucose metabolism in sediments of a eutrophic lake: tracer analysis of uptake and product formation. *Appl. Environ. Microbiol.* **44**, 1308-1317.

Kresge A. J. (1980) Correlation of kinetic isotope effects with free-energies of reaction. *J. Am. Chem. Soc.* **102**, 7797-7798.

Krüger M., Frenzel P., Kemnitz D., und Conrad R. (2005) Activity, structure and dynamics of the methanogenic archaeal community in a flooded Italian rice field. *FEMS Microbiol. Ecol.* **51**, 323-331.

Krummen M., Hilkert A. W., Juchelka D., Duhr A., Schluter H. J., und Pesch R. (2004) A new concept for isotope ratio monitoring liquid chromatography/mass spectrometry. *Rapid Commun. Mass Sp.* **18**, 2260-2266.

Krylova N. I. und Conrad R. (1998) Thermodynamics of propionate degradation in methanogenic paddy soil. *FEMS Microbiol. Ecol.* **26**, 281-288.

Krylova N. I., Janssen P. H., und Conrad R. (1997) Turnover of propionate in methanogenic paddy soil. *FEMS Microbiol. Ecol.* **23**, 107-117.

Krzycki J. A., Kenealy W. R., De Niro M. J., und Zeikus J. G. (1987) Stable carbon isotope fractionation by *Methanosarcina barkeri* during methanogenesis from acetate, methanol, or carbon dioxide-hydrogen. *Appl. Environ. Microbiol.* **53**, 2597-2599.

Lehmann-Richter S., Grosskopf R., Liesack W., Frenzel P., und Conrad R. (1999) Methanogenic archaea and CO_2-dependent methanogenesis on washed rice roots. *Environ. Microbiol.* **1**, 159-166.

Leschine S. B. und Canaleparola E. (1983) Mesophilic cellulolytic clostridia from freshwater environments. *Appl. Environ. Microbiol.* **46**, 728-737.

Liu W. T., Marsh T. L., Cheng H., und Forney L. J. (1997) Characterization of microbial diversity by determining terminal restriction fragment length polymorphisms of genes encoding 16S rRNA. *Appl. Environ. Microbiol.* **63**, 4516-4522.

Lovley D. R. und Klug M. J. (1983) Methanogenesis from methanol and methylamines and acetogenesis from hydrogen and carbon dioxide in sediments of a eutrophic lake. *Appl. Environ. Microbiol.* **45**, 1310-1315.

Lowe D. C., Brenninkmeijer C. A. M., Brailsford G. W., Lassey K. R., Gomez A. J., und Nisbet E. G. (1994) Concentration and ^{13}C records of atmospheric methane in New Zealand and Antarctica: Evidence for changes in methane sources. *J. Geophys. Res.* **99**, 16913-16925.

Ludwig W. (1995) Sequence database. In *Molecular microbial ecology manual* (ed. A. D. L. Akkermans, J. E. van Elsas, and F. J. de Bruijn). Kluwer Academic Publishers.

Ludwig W., Bauer S. H., Bauer M., Held I., Kirchhof G., Schulze R., Huber I., Spring S., Hartmann A., und Schleifer K. H. (1997) Detection and in situ identification of representatives of a widely distributed new bacterial phylum. *FEMS Microbiol. Lett.* **153**, 181-190.

Ludwig W., Strunk O., Westram R., Richter L., Meier H., Yadhukumar, Buchner A., Lai T., Steppi S., Jobb G., Forster W., Brettske I., Gerber S., Ginhart A. W., Gross O., Grumann S., Hermann S., Jost R., Konig A., Liss T., Lussmann R., May M., Nonhoff B., Reichel B., Strehlow R., Stamatakis A., Stuckmann N., Vilbig A., Lenke M., Ludwig T., Bode A., und Schleifer K. H. (2004) ARB: a software environment for sequence data. *Nucleic Acids Res.* **32**, 1363-1371.

Lueders T. und Friedrich M. W. (2002) Effects of amendment with ferrihydrite and gypsum on the structure and activity of methanogenic populations in rice field soil. *Appl. Environ. Microbiol.* **68**, 2484-2494.

Lueders T., Manefield M., und Friedrich M. W. (2004) Enhanced sensitivity of DNA- and rRNA-based stable isotope probing by fractionation and quantitative analysis of isopycnic centrifugation gradients. *Environ. Microbiol.* **6**, 73-78.

Lynd L. R., Weimer P. J., van Zyl W. H., und Pretorius I. S. (2002) Microbial cellulose utilization: Fundamentals and biotechnology. *Microbiol. Mol. Biol. R.* **66**, 506-577.

Madden R. H., Bryder M. J., und Poole N. J. (1982) Isolation and characterization of an anaerobic, cellulolytic bacterium, *Clostridium papyrosolvens* sp.nov. *Int. J. Syst. Bacteriol.* **32**, 87-91.

Mariotti A., Germon J. C., Hubert P., Kaiser P., Letolle R., Tardieux A., und Tardieux P. (1981) Experimental determination of nitrogen kinetic isotope fractionation - Some principles - Illustration for the denitrification and nitrification processes. *Plant Soil* **62**, 413-430.

Metje M. und Frenzel P. (2005) The effect of temperature on anaerobic ethanol oxidation and methanogenesis in an acid peat from a northern wetland. *Appl. Environ. Microbiol.* **in press**.

Mook W. G., Bommerso J. C., und Staverma W. H. (1974) Carbon isotope fractionation between dissolved bicarbonate and gaseous carbon dioxide. *Earth. Planet. Sc. Lett.* **22**, 169-176.

Müller V. (2004) An exceptional variability in the motor of archaeal A(1)A(0) ATPases: From multimeric to monomeric rotors comprising 6-13 ion binding sites. *J. Bioenerg. Biomembr.* **36**, 115-125.

Nüsslein B., Chin K. J., Eckert W., und Conrad R. (2001) Evidence for anaerobic syntrophic acetate oxidation during methane production in the profundal sediment of subtropical Lake Kinneret (Israel). *Environ. Microbiol.* **3**, 460-470.

O'Leary M. H. (1988) Carbon Isotopes in Photosynthesis. *Bioscience* **38**, 328-336.

Peters V. und Conrad R. (1996) Sequential reduction processes and initiation of CH_4 production upon flooding of oxic upland soils. *Soil Biol. Biochem.* **28**, 371-382.

Pohlschroder M., Leschine S. B., und Canaleparola E. (1994) Multicomplex cellulase xylanase system of *Clostridium papyrosolvens* C7. *J. Bacteriol.* **176**, 70-76.

Quay P. D., King S. L., Stutsman J., Wilbur D. O., Steele L. P., Fung I., Gammon R. H., Brown T. A., Farwell G. W., Grootes P. M., und Schmidt F. H. (1991) Carbon isotopic composition of atmospheric CH4: fossil and biomass burning source strengths. *Global Biogeochem. Cy.* **5**, 25-47.

Raeymaekers L. (2000) Basic principles of quantitative PCR. *Molecular Biotechnology* **15**, 115-122.

Ricke P., Kolb S., und Braker G. (2005) Application of a newly developed ARB software-integrated tool for in silico terminal restriction fragment length polymorphism analysis reveals the dominance of a novel pmoA cluster in a forest soil. *Appl. Environ. Microbiol.* **71**, 1671-1673.

Sanger F., Nicklen S., und Coulson A. R. (1977) DNA sequencing with chain-terminating inhibitors. *PNAS* **74**, 5463-5467.

Scheid D., Stubner S., und Conrad R. (2004) Identification of rice root associated nitrate, sulfate and ferric iron reducing bacteria during root decomposition. *FEMS Microbiol. Ecol.* **50**, 101-110.

Schink B. (1997) Energetics of syntrophic cooperation in methanogenic degradation. *Microbiol. Mol. Biol. R.* **61**, 262-&.

Schink B. und Stams A. J. M. (2003) Syntrophism among prokaryotes. In *The Prokaryotes: An evolving electronic resource for the microbiological community* (ed. M. Dworkin). http://link.springer-ny.com/link/service/books/10125/. Springer.

Schütz H., Holzapfel-Pschorn A., Conrad R., Rennenberg H., und Seiler W. (1989a) A 3-year continuous record on the influence of daytime, season, and fertilizer treatment on methane emission rates from an Italian rice paddy. *J. Geophys. Res.* **94**, 16405-16416.

Schütz H., Seiler W., und Conrad R. (1989b) Processes involved in formation and emission of methane in rice paddies. *Biogeochem.* **7**, 33-53.

Stahl D. A. und Amann R. (1991) Development and application of nucleic acid probes. In *Nucleic acid techniques in bacterial systematics* (ed. E. Stackebrandt and M. A. Goodfellow). 205-248. Wiley.

Stams A. J. M., Vandijk J. B., Dijkema C., und Plugge C. M. (1993) Growth of syntrophic propionate-oxidizing bacteria with fumarate in the absence of methanogenic bacteria. *Appl. Environ. Microbiol.* **59**, 1114-1119.

Stumm W. und Morgan J. J. (1995) *Aquatic Chemistry*. Wiley-Interscience.

Sühnel J. (1990) The kinetic deuterium-isotope effect of proton-transfer reactions in solution - comparison of the marcus and the quantum-statistical mechanical models. *J. Phys. Org. Chem.* **3**, 62-68.

Suzuki M. T., Taylor L. T., und Delong E. F. (2000) Quantitative analysis of small-subunit rRNA genes in mixed microbial populations via 5 '-nuclease assays. *Appl. Environ. Microbiol.* **66**, 4605-4614.

Thauer R. K. (1998) Biochemistry of methanogenesis: a tribute to Marjory Stephenson. *Microbiology-Sgm* **144**, 2377-2406.

Tsutsuki K. und Ponnamperuma F. N. (1987) Behavior of anaerobic decomposition products in submerged soils . Effects of organic material amendment, soil properties, and temperature. *Soil Sci. Plant Nutr.* **33**, 13-33.

Tyler S. C., Ajie H. O., Gupta M. L., Cicerone R. J., Blake D. R., und Dlugokencky E. J. (1999) Stable carbon isotopic composition of atmospheric methane: A comparison of surface level and free tropospheric air. *J. Geophys. Res.* **104**, 13895-13910.

Valentine D. L., Chidthaisong A., Rice A., Reeburgh W. S., und Tyler S. C. (2004) Carbon and hydrogen isotope fractionation by moderately thermophilic methanogens. *Geochim. Cosmochim. Acta* **68**, 1571-1590.

Wasserfallen A., Nolling J., Pfister P., Reeve J., und de Macario E. C. (2000) Phylogenetic analysis of 18 thermophilic *Methanobacterium* isolates supports the proposals to create a new genus, *Methanothermobacter* gen. nov., and to reclassify several isolates in three species, *Methanothermobacter thermautotrophicus* comb. nov.,

Methanothermobacter wolfeii comb. nov., and *Methanothermobacter marburgensis* sp. nov. *Int J Syst Bacteriol* **50**, 43-53.

Werner R. A. und Brand W. A. (2001) Referencing strategies and techniques in stable isotope ratio analysis. *Rapid Commun. Mass Sp.* **15**, 501-519.

Werner R. A., Bruch B. A., und Brand W. A. (1999) ConFlo III - An interface for high precision $\delta^{13}C$ and $\delta^{15}N$ analysis with an extended dynamic range. *Rapid Commun. Mass Sp.* **13**, 1237-1241.

Wolin E. A., Wolin M. J., und Wolfe R. S. (1963) Formation of methane by bacterial extracts. *J. Biol. Chem.* **238**, 2882-&.

Yao H. und Conrad R. (1999) Thermodynamics of methane production in different rice paddy soils from China, the Philippines and Italy. *Soil Biol. Biochem.* **31**, 463-473.

Zyakun A. M., Bondar V. A., Laurinavichus K. S., Shipin O. V., Belyaev S. S., und Ivanov M. V. (1988) Fractionation of carbon isotopes under the growth of methane-producing bacteria on various substrates. *Mikrobiologiceskij Zhurnal* **50**, 16-22.

Lebenslauf

Persönliche Daten

Holger Penning	geboren am 20. 04. 1977 in Erlangen deutsch ledig

Wissenschaftlicher Werdegang

seit 01/2003	Doktorand am Max-Planck-Institut für terrestrische Mikrobiologie (Marburg) in der Arbeitsgruppe von Prof. Conrad (Biogeochemie).
06/1999 – 11/2002	Hauptstudium Geologie/Paläontologie an der Friedrich-Alexander-Universität Erlangen-Nürnberg **Diplomarbeit:** „Phytoremediation of Perchlorate and Trichloroethylene contaminated Water using Willow Trees" (Prof. Nzengung, Department of Geology, University of Georgia, USA; Prof. Tobschall, Angewandte Geologie, Erlangen-Nürnberg). **Diplomkartierung:** „Aufbau und Beschaffenheit der Böden im Kartenblatt 5931 Ebensfeld unter besonderer Berücksichtigung der Lößlehmablagerungen" (Prof. Roßner, Allgemeine Geologie, Erlangen-Nürnberg; Prof. Tobschall, Angewandte Geologie, Erlangen-Nürnberg).
08/2000 – 06/2001	Geologieauslandsstudium an der University of Georgia in Athens, GA, USA (Fulbright-Stipendium).
01/2000	Aufnahme in die Studienstiftung des deutschen Volkes.
11/1997 – 05/1999	Grundstudium Geologie/Paläontologie an der Friedrich-Alexander-Universität Erlangen-Nürnberg.

Zivildienst

04/1998	Rettungssanitäterabschlussprüfung in Mainz
10/1996 – 10/1997	Rettungsdienst des Bayerischen Roten Kreuzes (Erlangen)

Schulbildung

1987 – 1996	Marie-Therese-Gymnasium Erlangen
1983 – 1987	Grundschule Bubenreuth

Danksagung

Mein besonderer Dank gilt Prof. Dr. Ralf Conrad für die Anleitung, die Überlassung des Themas und die finanzielle Unterstützung. Er gewährte mir großen forscherischen Freiraum mit der Möglichkeit stets ein offenes Ohr für Diskussionen und neue Ideen zu finden, so dass ich meine Arbeit genießen und erfolgreich durchführen konnte.

Prof. Dr. Ralf Conrad und Prof. Dr. Thauer möchte ich herzlich für die Erstellung der Gutachten für diese Arbeit danken.

Besonderer Dank auch an Dr. Stan C. Tyler, Dr. Roland Werner und Dr. Gerd Gleixner, die mich in ihren Labors in einige Geheimnisse der Isotopenanalytik eingewiesen haben. Weiterhin bedanke ich mich bei Dr. Carolin Plugge und Dr. Pierre Galand für die angenehme und erfolgreiche Zusammenarbeit an verschiedenen Projekten.

Für die sehr gute und erbauende Zusammenarbeit im Labor möchte ich Dr. Gesche Braker, Dr. Dana Kemnitz, Peter Claus, Melanie Klose, Dr. Bernhard Nüßlein und gesamten Abteilung Biogeochemie danken.

Meinen lieben Eltern möchte ich dafür danken, dass sie mir das Studium ermöglicht haben und mich stets von fern oder nah in jeglicher Angelegenheit unterstützt haben und dies hoffentlich auch weiterhin tun werden.

Ganz besonders danke ich meiner Verena, die mir in allen Lebenslagen eine große Freude und wichtige Stütze ist.

Erklärung

Ich versichere, dass ich meine Dissertation

„Fraktionierung stabiler Isotope durch anaerobe Bodenmikroorganismen“

selbständig und ohne unerlaubte Hilfe angefertigt habe und mich keiner anderen als der von mit ausdrücklich bezeichneten Quellen und Hilfen bedient habe.
Diese Dissertation wurde in der jetzigen oder einer ähnlichen Form noch bei keiner anderen Hochschule eingereicht und hat noch keinen sonstigen Prüfungszwecken gedient.

Marburg, im Oktober 2005